Synthesis and Characterisation of Non-Interacting Multichromophore Arrays

Stephanie Ryan

This Thesis is submitted in part fulfilment of the requirements for the degree of Doctor of Philosophy at the University of East Anglia

July 2011

© This Copy of the thesis has been supplied on condition that anyone who consults it is understood to recognise that its copyright rests with the author and that no quotation from the thesis, nor any information derived therefrom, may be published without the author's prior consent.

Declaration

The research described in this thesis is, to the best of my knowledge, original and my own work except where due reference has been made.

Stephanie Ryan

Abstract

Multiporphyrin arrays are important for helping us understand the energy migration process in photosynthetic organisms. However these arrays must have some important attributes that mimic naturally occurring light harvesting synthesis *i.e*. architectural rigidity, organic solubility and incorporation of numerous chromophores (porphyrins) with controlled metalation. Light harvesting systems in purple bacteria are known to have highly ordered cyclic architectures of bacterial chlorophylls. These cyclic chromophore structures are held in place by a protein frame, preventing the chromophores from interacting and therefore losing energy by quenching.

Triphenylene cores have been employed in the synthesis of model compounds for investigation of such non-interacting multichromophore arrays. Two regioisomeric models were successfully synthesised in which the chromophore (a zinc porphyrin) was linked to the 2,3 or 3,6-positions of the triphenylene core via a flexible spacer. The binding was investigated quantitatively through UV-vis titrations and, as expected, the models showed strong, cooperative binding to matched bispyridyl ligands.

Synthesis of the related hexaporphyrin array initially appeared successful. However, analysis of binding gave unexpected results that matched binding to simple monomeric zinc porphyrins. These results led to further investigation and it was found that the synthesised compound was in fact the monomeric porphyrin substituted with a terminal formate ester. The origin of this compound is likely to stem from decomposition of the DMF reaction solvent.

Further metalation of the model diporphyrins was undertaken to give the copper and ruthenium analalogues.

Acknowledgements

I would firstly like to thank my supervisor Dr Andrew N Cammidge for all his help, encouragement and support not only as my PhD supervisor but also as my undergraduate advisor. Andy has been excellent in his guidance and I am grateful to him for his attentiveness, patience and help in all fields during my studies at UEA.

I am also grateful to the teaching, technical and administrative staff of the school of chemistry at UEA for their help and assistance throughout my degree.

I would like to thank my friends with whom I have shared lab 3.17 and worked with throughout my time at UEA. Specifically Hemant Gopee and Isabelle Chambrier for their help and guidance during my PhD. Also a special thanks to my friends from other labs, departments and areas within UEA with whom I have had a great time and will carry with me the great memories of our time spent together. A special mention must go to Jamie Leeder who had the very difficult job of helping me with everything computer related and to all my friends outside of UEA, especially Vicki White, that have been incredibly supportive and I hope I will be able to return this support in all of your endeavours.

I wish to express my greatest gratitude and thanks to my parents, Michele and Graham Ryan, and to Kyle Cooke, without whom, I would not have had the strength or means to complete my PhD. Their encouragement, love and support is without bounds and I only hope my achievement in writing this thesis will go some way to repaying this debt.

Dedicated to my parents Michele and Graham Ryan

Abbreviations

d	Doublet
DCM	Dichloromethane
dd	Doublet of doublets
DDQ	2,3-Dichloro-5,6-dicyanobenzoquinone
DME	1,2-dimethoxyethane
DMF	Dimethylformamide
EPSRC	Engineering and Physical Sciences Research Council
Et	Ethyl
h	Hour
HOMO	Highest Occupied Molecular Orbital
Hz	Hertz
IR	Infrared
IUPAC	International Union of Pure and Applied Chemistry
J	Coupling constant in Hertz
LUMO	Lowest Unoccupied Molecular Orbital
m	meta
m	Multiplet
M	Molar
MALDI	Matrix assisted laser desorption ionisation
Me	Methyl
MEK	Methylethylketone
MS	Mass Spectrum

MSDS	Materials Safety Data Sheet
NMP	N-methyl-2-pyrrolidone
NMR	Nuclear Magnetic Resonance Spectroscopy
NLO	Non-Linear Optical
o	ortho
p	para
PET	Petroleum ether
Ph	Phenyl
ps	picoseconds
Py	Pyridine
s	Singlet
TBLAH	Lithium tri-tert-butoxyaluminum hydride
TFA	Triflouroactetic acid
THF	Tetrahydrofurran
TLC	Thin Layer Chromatography
TPP	Tetraphenylporphyrin
TsCl	*p*-Toluenesulfenylchloride
UV-Vis	Ultra violet-Visible

Chapter 1: Introduction

1.1. Structure and Properties of porphyrins

1.1.1. Background and Structure

Porphyrin is the name given to a highly coloured group of compounds comprising a particular macrocycle. This macrocycle is made up of four smaller rings (pyrrole) each joined together by a methine bridging group (figure 1). The structure of porphyrins was first suggested by Küster in 1912, but was not accepted until the total synthesis of a heme was achieved by Fisher in 1929.[1] The word Porphyrin is derived from the Greek word for purple, *porphura*.[2] The name illustrates the most obvious property of porphyrins, their intense colour, in this case purple. Purple dye was used to colour the clothes of royalty and we still associate purple with royalty and wealth today. However purple porphyrins are only one group of pigments, in general the colour and many other properties are dependent on a metal atom at the centre of the macrocycle bound by the four nitrogen atoms. For example, a porphyrin with an iron at its centre is called a heme and is essential to life as it is responsible for oxygen transportation in the blood and many redox enzymes used in metabolic processes.[3]

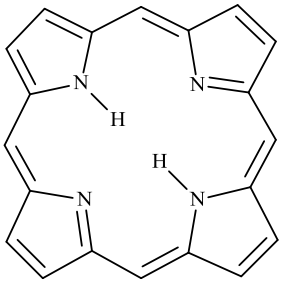

Figure 1. Porphyrin macrocycle

Chlorophyll is a reduced porphyrin with a magnesium atom at its centre, and is responsible for photosynthesis is plants.[4] The reason that porphyrins have such a wide range of properties is largely due to their electronic structure, they belong to a group of compounds called aromatics *i.e.* a coplanar ring or rings that consist of a delocalized conjugated π system, most commonly an arrangement of alternating single and double bonds containing $(4n+2)\pi$ electrons (obey Huckel's rule). Porphyrins have 22 π electrons 18 of which are involved in the aromatic system, therefore according to Huckel n = 4.

1.1.2. Nomenclature

Fischer[5] was the first to introduce a nomenclature and numbering system for the porphyrin. Each carbon on the pyrrole unit that can be substituted was named the β-carbon and numbered 1 to 8. The positions that cannot be substituted were referred to as α-carbons and are unnumbered. The bridging carbons (the meso positions) were given the Greek letters α to δ (figure 2).

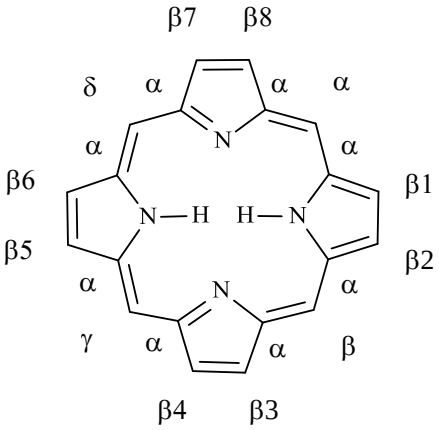

Figure 2. Ficsher's nomenclature system.

This system was efficient for basic porphyrins but when they were fully substituted the nomenclature became very complicated. The systematic IUPAC nomenclature was introduced in 1974 and completed in 1987.[1] In this system all of the atoms are numbered including the nitrogen atoms in the macrocycle (figure 3).

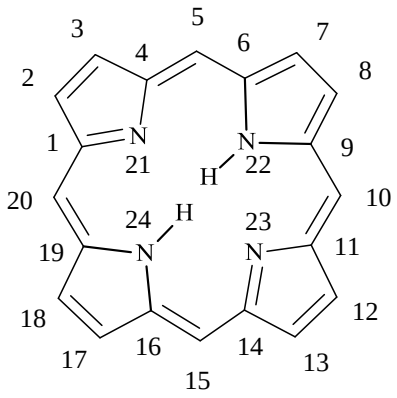

Figure 3. IUPAC nomenclature system.

1.1.3. Spectral Properties

1.1.3.1. UV-Vis absorption spectra

Porphyrins are intensely coloured compounds with very high extinction coefficients (10^6). The colour of which can be seen at very low concentrations. These properties allow for easy analysis of porphyrin compounds by UV-Vis absorption spectroscopy. Different porphyrin derivatives, such as different substitution patterns, cause changes in the UV-Vis spectra. The shape and relative intensities of the bands within the spectra can give important clues to the substitution in a porphyrin [6] whereas stereoisomers and atropisomers of a specific porphyrin will often produce identical, indistinguishable spectra. [7]

The archetypal aromatic compound, benzene, has three conjugated electron pairs and absorbs at very high energy wavelengths. However porphyrins have a minimum of nine conjugated electron pairs and this decreases the gap between the HOMO and the LUMO considerably and therefore brings the absorption bands down to the near UV-Visible region of the spectrum (figure 4).[7]

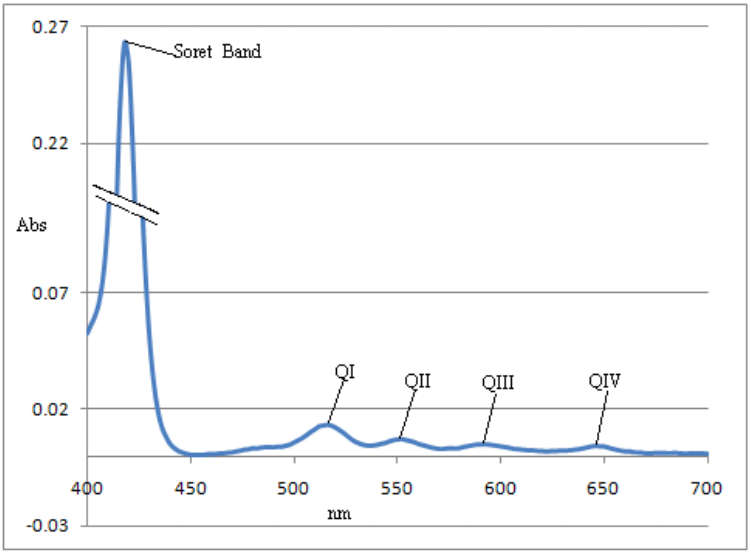

Figure 4. Typical H_2-Porphyrin UV-Vis Spectrum.

Porphyrin compounds have this absorption spectrum because of the electronic transitions between the highest occupied molecular orbital (π-bonding orbital) (HOMO) and the lowest unoccupied molecular orbital (π*-anti-bonding orbital) (LUMO) associated with the

conjugated ring system (the Gouterman four orbital model). Martin Gouterman first proposed the four-orbital model in the 1960s to explain the absorption spectra of porphyrins.[6] According to this theory, the absorption bands in porphyrin systems arise from transitions between two HOMOs and two LUMOs, and it is the identities of the metal centre and the substituents on the ring that affect the relative energies of these transitions. The HOMOs were calculated to be an a_{1u} and an a_{2u} orbital, while the LUMOs were calculated to be a degenerate set of e_g orbitals (figure 5). Transitions between these orbitals gave rise to two excited states, both of ^1E_u character. Orbital mixing splits these two states in energy. This creates a higher energy ^1E_u state with greater oscillator strength and an angular momentum of 4 units i.e. the Soret band, and a lower energy ^1E_u state with less oscillator strength and an angular momentum of nine units, giving rise to the Q-bands. The Q bands are only partially allowed due to the lower angular momentum so therefore have a much lower intensity.

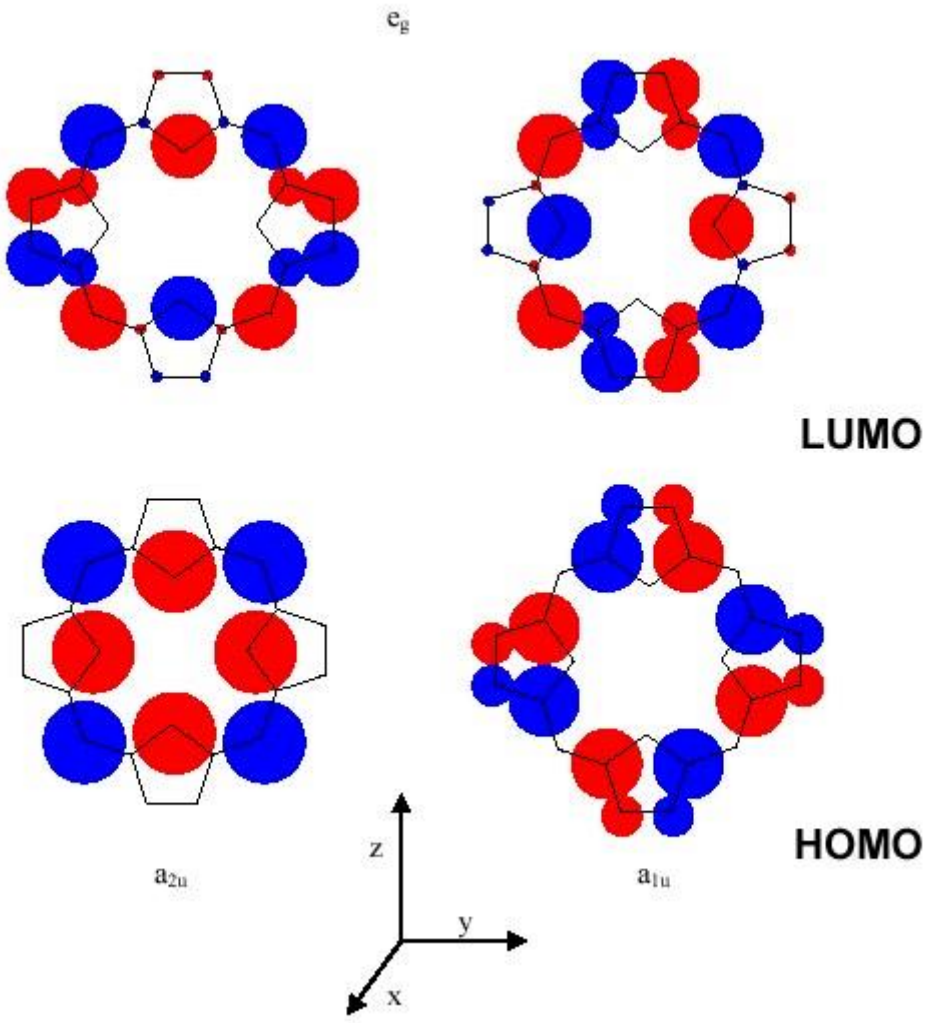

Figure 5. The Frontier Orbitals relevant to the Gouterman Four-Orbital Model [6]

The Soret band was named after J. L. Soret who first discovered an intense absorption band around 400 nm in haemoglobin in 1883.[8] Free porphyrins have four smaller bands between 480-700 nm called Q bands (figure 4) and metalloporphyrins have two smaller Q bands between 480-700 nm (figure 6).

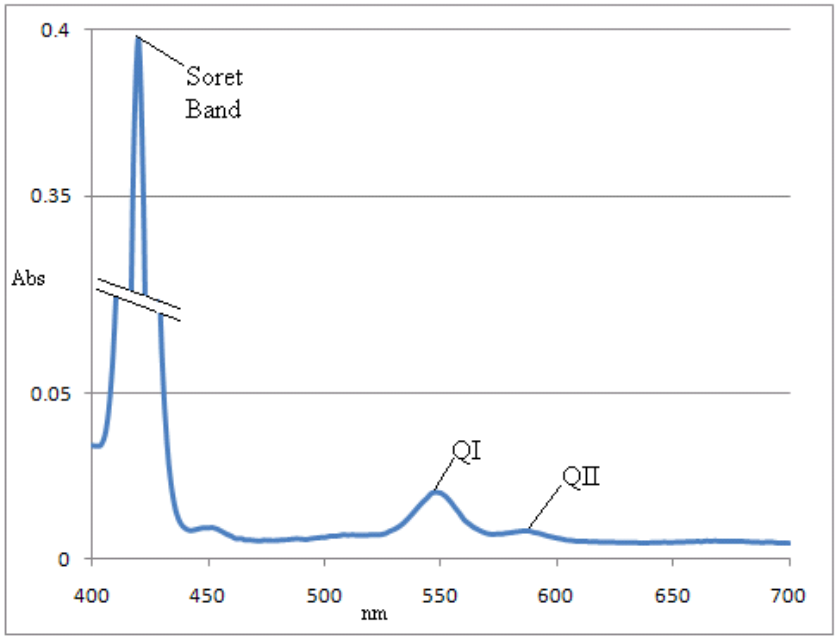

Figure 6. Typical Zinc-Porphyrin UV-Vis Spectrum.

The difference in spectra between the metalloporphyrins and the free porphyrin occur because they have two different symmetry point groups. Free porphyrins have D_{2h} symmetry and metalloporphyrins have D_{4h} symmetry. This causes some of the energy levels to become degenerate decreasing the number of Q bands.

1.1.3.2. NMR Spectra

Porphyrins are large macroheterocycles with an extended conjugated system. The porphyrin macrocycle has 22 π electrons 18 of which are involved in the conjugated aromatic system (supported by Huckel's rule). This aromaticity causes porphyrins to have remarkable NMR properties. The β-pyrrole and meso-protons are strongly shifted downfield due to the paramagnetic ring current de-shielding effect and the –NH protons of the pyrrole rings are shifted up field to the negative region of the spectrum as a result of the shielding effect of the ring current (figure 7).[9]

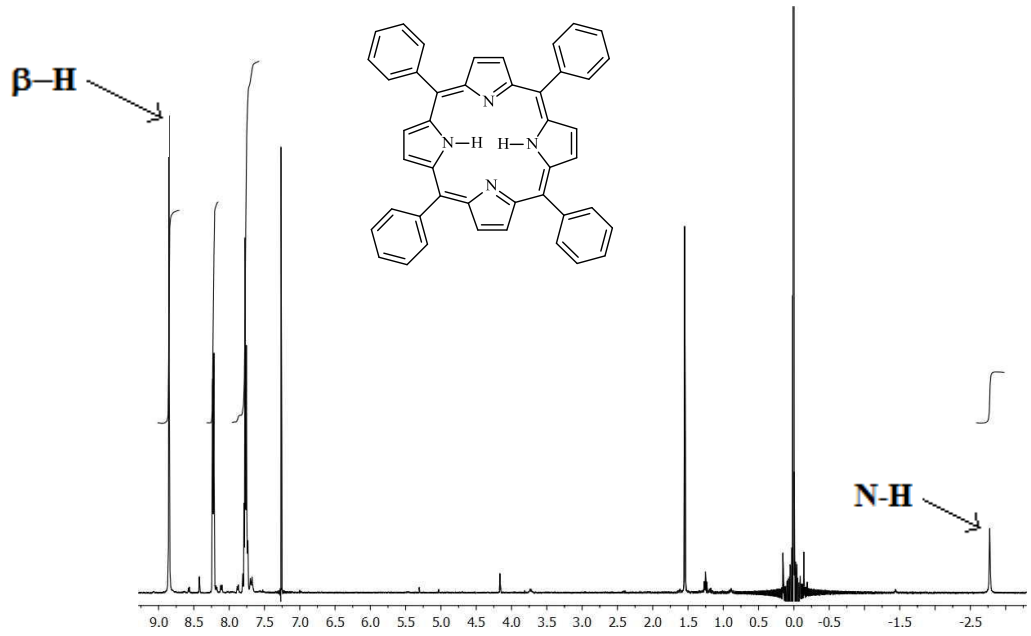

Figure 7. NMR spectrum of Tetraphenylporphyrin.

1.2. Meso-Substituted Porphyrins

1.2.1. Porphyrins with four identical meso-substituents

1.2.1.1. Background

The reason porphyrins are so diverse is because many different substituents can be placed on many different positions in the macrocycle. Control over these substituents allows us to tailor the macrocycle for specific applications. There are two main porphyrin substitution patterns i.e. β-substituted porphyrins and *meso*-substituted porphyrins (figure 8). The β-substituted porphyrins are more commonly found in nature but *meso* substituted porphyrins have sparked perhaps the most interest in synthetic chemistry.[10] They have biomimetic model applications, are useful in materials chemistry and are relatively easy to synthesise. Porphyrins are essentially synthesised from a mixture of pyrrole and aldehydes. One of the advantages to this is that aldehydes are widely available, easy to manipulate and are ideal for making a huge range of porphyrins without complicated multistep syntheses of precursors. Components incorporated into the aldehyde unit give rise to convenient handles on the porphyrin for further synthetic elaboration.[11]

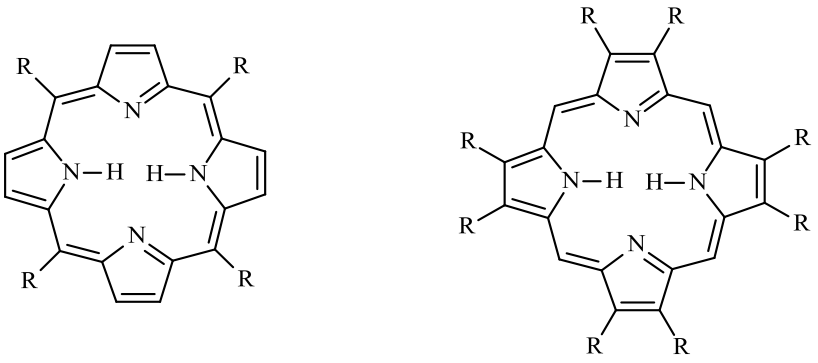

Meso-substituted porphyrin β-substituted porphyrin

Figure 8. Structure of *meso*-substituted and β-substituted porphyrins

1.2.1.2. Rothemund method

There are a number of methods for preparing porphyrins, from simple one-flask reaction of pyrrole and an aldehyde to extensive multistep synthesis, each one having its advantages and disadvantages. A pioneer in this research was Rothemund in 1935.[12] Rothemund reacted acetaldehyde and pyrrole in methanol to obtain *meso*-tetramethylporphyrin as a crystalline solid along with its copper and iron complexes. He then expanded this research to include a variety of aldehydes creating a large catalogue of porphyrins substituted at the meso positions, some examples of such substituents are methyl, propyl, phenyl, isobutyl, butyl and some more complicated substituents such as 3-methoxy-4-hydroxyphenyl, 2-hydroxyphenyl, 3-hydroxyphenyl and 4-methoxyphenyl. The reaction conditions for most of these porphyrins were 140-150˚C for ~24hrs in a sealed flask under nitrogen,[13] i.e. high temperatures, high pressures in a sealed container with no added oxidant (Scheme 1).

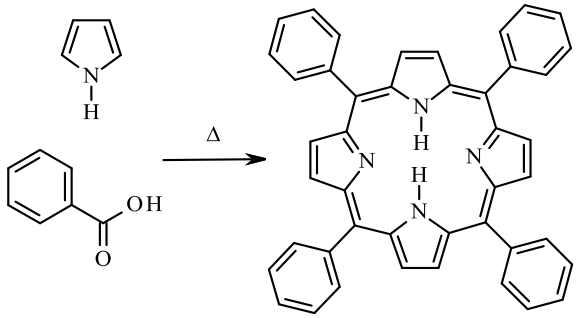

Scheme 1. Rothemund method for synthesis of *meso*-substituted porphyrins, exemplified for *meso*-tetraphenylporphyrin [H_2(TPP)]

However Rothemund's yields where very low and studies show a large amount of a by-product, chlorins, was present in his reactions. Chlorin is a reduced porphyrin (figure 9). Leaving the reaction mixture open to air overnight after the reaction has completed allows the chlorin to be oxidised to porphyrin. Calvin and co-workers discovered that the yield of the majority of porphyrins can be improved by adding zinc acetate, creating the zinc complex of the porphyrin. This raised the average yield of meso-tetraphenylporphyrin from 4-5 % to 10-11 %.[14]

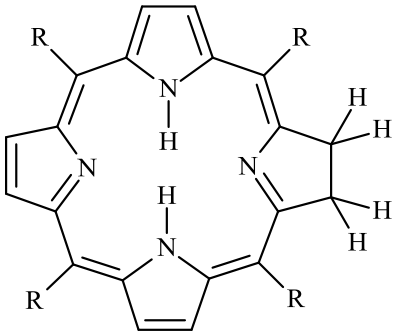

Meso-substituted chlorin

Figure 9. Structure of chlorin

1.2.1.3. Alder-Longo method

In the mid-1960's *meso*-substituted porphyrin synthesis was revolutionised by the Adler-Longo method (Scheme 2). They discovered that if pyrrole is reacted in acidic conditions, open to the air, the yields are greatly increased. Yields of 30-40 % were obtained using propionic acid with the aldehyde and pyrrole at a concentration of 0.27 M, refluxing for 30 minutes, open to air.[15] Propionic acid is ideal to use because many aldehydes are soluble in it and the porphyrin product crystallises out easily with relatively high yield. Other acids such as acetic acid can be used and for a few aldehydes, produce better yields, but it is propionic acid that in generally favoured. Isolation of these porphyrins is generally easy and just involves filtration and washing but in some cases crystallisation does not occur. In these cases the propionic acid is removed by vacuum evaporation to leave a black residue which is subjected to column chromatography to isolate the product. One limitation to this method is *o*-substituted benzaldehydes. *P*-substituted benzaldehydes such as *p*-chlorobenzaldehyde produce porphyrins in yields of 23 % where as *o*-chlorobenzaldehyde produces porphyrin in yields of just 3.3 %. A way around some of the problems with the Alder method is to use

protecting groups, for example to make *o*-hydroxyphenyl porphyrin, *o*-methoxybenzaldehyde is first employed. There are also some problems with *m*- *p*- benzaldehyde substituents e.g. nitrobenzene. This has led to modifications to the reaction and workup conditions. For example *p*-nitrobenzaldehyde can be reacted with pyrrole in propionic acid with some acetic anhydride present and filtered to leave a black residue which is then refluxed in pyridine, cooled and filtered to gain the desired porphyrin in yields of 19-20 %.[16]

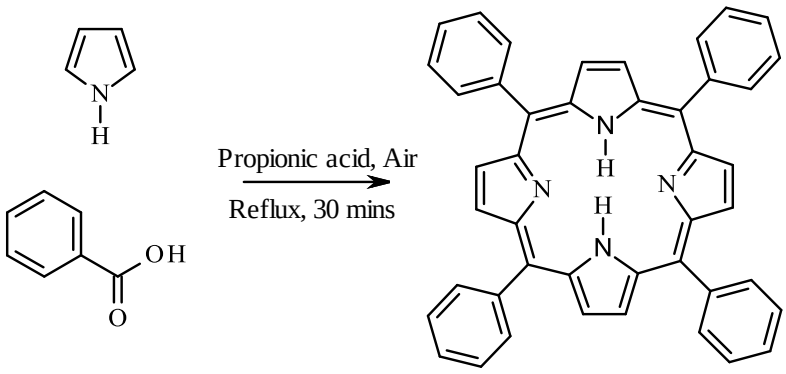

Scheme 2. Alder method for preparing *meso*-substituted porphyrins

1.2.1.4. Collman group

Another pioneer in *meso* substituted porphyrin synthesis is Collman, who reacted o-nitrobenzene with pyrrole and reduced the product with stannous chloride to create *meso*-tetrakis(*o*-aminophenyl)porphyrin. This produces the atropisomers shown in figure 10, all of which were shown to be stable and easily separated.[17] The atropisomers are caused by the NO_2 groups on the phenyl substituents preventing rotation around the single bond attached to the meso position of the porphyrin. These porphyrins are now known as "picket-fence" porphyrins i.e. a porphyrin with a protective enclosure for binding oxygen at one side of the ring that is used to mimic the dioxygen-carrying properties of the heme group**.** The amines can be easily derivatized and a wide variety of superstructural porphyrins can be and has been built using this simple molecule.[18] One example is as a synthetic model for oxygen binding hemoproteins. Collman *et al* separated the isomers to isolate the α,α,α,α-atropisomer. They inserted iron into the porphyrin cavity then reacted the NH_2 substituent with a bulky group such as p-toluenesulfonyl chloride to create a porphyrin that has great steric bulk on one side of the plane of the porphyrin yet leaves the other side unencumbered, thus leaving a hydrophobic pocket for complexation of dioxygen. This allowed Collman to investigate the

binding of dioxygen to the iron centre. They found their model systems suggest that molecular oxygen coordinates in the hemoproteins, Hb and Mb, in an angular, end-on fashion, possibly with multiple bond character in the iron-oxygen bond.

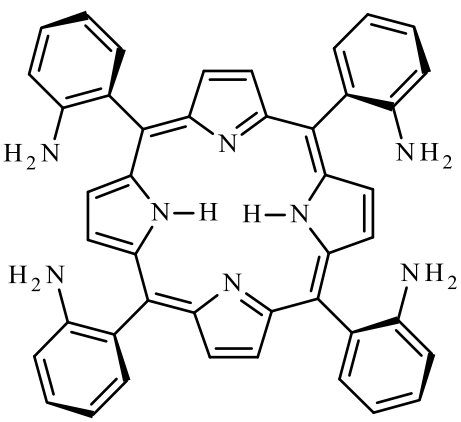

α,α,β,β-atropisomer

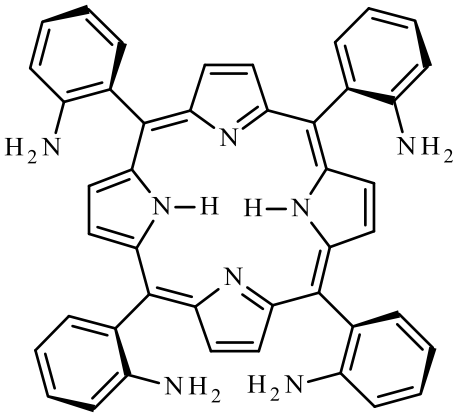

α,β,α,β-atropisomer

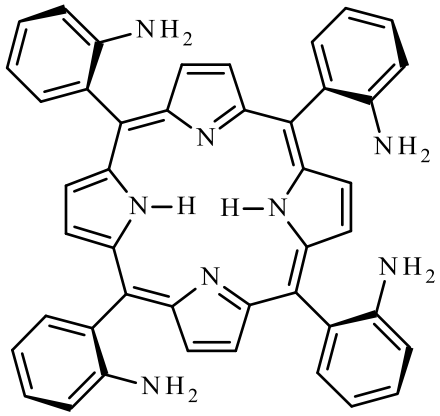

α,α,α,α–atropisomer

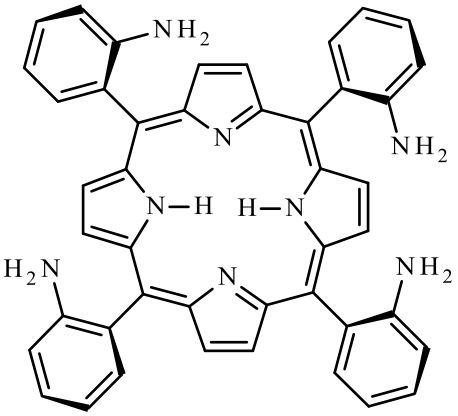

α,α,α,β–atropisomer

Figure 10. Atropisomers derived from *meso*-tetrakis(*o*-aminophenyl)porphyrin.

1.2.1.5. Pyrrole-Carbinols

One of the key steps in the porphyrin synthesis is thought to be the production of pyrrole-carbinols (figure 11). Pyrrole-carbinols undergo self-condensation forming the porphyrin upon reaction under a variety of conditions. However the most common is to treat the pyrrole-carbinols in hot propionic acid under conditions identical to that used in the Alder

method. This produces yields similar to that obtained by condensation of pyrrole with an aldehyde.

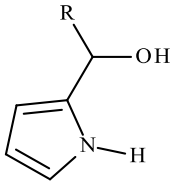

Figure 11. Structure of a Pyrrole-Carbinol

Volz[19] developed a method for using pyrrole-carbinols to synthesise porphyrins. This was done by reaction of pyrrole-carbinols in propionic acid and pyrrole to produce porphyrins with both alkyl and aryl meso substituents with yields of 10 %.

1.2.1.6. Lindsey method

Lindsey and co-workers noticed that since both pyrrole and aldehydes are quite reactive there should not be the need for the high reaction temperatures seen in the Alder-Longo method. Also porphyrins in nature are built using sequential steps of condensation and oxidation.[11] This prompted Lindsey to develop a new method over seven years. He found that if pyrrole is reacted with benzaldehyde in dichloromethane at room temperature and then treated with trifluoroacetic acid for about 60 minutes, followed by the addition of stoichiometric amount of an oxidising agent such as DDQ, yields of 35-40 % could be gained (Scheme 3).

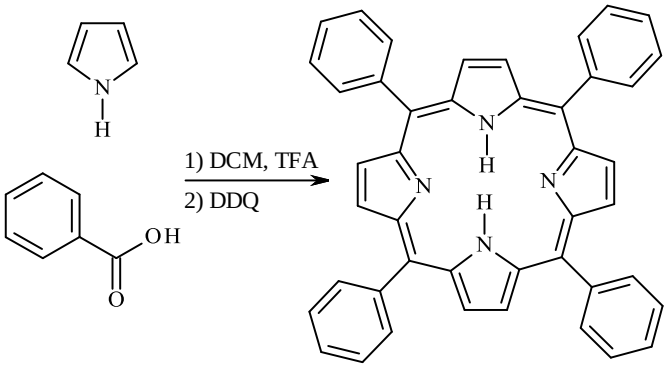

Scheme 3. Lindsey method for synthesis of porphyrins.

This two-step one flask method soon became known as the Lindsey method.[20,21] The reaction was found to be sensitive to the concentration of reactants, the optimum being 10 mM and sensitive to the concentration of the acid catalyst i.e. optimum for BF_3-etherate being 1 mM and trifluoroacetic acid being 20-50 mM.[21] With just a little refinement of the concentrations of the reagents and a slight adaption of the acids, the Lindsey method can be used to create a large number of different *meso*-substituted porphyrins in relatively high yields.[22,23] Since the Lindsey method was established, a few changes have been found to improve the yield of some of the porphyrins, for example by adding salts such as NaCl or Bu_4N + Ph_4B- the yields of such porphyrins as tetraphenylporphyrin can be doubled.[24] One of the main problems with the Lindsey method is that it cannot be used with polar aldehydes that are not soluble in chlorinated solvents.

1.2.1.7. Conclusions

In conclusion there are three main methods to making *meso*-substituted porphyrins, the Rothemund method, the Alder method and the Lindsey method. The Rothemund method does not seem to have any advantages over the other two methods so the choice of method is usually between the Alder and Lindsey methods. The Alder method is generally better for synthesising porphyrins from aldehydes that are relatively stable, it is not so good with porphyrins that are created from aldehydes that cannot survive refluxing propionic acid, or that have 2,6-diaryl substituents, aliphatic aldehydes and aldehydes that produce porphyrins that do not crystallise from propionic acid. The major benefit to this method is that the porphyrin crystallises from the slowly cooling propionic acid. The Lindsey method has the mildest reaction conditions and generally has higher yields than the other methods. It is particularly good for preparing porphyrins from aldehydes that have 2,6-diarylsubstituents, aliphatic aldehydes and expensive aldehydes. One drawback to this method is that the purification usually involves chromatography. If this causes a problem it may be better to use the Alder method.

1.2.2. Synthesis of porphyrins bearing up to four different *meso* substituents.

All of the above methods were developed for tetra meso-substituted porphyrins where all of the substituents are the same. However the synthesis becomes much more difficult when there is a range of substituents around the porphyrin. There are seven types of meso-substituted porphyrin (Figure 12). The methods for synthesising porphyrins with these substitution patterns vary for each porphyrin and in general become more elaborate as the number of different substituents increases.[25]

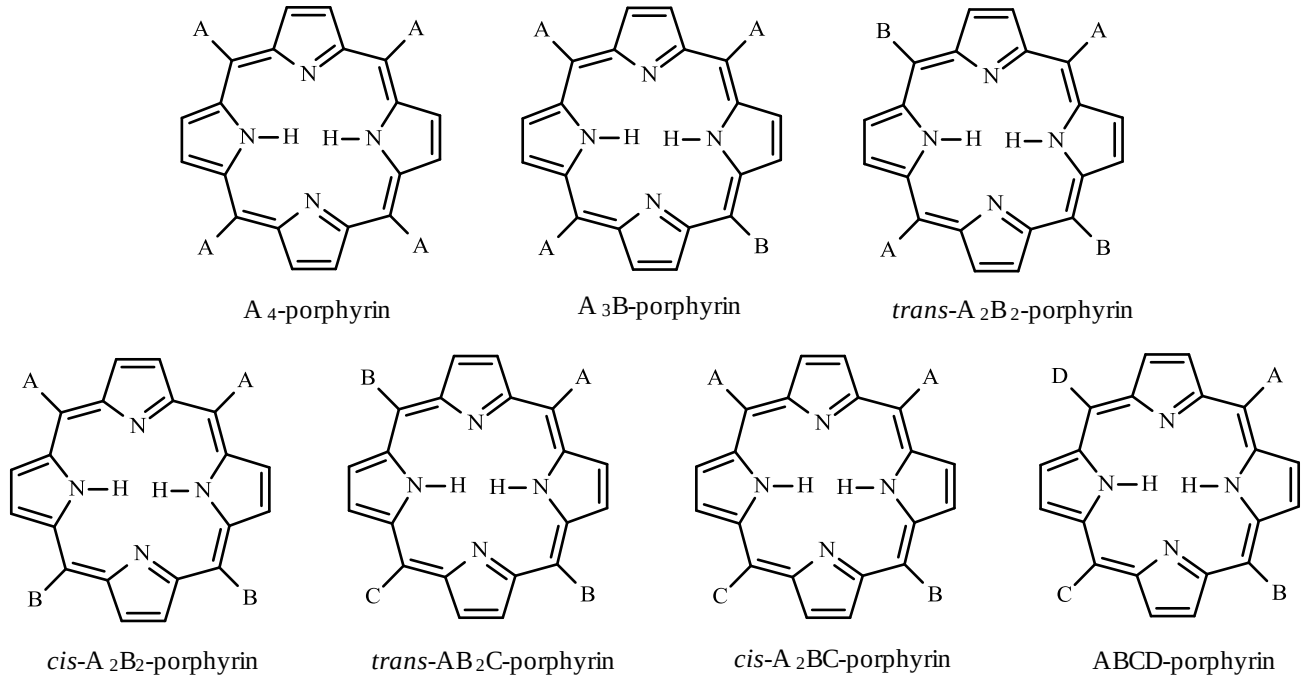

Figure 12. meso-substitution patterns for porphyrins.

1.2.2.1. A_4-porphyrins

A_4-porphyrins are prepared using one of the methods described above. The method used is dependent on the substituents that are to be placed on the meso position of the porphyrin.

1.2.2.2. A_3B-porphyrins

A_3B-porphyrins however have a much more complicated synthesis. The usual method used is the Alder method i.e. reacting pyrrole with two different aldehydes in a 3:1 ratio. However the reaction conditions are very harsh and the reaction results in the formation of a statistical mixture of all six substituted porphyrins (Scheme 4). This must then be separated by column chromatography resulting in very low yields.[26] Therefore a more stepwise synthesis maybe required.

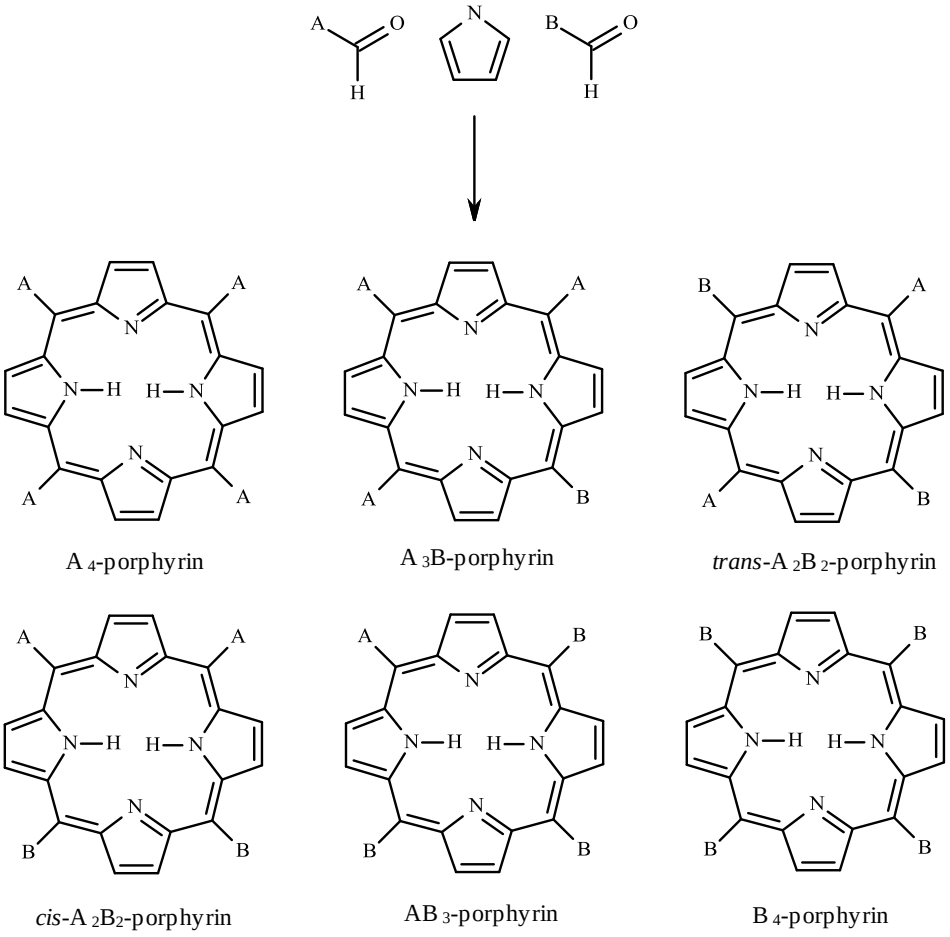

Scheme 4. Porphyrins formed from a mixed-aldehyde condensation.

Dipyrromethanes and dipyrromethane-dicarbinols are important precursors for the synthesis of porphyrins in a stepwise manner. Dipyrromethanes are prepared by a one-flask reaction of an aldehyde with pyrrole (Scheme 5).

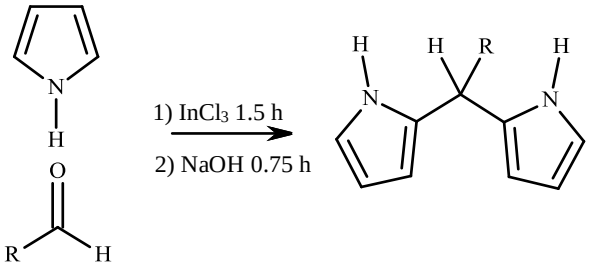

Scheme 5. Synthesis of dipyrromethane.

These dipyrromethanes can then undergo sequential acylation to form diacyl dipyrromethane. This is done by first treating the dipyrromethane with EtMgBr followed by an *S*-2-pyridyl-substituted benzothioate to produce 1-acyldipyrromethane. This is then reacted with more EtMgBr followed by an acid chloride to produce the diacyl dipyrromethane (Scheme 6).

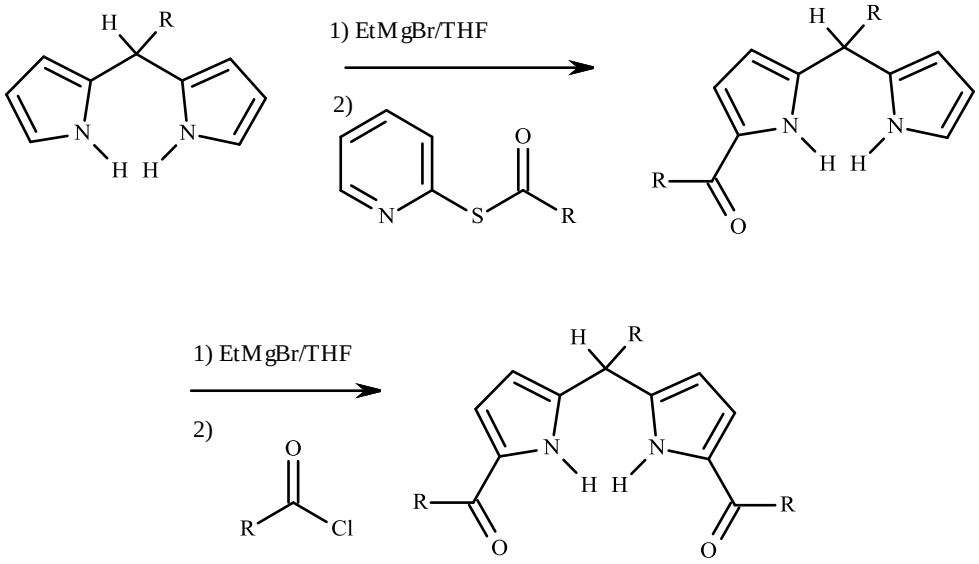

Scheme 6. Synthesis of diacyl dipyrromethane.

The reduction of diacyl dipyrromethane to dipyrromethane-dicarbinol can be achieved with excess $NaBH_4$ in THF/methanol (Scheme 7).

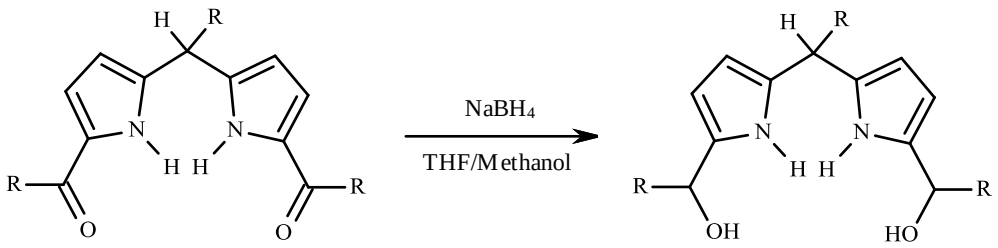

Scheme 7. Reduction of diacyl dipyrromethane.

Using these two precursors A_3B-porphyrins can be prepared in two different ways, either by an A_3-dipyromethane-dicarbinol + B-dipyrromethane, or an ABA-dipyrromethane-dicarbinol + A-dipyrromethane (Scheme 8).[27]

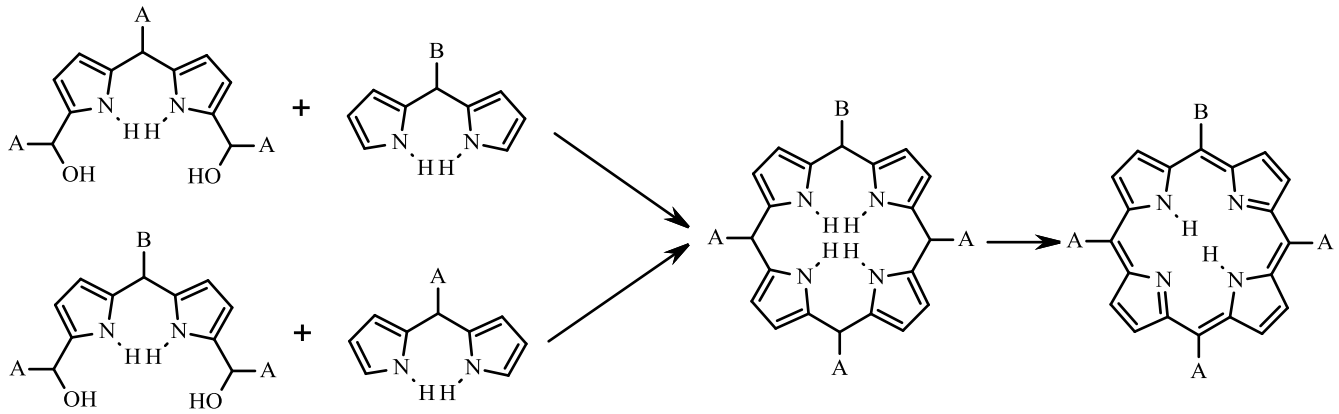

Scheme 8. Synthesis of A_3B-porphyrins.

1.2.2.3. *Trans*-A_2B_2-Porphyrins

Trans-A_2B_2-porphyrins are typically prepared in a slightly different manner, usually by reaction of an aldehyde and a dipyrromethane. Although the methods described earlier can still be used i.e. reaction of pyrrole with two aldehydes, the products from this reaction usually involve difficult separations and therefore may not be practical. There has been a lot of research into the preparation of *trans*-A_2B_2-porphyrins as they provide a linear substitution pattern that may be used for the construction of porphyrin-based architectures with a well defined structure i.e. porphyrin wires. The most common method used for creating these *trans*-porphyrins is via the Macdonald-type 2 + 2 condensation[28] as illustrated in Scheme 9.

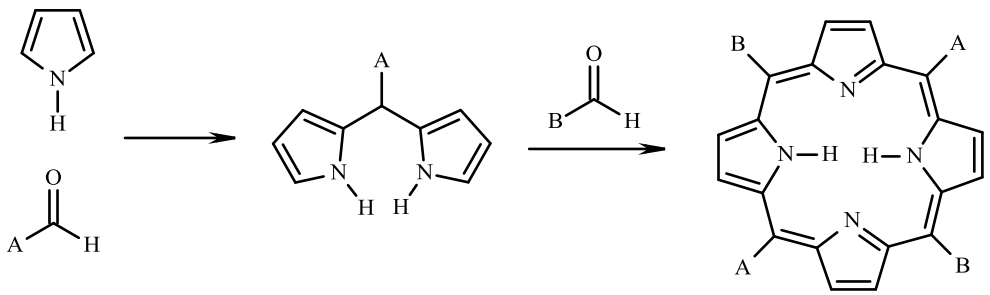

Scheme 9**.** MacDonald 2 + 2 condensation.

However this reaction has its downfalls. The condensation must be performed in dilute conditions, the yields are modest (10-30 %) and any acid catalysed reaction involving polypyrromethanes results in scrambling (Scheme 10). This produces a mixture of porphyrins which may be very hard to separate (especially the *trans*-A_2B_2 and *cis*-A_2B_2 isomers).[29] This scrambling of the *meso*-substituents is thought to occur by the acid catalysed fragmentation of a polypyrrane as illustrated in Scheme 10. The polypyrrane fragments into pyrrolic and azafulvene recombination of these units results in a mixture of porphyrin isomers.[30]

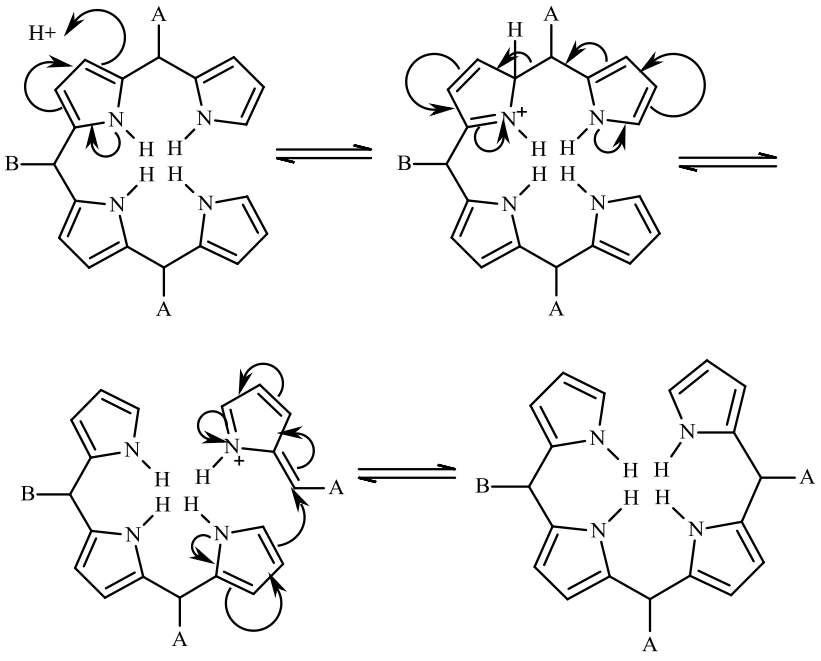

Scheme 10. Acid catalysed scrambling.

Lindsey *et al*[29] identified reaction conditions involving sterically hindered dipyrromethane that resulted in no scrambling (10 nM in CH_2Cl_2 containing 17.8 nM TFA for 1 h followed by DDQ oxidation).[10] However they were not able to produce high yields of *trans*-porphyrins with unhindered substituents via the MacDonald 2 + 2 method. An alternative method to *trans*-A_2B_2-porphyrins is the self-condensation of a dipyrromethane-carbinol (Scheme 11). Here the monoacyl dipyrromethane is prepared in the same manner as mentioned previously. However the second acylation is not necessary. Reduction of the monoacyl dipyrromethane to dipyrromethane-carbinol followed by self condensation gives the desired *trans*-A_2B_2-porphyrin without scrambling.[31]

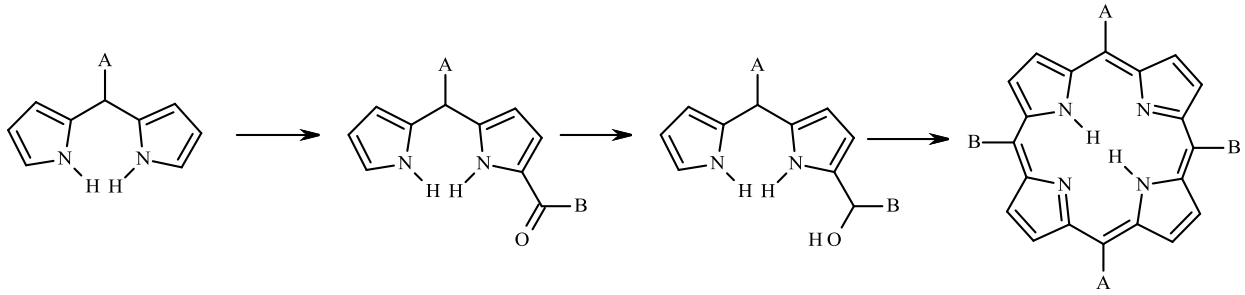

Scheme 11. Synthesis of monoacyl dipyrromethane, and route to trans-A_2B_2-porphyrins.

1.2.2.4. *Cis*-A_2B_2-Porphyrins

Cis-A_2B_2-porphyrins can be synthesised by reaction of a pyrrole and two aldehydes followed by separation of the products as described earlier. An alternative route is the reaction of A_2B-dipyrromethane-dicarbinol with B-dipyrromethane (Scheme 12) as described earlier.

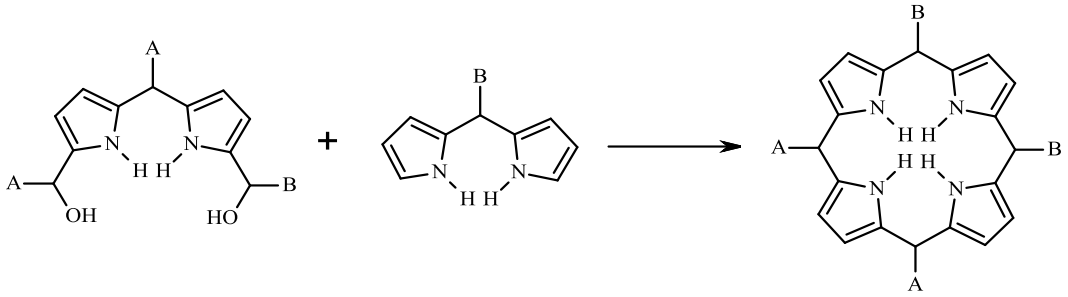

Scheme 12. Reaction of A_2B-dipyrromethane-dicarbinol with B-dipyrromethane.

1.2.2.5. More complicated substitution patterns

Trans-AB_2C-porphyrins could be created using any of the previous methods mentioned, however, with the more complicated substitution pattern the yields are very low. One alternative route to *trans*-AB_2C-porphyrins involves treating a 5,15-disubstituted porphyrin with an organolithium reagent, quenching with water and then treating with an alkyl iodide followed by oxidation (Scheme 13, route 1).[32] Or on similar lines, a 5,15-disubstituted porphyrin can be selectively brominated on the 10 and/or 20 position, which would produce a suitable precursor for the synthesis of more complicated porphyrin systems (Scheme 13, route 2).[33] The 5,15-disubstituted porphyrin is an A_2-porphyrin with both the B positions being H and usually prepared from reaction of dipyrromethane and formaldehyde.

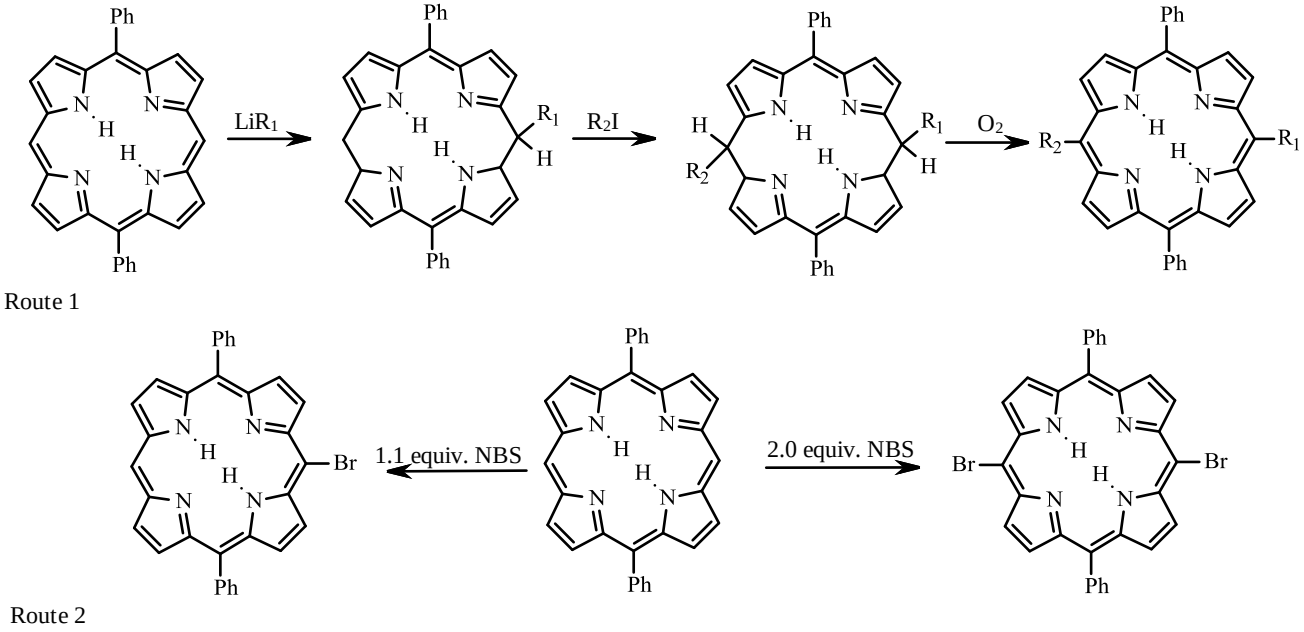

Scheme 13. Alternative synthetic routes to *trans*-AB_2C-porphyrins.

The synthesis of a *cis*-A_2BC-porphyrin requires an unsymmetrical diacyl dipyrromethane. One route involves the reaction of an ABC-dipyrromethane-dicarbinol with an A-dipyrromethane (Scheme 14, route A). While an alternative approach reacts AAB-dipyrromethane-dicarbinol with C-dipyrromethane (Scheme 14, route B).[10]

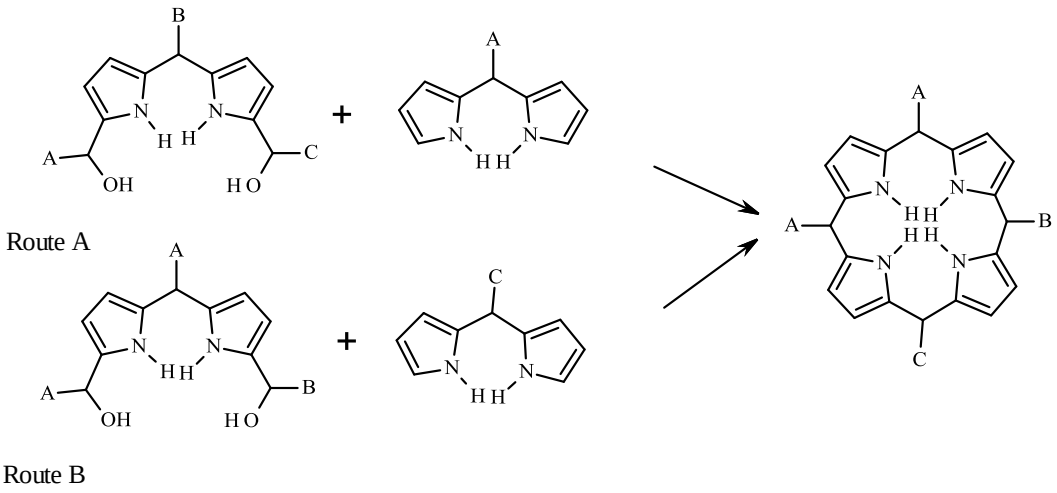

Scheme 14. Routes to cis-A_2BC-porphyrins.

ABCD-substituted porphyrins are the most complex of all as the number of isomers is very large. They have been prepared stepwise by sequential introduction of acyl groups onto a dipyrromethane, followed by reduction to the dipyrromethane-dicarbinol and then condensation with another dipyrromethane.[25] However only low yields (<10 %) are afforded from this reaction. A better method to the synthesis of ABCD-porphyrins is via the bilane route. The new strategy relies on producing two halves of the porphyrin then reacting them together. The CD half is a 1-acyldipyrromethane and the AB half is 9-protected dipyrromethane-1-carbinol derived from a 9-protected 1-acyldipyromethane. These are reacted together by means of a condensation reaction to produce a 1-protected 19-acylbilane. This can then undergo a one-flask transformation to give the ABCD-metalloporphyrin (Scheme 15).[34] [10] Some ABCD-porphyrins can reach up to 65% yield using this method.

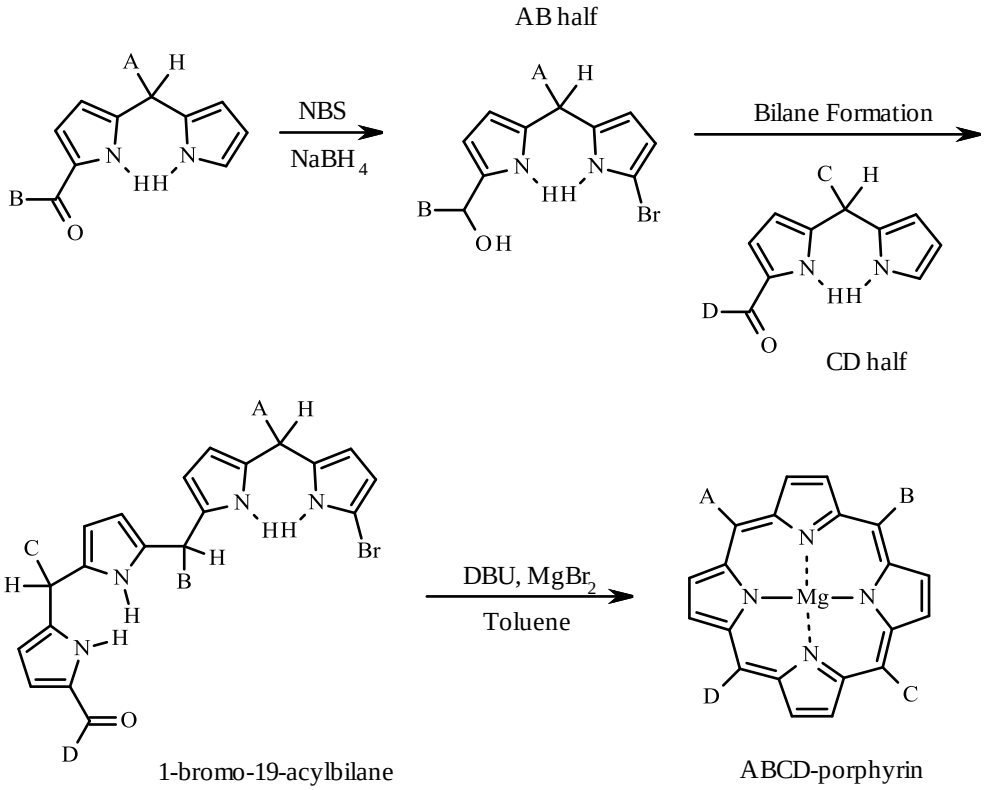

Scheme 15. ABCD-porphyrin via ABCD-Bilanes

In conclusion, porphyrins bearing two different substituents i.e. A_3B, *trans*-A_2B_2 and *cis*-A_2B_2, are usually produced via a statistical condensation of pyrrole with two aldehydes, albeit in small quantities after extensive chromatography. Porphyrins with three or four substituents (*trans*-AB_2C, *cis*-A_2BC or ABCD) require rational synthesis whilst trying to avoid acid catalysed scrambling of the substituents. To achieve this we must use a methodology at the other extreme to the one-flask pyrrole-aldehyde condensations leading to A_4-porphyrins. For example using the methods developed by Lindsey [25] *i.e.* in a step wise manner.

1.3. Porphyrin arrays

1.3.1. Multiporphyrin arrays

Multiporphyrin arrays are important for helping us understand the energy migration process in photosynthetic organisms. However these arrays must have some important attributes that mimic naturally occurring light harvesting synthesis i.e. architectural rigidity, organic solubility and incorporation of numerous porphyrins in controlled metalation states including

metalloporphyrins and free base porphyrins.[35] Lindsey produced just such an array. This was done by preparing a tetraarylporphyrin bearing peripheral iodo groups which was then combined with a free base porphyrin via homogeneous palladium mediated coupling reaction under basic conditions to produce pentameric arrays of porphyrins (figure 13). The fluorescence spectrum of the pentameric porphyrin array shows emission from the core free base porphyrin, whereas the zinc porphyrin emission yield is diminished twelve fold compared with that of a corresponding monomeric zinc porphyrin. This shows that there is an energy transfer from the peripheral zinc porphyrins to the free base core porphyrin with a yield of around 90%.

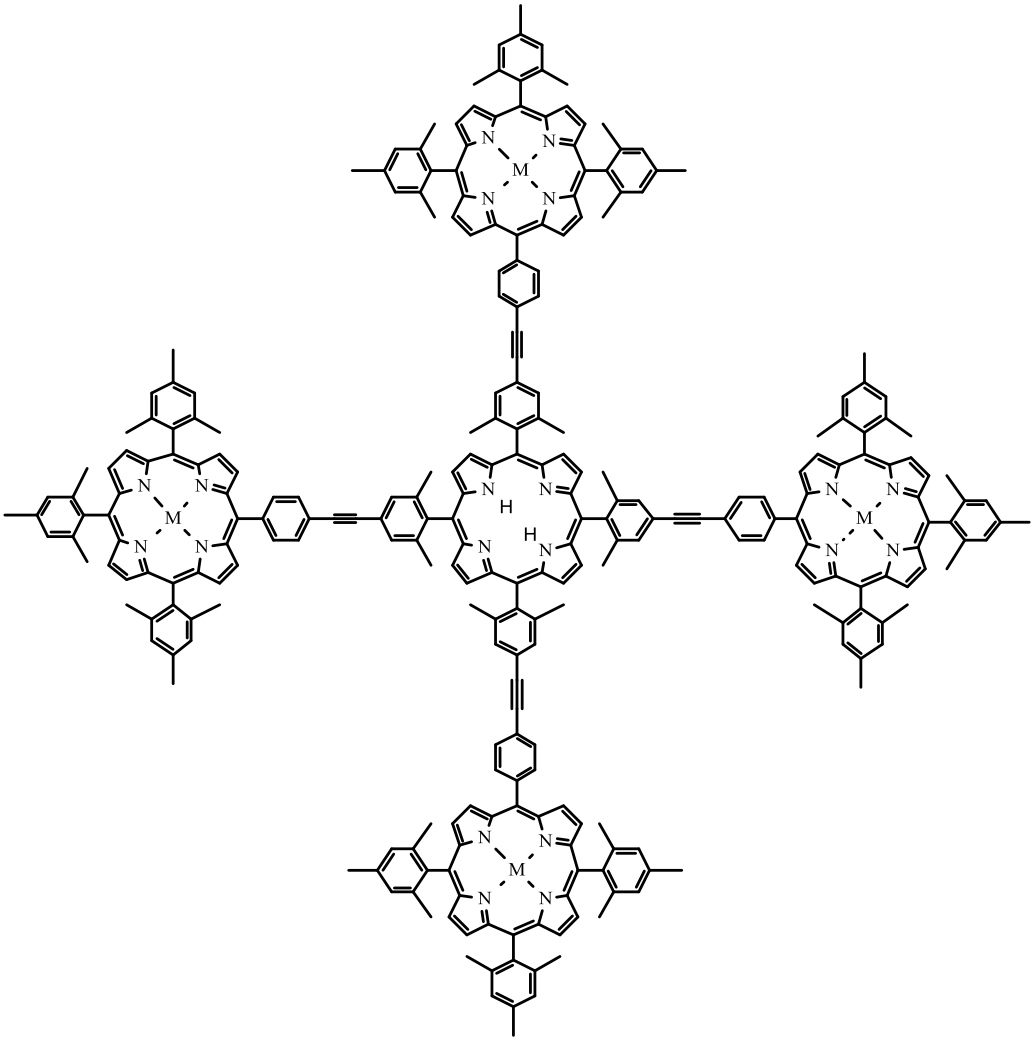

Figure 13. Lindsey's pentameric porphyrin.

Larger arrays of covalently linked porphyrins have also been produced known as multiporphyrin dendrimers,[36] and have attracted increasing attention as artificial light harvesting systems because of their structural analogy to natural antenna complexes. As expected the larger the complex the less efficient the energy transfer. For example a dendrimer with one porphyrin unit has 87 % efficiency where as a dendrimer with seven porphyrin units has 71% efficiency. It was also shown that the four dendritic zinc porphyrin wedges in the large $(7ZnP)_4H_2P$ molecule do not work completely individually but cooperate, thus facilitating energy migration and energy transfer (Figure 14).

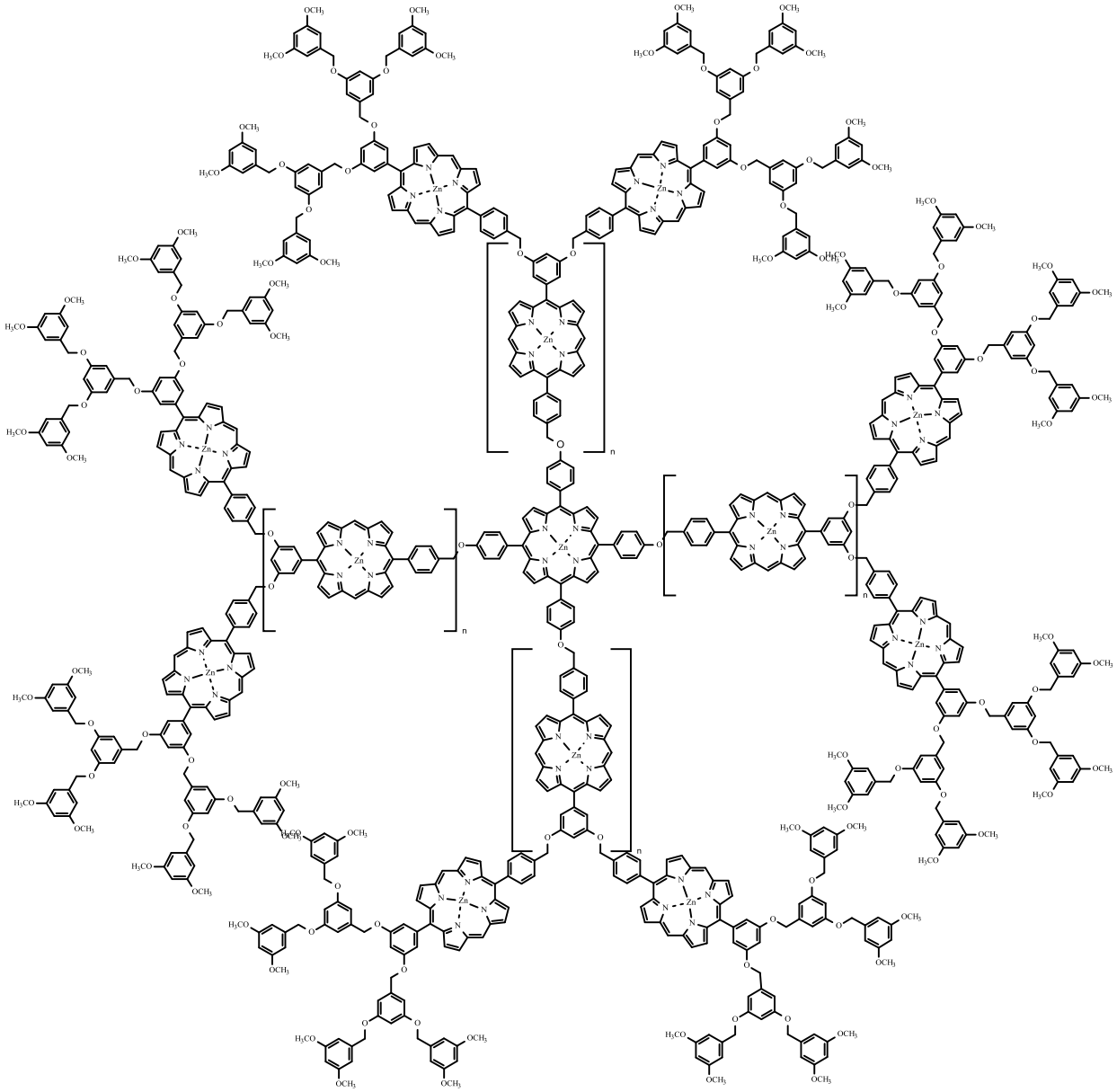

Figure 14. Porphyrin dendrimer.

Cooperativity is seen in the light harvesting process of photosynthesis. The number of porphyrins in the array is not the only thing that can affect energy transfer efficiency. The linking unit between porphyrins plays a major role in the energy transfer process. The rate constant for energy transfer from a zinc metalated porphyrin to a free base porphyrin with a diphenylethyne linker is around 24 ps^{-1}. A simple linker would be a phenyl group (Figure 15). This linker produces a much shorter distance between porphyrins and has a zinc metalated to free base porphyrin energy transfer rate of just 2.8 ps^{-1}. This is much faster than with the diphenylethyne linker. It is suspected this is due to the distance between porphyrins.[37]

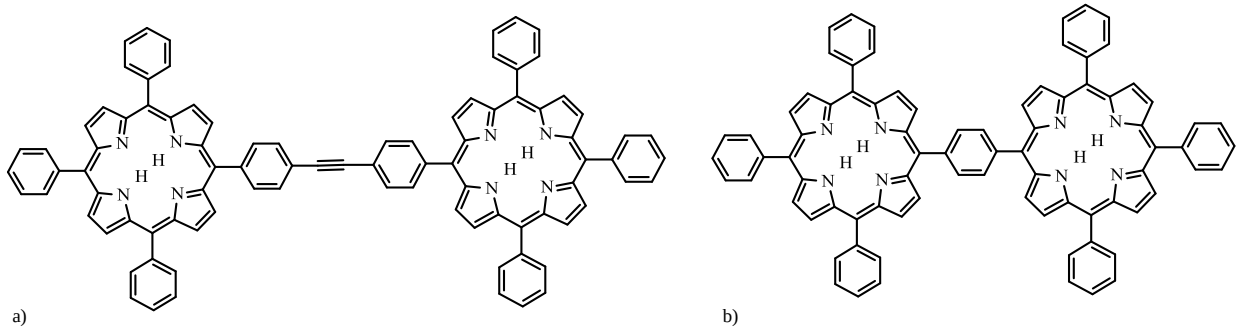

Figure 15. Porphyrins linked by a) a phenylyne linkage and b) a phenyl linker.

1.3.2. Porphyrin and Phthalocyanine hetero arrays.

Porphyrins can also be combined with other macrocycles to form hetero arrays. One such group of macrocycles are phthalocyanines. Phthalocyanines are structurally related to porphyrins and are traditionally used as industrial dyes, they also have technological applications as molecular electronic devices, optical recording materials, catalysts for oxidative degradation of pollutants and photosensitisers for photo dynamic therapy.[38] We know that porphyrins exhibit a Soret band at ca. 410-450 nm together with a number of weaker Q bands at ca 500-600 nm due to their highly conjugated π system. Phthalocyanines also have a highly conjugated π system which has absorptions at ca 320-360 nm and 670-700 nm. So despite their similar structures, redox potentials and photophysical properties their absorptions are very different and can be altered by changing their metal centre and peripheral substituents. A resulting hybrid of the two can be fine tuned to absorb a large part of the solar spectrum and may also interact through photo-induced electron and/or energy transfer pathways. A large number of mixed porphyrin phthalocyanine arrays have been reported and there are many ways to bridge the two chromophores, for example via large

metal centres, bridging ligation, electrostatic interactions and axial coordination. However a large area of current research is in covalently linked tetrapyrrole systems. The first covalently linked porphyrin and phthalocyanine was reported by Maillard in 1986.[39] This was done by reacting hydroxyphenylporphyrin with 4-nitrophthalonitrile to obtain porphyrin substituted phthalonitrile which is then condensed with excess 4-*tert*-butylphthalonitrile to produce the product (Scheme 16).

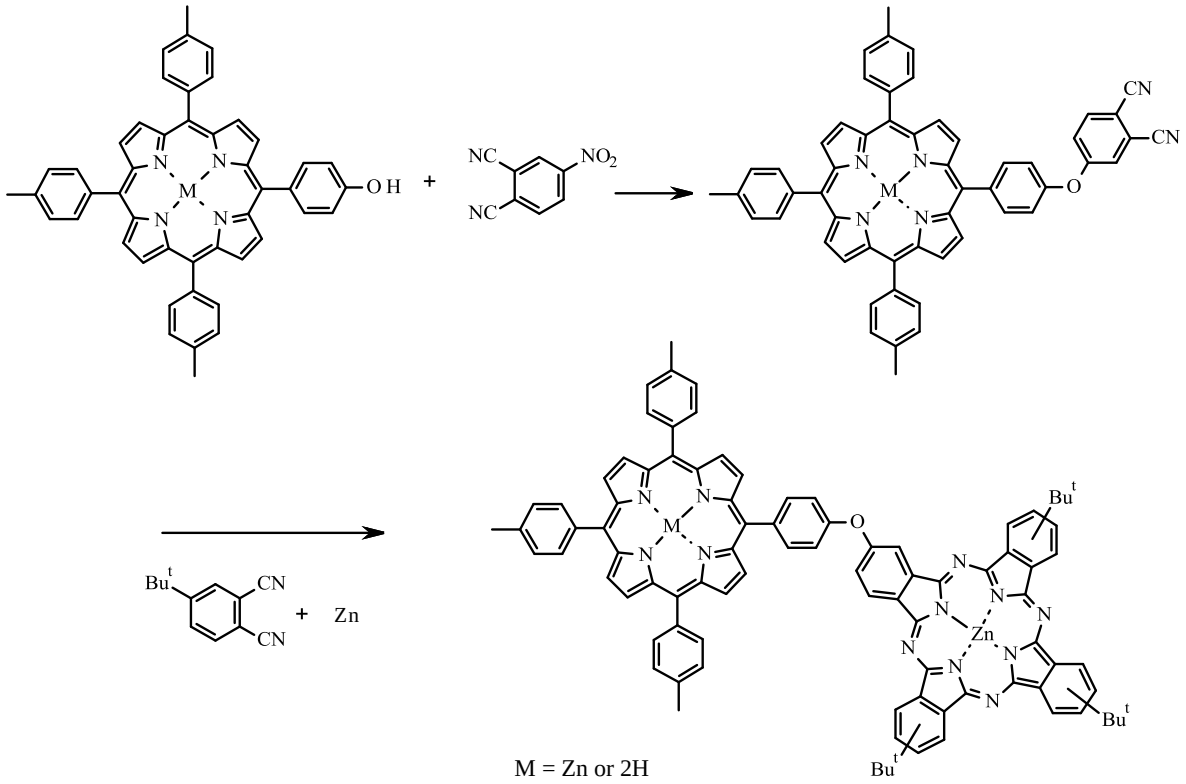

Scheme 16. Mixed Porphyrin-Phthalocyanine dyad.

There is no significant ground-state interaction between the two chromophores. However upon selective excitation of the porphyrin chromophore at 424 nm in toluene the dyad shows a strong emission due to the phthalocyanine moiety (at 690 nm).[40] This indicates the occurrence of an efficient energy transfer from the porphyrin to the phthalocyanine. The efficiency of the energy transfer is very good as the excitation spectrum and the ground state absorption spectrum are virtually identical. This energy transfer occurs via both a singlet-singlet and a triplet-triplet process, once the energy has been transferred the phthalocyanine moiety returns to its ground state via normal routes. If the solvent is changed from toluene to a polar solvent such as dimethyl sulfoxide the efficiency of the energy transfer is decreased

where as an electron transfer becomes the predominant process. This can be explained by the stabilisation of the charge separated species by the solvent and the conformational change of the dyad due to the nature of the solvent interactions. A series of porphyrin and phthalocyanine dyads linked by a flexible alkyl chain were also prepared by standard O-alkylation[41]. However due to the greater conformational flexibility and greater distance between the chromophores the energy transfer is less likely. As with the previous dyads there is a competing electron transfer process that is made more efficient with increasing polarity of the solvent.

Xu and co-workers reported a porphyrin-phthalocyanine dyad which has a very efficient electron transfer in DMF.[42] This dyad has a piperazine spacer and the synthesis is shown in Scheme 17. The rational for its increased efficiency in electron transfer is that the piperazine adopts a boat configuration instead of a chair configuration which would bring the two chromophores in close proximity facilitating the electron transfer process.

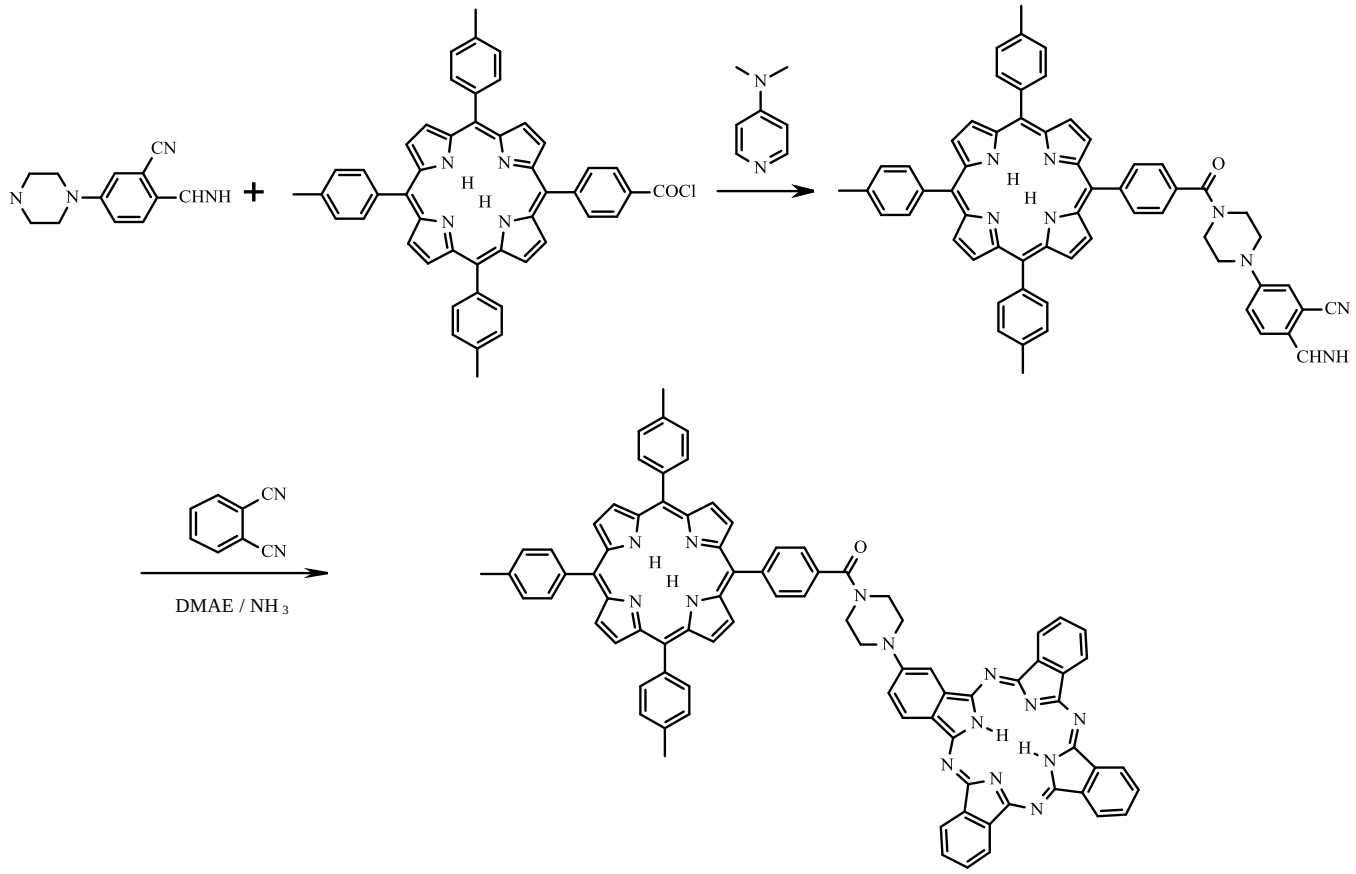

Scheme 17. Preparation of piperazine-bridged porphyrin-phthalocyanine dyad.

As a contrast Lindsey and co-workers produced a porphyrin phthalocyanine dyad with a phenylethynyl linker that has a very fast highly efficient energy transfer (Figure 16).[43] The singlet-singlet energy transfer from the phthalocyanine moiety is around 10 ps^{-1} with an efficiency of 90 %.

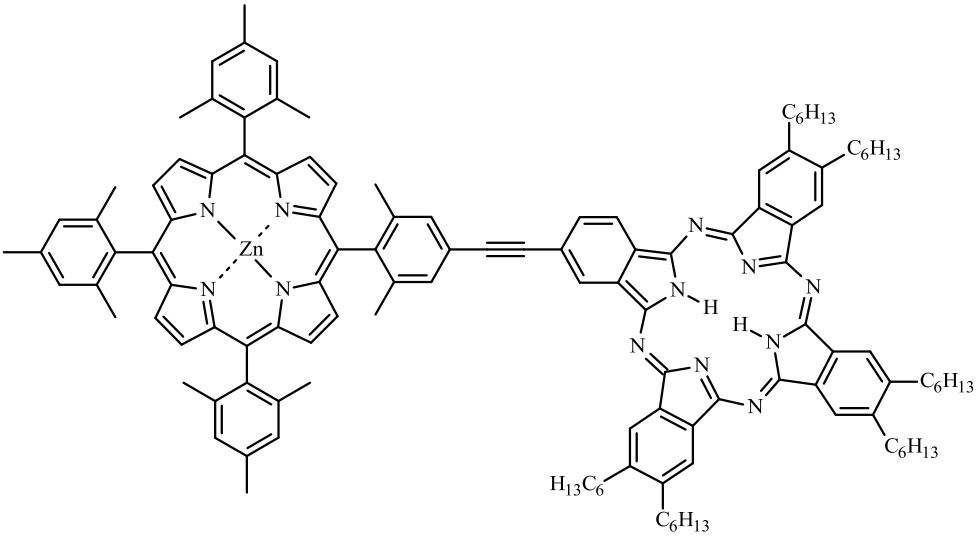

Figure 16. Phenylethynyl-linked porphyrin-phthalocyanine dyad.

All dyads mentioned so far have a linking unit, however the porphyrin and phthalocyanine can be linked directly.[44] This gives a shorter edge to edge distance between the macrocycles leading to strong excitonic coupling and very efficient energy transfer. Figure 17 shows a dyad linked at the meso position of the porphyrin and the beta position of the phthalocyanine.

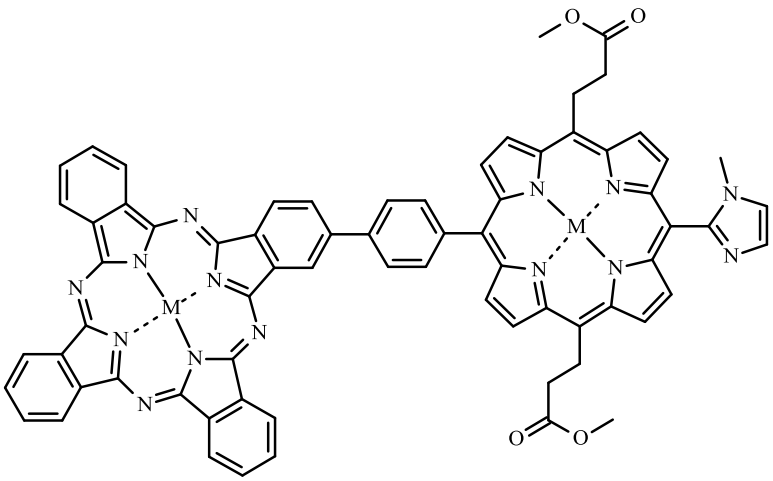

Figure 17. Directly linked porphyrin-phthalocyanine dyad

Porphyrin and phthalocyanine hetero arrays can also contain more than two units e.g. triads. Lindsey and co workers produced a linear array of chromophores consisting of a perylene input unit, a bis porphyrin transmission unit and a phthalocyanine output unit (figure 18).[45] This array absorbs strongly across much of the visible region. Analysis shows there to be an extremely fast and efficient funnelling of energy from the perylene through bis(porphyrin) to the phthalocyanine unit. This compound has two major advantages over other light harvesting/energy funnelling systems. Firstly it has a good coverage across the blue and red region of the spectrum and secondly it exhibits ultrafast and essentially quantitative energy transfer from the perylene to the phthalocyanine.

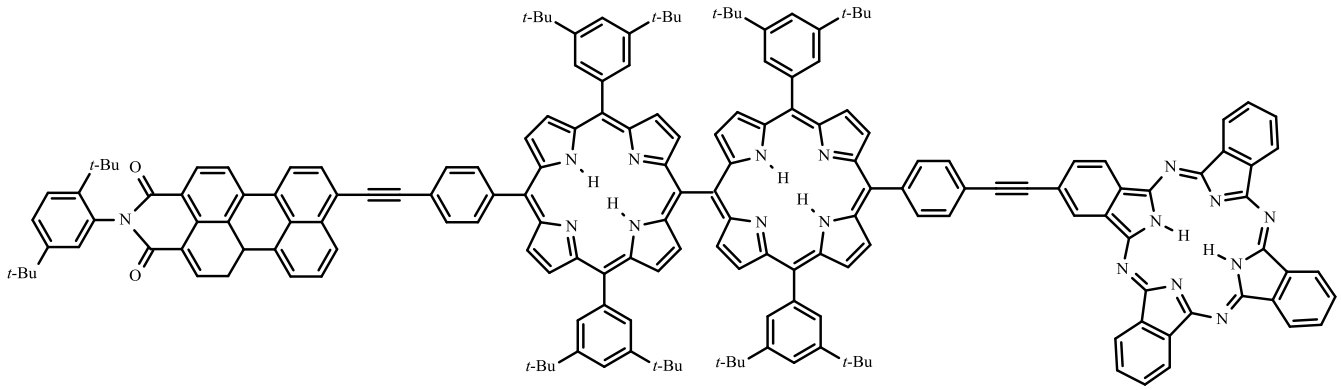

Figure 18. Perylene-substituted porphyrin-phthalocyanine triad.

Porphyrin-phthalocyanine triads can be linked using a simple oxo group (similar to dyads shown previously) (Figure 19). This compound shows similar attributes to the related dyads including the competing process of energy transfer verses electron transfer. However the phthalocyanine-porphyrin conjugate in figure 19 is an effective light harvester. The two porphyrin units are especially efficient at transferring energy to the phthalocyanine upon excitation at their Soret or Q- bands and the zinc-phthalocyanine is a good accepter of this energy.[46]

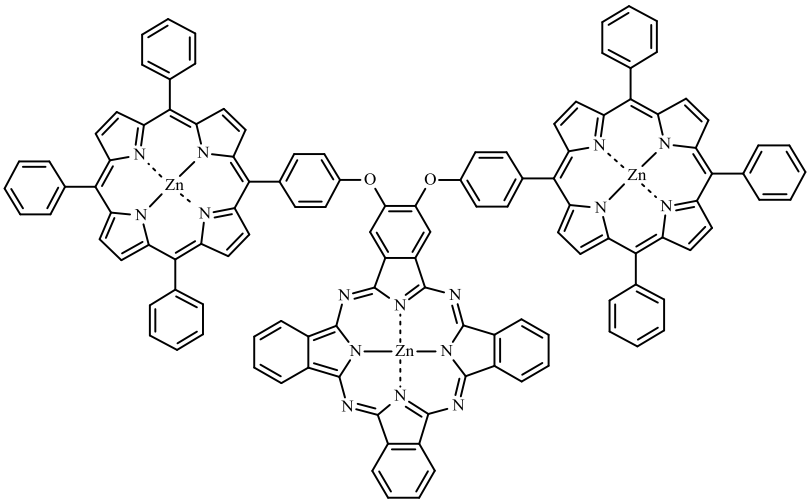

Figure 19. Hetero porphyrin-phthalocyanine triad.

Porphyrin-phthalocyanine pentads were reported by Kobayashi *et al* in 1987.[47,48] 2,3,9,10,16,17,23,24-Octacarboxyphthalocyanine was condensed with 5-(-4-aminophenyl)-10,15,20-triphenylporphyrin to give the tetra-porphyrin substituted phthalocyanine (figure 20).

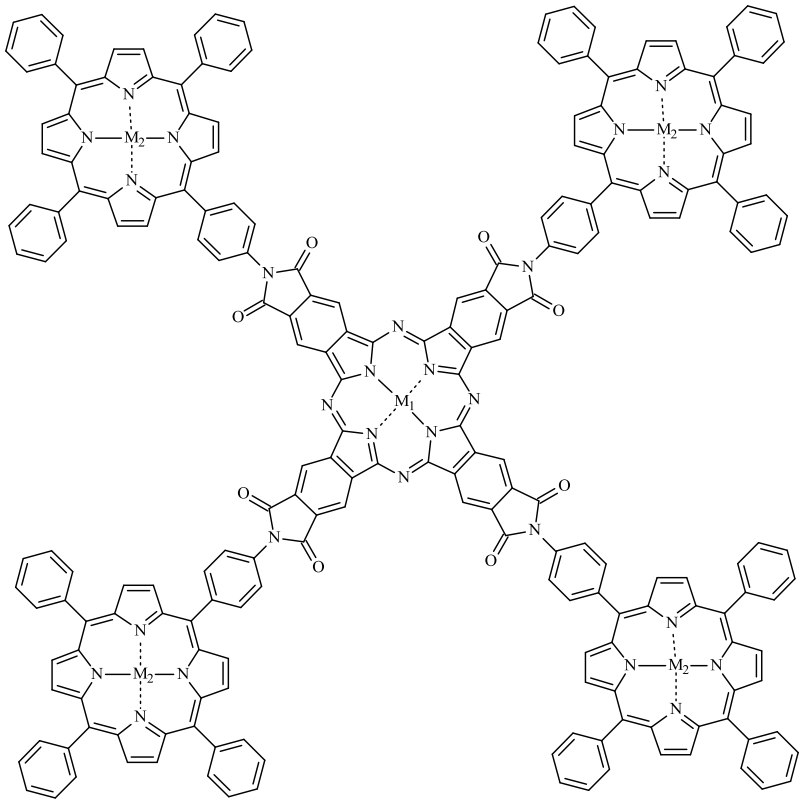

Figure 20. Porphyrin-phthalocyanine pentad.

Lindsey and co workers produced similar pentads in which four porphyrin moieties are covalently linked to a phthalocyanine core through ethynyl linkers (figure 21). These show similar traits to the dyads shown earlier in that they absorb in the blue and red regions and show rapid, efficient energy transfer from the porphyrin moieties to the phthalocyanine core.[49] Nyokong and co-workers produced a similar pentad using the oxo linkage.[50]

When the phthalocyanine core in figure 21 is selectively excited it is quenched by electron transfer. However when the porphyrin is selectively excited it is quenched by a combination of both electron transfer and energy transfer.[38]

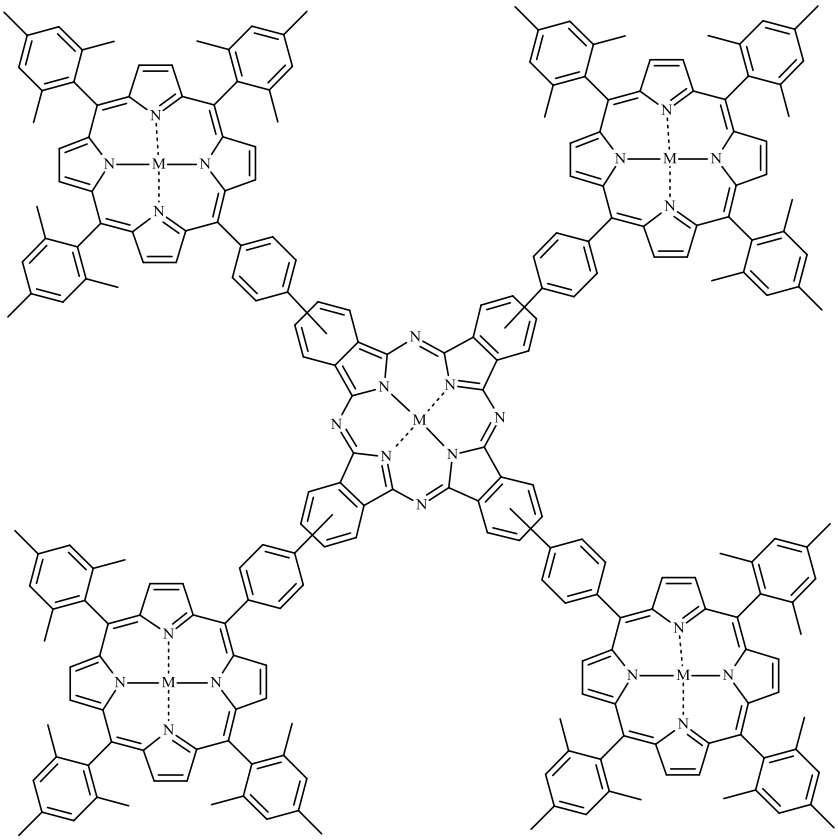

Figure 21. Phthalocyanine porphyrin mixed pentad.

Larger hetero arrays such as hetero-nonamers of porphyrins and phthalocyanines have been prepared.[38] These all show similar properties i.e. a wide absorption spectrum and a singlet excited state energy transfer from porphyrin to the phthalocyanine core.

1.3.3. Molecular wires

Porphyrins have a large number of impressive properties which make them desirable for incorporation into supramolecular systems and polymers such as molecular wires and stacks. The optical electronic and photochemical properties of porphyrins means they are central to the development of the biomimetic chemistry of multichromophoric assemblies in biology as well as sensing, opto-electronic, magnetic, artificial photosynthetic, catalytic and photosensitizing-pharmaceutical materials.[51]

Molecular wires have been created for a variety of applications, such as organic conducting materials and non-linear optical materials.[52] For most molecular wires the conjugation arises through linear π-π overlap, these are becoming more and more attractive as the drive for smaller circuits is increasing.[53] π-Conjugated porphyrins are of interest because they have a small HOMO-LUMO gap,[52] their properties can be altered to specific applications and be modified, non covalently, causing self-organizing electronics. They have high stability which makes them ideal for molecular scale electronics.[54] Not only can the metal centre of the porphyrins be changed to alter the oxidation/reduction properties of the wire[55] and the ligands on the porphyrin be altered to change the stability, solubility and self-assembling properties of the conjugated porphyrin[54] but the bridging molecule can also be altered. Acetylene, thiophene, phenylacetylene and viologen have all been used as porphyrin linkers in polymers.[56] One example of a molecular wire is the polymer shown in figure 22, which consists of zinc porphyrins, joined by butadiyne units at the 5,15-*meso*-positions. It has been shown that this polymer can transfer charge over long distances efficiently but the conjugation of these polymers is limited by the rotation of one porphyrin unit with respect to another, one way around this is to link the wires using a bi-dentate ligand such as 4,4-bipyridyl (Bipy) creating a ladder like conformation and increasing conjugation.[54]

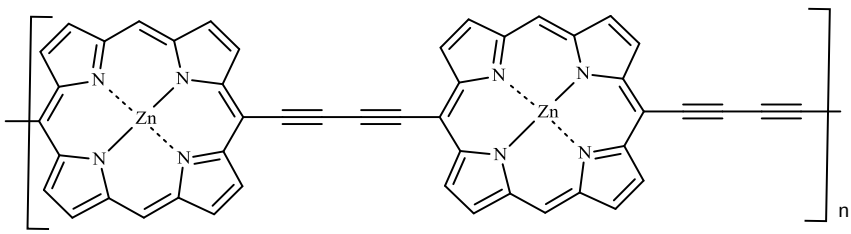

Figure 22. Porphyrin wire linked by a butadiyne bridge.

Another class of porphyrin wires has been prepared from ethyne-elaborated porphyrin precursors through the use of metal-mediated cross-coupling to produce porphyrin wires in which the porphyrin rings are bridged by single ethynyl linkages (Figure 23). It has been shown that this polymer affords exceptional electronic interactions proven by room temperature photophysics, optical spectroscopy and electrochemistry and so models many of the characteristics essential for biological light harvesting antenna systems. The production of such materials has long been of interest as this precedes the development of artificial systems that could convert light into chemical energy. It has been shown that the trimeric porphyrin shown in figure 23 bears many of the spectroscopic similarities to purple bacterial light-harvesting complexes (i.e. the B820 subunit of the core antenna complexes of *Rhodospirillum rubum*, *Rhodobacter capsulatus*, and *Rhodobacter sphaeroides*), as well as to the light harvesting structures in green photosynthetic bacteria.[51]

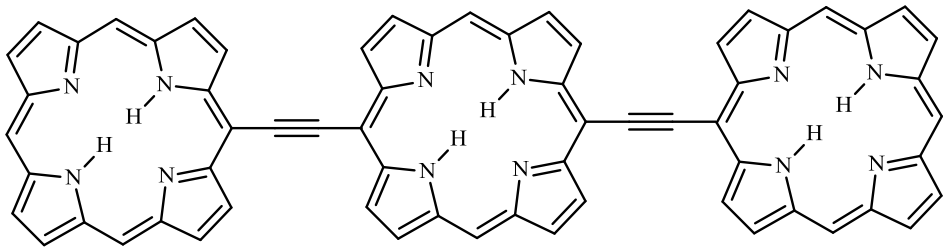

Figure 23. Porphyrin rings bridged by single ethynyl linkages.

Non-linear optical (NLO) materials are of great interest for their photonic applications in ultra fast optical switching and modulations.[55] Thus far, very few materials can combine a suitably large optical nonlinearity with a good enough transparency. Porphyrin wires are ideal NLO materials as they are conjugated, their structure and metal centre can be modified to shift the energies of their electronic transitions and they can survive high heat and intense optical irradiation. The porphyrin wire shown in figure 24 has been shown to have one of the largest nonlinearities studied to date due to the extensive delocalisation of electrons over not only the porphyrin but across the bridging butadiynes.[57] It has been shown that the butadiene linked porphyrin wires exhibit among the largest third-order susceptibilities χ^3 of any organic material.[55] The polymer has not only a large nonlinearity and χ^3 but is also robust, highly processible and easily derivatized putting it in a class of its own.[57]

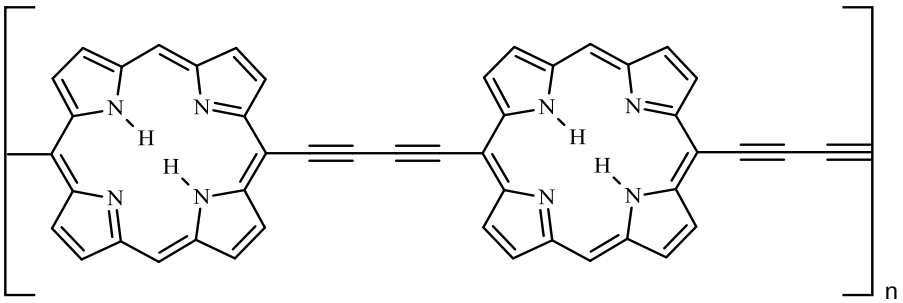

Figure 24. Porphyrins bridged by butadiyne.

1.3.4. Porphyrin stacks

Porphyrins can not only be linked in a horizontal fashion as in porphyrin wires but also in a vertical fashion as in porphyrin stacks. Porphyrin stacks usually consist of a vertically stacked porphyrin and another molecule such as quinone.[58-60] There is much interest in finding synthetic analogs of naturally occurring biological processes, such as photosynthesis. The ability to turn light in to energy efficiently could revolutionise the way we live. Porphyrin stacks show many of the same properties as the complexes found in the photosynthetic reaction centre. For example long-lived charge-separated states and an ever decreasing distance between a cofacial porphyrin pair. This is important as in photosynthetic reaction centres the porphyrin-porphyrin separation distance is around 3Å.[60]

There are a few porphyrin stacks that have been produced that do not have this small porphyrin-porphyrin separation distance but still exhibit interesting properties. Vertically stacked porphyrin-quinone structures are of interest because the porphyrin acts as an electron donor and the quinone as an electron accepter, mimicking the primary process in biological photosynthesis. Porphyrin(1)-porphyrin(2)-quinone cyclophane (figure 25) is ideal for study, as steric and electronic structures can be defined and varied systematically. It was found that the electron transfer occurred approximately a thousand times faster than expected and the conclusion was reached that the photoinduced electron transfer actually occurred between the porphyrin(1) and quinone and was electronically coupled by the central π-electron system of the porphyrin(1). [59]

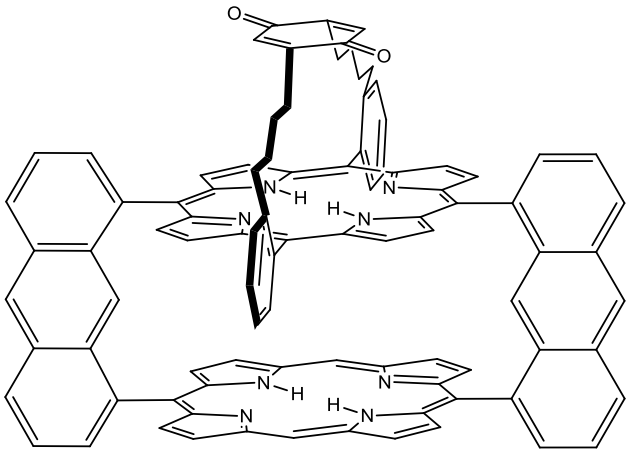

Figure 25. Porphyrin(1)-porphyrin(2)-quinone cyclophane

A porphyrin stack has been synthesised with a porphyrin-porphyrin separation distance of less than 3Å. Rather than consisting of stacked macrocycles tethered together by organic molecules, these stacks consist of bis(porphyrin) metal sandwich complexes (Figure 26).

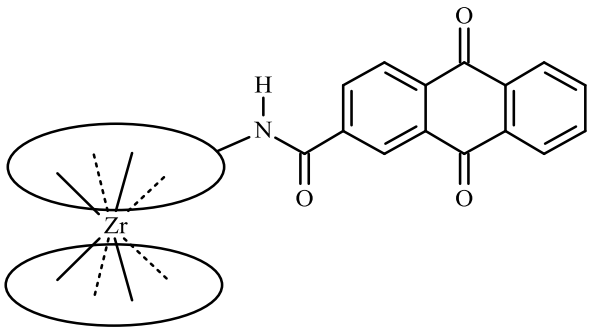

Figure 26. Quinone-derivatized bis(porphyrin) complex [Zr(TTP)(TTP-NHCOAQ)]

These complexes not only have a similar separation distance to chlorophyll but also have similar electronic properties. These properties can be tuned by adding substituents to the porphyrin rings to increase the similarity between the synthetic complexes and the naturally occurring light harvesting complexes such as chlorophyll.[60] The porphyrins in porphyrin stacks need not be directly above one another but may be slightly out of line, in this way they can be held together not by molecules or atoms as previously mentioned but by forces. For example mono(imidazolyl)-substituted cobalt(II) porphyrins can form a dimer, (figure 27) where the imidazolyl group of one porphyrin coordinates to the cobalt ion of the other porphyrin, in a slipped cofacial arrangement. This dimer is of great interest as it not only has

a similar structure and function as the reaction centre of bacterial photosynthesis, but it is also a new artificial haemoglobin model containing two binding sites.

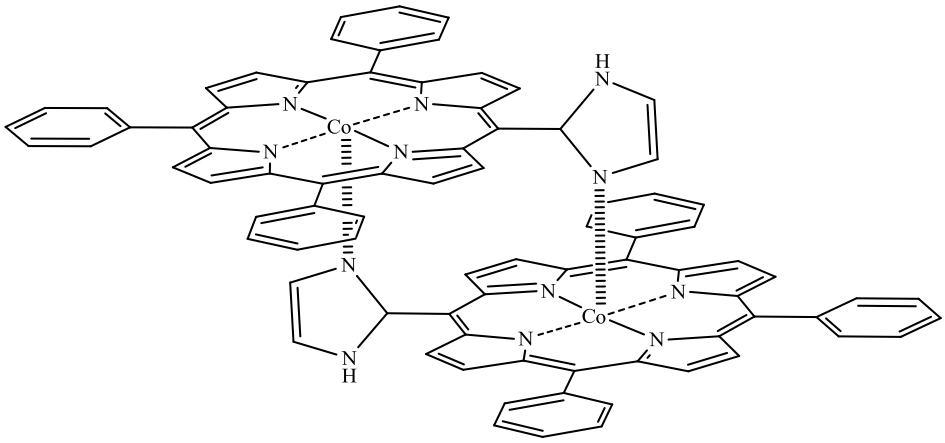

Figure 27. 5-(2-Imidazolyl)-10,15,20-tris(a,a,a-o-pivalamidophenyl)porphyrinatocobalt(II) dimer

The dimer creates a picket fence formation (a porphyrin with a protective enclosure for binding oxygen at one side of the ring that is used to mimic the dioxygen-carrying properties of the heme group) and reversibly binds dioxygen by stabilizing the adduct through hydrogen bonding in the picket fence cavity. Although some similar dimers have been previously prepared, they have needed additions of excess bidentate bases as axial ligands; this can cause oxidation of the Co(II) porphyrin.[61]

1.3.5. Porphyrin cyclic arrays

Photosynthesis has driven researchers to find ways to mimic the fundamental structures of light harvesting antenna within Nature. Light harvesting systems in purple bacteria have been characterised at atomic resolution and are known to have highly ordered cyclic architectures of bacterial chlorophylls. These cyclic structures enable the chlorophylls to pack densely into two-dimensional organizations.[62,63] This has inspired much research into cyclic porphyrin arrays. Kim and co-workers [64] have created a variety of covalent and non-covalently assembled cyclic porphyrin arrays as biomimetic models of light harvesting antenna. The key to producing these systems is the Ag(I)-promoted coupling reaction of 5,15-diarylzinc(II) porphyrin that provides a meso-meso-linked diporphyrin regioselectively (figure 28).[65]

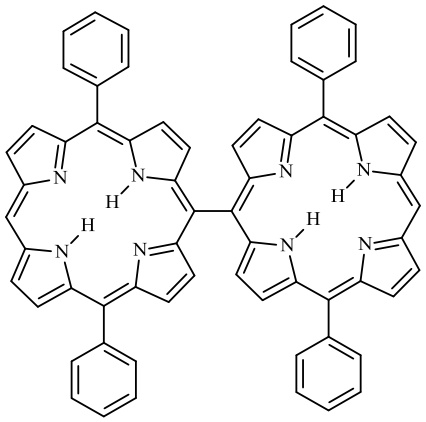

Figure 28. Meso-meso-linked diporphyrin

Meso-meso directly linked porphyrins have rapid energy and electron transfer rates due to a short centre-to-centre distance and a large excitonic interaction.[65] These meso linked porphyrins can undergo intramolecular coupling reactions to form cyclic tetramers, hexamers and octamers. All of these structures exhibit efficient excitation energy transfers which rival those in natural cyclic antenna systems.[65] Kim and co-workers also produced larger cyclic systems by reacting the meso-meso linked porphyrin dimmers and tetramers with a phenylene bridge via a Suzuki reaction (figure 29). [66-68]

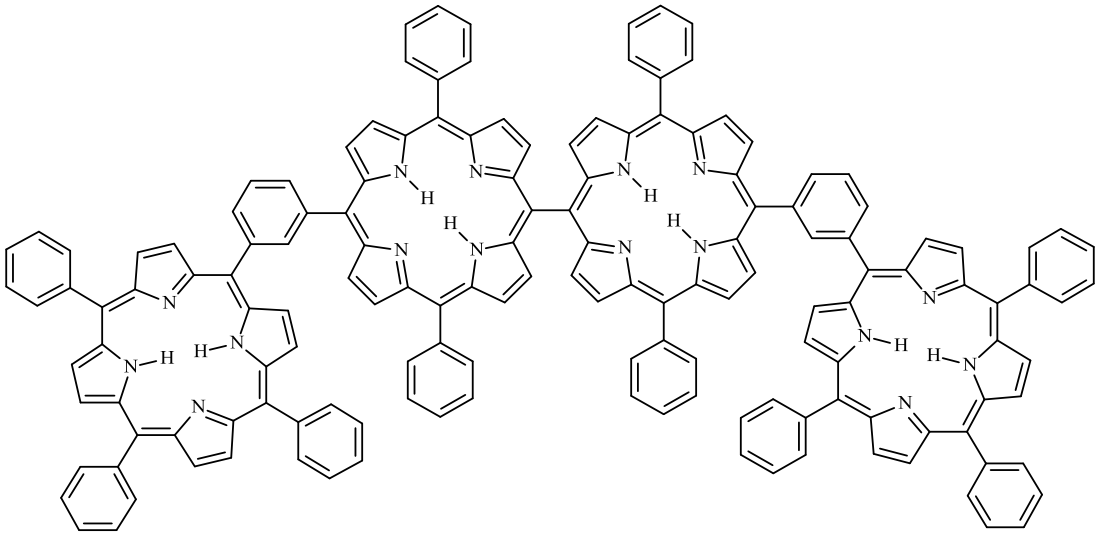

Figure 29. Tetramer with a phenylene bridge

An alternative route to creating cyclic porphyrins is via self sorting non-covalent interactions. This assembling process is especially effective for the construction of discrete cyclic arrays due to the associated entropic advantage.[64] These porphyrins self assemble due to a coordinating side arm and a metal centre. Kim and co-workers created a porphyrin cyclic array consisting of four porphyrin units (figure 30).[69,70] However only the directly linked meso-meso linked cyclic porphyrin structures had the excited energy transfer that rivalled those found in nature.

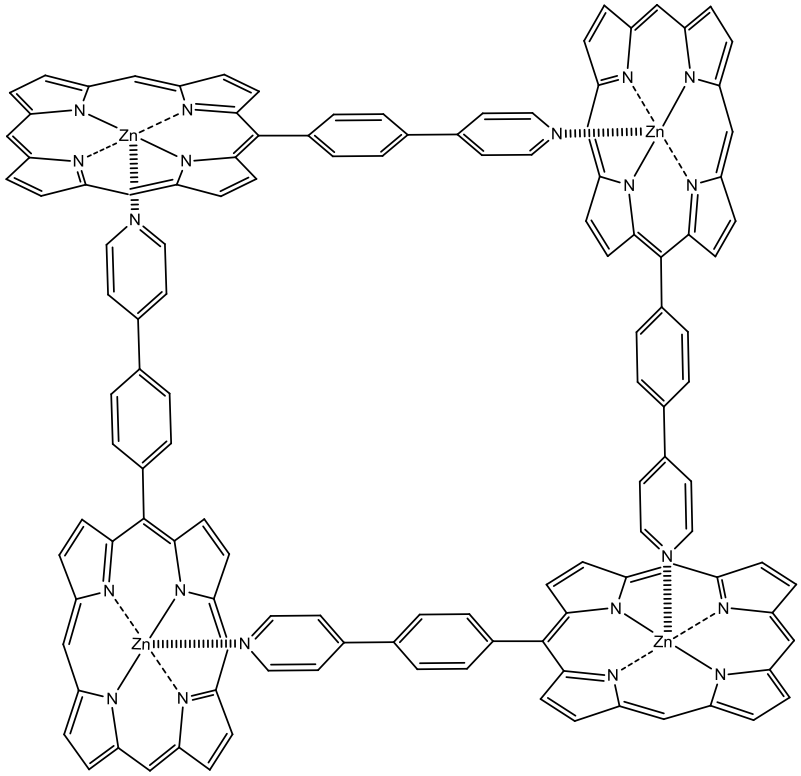

Figure 30. Porphyrin cyclic array

Another group of cyclic porphyrin antenna structures that act as light harvesting arrays are those where a number of porphyrins are attached to a central energy/electron acceptor via a linker. One such compound is 1,7,N,N'-tetrakis(zinc porphyrin)-perylene-3,4:9,10-bis(dicarboximide) synthesised by Wasielewski and co-workers (Figure 31).[71] The perylene-3,4:9,10-bis(dicarboximide) (PDI) core is a chromophore which has four distinct sites on which to attach electron donating porphyrin chromophores. The porphyrins and the core have complementary electronic spectra which results in absorption of most of the solar spectrum between 400 and 650 nm. This molecule shows rapid and efficient photo induced electron transfer from the porphyrins to the PDI core.

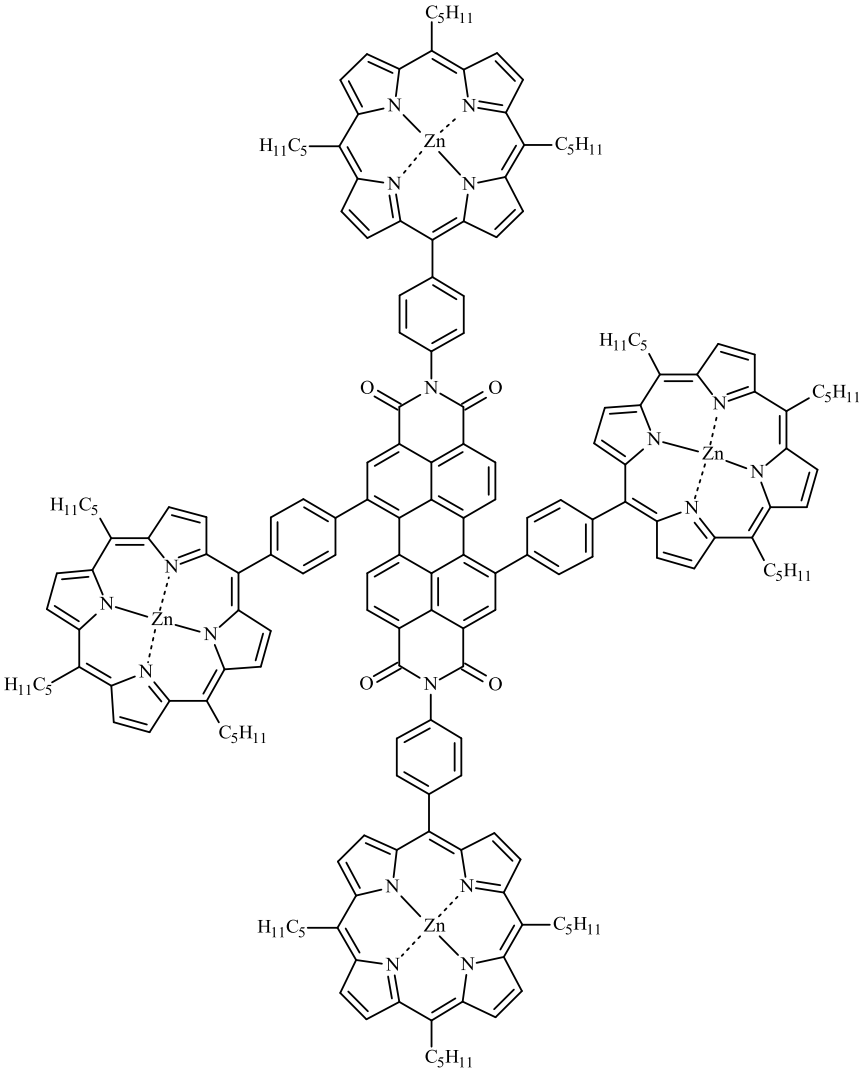

Figure 31. 1,7-N,N'-tetrakis(zinc porphyrin)-perylene-3,4:9,10-bis(dicarboximide)

When the cyclic array is mixed with a bidentate ligand such as 1,4-diazabicyclo[2.2.2]octane (DABCO) an unexpected co-facial dimer is formed. The aim was to insert the ligand between two of the porphyrins within the same molecule, however this did not occur.[71]

In a similar fashion Flamigni *et al* produced star-shaped pentaporphyrin with nucleosidic linkers.[72] However in this system four metalloporphyrin units are attached to a central metal free porphyrin core (figure 32). This allows light energy to be collected at the peripheral porphyrins and transferred quickly and efficiently to the central free porphyrin electron acceptor.

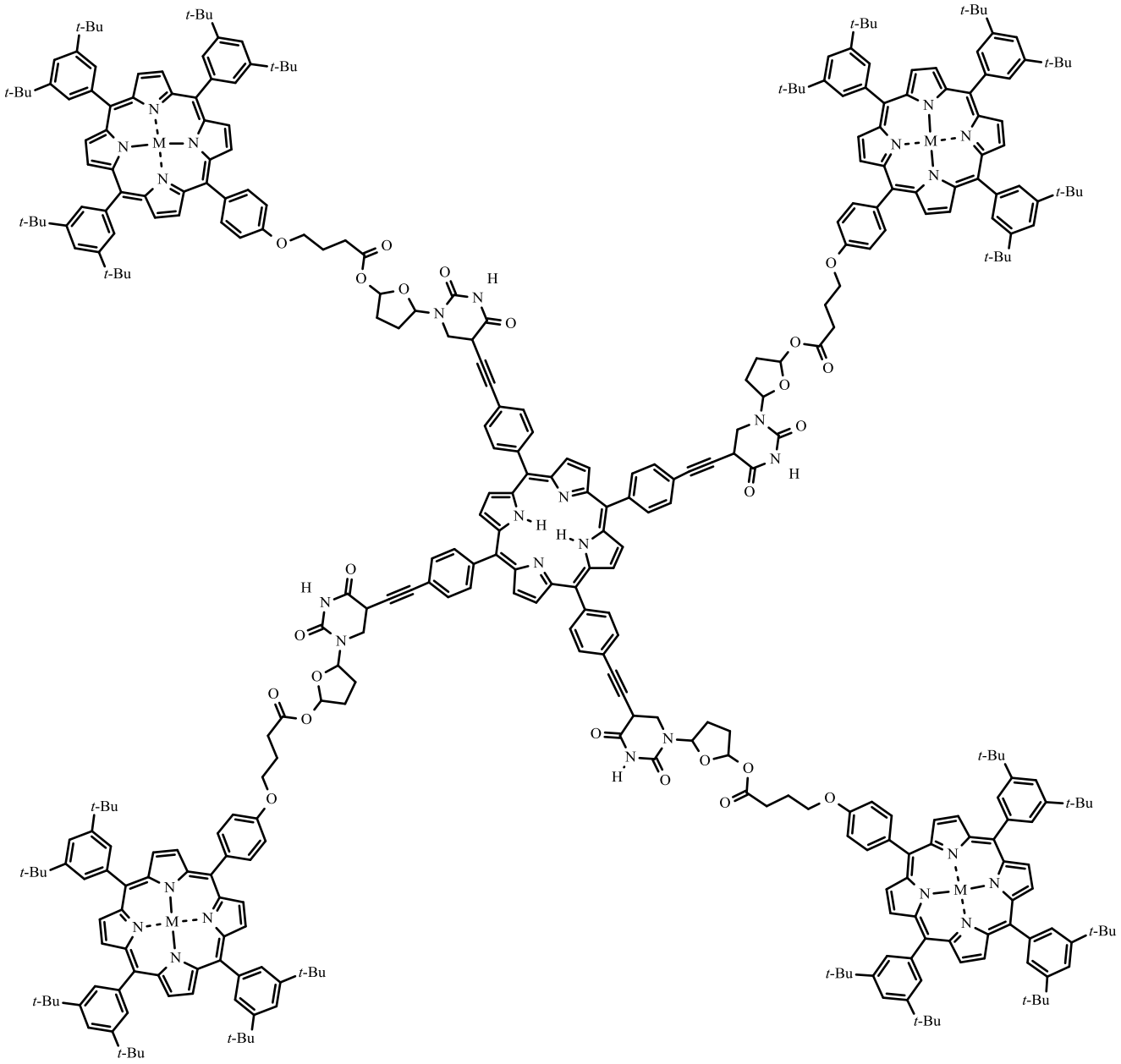

Figure 32. Star-shaped pentaporphyrin with nucleosidic linkers

Flamigni *et al*[72] also tried to insert a bidentate ligand (such as DABCO and 4,4-bipyridine) between the porphyrin units. However the association constants for the bidentate ligands were very similar to that of pyridine (a monodentate ligand) i.e. it shows no cooperative effects. It was suspected that the metalloporphyrin units were too far apart to bind both sides of the DABCO ligand.

One group that has achieved the aim of insertion of a ligand between two porphyrins attached to a central core is Carofiglio and co-workers.[73] They describe the efficient synthesis of melamine-bridged bis-porphyrin dyads which they call porphyrin tweezers (figure 33).

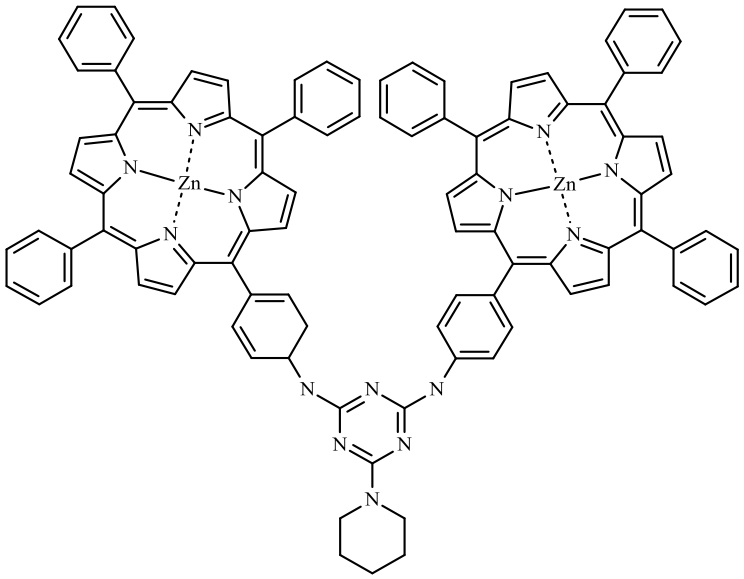

Figure 33. Melamine-bridged porphyrin tweezer.

The zinc metalated tweezers feature a ditopic binding interaction with diamines, resulting in supramolecular complexes with more than three orders of magnitude higher stability constants as compared to a monodentate amine.[73]

Getting back to the cyclic porphyrin arrays, Kobuke et al[74] took a slightly different approach. They created a central core that consisted of a tripod with three arms each able to bind to a porphyrin and a stem of a porphyrin and a fullerene (C_{60}) which acts as an electron acceptor (figure 34a). This core can bind three porphyrin structures via the central metal atom creating a cyclic porphyrin antenna system. Each porphyrin unit itself is made up of three porphyrin subunits joined by a phenyl bridge (figure 34b). Energy collected by the nine antenna ring porphyrins is transferred efficiently to the central acceptor porphyrin moiety followed by photoinduced electron transfer to the C_{60} moiety. This system mimics the combined structure of light-harvesting complex and the reaction centre in natural photosynthesis.[75]

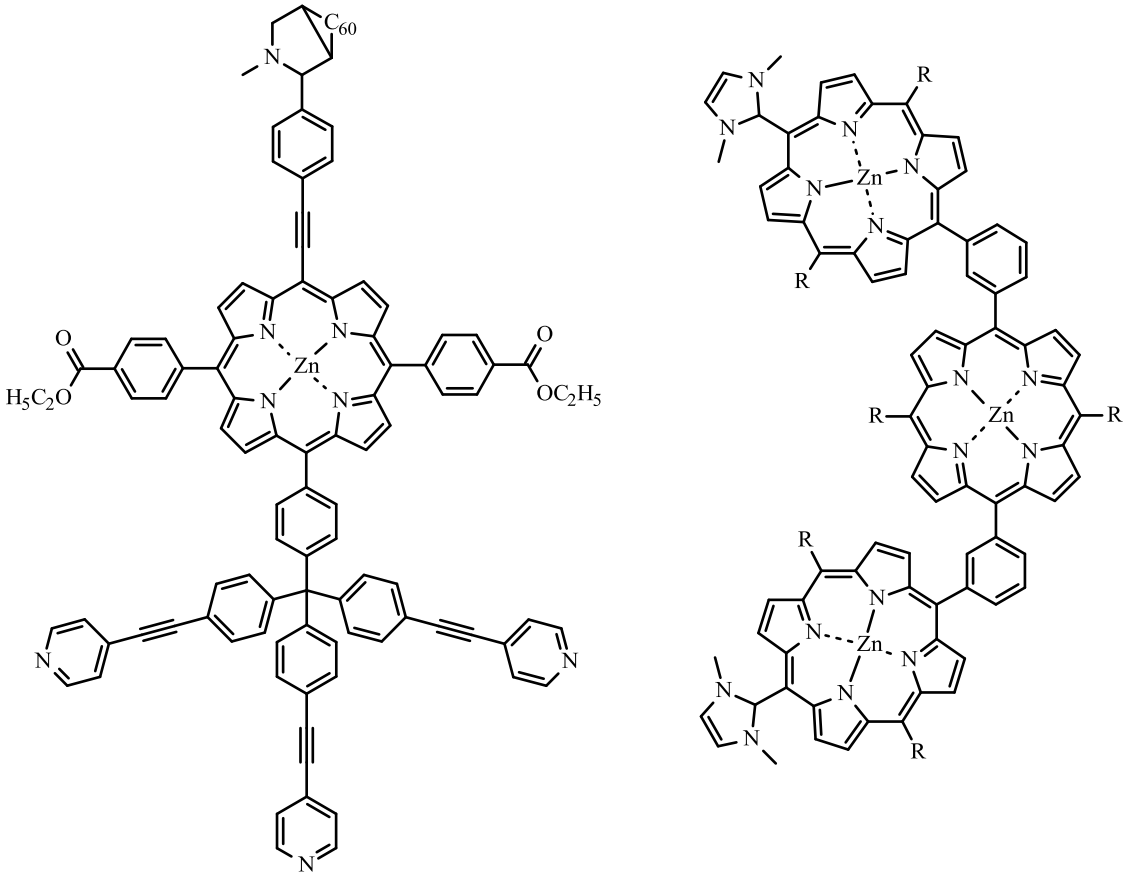

a) Tripod stem, C_{60} = Buckminsterfullerene

b) Three porphyrin unit

Figure 34. Kobuke's cyclic antenna system

1.4. Photoinduced electron-transfer reactions

Much of the interest in the photochemistry of porphyrins stems from their involvement in photosynthesis and the drive to mimic the natural photosynthetic process of converting light into energy.

Photosynthesis begins with the absorption of light by a chromophore. Porphyrins make an ideal chromophore for absorbing light as they absorb strongly in the visible region. Very little UV light reaches the earth's surface and IR and longer wavelengths would not provide enough energy for photosynthesis so visible light is the most useful. When this light is absorbed it creates a singlet excited state which can then be transferred to an acceptor molecule. The lifetime of the singlet state is very short so the transfer of the singlet state must be very quick. In photosynthesis this singlet state is then transferred to the reaction centre where it is converted to chemical energy. This occurs in the form of a transmembrane charge

separation. The electron and the positively charged "hole" are separated and recombination is slowed long enough for the organism to use the stored energy for subsequent reactions.[76]

Artificial photosynthesis describes any attempt to copy the photosynthetic conversion of light into chemical energy. As mentioned above porphyrins make an ideal light harvesting chromophore not only for their great absorption in the visible range but because of their stability, their redox properties, their relative ease of synthesis and above all the huge number of structural variations available. The structure of a porphyrin can be altered to achieve the ideal light absorption, redox, electronic coupling and many more properties.[76] When the porphyrin absorbs light it produces an excited state, that is, an electron is promoted from the highest occupied molecular orbital (HOMO) to the lowest unoccupied molecular orbital (LUMO) (Figure 35).

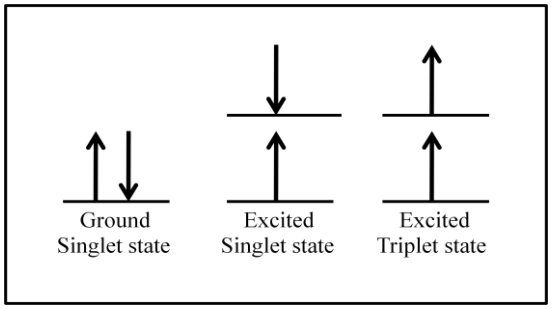

Figure 35. Orbital diagram.

We can see from the Jablonski diagram (Figure 36) that this excited state can undergo a number of transitions. It can relax back down to the ground state, *i.e.* fluorescence, or it can undergo intersystem crossing to a triplet state which can then relax causing phosphorescence.[77]

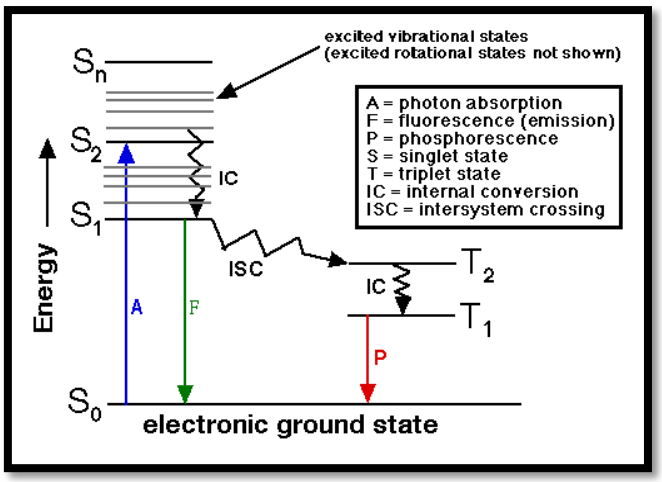

Figure 36. Jablonski diagram.[78]

When the porphyrin is in an excited state, electron transfer of the high energy electron in its LUMO can occur and compete with the unimolecular relaxation. The lifetime for a singlet excited state of a porphyrin is less than 10 ns, so the electron transfer must be 10-100 times faster than this to get a good yield. The porphyrin and the acceptor must have the optimum redox potentials and a strong electronic interaction so that the electron can move quickly from one to the other. Other things that affect the speed and efficiency of electron transfer are the distance between the acceptor, the donor and the solvent. The speed of the electron transfer will decrease with increasing distance. In the case of the solvent it is more to do with the stability of the charges. When an electron is donated by one molecule and accepted by another, charges are created, an ionic solvent stabilises these charges and so prolongs their lifetime giving the charge longer to transfer.[79]

Early attempts to look at this electron transfer involved mixing porphyrins with an acceptor in a solvent however the distance between the molecules cannot be controlled using this method. The transfer requires orbital overlap, so the molecules have to collide to observe the electron transfer. A much better way to create an electron transfer between a porphyrin and an acceptor is to have them bound together. In photosynthesis the position and therefore distance between the two molecules is controlled by a protein complex holding the molecules in place. For artificial photosynthesis the porphyrin and acceptor can be bound with covalent bonds. The porphyrins often used are free-base, zinc or magnesium porphyrins as they have the longest singlet state lifetime, these are then linked to an acceptor that will not oxidise the porphyrin e.g. quinines and larger organic aromatic molecules. [76]

1.5. References

(1) Milgrom, L. *The Colours of life.* Oxford University Press: Oxford, **1997**, p4.

(2) *The Oxford English Dictionary*; 2nd ed. Clarendon Press, 1989; Vol. XII, p138-140.

(3) Feng, X.-T. Yu, J.-G. Lei, M. Fang, W.-H.; Liu, S. *J. Phys. Chem. B* **2009**, *113*, 13381-13389.

(4) Woodward, R. B. Ayer, W. A. Beaton, J. M. Bickelhaupt, F. Bonnett, R. Buchschacher, P. Closs, G. L. Dutler, H. Hannah, J.; Hauck, F. P. *J. Am. Chem. Soc.* **1960**, *82*, 3800–3802.

(5) Fisher, H.; Orth, H. *Die Chemie des Pyrroles.* Akad. Verlagsges. Leipzig, **1937**; Vol. 1, p193.

(6) Gouterman, M. *J. Chem. Phys* **1956**, *30*, 1139.

(7) Falk, J. *Porphyrins and Metalloporphyrins*; Elservier: Amsterdam, **1964**; Vol. 2, p72-77.

(8) Soret, J. *Comptes rendus* **1883**, *97*, 1269-1270.

(9) Ozturk, O. Synthesis and Characterisation of Novel Meso-Naphthyl Porphyrins, University of East Anglia: Norwich, **1999**, p9-10.

(10) Lindsey, J. S. *Acc. Chem. Res.* **2010**, *43*, 300-311.

(11) Lindsey, J. S. Kadish, K. M. Smith, K. M.; Guilard, R. *The Porphyrin Handbook*; Achademic Press, **2000**; Vol. 1, p60-80.

(12) Rothemund, P. *J. Am. Chem. Soc.* **1935**, *57*, 2010–2011.

(13) Rothemund, P. *J. Am. Chem. Soc.* **1939**, *61*, 2912–2915.

(14) Ball, R. H. Dorough, G. D.; Calvin, M. *J. Am. Chem. Soc.* **1946**, *68*, 2278–2281.

(15) Berenbaum, M. Bonnett, R. Ioannous, S.; White, R. *J. Cancer* **1986**, *54*, 717-725.

(16) Bettelheim, A. White, B. A. Raybuck, S. A.; Murray, R. W. *Inorg. Chem.* **1987**, *26*, 1009–1017.

(17) Collman, J. P. Gagne, R. R. Reed, C. Halbert, T. R. Lang, G.; Robinson, W. T. *J. Am. Chem. Soc.* **1975**, *97*, 1427–1439.

(18) Collman, J. P. *Inorg. Chem.* **1997**, *36*, 5145-5155.

(19) Voltz, H.; Herb, G. *Naturforsch B* **1983**, *38*, 1240.

(20) Lindsey, J. S. *Tetrahedron Lett.* **1986**, *27*, 4969-4970.

(21) Lindsey, J. S. Schreiman, I. C. Hsu, H. C. Kearney, P. C.; Marguerettaz, A. M. *J. Org. Chem.* **1987**, *52*, 827–836.

(22) Lindsey, J. S.; Wagner, R. W. *J. Org. Chem.* **1989**, *54*, 828–836.

(23) Lindsey, J. S. *In Metalloporphyrin-Catalyzed Oxidation*; K. A. Publishers: The Netherlands, **1994**, p49.

(24) Li, F. Yang, K. Tyhonas, J. S. MacCrum, K. A.; Lindsey, J. S. *Tetrahedron* **1997**, *53*, 12339–12360.

(25) Rao, P. D. Dhanalekshmi, S. Littler, B. J.; Lindsey, J. S. *J. Org. Chem.* **2000**, *65*, 7323-7344.

(26) Kadish, K. Smith, K.; Guilard, R. *The Porphyrin Handbook*; Achademic Press, **2000**; Vol. 1, p53.

(27) Zaidi, S. H. H. Loewe, R. S. Clark, B. A. Jacob, M. J.; Lindsey, J. S. *Org Process Res Dev* **2006**, *10*, 304–314.

(28) Arsenault, G. P. Bullock, E.; MacDonald, S. F. *J. Am. Chem. Soc.* **1960**, *82*, 4384–4389.

(29) Littler, B. J. Ciringh, Y.; Lindsey, J. S. *J. Org. Chem.* **1999**, *64*, 2864-2872.

(30) Smith, K. *Porphyrins and Metalloporphyrins*; Elservier: Amsterdam, **1975**, p96-101.

(31) Rao, P. Littler, B. Geier, G.; Lindsey, J. *J. Org. Chem.* **2000**, *65*, 1084-1092.

(32) Feng, X.; Senge, M. O. *Tetrahedron* **2000**, *56*, 587–590.

(33) Liu, C. Shen, D.; Chen, Q. *Chem. Commun.* **2006**, *7*, 770-772.

(34) Rao, P. D. Littler, B. J. Geier, G. R.; Lindsey, J. S. *J. Org. Chem.* **2000**, *65*, 1084-1092.

(35) Prathapan, S. Johnson, T. E.; Lindsey, J. S. *J. Am. Chem. Soc.* **1993**, *115*, 7519–7520.

(36) Imahori, H. *J. Phys. Chem. B* **2004**, *108*, 6130-6143.

(37) Song, H. Taniguchi, M. Speckbacher, M. Yu, L. Bocian, D. Lindsey, J.; Holten, D. *J. Phys. Chem. B* **2009**, *113*, 8011-8019.

(38) Lo, P. C. Leng, X.; Ng, D. K. P. *Coordin Chem Rev* **2007**, *251*, 2334–2353.

(39) Gaspard, S. Giannotti, C. Maillard, P. Schaeffer, C.; Tran-Thi, T. *J. Chem. Soc., Chem. Commun.* **1986**, *16*, 1239-1241.

(40) Tran Thi, T. H. Desforge, C. Thiec, C.; Gaspard, S. *J. Phys. Chem.* **1989**, *93*, 1226–1233.

(41) Král, V. Rusin, O.; Schmidtchen, F. *Org. Lett.* **2001**, *3*, 873-876.

(42) Li, X. Zhou, Q. Tian, H.; Xu, H. *Chin. J. Chem.* **1998**, *16*, 97-108.

(43) Yang, S. I. Li, J. Sun Cho, H. Kim, D. Bocian, D. Holten, D.; Lindsey, J. S. *J. Mater. Chem.* **2000**, *10*, 283-296.

(44) Kameyama, K. Satake, A.; Kobuke, Y. *Tetrahedron Lett.* **2004**, *45*, 7617–7620.

(45) Miller, M. A. Lammi, R. K. Prathapan, S. Holten, D.; Lindsey, J. S. *J. Org. Chem.* **2000**, *65*, 6634-6649.

(46) Haufe, G. Alvernhe, G. Laurent, A. Ernet, T. Goj, O. Kroger, S.; Sattler, A. *Org. Synth.* **2004**, *10*, 128-132.

(47) Kobayashi, N. Nishiyama, Y. Ohya, T.; Sato, M. *J. Chem. Soc., Chem. Commun.* **1987**, 390-392.

(48) Kobayashi, N. Ohya, T. Sato, M.; Nakajima, S. *Inorg. Chem.* **1993**, *32*, 1803–1808.

(49) Li, J. Diers, J. R. Seth, J. Yang, S. I. Bocian, D. F. Holten, D.; Lindsey, J. S. *J. Org. Chem.* **1999**, *64*, 9090-9100.

(50) Zhao, Z. Ogunsipe, A. O. Maree, M. D.; Nyokong, T. *J. Porphyrins. Phthalocyanins.* **2005**, *9*, 186.

(51) Lin, V. DiMagno, S. G.; Therien, M. J. *Research* **1994**, *264*, 1105-1111.

(52) Kawao, M. Ozawa, H. Tanaka, H.; Ogawa, T. *Thin Solid Films* **2006**, *499*, 23–28.

(53) Cammidge, A. N. Scaife, P. J. Berber, G.; Hughes, D. L. *Org. Lett.* **2005**, *7*, 3413-3416.

(54) Grozema, F. C. Houarner-Rassin, C. Prins, P. Siebbeles, L. D. A.; Anderson, H. L. *J. Am. Chem. Soc.* **2007**, *129*, 13370–13371.

(55) Ogawa, K. Zhang, T. Yoshihara, K.; Kobuke, Y. *J. Am. Chem. Soc.* **2002**, *124*, 22–23.

(56) Li, G. Wang, T. Schulz, A. Bhosale, S. Lauer, M. Espindola, P. Heinze, J.; Fuhrhop, J. *Chem. Commun.* **2004**, *5*, 552-553.

(57) Kuebler, S. Denning, R.; Anderson, H. *J. Am. Chem. Soc.* **2000**, *122*, 339-347.

(58) Staab, H. A. Tercel, M. Fischer, R.; Krieger, C. *Angew. Chem., Int. Ed. Engl.* **1994**, *33*, 1463-1466.

(59) Staab, H. A.; Carell, T. *Angew. Chem. Int . Ed. Engl.* **1994**, *33*, 1466-1468.

(60) Girolami, G. S. Hein, C. L.; Suslick, K. S. *Angew. Chem., Int. Ed. Engl.* **1996**, *35*, 1223-1225.

(61) Inaba, Y.; Kobuke, Y. *Tetrahedron* **2004**, *60*, 3097–3107.

(62) Karrasch, S. Bullough, P. A.; Ghosh, R. *EMBO J.* **1995**, *14*, 631-638.

(63) Roszak, A. W. Howard, T. D. Southall, J. Gardiner, A. T. Law, C. J. Isaccs, N. W.; Cogdell, R. J. *Science* **2003**, *302*, 1969-1972.

(64) Aratani, N. Kim, D.; Osuka, A. *Acc. Chem. Res.* **2009**, *42*, 1922-1934.

(65) Osuka, A.; Shimidzu, H. *Angew. Chem., Int. Ed. Engl.* **1997**, *36*, 135-137.

(66) Peng, X. Aratani, N. Takagi, A. Matsumoto, T. Kawai, T. Hwang, I. W. Ahn, T. K. Kim, D.; Osuka, A. *J. Am. Chem. Soc.* **2004**, *126*, 4468–4469.

(67) Hwang, I. Ko, D. Ahn, T. Yoon, Z. Kim, D. Peng, X. Aratani, N.; Osuka, A. *J. Phys. Chem. B* **2005**, *109*, 8643-8651.

(68) Hori, T. Aratani, N. Takagi, A. Matsumoto, T. Kawai, T. Yoon, M. Yoon, Z. Cho, S. Kim, D.; Osuka, A. *Chem. Eur. J.* **2006**, *12*, 1319-1327.

(69) Tsuda, A. Nakamura, T. Sakamoto, S. Yamaguchi, K.; Osuka, A. *Angewandte Chemie* **2002**, *114*, 2941–2945.

(70) Hwang, I. Kamada, T. Ahn, T. Ko, D. Nakamura, T. Tsuda, A. Osuka, A.; Kim, D. *J. Am. Chem. Soc.* **2004**, *126*, 16187-16198.

(71) Kelley, R. F. Shin, W. S. Rybtchinski, B. Sinks, L. E.; Wasielewski, M. *J. Am. Chem. Soc.* **2007**, *129*, 3173-3181.

(72) Flamigni, L. Talarico, A. M. Ventura, B. Marconi, G. Sooambar, C.; Solladié, N. *Eur. J. Inorg. Chem.* **2004**, *12*, 2557–2569.

(73) Elisa, L. Baldini, F. Giannetti, A. Trono, C.; Carofiglio, T. *Chem. Commun.* **2010**, *46*, 3678-3680.

(74) Kobuke, Y. *Eur. J. Inorg. Chem.* **2006**, *2006*, 2333-2351.

(75) Kuramochi, Y. Sandanayaka, A. Satake, A. Araki, Y. Ogawa, K. Ito, O.; Kobuke, Y. *Chem. Eur. J.* **2009**, *15*, 2317-2327.

(76) Smith, K. Kadish, K. M.; Guilard, R. *The Porphyrin Handbook*; Academic Press: San Diego, **2000**; Vol. 8, p3-8.

(77) Atkins, P.; Paula, J. *Atkins Physical Chemistry*; 8th ed. Oxford University Press: Oxford, **2002**, p492-496.

(78) The Chemistry Hypermedia Project http://www.files.chem.vt.edu/chem-ed/quantum/jablonsk.html **17/07/2011**.

(79) Wasielewski, M. R. *Chem. Rev.* **1992**, *92*, 435–461.

Chapter 2: Discussion

2.1. Aims

A year long, research project into porphyrin stacked directly above one another linked by naphthyl groups, proved to be unsuccessful. Therefore the decision was taken to investigate a different class of multichromophore assemblies. The original multichromophore targets of this project had chromophores in the form of porphyrins packed very close together one above the other. These were to be linked by naphthyl groups attached at the *meso* positions of the porphyrin. This small separation of the chromophores allows a strong interaction between them, for example a pathway for electrons along the stack is present. Such interaction is not always favourable, however, and the focus of our project shifted towards design and preparation of non-interacting multichromophore arrays. We reasoned that assembly of a high concentration of chromophores around a central, functional unit would lead to interesting materials with potential applications. In particular, the potential for multiple electron processes could become possible. To achieve this goal we would need to generate two excited chromophores in close proximity to a third unit. A high concentration of chromophores (with a long excited state lifetime) would be required to achieve this with normal (non-laser) irradiation. For this process to be efficient there would have to be no interaction or quenching between the chromophore units. The chromophores could not simply be placed in solution in large concentrations as they would aggregate *i.e.* come together in solution. This would cause quenching between the chromophores (figure 1).

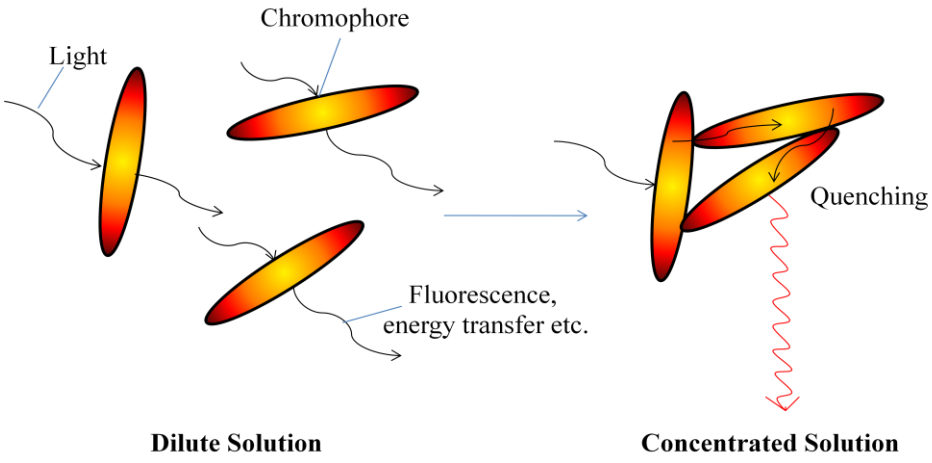

Figure 1. Quenching of chromophores

Inspiration for a structure that could achieve a high concentration of chromophores without quenching came from nature. The chromophores in the light harvesting antenna within purple bacteria are arranged in a cyclic manner held in position by a protein framework.[1] A similar structure could be achieved by attaching a number of chromophores around a central core. However we expect that the chromophores in this structure could still come together, possibly in pairs. This would again cause quenching of the excited states (Scheme 1).

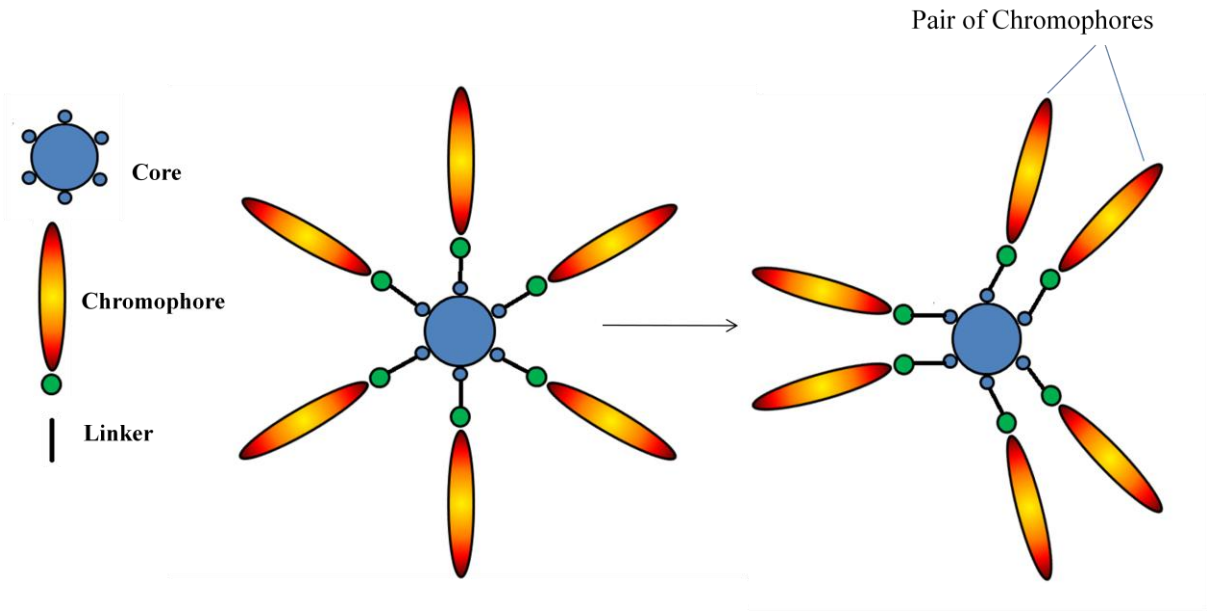

Scheme 1. Chromophores attached to a central core

To prevent this, we reasoned that an inert spacer could be used to separate the chromophore units preventing them from coming together. An illustration of a possible structure is given below in figure 2.

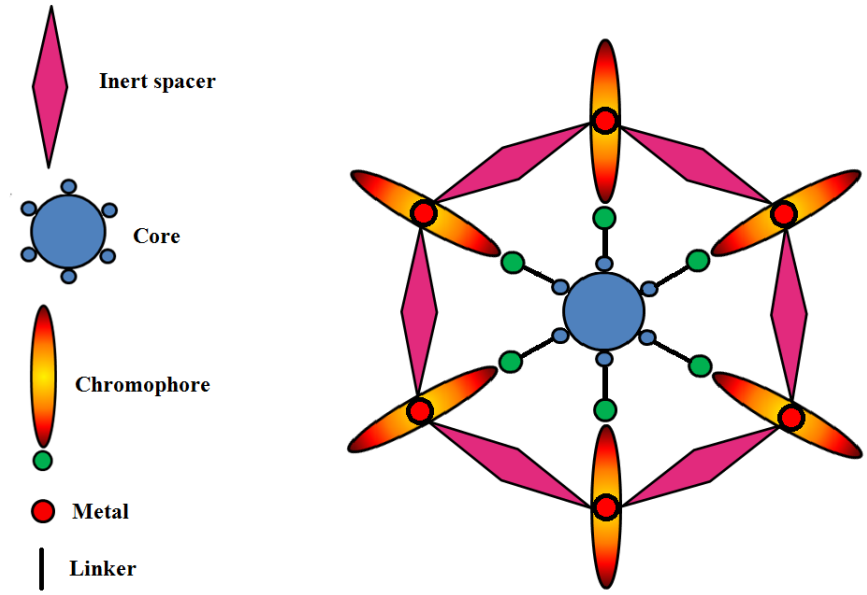

Figure 2. Spacer groups between chromophores attached to a central core

Each part of the molecule depicted in the illustration above must be considered carefully and there are a large number of compounds to choose from for each component. The chromophore must be versatile and easily produced. Porphyrins are ideal candidates as the knowledge gained from the research on the previous multichromophore can be drawn upon. They are also easily tuneable through synthesis *i.e.* our lab has experience placing a range of substituents on the *meso* positions of the porphyrin.[2-4] The ideal prophyrin for this would be tetraphenylporphyrin (TPP) as it has been researched thoroughly and is easy to produce by reaction between benzaldehyde and pyrrole.[5] As the porphyrin will be attached to the central core by a single linker, an unsymmetrical mono substituted porphyrin will be required. With this in mind we expected that a hydroxyl group could easily be introduced on the 4 position of one of the phenyl groups within TPP. This could be done by reaction between 4-hydroxybenzaldehyde and benzaldehyde (in a 1:3 ratio), with pyrrole to produce an unsymmetrical mono substituted porphyrin like **1** (Scheme 2).[6] The hydroxyl group on the phenyl group provides a position where the linker could be attached using versatile methods e.g. via a simple S_N2 reaction with a bromoalkyl linker.

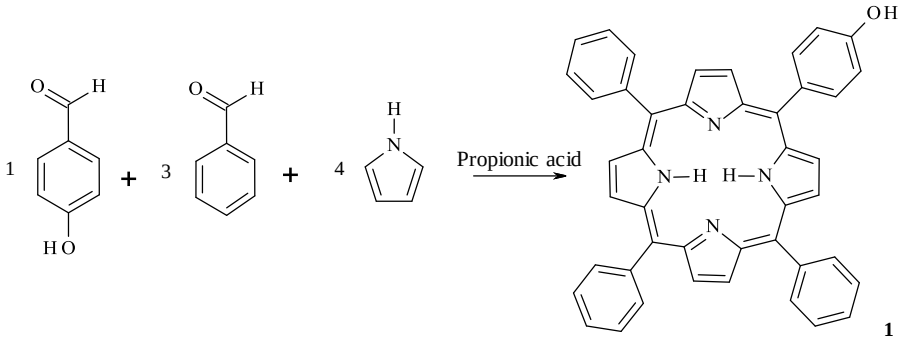

Scheme 2. Synthesis of hydroxyphenylporphyrin **1**

There are also a large number of molecules that could be considered for the core. In the final functioning system the core will itself be a purpose designed unit, perhaps a catalytically active two electron acceptor or donor. Nevertheless for these model compounds a simple core was to be chosen to demonstrate the overall strategy. For example a porphyrin could be used for the core as well as the outer chromophore.[7] However, we reasoned that this would complicate the results making them hard to interpret for the model compounds. Benzene could also be considered as the simplest possible core with six possible substitution sites, but we anticipated that synthesis might not be straightforward. Based on these considerations, triphenylenes were the next logical step as they are simple, yet bigger than benzene. Our lab also has much experience when producing triphenylenes due to their use as liquid crystals.[8-11] This experience could therefore be drawn upon when producing new triphenylenes. Triphenylenes have twelve possible substitution sites. However the 2,3,6,7,10,11 positions are the most accessible for substitution (Figure 3).

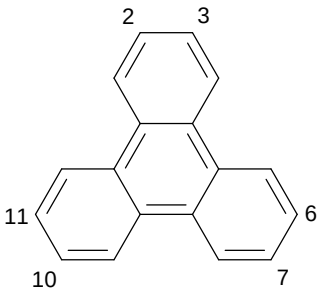

Figure 3. Substitution positions on a triphenylene

We will also need to provide a functional group on these positions with which the linker to the porphyrin can react. As with the porphyrin above, a hydroxyl group would be ideal. A triphenylene with hydroxyl groups on the 2,3,6,7,10,11 positions can easily be synthesised by cyclising veratrole to produce hexa(methoxy)triphenylene **2**, followed by deprotection of the methoxy groups to give hexahydroxytriphenylene **3** (Scheme 3).[12]

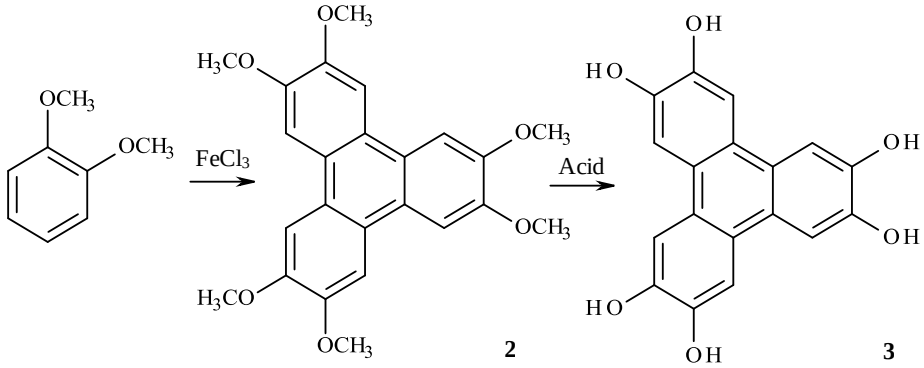

Scheme 3. Synthesis of hexahydroxytriphenylene **3**

It is obvious from looking at the triphenylene that the separation between positions 2 and 3 is much smaller than the separation between positions 3 and 6. However it is possible that if a flexible enough linker is used the porphyrins could still spread out evenly with the aid of the inert spacer group. Nonetheless synthesis allows two models to be produced where the hydroxyl groups are on the 2 and 3 positions of one and the 3 and 6 positions of the other. Similar groups to the linker could also be placed on the other positions within the triphenylene without the porphyrins attached so that comparisons can be made between the model compound and the final multichromophore (figure 4). The two model compounds could be used to test the spacer groups for the correct size and shape for each of the gaps. The results for these two model compounds will also make the results for the final hexa-porphyrin array much easier to interpret.

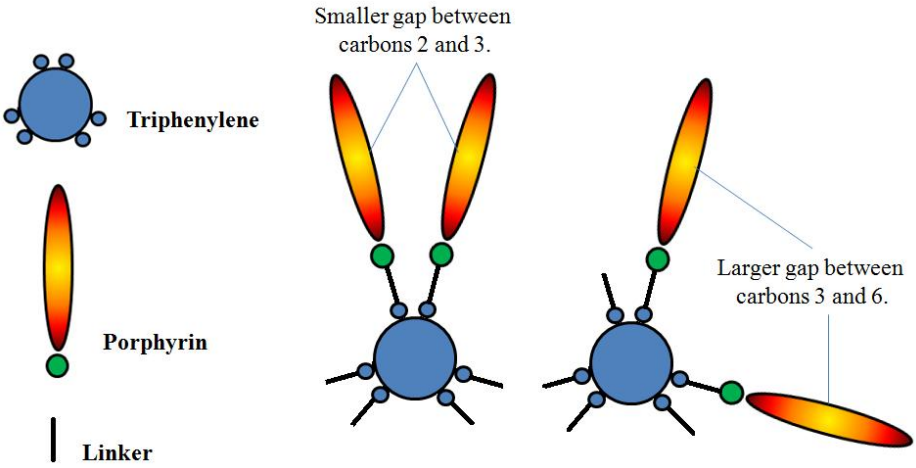

Figure 4. Model compounds to demonstrate the different sized gaps between substitution positions on triphenylenes

The linker between the porphyrin and the triphenylene is very important. The linker could be made either flexible or rigid. A rigid linker such as benzene would provide some control over the porphyrins, separating them. However, if a spacer group is still needed it would be very difficult to insert a group without flexibility of the porphyrins. Therefore a flexible chain would be preferable. This would allow the porphyrins to move around to accommodate a spacer group and distribute evenly. It may also prevent the need for two different sized spacer groups due to the two different gaps in the triphenylene substituents. The length of linker is also important to balance flexibility with function of discrete arrays. Therefore an intermediate length of six carbons was chosen for our initial investigation. 1,6-Dibromohexane would react easily with the hydroxyl groups on both the porphyrin and the triphenylene producing 2,3-linked bis(porphyrin)triphenylene **4** with a diether linker between them (Scheme 4), although a stepwise synthesis is clearly required in practice.

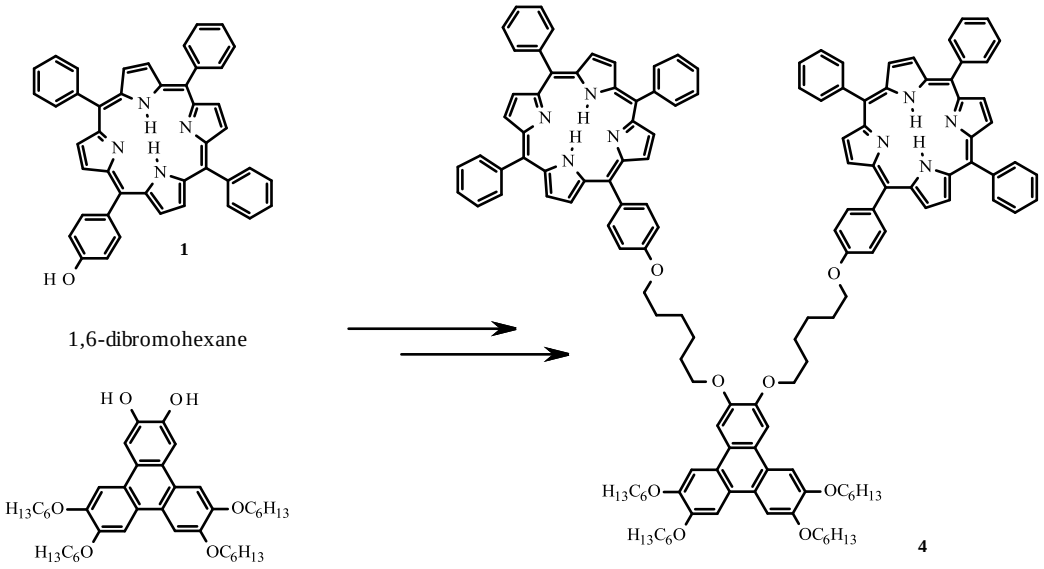

Scheme 4. Systematic illustration of the synthesis of model compound 2,3-bis(porphyrin)triphenylene **4**

The next step will be to find an inert spacer group. The porphyrins could be joined via the phenyl groups at the 10 and 20 meso positions to produce a planar complex. However the porphyrins could interact through this spacer as it is directly linked. Another option would be to metalate the porphyrin centres and separate them by inserting a ligand between them. The ligand would have to bind to a metal strongly, for example through a nitrogen based functional group such as pyridine. The ligand would also have to be able to bind two metals to be able to insert between the porphyrins. A range of ligands are available to get the right size and shape to fit between the porphyrins. Examples of different sized bidentate nitrogen based ligands are 4,4-bipyridine and 1,2-bispyridylethane (figure 5).

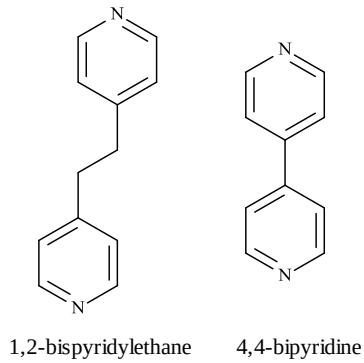

Figure 5. Examples of linear bidentate ligands

There are also many possibilities for the central metal element. A metal that can sit comfortably in the centre of the porphyrin and also bind two ligands such as ruthenium would be ideal for the final multichromophore molecule. However zinc would make a good model; it is easily inserted into the porphyrin and we have experience in doing this. Zinc-TPP and its binding properties to a number of ligands are well documented and so could be compared to our results.[13-15] Zinc would also still be able to bind a bidentate ligand between two of the porphyrins. This could also simplify the results making them easier to interpret as there would be three ligands inserted between three pairs of porphyrins (similar to the two model compounds) rather than six ligands between six porphyrins (figure 6).

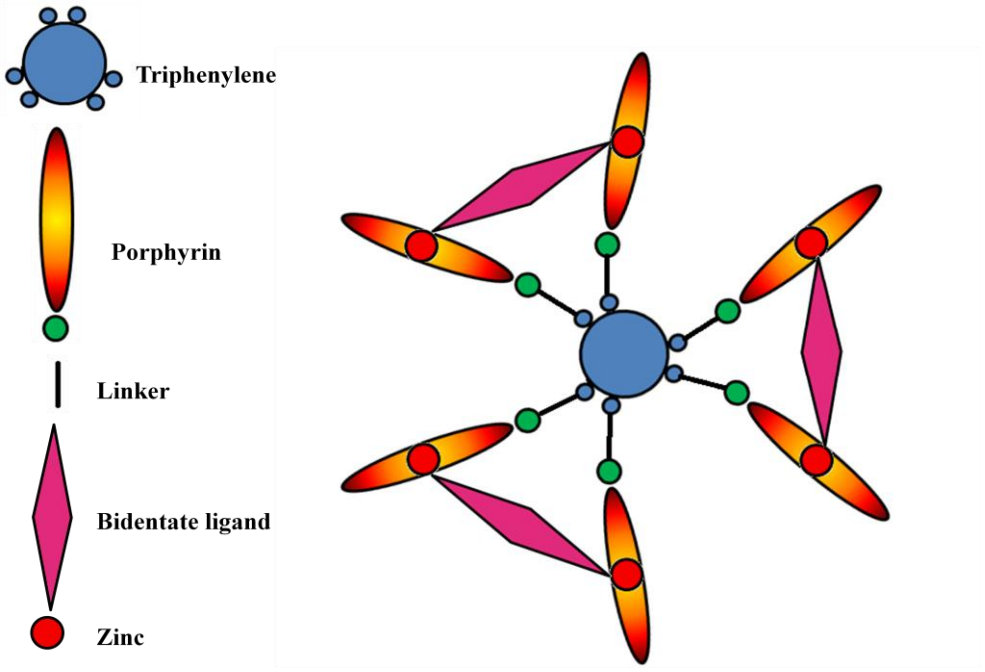

Figure 6. Cartoon of a zinc hexa(porphyrin)triphenylene bound to a bidentate ligand

A lot of thought and consideration has gone in to each part of the final target molecule and the two model compounds that will allow investigation of the effect of the different sized gaps between the substitution positions on the triphenylene. Figure 7 shows the three molecules that were targeted, zinc-2,3-bis(porphyrin)triphenylene **5**, zinc-3,6-bis(porphyrin)triphenylene **6** and zinc-hexa(porphyrin)triphenylene **7**.

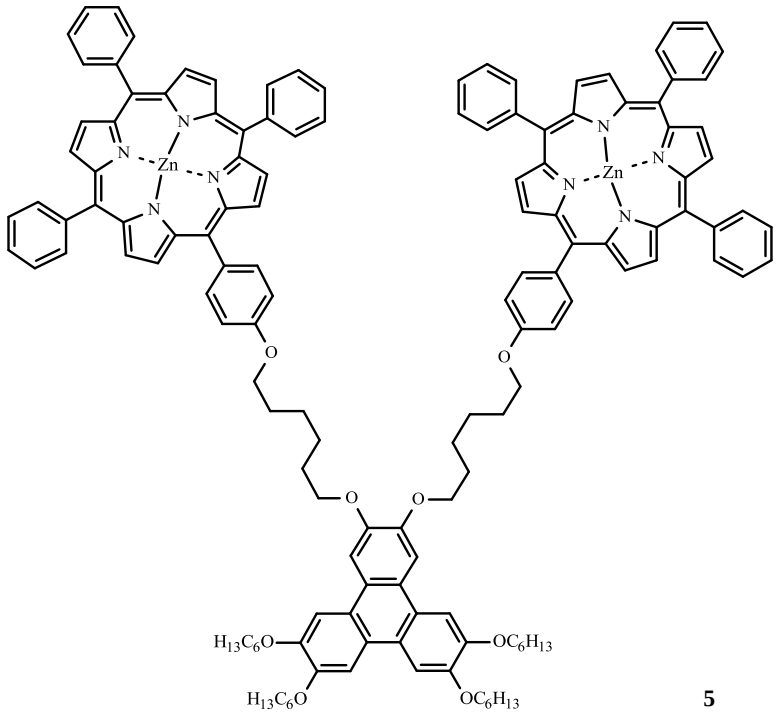

5

Zinc-2,3-bis(porphyrin)triphenylene **5**

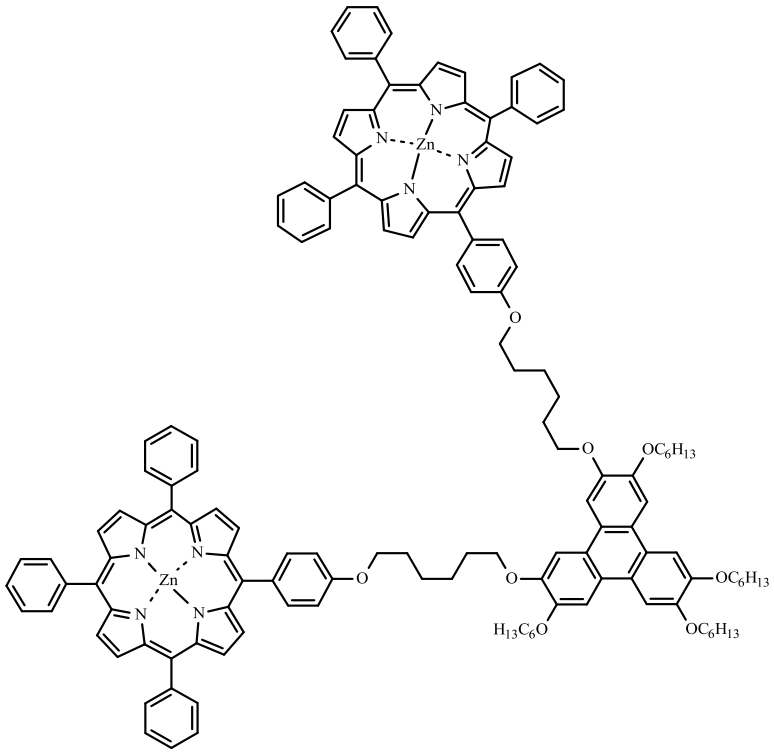

6

Zinc-3,6-bis(porphyrin)triphenylene **6**

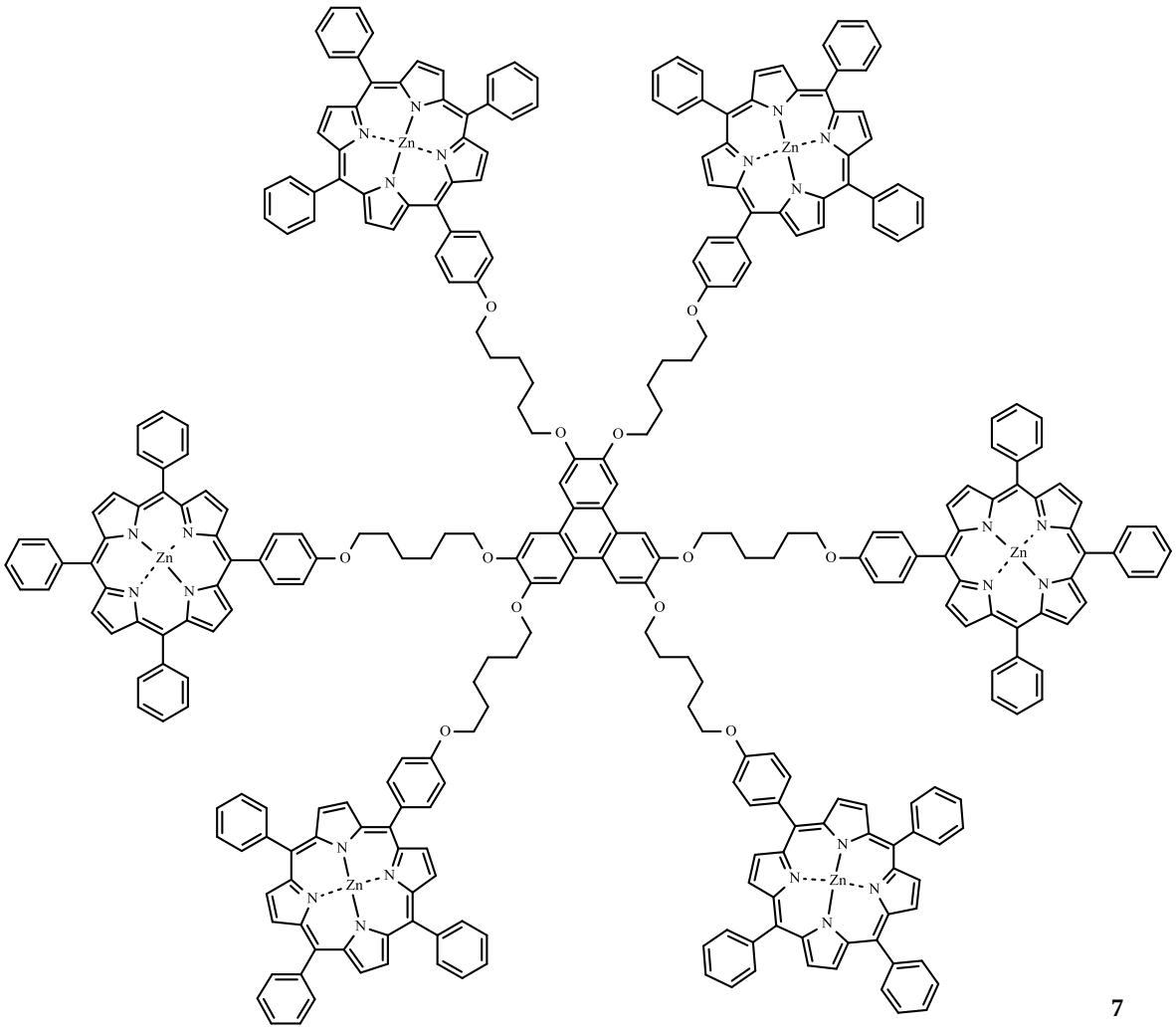

7

Zinc-hexa(porphyrin)triphenylene **7**

Figure 7. The final target molecule plus the two model compounds

Finally we recognised that extension of this strategy to systems with a greater number of chromophores would be straightforward. We could use similar chemistry to that used for the molecules already mentioned, to produce, for example, structures such as **8** (figure 8).

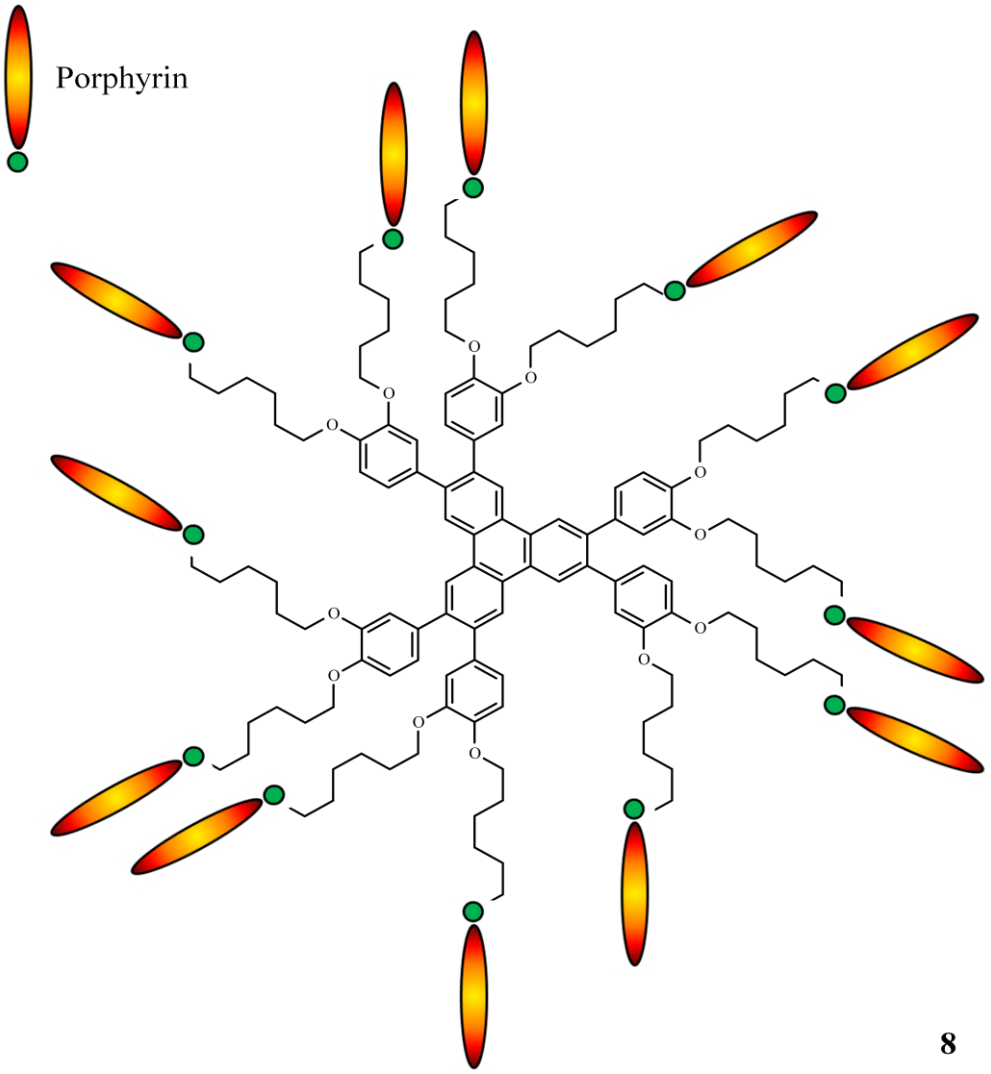

Figure 8. An example of a molecule with a higher concentration of chromophores around a central core

2.2. Preparation of the porphyrin component

The first part of the final molecule that was synthesised was the hydroxyphenylporphyrin **1**. There are many ways to produce a *meso*-substituted porphyrin with an A_3B substitution pattern.[16-18] As mentioned previously we could react pyrrole, benzaldehyde and a substituted benzaldehyde in a 4:3:1 ratio (Scheme 5).[6] This might produce a large number of products which would need to be separated via column chromatography possibly resulting in low yields.

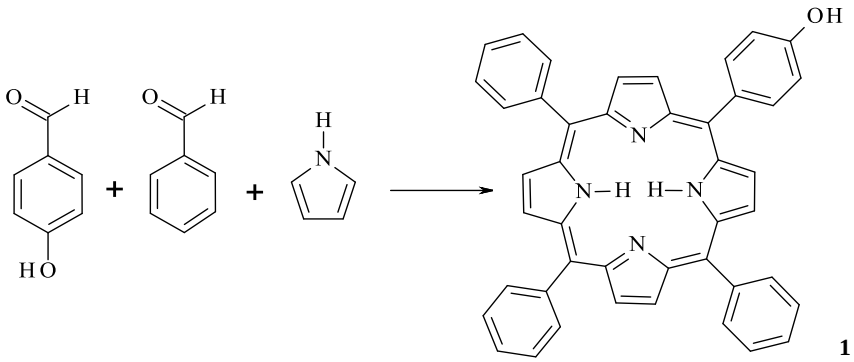

1

Scheme 5. Synthesis of hydroxyphenylporphyrin **1** via the one pot method

We could also build the molecule in a stepwise manner introducing one *meso* substituent at a time, regioselectivly (Scheme 6).[19] However the number of steps in this process means that overall the full synthesis would take a number of weeks and although the yield would perhaps be more than the all-in-one process above it would still be quite low. Taking this into consideration it was thought that the one-step synthesis would be more efficient.

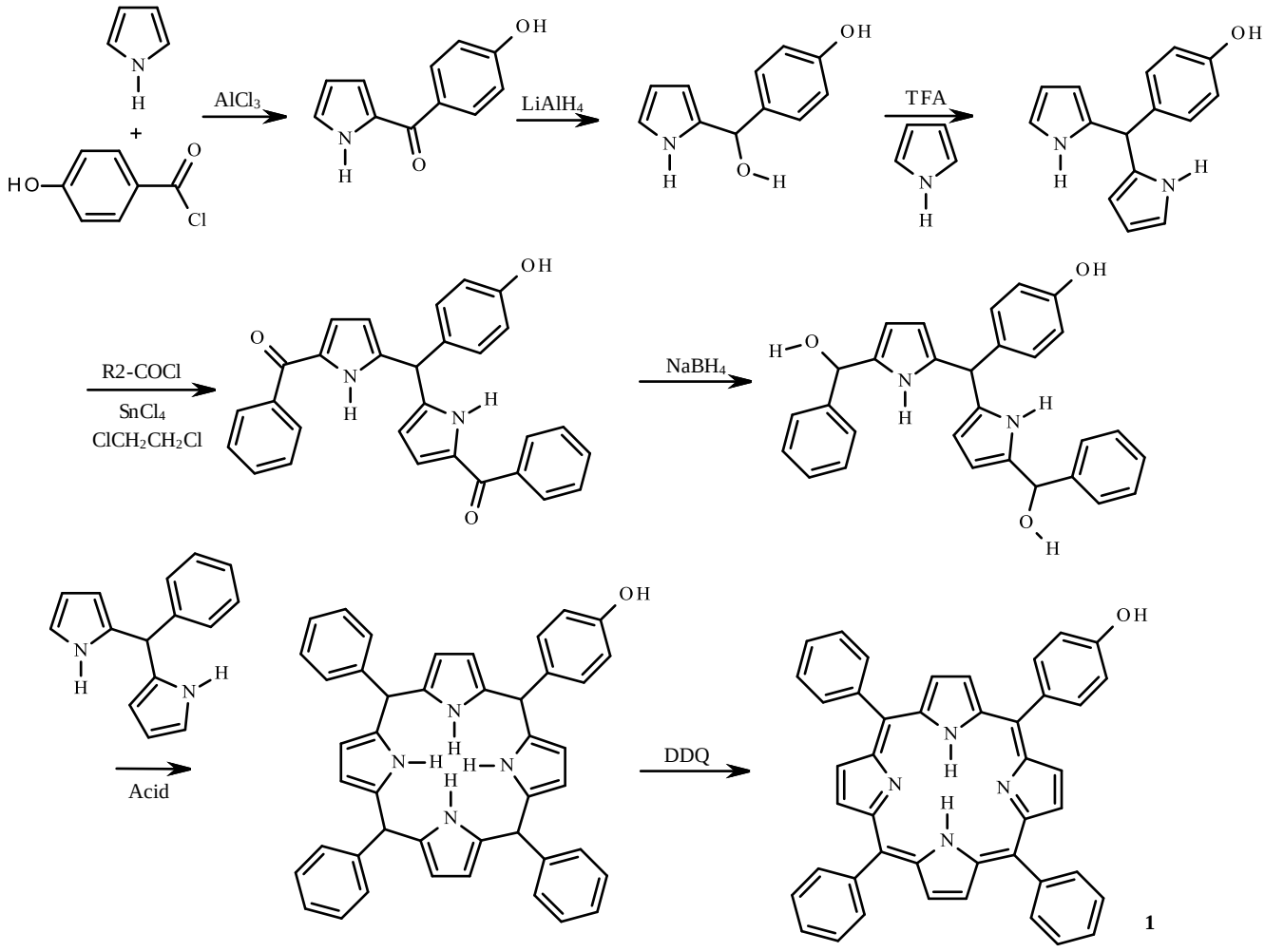

Scheme 6. Synthesis of hydroxyphenylporphyrin **1** via the stepwise method

There are a number of reported reaction conditions for the single step synthesis of *meso*-substituted porphyrins with an A_3B substitution pattern, including the Alder method[20-23] and the Lindsey method.[6,16,19,24] In the Alder method, benzaldehyde, 4-hydroxybenzaldehyde and pyrrole are refluxed in propionic acid in a 3:1:4 ratio open to the air to oxidise the intermediate formed. The Lindsey method is different in that pyrrole, benzaldehyde and 4-hydroxybenzaldehyde are reacted at room temperature in DCM and treated with trifluoroacetic acid for around an hour before adding a stoichiometric amount of an oxidising agent such as DDQ to oxidise the intermediate to the porphyrin. The Lindsey method was investigated first. Pyrrole, benzaldehyde and 4-hydroxybenzaldehyde (in a 4:3:1 ratio) were dissolved in DCM followed by addition of trifluoroacetic acid. The intermediate created was oxidised by DDQ, worked up and purified by column chromatography to produce hydroxyphenylporphyrin **1** in a yield of 3 %. However when the solvents were removed to perform the column chromatography, a very thick, sticky tar (polypyrroles) remained. This

was very hard to handle resulting in loss of yield. Therefore we chose to investigate the Alder method.

Benzaldehyde, 4-hydroxybenzaldehyde and pyrrole (in a 3:1:4 ratio) were reacted in refluxing propionic acid for 30 minutes open to the atmosphere. Crystallisation occurred after cooling and on addition of ethanol, and the isolated solid was purified by column chromatography to produce hydroxyphenylporphyrin **1** in a yield of 4%. Both methods therefore produced similar yields. However the Alder method's purification procedure was much easier due to the porphyrin products crystallising out of solution on addition of ethanol. Therefore, the Alder method was chosen to produce hydroxyphenylporphyrin **1** (Scheme 7) for subsequent syntheses.

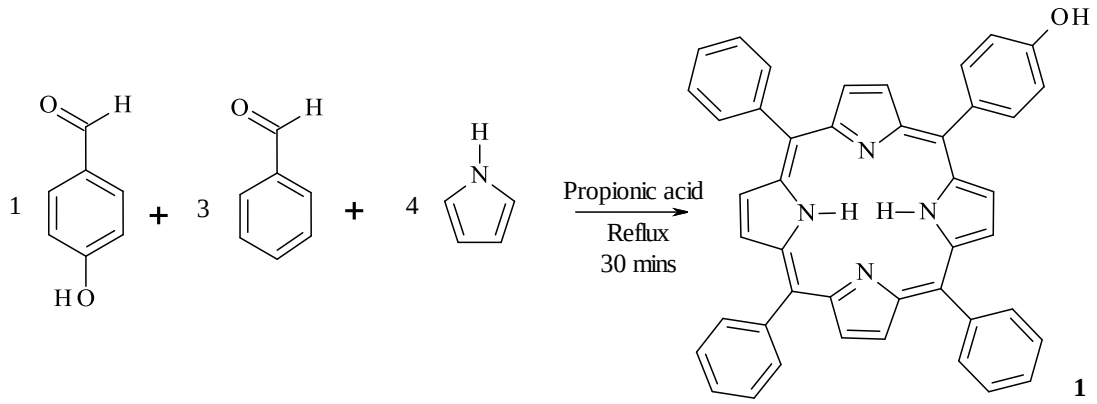

Scheme 7. Synthesis of hydroxyphenylporphyrin **1**

2.3. Preparation of the triphenylene components

2.3.1. Synthesis of hexamethoxytriphenylene 2

The synthesis of the symmetrical triphenylene core, required for attachment of six chromophores, was relatively straightforward. The method of synthesis of hexamethoxytriphenylene **2** was based on the research knowledge gained from our lab. Hexamethoxytriphenylene **2** can be created easily from veratrole using iron trichloride in DCM followed by a reductive methanol workup. This procedure produced hexamethoxytriphenylene **2** in a yield of 24 % (Scheme 8).[12]

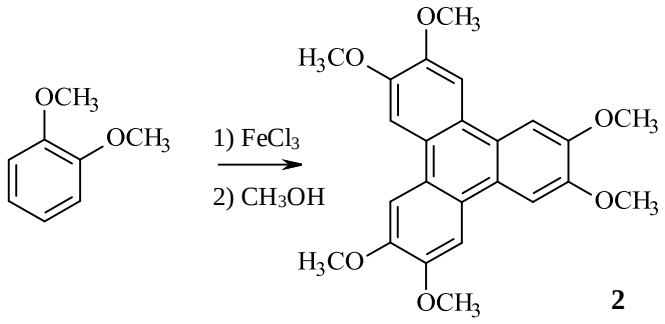

Scheme 8. Synthesis of hexa(methoxy)triphenylene **2**

2.3.2. Synthesis of hexahydroxytriphenylene 3

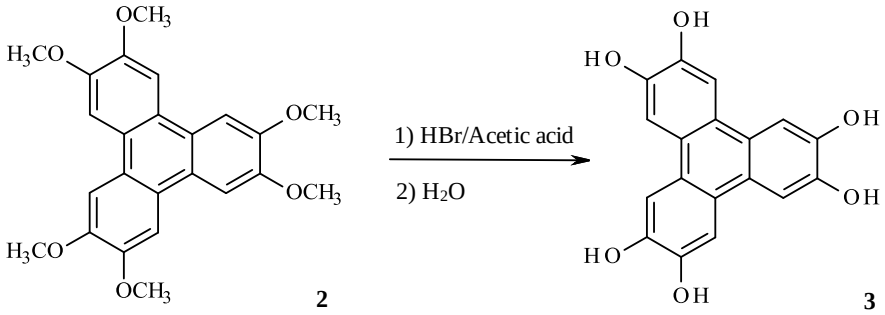

Scheme 9. Synthesis of hexa(hydroxy)triphenylene **3**

Piattelli *et al*[25] synthesised hexahydroxytriphenylene **3** by deprotection of hexamethoxytriphenylene **2** using acid. Therefore we carried out the deprotection in a mixture of refluxing HBr and glacial acetic acid (1:1) (Scheme 9). A good yield of 84 % is obtained so long as oxygen is excluded from the reaction.

2.3.3. Synthesis of 2,3-dimethoxytriphenylene 9

The core for the two model compounds **5** and **6** cannot be synthesised by the same method as above. This is because hexyl chains need to be placed regiospecifically on four of the substitution positions. These must be added during the synthesis of the core so that the positions in which the porphyrins are attached can be controlled. The hexyl chains will also increase the solubility of the molecule allowing it to dissolve in organic solvents and this is

essential for the next step of the synthesis to occur. However this makes the synthesis of the cores much more complicated and they have to be synthesised in a stepwise fashion.

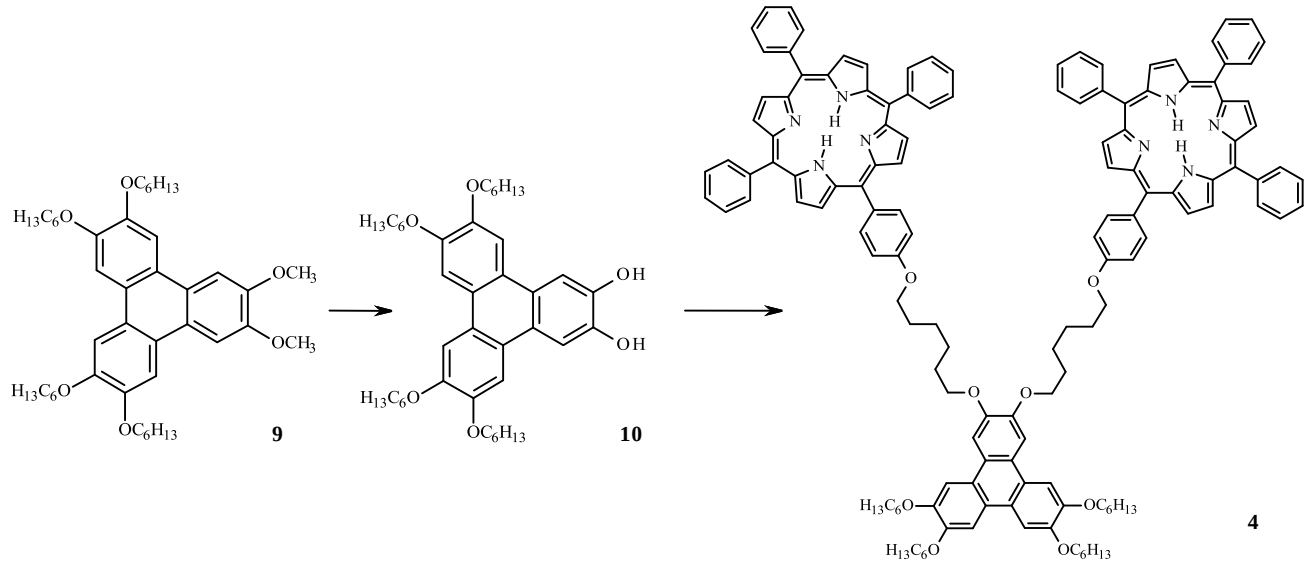

Scheme 10. Proposed synthesis of 2,3-bis(porphyrin)triphenylene **4**

The core for 2,3-bis(porphyrin)triphenylene **4** is formed by deprotection of 2,3-dimethoxytriphenylene **9** to produce 2,3-dihydroxytriphenylene **10** (Scheme 10). 2,3-Dimethoxytriphenylene **9** cannot be synthesised as simply as the hexa(methoxy)triphenylene **2**. A mixed cyclization between veratrole and 1,2-bis(hexyloxy)benzene **11** is possible but results in a mixture of all possible products. We therefore chose a stepwise synthesise which is illustrated in Scheme 11.

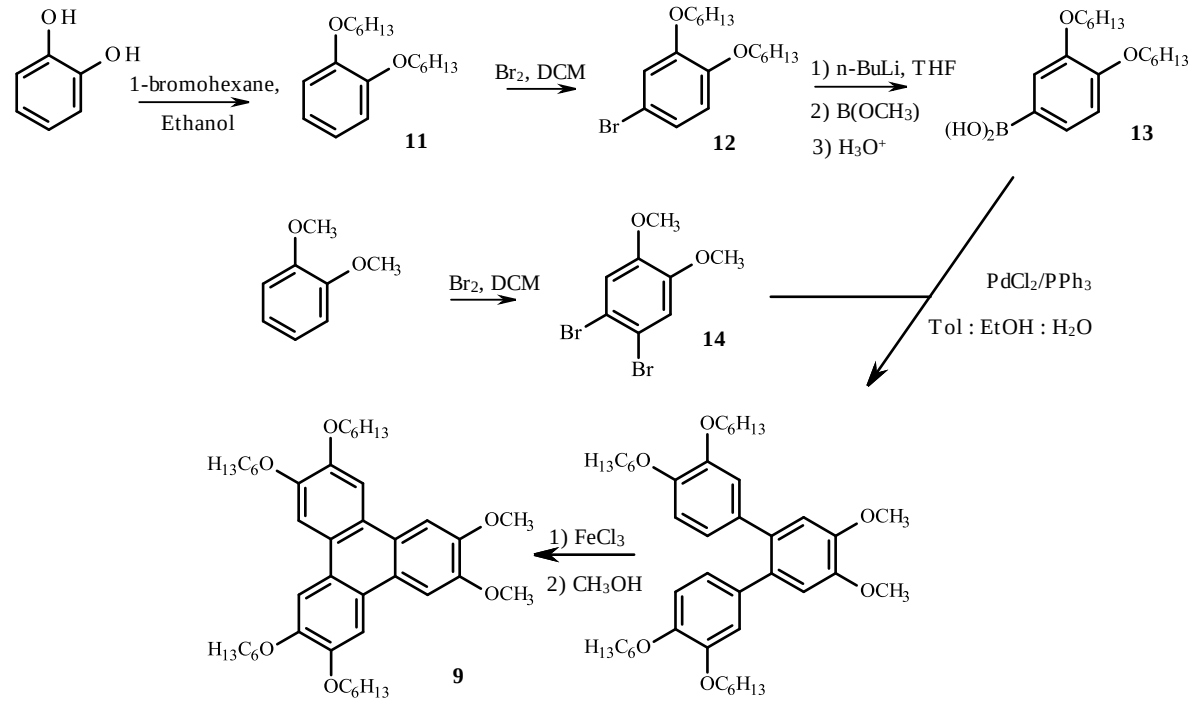

Scheme 11. Synthesis of 2,3-dimethoxytriphenylene **9**

1,2-Bis(hexyloxy)benzene **11** was prepared by alkylation of catechol with 1-bromohexane in refluxing ethanol, using potassium carbonate as a base, and the crude product was purified by distillation.[26] Bromination of **11** was initially achieved using NBS in DCM in the dark.[27] However, this method generally resulted in low yields and it was found to be more efficient to employ molecular bromine in DCM at -5 °C for this transformation. These improved conditions gave essentially quantitative yields in a reproducible reaction. Bis(hexyloxy)phenylbromide **12** was converted to the corresponding boronic acid **13** by lithiation with BuLi at -80 °C followed by addition of trimethylborate and work up.[28] Dibromodimethoxybenzene **14** was prepared by bromination (using 2 equivalents of bromine) of catechol in DCM at 0 °C. Suzuki-Miyaura[29,30] cross coupling between **14** and **13** (2 equivalents) employed $PdCl_2/PPh_3$ in a refluxing mixed solvent system (toluene : ethanol : water). The resulting *o*-terphenyl intermediate **15** was purified by column chromatography and cyclised to the triphenylene using $FeCl_3$ in DCM. The mechanism of the cyclization is shown in Scheme 12. [31]

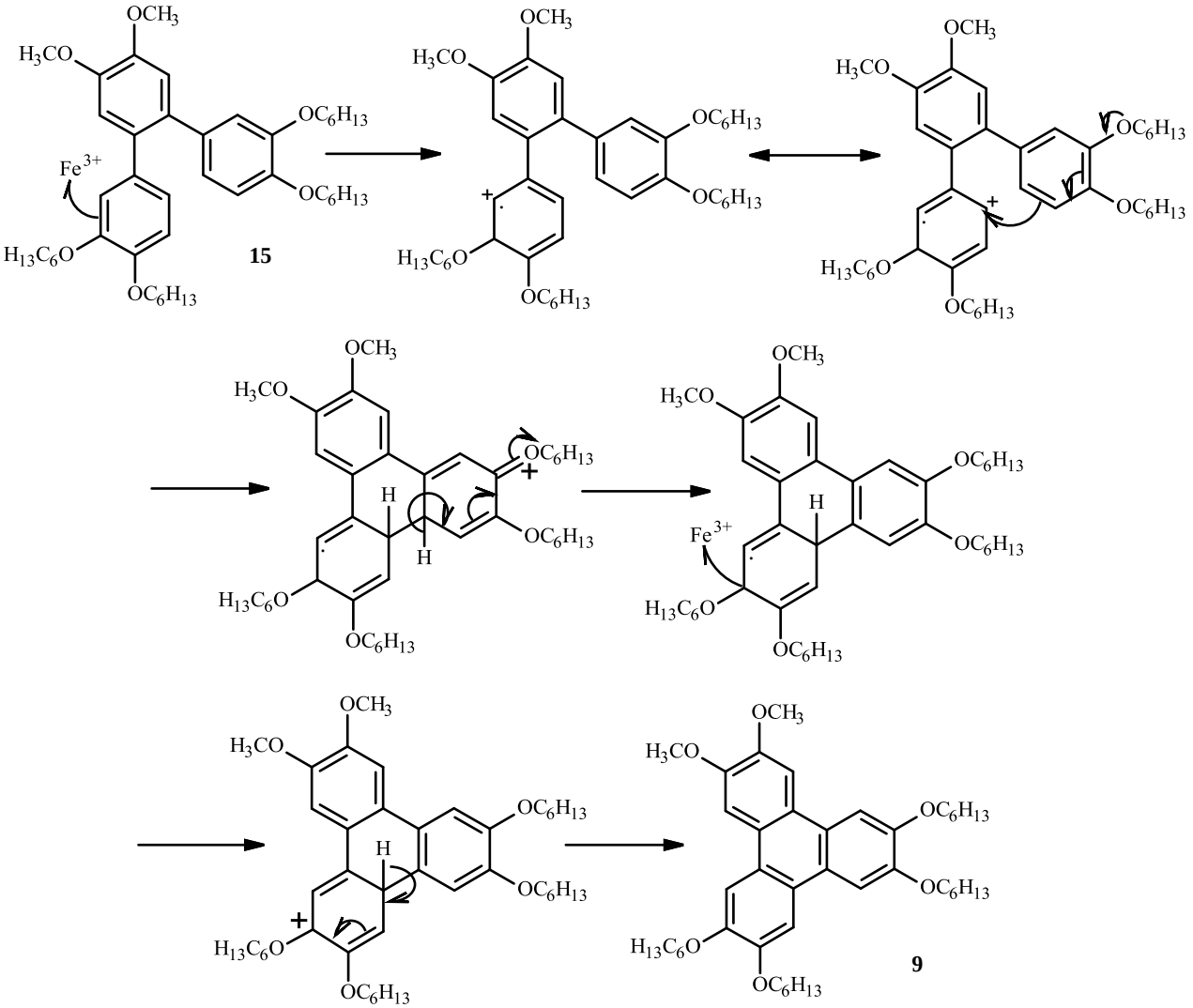

Scheme 12. Cyclization of the *o*-terphenyl **15**

Although the method shown in Scheme 11 does easily produce the desired triphenylene in good yields, the bis(hexyloxy)phenylboronic acid **13** must be used in excess. The production of bis(hexyloxy)phenylboronic acid **13** is a relatively low yielding reaction and so having to use an excess is not practical. This stimulated us find a different method that involved using less bis(hexyloxy)phenylboronic acid **13**. We found that by adding an extra step into the process only one equivalent of the boronic acid would be needed and this revised approach is shown in Scheme 13.

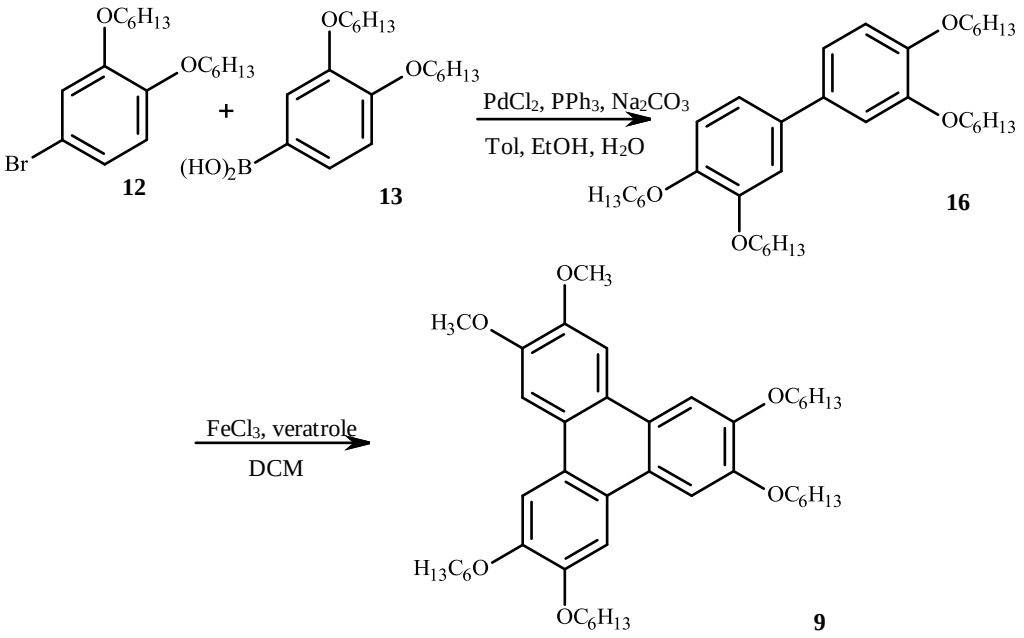

Scheme 13. Synthesis of 2,3-bis(methoxy)triphenylene **9** via a biphenyl

The extra step involves creating a biphenyl and only one equivalent of the bis(hexyloxy)phenylboronic acid **13** is used making the reaction more efficient. Reaction between 4-bromo-1,2-bis(hexyloxy)benzene **12** and bis(hexyloxy)phenylboronic acid **13** (in a 1:1 ratio) in a refluxing mixture of toluene, ethanol and water (in a 3:3:1 ratio) employed $Pd(PPh_3)_4$ as catalyst and Na_2CO_3 as base. The crude product was then recrystallised from ethanol to produce tetrakis(hexyloxy)biphenyl **16**.[8] This biphenyl was then cyclised with veratrole easily using $FeCl_3$ to produce the triphenylene product 2,3-bis(methoxy)triphenylene **9**.[18]

2.3.4. Synthesis of 2,3-bis(hydroxy)triphenylene 10

The deprotection of 2,3-dimethoxytriphenylene **9** involves the cleavage of the methoxy groups to phenolic groups. There are many known reactions that will perform such a hydrolysis e.g. using boron tribromide at room temperature[32] or refluxing the methoxy substrate in a mixture of hydrobromic acid and acetic acid as described by Bechgaard *et al.*[12] However both of these methods were thought to be too harsh to use on 2,3-dimethoxytriphenylene **9** because the hexyloxy groups present on the molecule are also susceptible to hydrolysis. Selective removal of methyl ethers can be achieved using lithium

diphenylphosphide and this method has been successfully applied to triphenylenes.[33] However, we chose to use a newer, mild method employing thiophenol.[34] Consequently 2,3-dimethoxytriphenylene **9** in refluxing dry DMF was reacted with $PhSH/K_2CO_3$. The mixture was acidified, cooled and the crude product purified by column chromatography to smoothly produce 2,3-dihydroxytriphenylene **10** (Scheme 14).

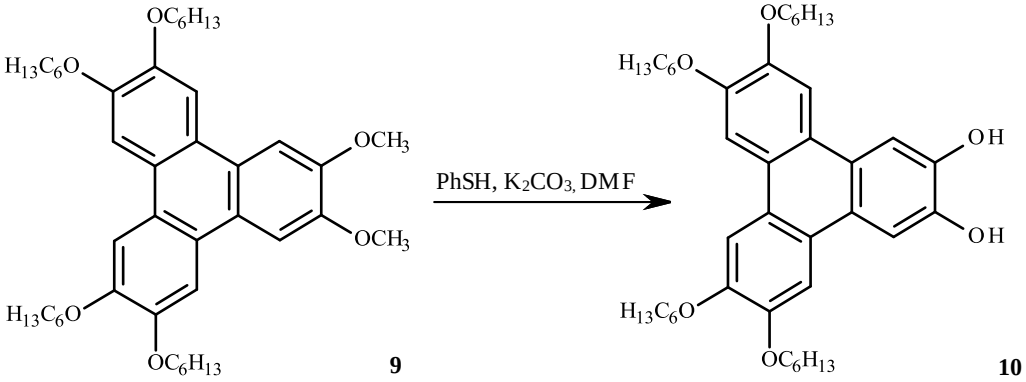

Scheme 14. Selective deprotection of 2,3-dimethoxytriphenylene **9**

2.3.5. Synthesis of 3,6-dimethoxytriphenylene 17

Deprotection of the methoxy groups on 3,6-bis(methoxy)triphenylene **17** produces the core of the second model compound 3,6-dihydroxytriphenylene **18** (Scheme 15).

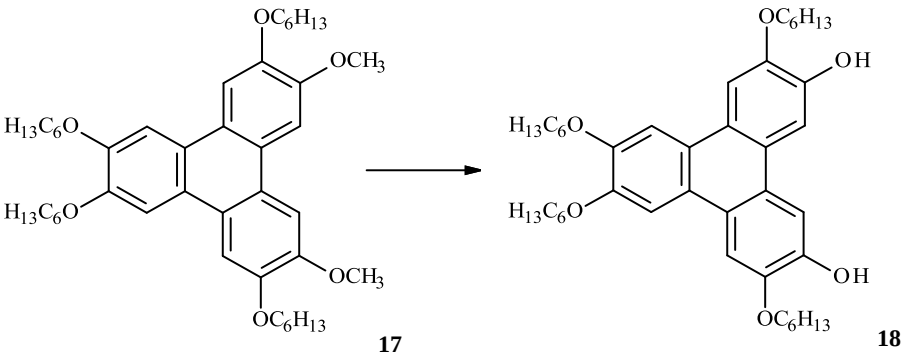

Scheme 15. Synthesis of 3,6-dihydroxytriphenylene **18**

The synthesis of 3,6-dihydroxytriphenylene **18** core could be performed by a similar method to that of the 2,3-dihydroxytriphenylene **10** core. This method was successful but the

synthesis still involves the production of a boronic acid and, as mentioned before, the yield of this is low. As a result we found a new method to synthesise the triphenylene 3,6-dimethoxytriphenylene **17** using a biphenyl without the need to synthesise a boronic acid (Scheme 16).

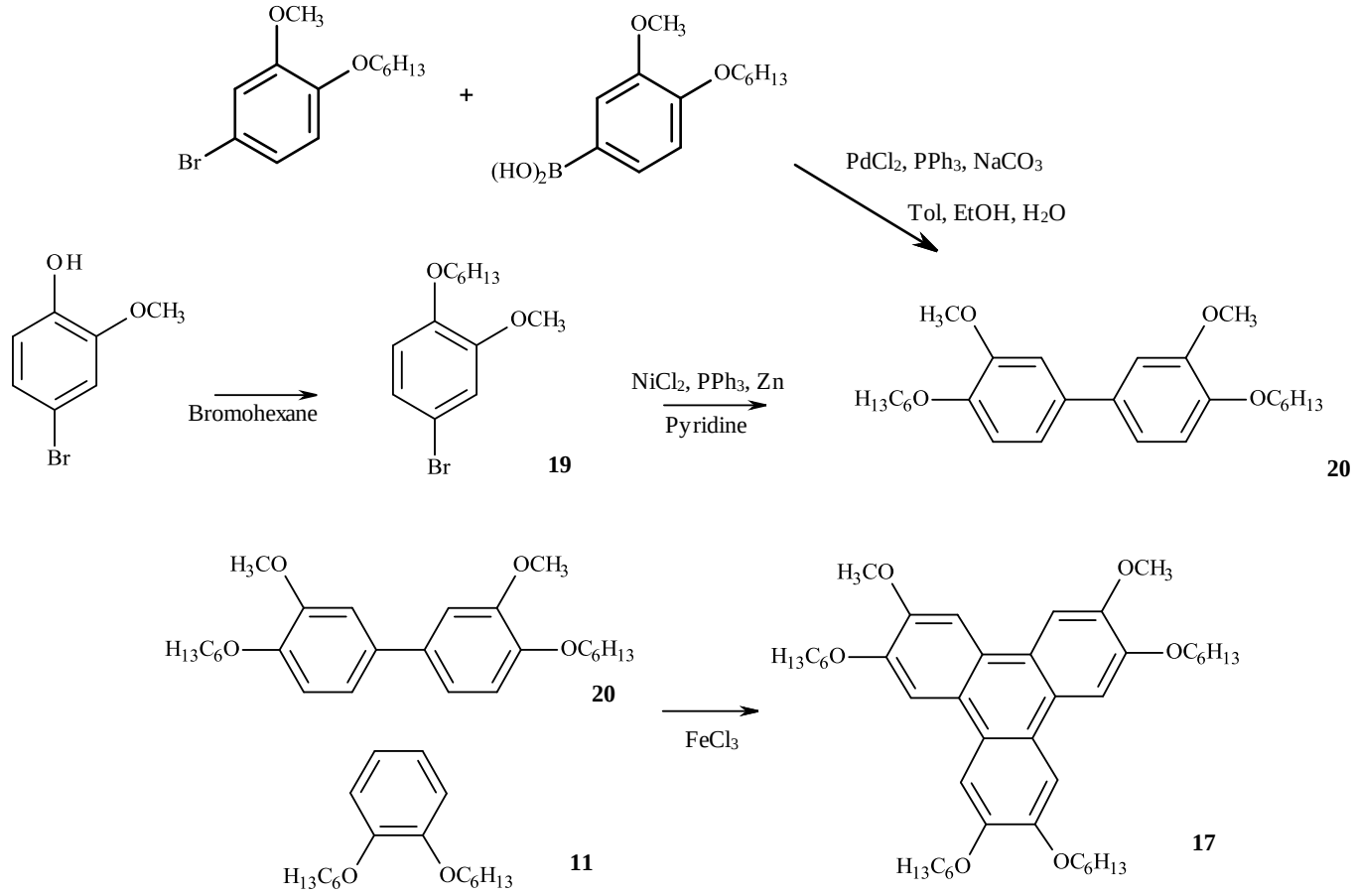

Scheme 16. The synthesis of 3,6-dimethoxytriphenylene **17**

The classic Ullmann coupling is the synthesis of biaryls via copper mediated coupling (figure 9). However, an adaption by Lin and co-workers utilizes nickel as a catalyst.[35] In our case, firstly the hydroxyl group on 4-bromo-2-methoxyphenol can be alkylated easily by an S_N2 reaction to produce 4-bromo-1-hexyloxy-2-methoxybenzene **19**. However rather than converting half of this product into a boronic acid to be used in a Suzuki reaction, the biphenyl **20** can be produced directly by reacting two molecules of bromide **19** catalysed by nickel.

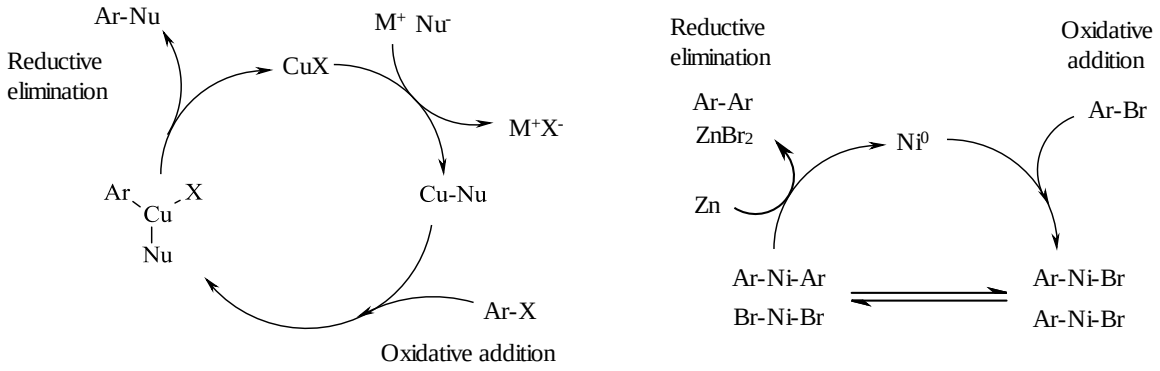

Figure 9. Ullmann coupling catalytic cycle with copper and with nickel

To synthesise dimethoxybishexyloxy biphenyl **20**, 4-bromo-2-methoxyhexyloxybenzene **19** was reacted in refluxing pyridine in the presence of $NiCl_2$, PPh_3 and Zn powder. After work up, biphenyl **20** was isolated in a yield of 31 %. This is a much higher overall yield than achieved by the production of tetrakis(hexyloxy)biphenyl **16** via the Suzuki-Miyaura coupling method. Biphenyl **20** was then cyclised with 1,2-bis(hexyloxy)benzene **11** to produce the 3,6-dimethoxytriphenylene core **17**, again employing iron trichloride. The crude product was then purified by column chromatography to produce the 3,6-dimethoxytriphenylene **17** (Scheme 17).[12]

2.3.6. Synthesis of 3,6-bis(hydroxy)triphenylene 18

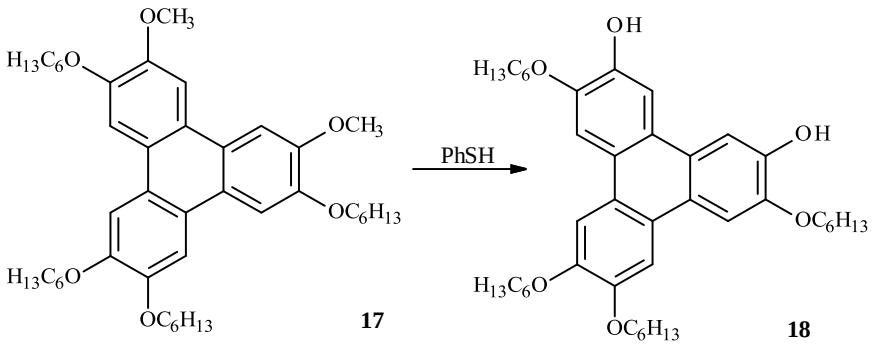

Scheme 17. Deprotection of 3,6-dimethoxytriphenylene **17**

The deprotection of 3,6-dimethoxytriphenylene **17** was achieved in the same way as for 2,3-dimethoxytriphenylene **9** described earlier using PhSH in refluxing DMF. The crude product

was purified by column chromatography to produce the 3,6-dihydroxytriphenylene core **18** (Scheme 17).[34]

2.4. Synthesis of 2,3-bis(porphyrin)triphenylene 4

2.4.1. Synthesis of 2,3-bis(bromohexyloxy)triphenylene 21

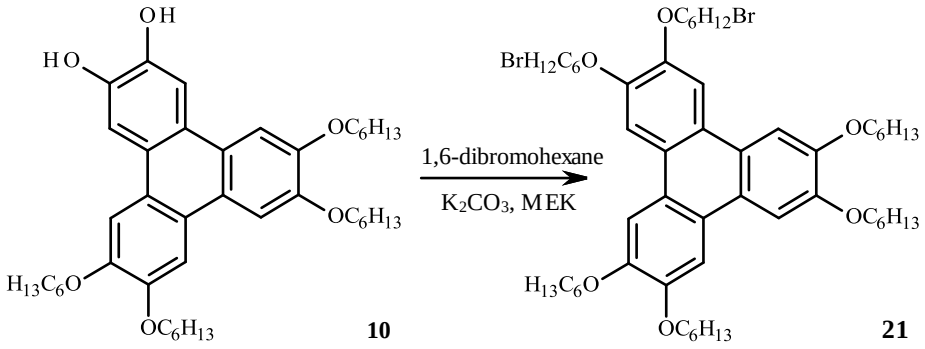

Scheme 18. Synthesis of 2,3-bis(bromohexyloxy)triphenylene **21**

The six carbon diether linker could be placed on either the triphenylene core or the porphyrin first, but the decision was taken to prepare the triphenylene intermediate and react it with the porphyrin. This decision was taken because it was thought that the chains will be relatively close together on the triphenylene and therefore the reaction would be easier without the bulky porphyrins attached. We also chose to perform this reaction on the triphenylene core of the model compound 2,3-bis(porphyrin)triphenylene **4** first as a test for the final multichromophore. The reaction between the hydroxyl groups on the triphenylene and the alkyl bromide group on the linking chains follows a simple S_N2 substitution reaction to produce the ether. So 2,3-dihydroxytriphenylene **10** in MEK, was reacted with 1,6-dibromohexane with K_2CO_3. The reaction was complete after 12 h and the crude product was purified by column chromatography to produce 2,3-bis(6-bromohexyloxy)triphenylene **21** in an overall yield of 13 % (Scheme 18).[36] This yield is relatively low, and it was suspected that this is due to the congestion associated with substitution at the 2 and 3 positions on the triphenylene.

Synthesis of 2,3-bis(porphyrin)triphenylene 4

The last step to making the first model compound 2,3-bis(porphyrin)triphenylene **4** was to combine the 2,3-bis(6-bromohexyloxy)triphenylene **21** with our chromophore hydroxyphenylporphyrin **1**. As this is another reaction between a hydroxyl group and an alkyl bromide, similar conditions were used to the above reaction between 1,6-dibromohexane and the triphenylene 2,3-dihydroxytriphenylene **10**. Consequently 2,3-bis(6-bromohexyloxy)triphenylene **21** was reacted with hydroxyphenylporphyrin **1** employing K_2CO_3 and KI in refluxing MEK. The reaction was monitored by TLC and stopped after 7 days. The crude product was purified by column chromatography to produce the first model compound 2,3-bis(porphyrin)triphenylene **4** in a low but acceptable yield of 12% (Scheme 19).

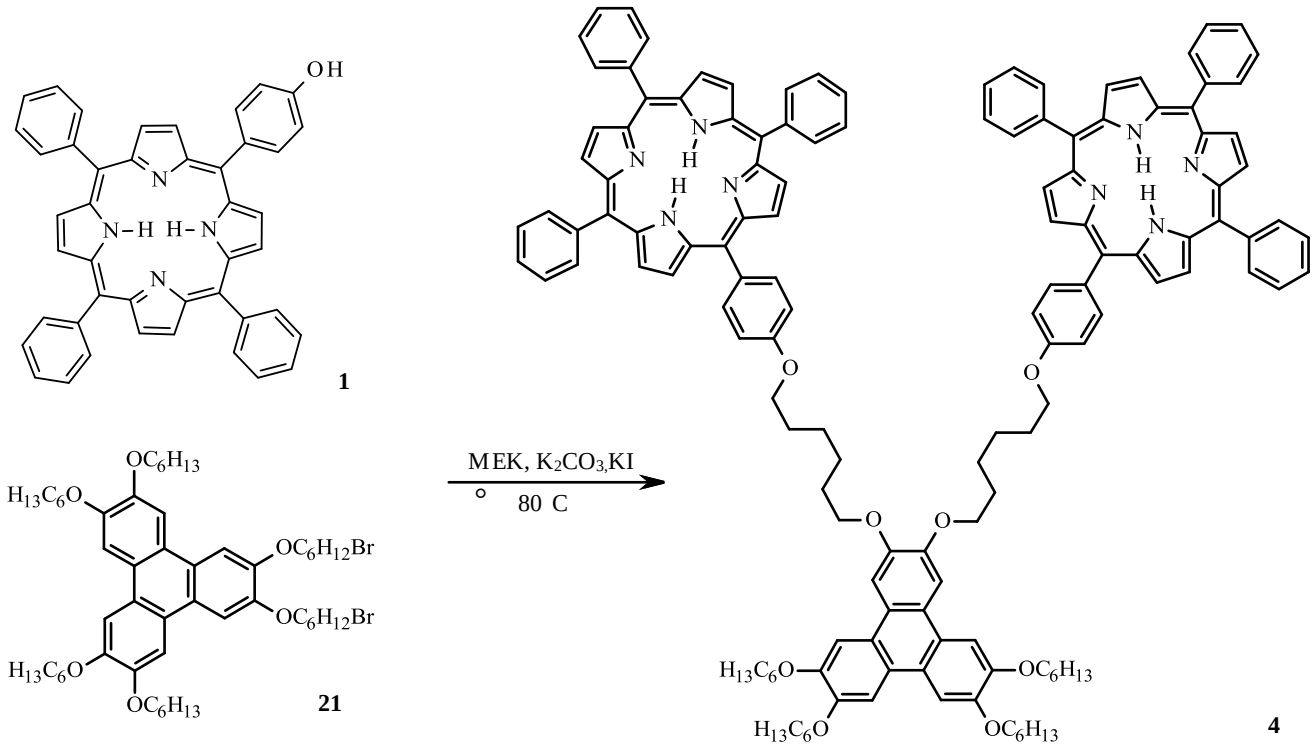

Scheme 19. Synthesis of 2,3-bis(porphyrin)triphenylene **4**

The yields of both the synthesis of 2,3-bis(6-bromohexyloxy)triphenylene **21** and of 2,3-bis(porphyrin)triphenylene **4** were very low. To try and rectify this we chose to take a slightly

different route. We chose to place the linker on the porphyrin rather than the triphenylene core to investigate whether this alternative sequence would be more efficient.

2.4.2. Synthesis of bromoalkoxyporphyrin 22

We reasoned that reaction between the porphyrin **1** and 1,6-dibromohexane should be very similar to that of the reaction between the triphenylene **10** and 1,6-dibromohexane. However, we identified that hydroxyphenylporphyrin **1** did not readily dissolve in MEK so the solvent was changed to DMF. Consequently hydroxyphenylporphyrin **1** in DMF was reacted with 1,6-dibromohexane employing K_2CO_3. The crude product was dissolved in DCM and then purified by column chromatography to isolate the product (6-bromohexyloxy)phenylporphyrin **22** in a yield of 47 % (Scheme 20).[36] This is a much higher yield than that of the reaction between the linker and the triphenylene core.

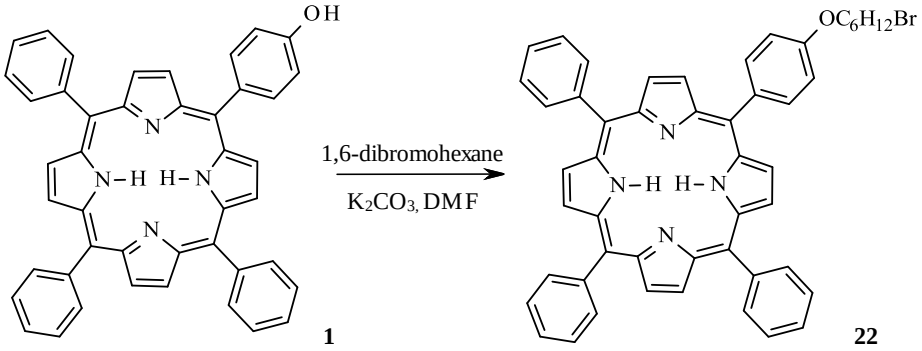

1 **22**

Scheme 20. Synthesis of bromoalkoxyporphyrin **22**

The unsymmetrical nature of bromoalkoxyporphyrin **22** is immediately apparent from inspection of its ^{1}H NMR spectrum, particularly when compared to the spectrum of TPP (Figure 10). We also expect a similar ^{1}H NMR spectrum for the porphyrin region of more complex arrays. At ca. 8.8 ppm we see signals corresponding to 8H for the porphyrin β-hydrogens. At ca. 8.2 and 7.8 ppm we find two broad signals integrating to 6H and 9H respectively that correspond to the hydrogens on the three unsubstituted phenyl rings (the phenyls are not equivalent which contributes to the broad signals observed). Signals for hydrogens on the substituted phenyl rings appear at 8.1 ppm and 7.2 ppm (masked by residual solvent peak). Characteristic signals for the methylene groups of the alkyl chain

appear at 4.25 ppm (-OCH_2-), 3.5 ppm (-CH_2Br), 2.0 ppm and 1.85 ppm. The distinctive signal for hydrogens in the centre of the porphyrins is observed at ca. -2.7 ppm.

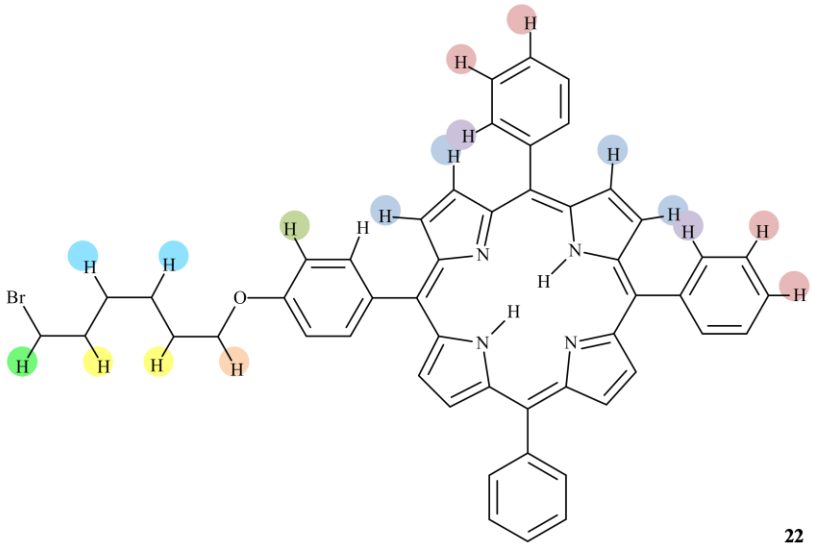

22

Bromoalkoxyporphyrin 22 showing dissimilar hydrogens

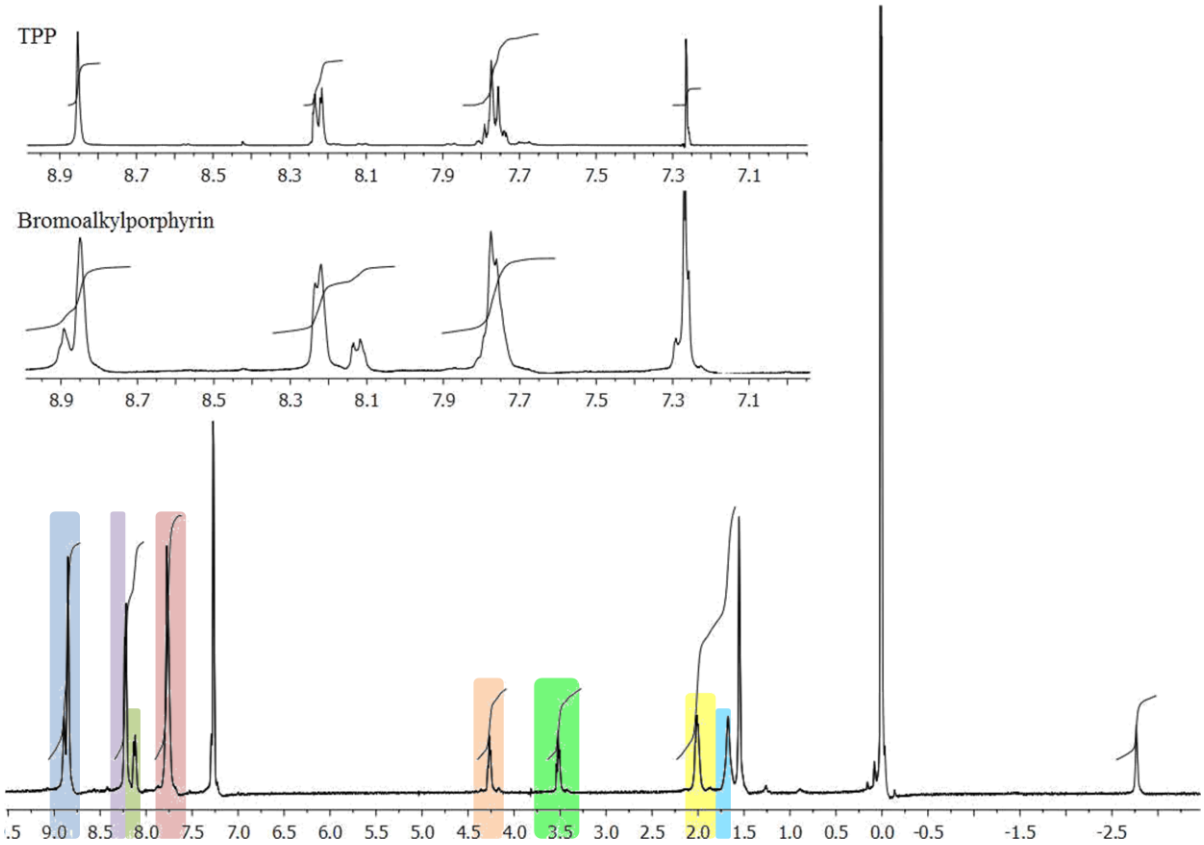

Figure 10. ^{1}H NMR of bromoalkylporphyrin **22** compared to ^{1}H NMR of TPP in $CDCl_3$

Alternative synthesis of 2,3-bis(porphyrin)triphenylene 4

The next step was to react the bromoalkoxyporphyrin **22** with the triphenylene core 2,3-dihydroxytriphenylene **10**. As the reaction is so similar to the reaction between 2,3-bis(6-bromohexyloxy)triphenylene **21** and hydroxyphenylporphyrin **1**, we chose to use the same reaction conditions. Therefore bromoalkoxyporphyrin **22** in refluxing MEK was reacted with 2,3-dihydroxytriphenylene **10** employing K_2CO_3 and KI. However no product was isolated from this reaction. The conclusion was reached that the reactants were not soluble enough in the MEK solvent so it was changed to DMF and the reaction repeated. The crude product was purified by column chromatography to produce 2,3-bis(porphyrin)triphenylene **4** in very small quantities. The column chromatography also revealed that there were many side products produced during the reaction. This caused us to investigate what could cause these results. It was found, according to the MSDS data sheet, that at high temperatures DMF can break down into dimethylamine and carbon monoxide or formic acid, especially in the presence of an acid or base and these could then react with our reactants producing side products (Scheme 21).[37]

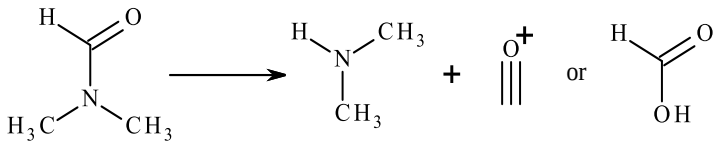

Scheme 21. Degradation of dimethylformamide

To try and prevent this we lowered the temperature of the reaction to 80 °C. Therefore bromoalkoxyporphyrin **22** in DMF was reacted with 2,3-dihydroxytriphenylene **10** employing K_2CO_3 and KI at 80 °C for 7 days. After work up the crude product was purified by column chromatography and this produced the desired product, 2.3-bis(porphyrin)triphenylene **4**, in a much higher yield of 48 % (Scheme 22).

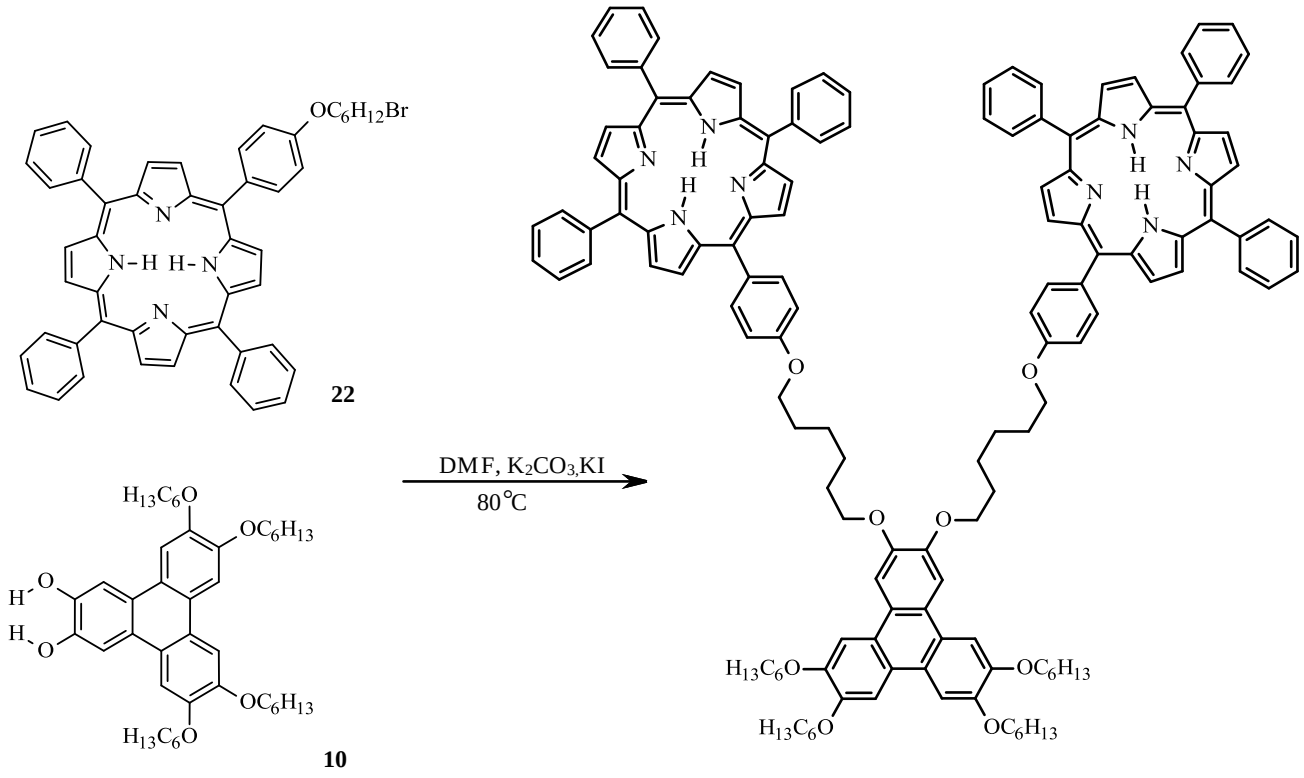

Scheme 22. Alternative synthesis of 2,3-bis(porphyrin)triphenylene **4**

The ^{1}H NMR spectrum of 2,3-bis(porphyrin)triphenylene **4** (figure 11) shows the same spectral pattern as that of the unsymmetrical bromoalkoxyporphyrin **22** with the addition of three peaks between ca. 7.8 – 8.0 ppm. Each peak integrates to two hydrogens and they are caused by the unsymmetrical nature of the triphenylene. The characteristic signal for the methylene group of the alkyl chain at 4.25 ppm (-OCH_2-) remains the same. However the signal at 3.5 ppm (-CH_2Br) no longer appears and instead a peak is present at ca. 4.2 ppm which integrates to 12 hydrogens. This corresponds to the methylene group of the alkyl chains (-OCH_2-) close to the triphenylene core. The remaining methylene groups of the alkyl chains appear as broad peaks between 0.90-2.19.

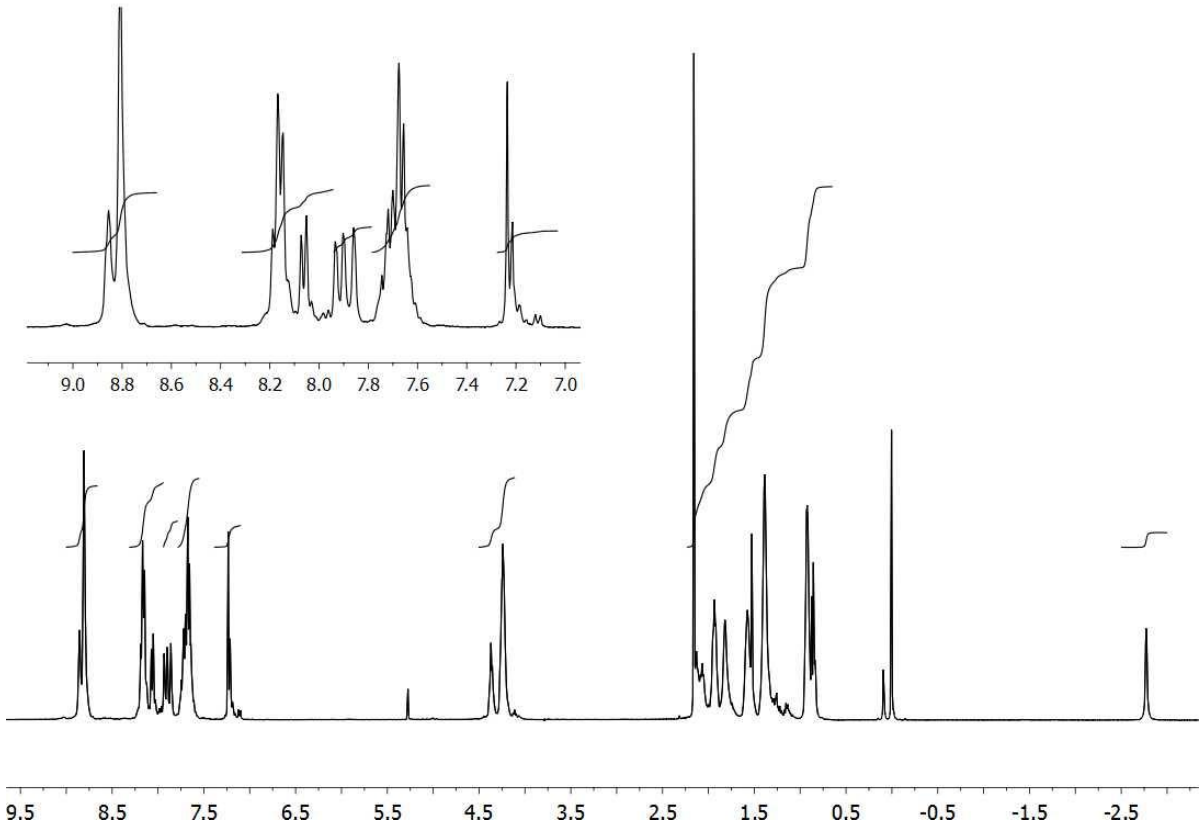

Figure 11. ^{1}H NMR Spectra of 2,3-bis(porphyrin)triphenylene **4** in $CDCl_3$

The MALDI mass spectrum of **4** is also shown in figure 12 and shows a peak at 2086 corresponding to the molecular ion. However, the spectrum was difficult to obtain and MALDI-MS were inconsistent run-to-run. It also showed clusters of peaks of low intensity around M^+ and higher intensity fragment ions.

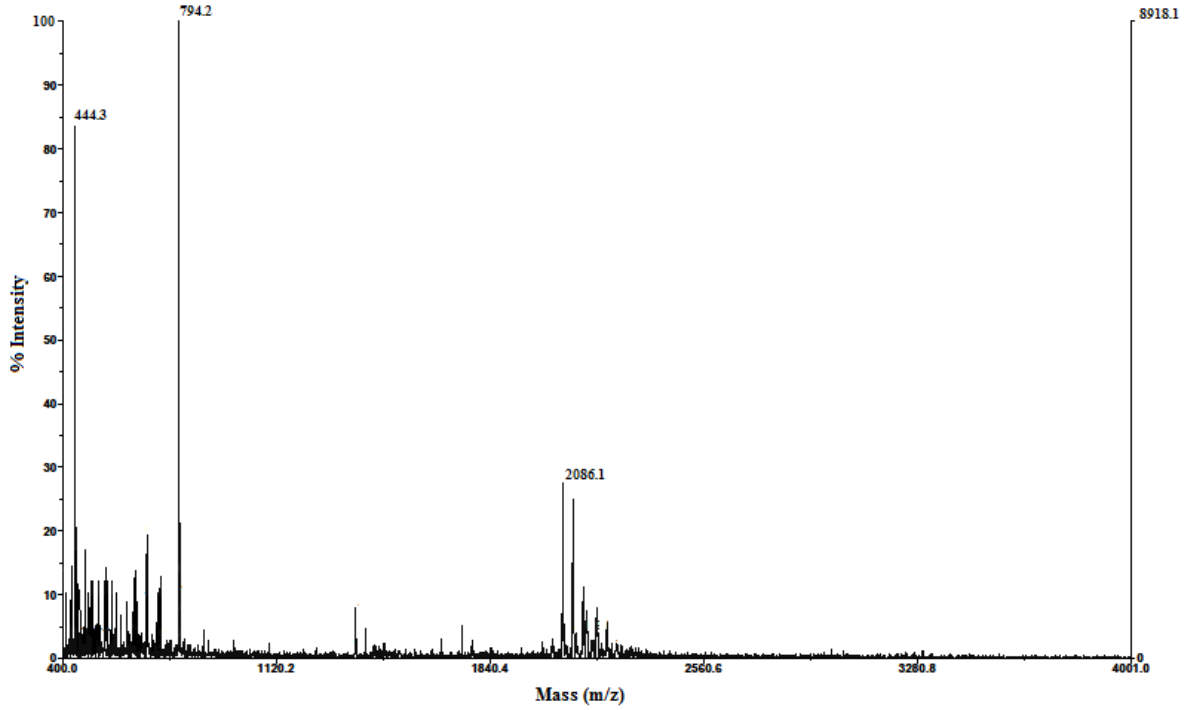

Figure 12. MALDI spectrum of 2,3-bis(porphyrin)triphenylene **4**

2.5. Synthesis of 3,6-bis(porphyrin)triphenylene 23

As this method produced such good yields the same method was performed to produce the second model compound 3,6-bis(porphyrin)triphenylene **23**. The bromoalkoxyporphyrin **22** in DMF was reacted with 3,6-dihydroxytriphenylene **18** employing K_2CO_3 and KI at 80 °C for 7 days. After work up and purification by column chromatography, the desired product, 3,6-bis(porphyrin)triphenylene **23** was produced with a yield of 31% (Scheme 23).

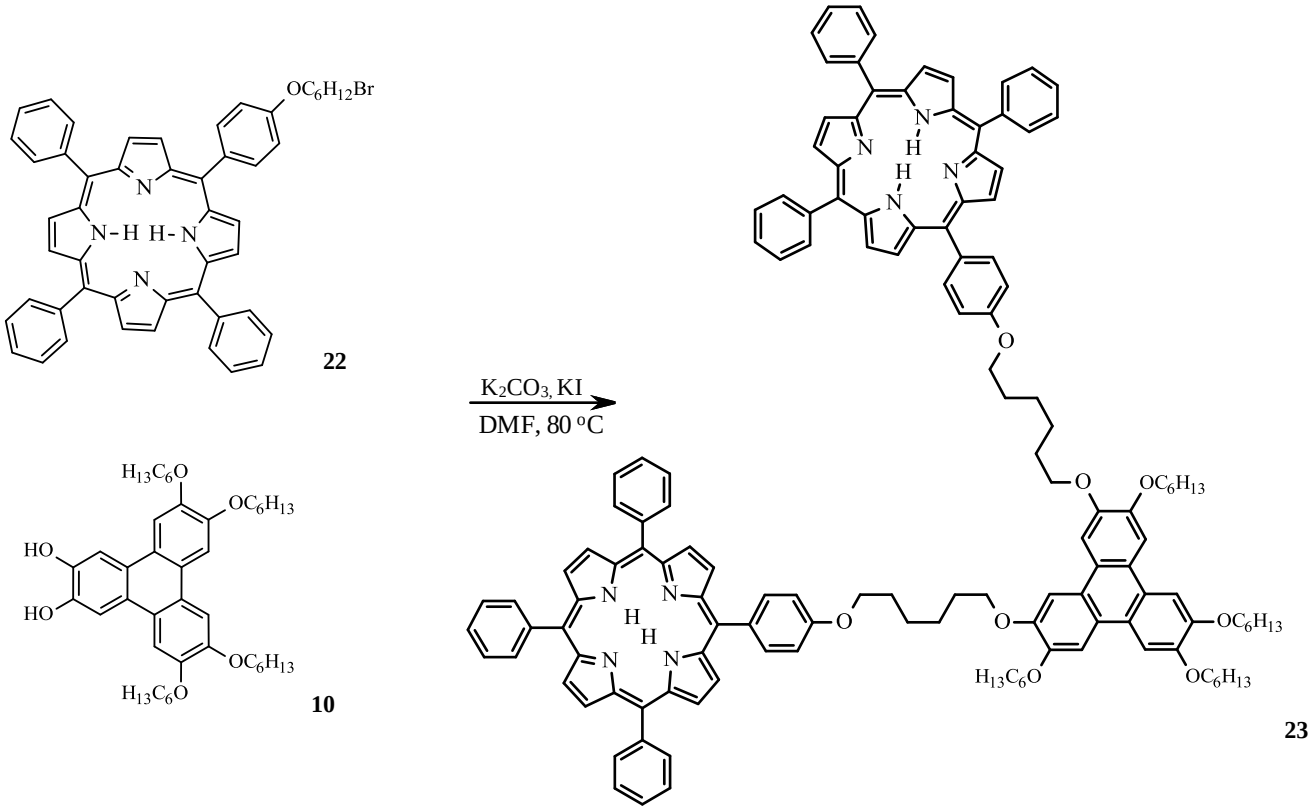

Scheme 23. Synthesis of 3,6-bis(porphyrin)triphenylene **23**

The ^{1}H NMR of 3,6-bis(porphyrin)triphenylene **23** (figure 13) is similar to that of 2,3-bis(porphyrin)triphenylene **4**. However there are some slight differences. The unsymmetrical porphyrins retain the spectral pattern of the bromoalkoxyporphyrin **22**. However the three triphenylene peaks between 7.8 ppm and 8.0 ppm are shifted and two are very close together. The characteristic signals for the methylene groups of the alkyl chain around 4.25 ppm (-OCH_2-) are now further resolved.

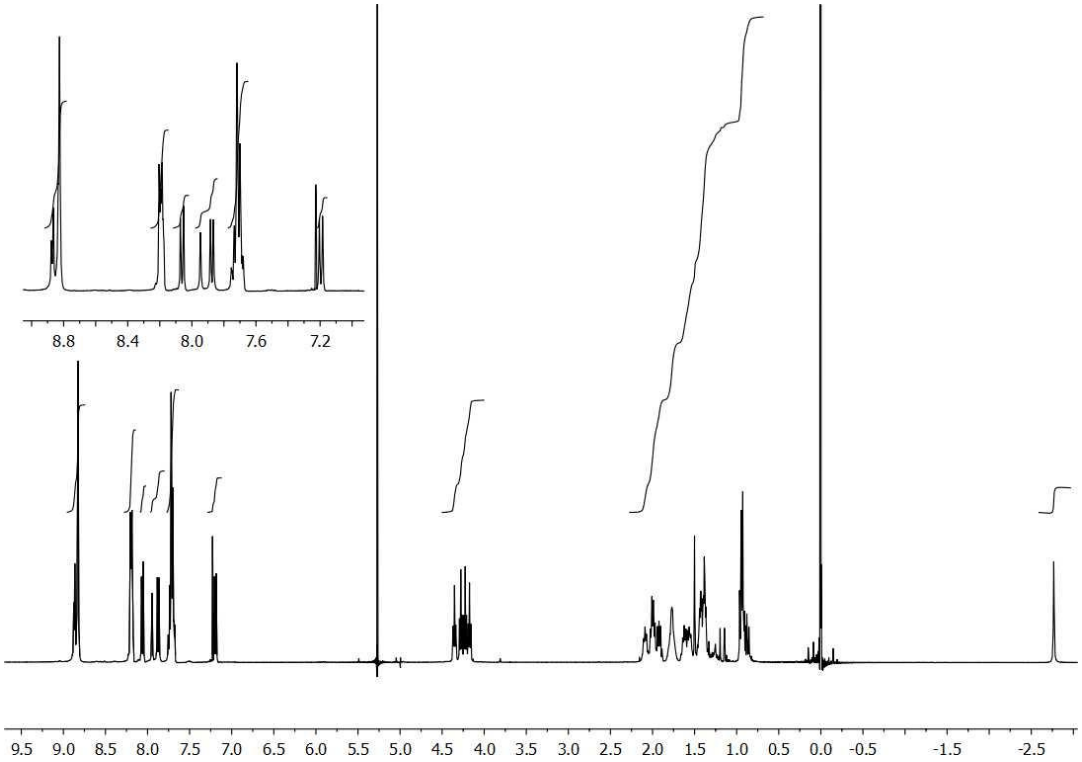

Figure 13. ^{1}H NMR spectra of 3,6-bis(porphyrin)triphenylene **23** in $CDCl_3$

The MALDI mass spectrum of 3,6-bis(porphyrin)triphenylene **23** is also shown in figure 14 and shows a peak at 2086 corresponding to the molecular ion.

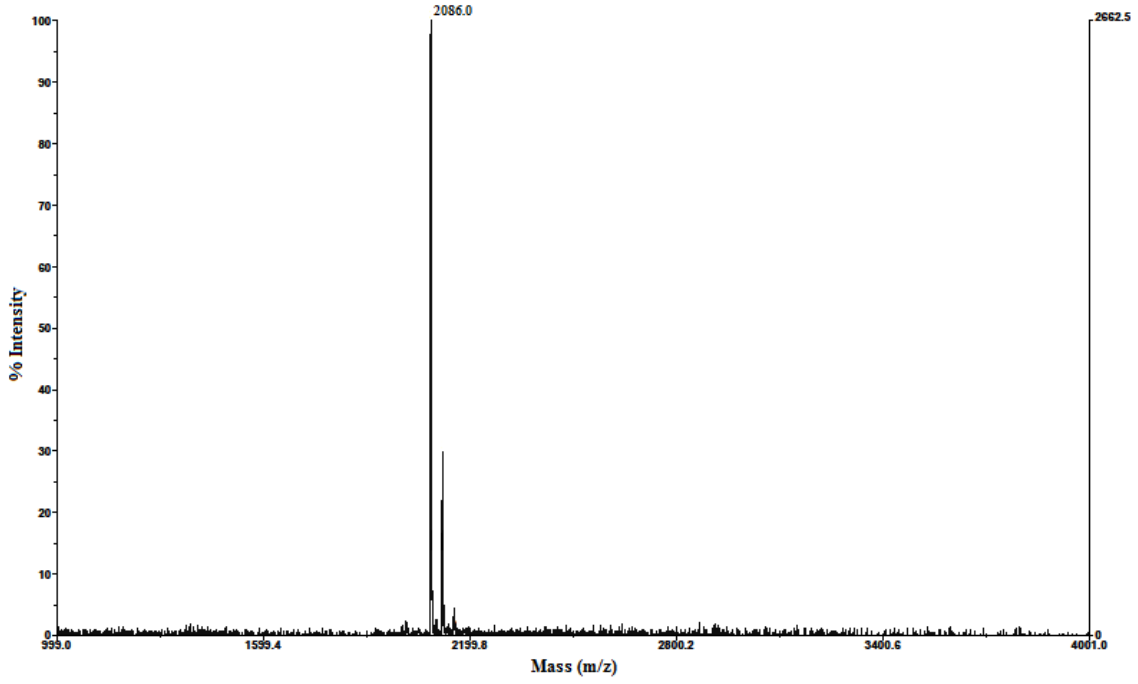

Figure 14. MALDI spectrum of 3,6-bis(porphyrin)triphenylene **23**

2.6. Synthesis of hexa(porphyrin)triphenylene 24

With both the model compounds produced we used the same reaction conditions to react the bromoalkoxyporphyrin **22** with the deprotected triphenylene core hexa(hydroxy)triphenylene **3**. The bromoalkoxyporphyrin **22** in DMF was reacted with hexa(hydroxy)triphenylene **3** employing K_2CO_3 and KI at 80 °C for 7 days. After word up and purification by column chromatography the product was isolated with yields of 22 % (Scheme 24).

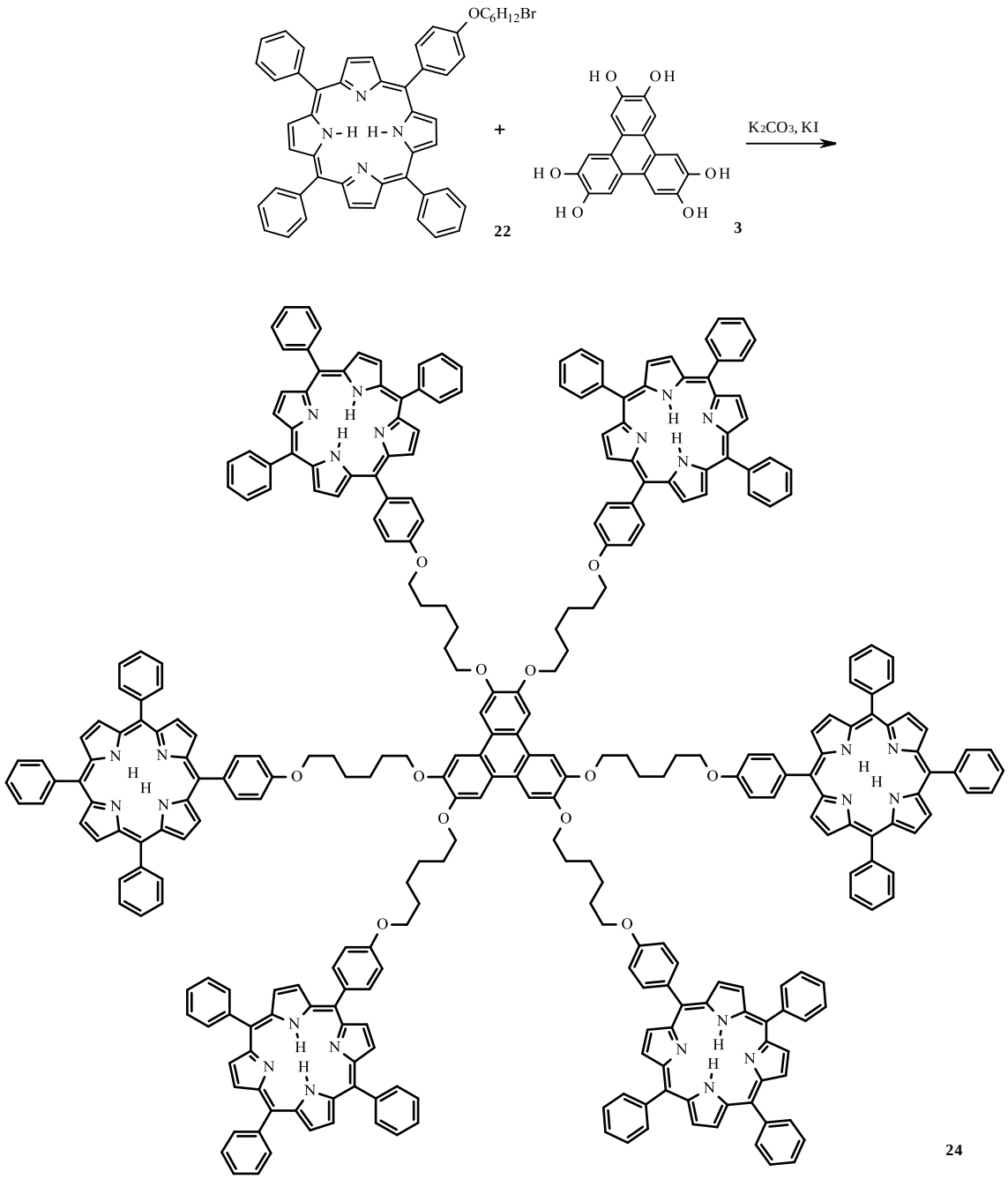

Scheme 24. Synthesis of hexa(porphyrin)triphenylene **24**

Spectral data corresponded to the hexa(porphyrin)triphenylene **24.** Figure 15 shows the ^{1}H NMR spectra and it can be seen that it is simplified due to the symmetrical nature of the molecule. The triphenylene should give a single peak, but this is not visible in the $CDCl_3$ spectrum. From looking at the integration of the porphyrin peaks it appears that the triphenylene peak is being masked by one of the porphyrin peaks. The solvent was changed from $CDCl_3$ to deuterated acetone and the expected signal is now visible at 8.15 ppm. The signals for the hydrogens on the substituted phenyl rings of the porphyrins now appear clearly. However the spectral pattern of the remainder of the porphyrin fragment remains the same as for the bromoalkoxyporphyrin **22**. Characteristic signals for the methyl groups of the alkyl chain appear around 4.25 ppm (porphyrin-OCH_2-) integrating to 12 hydrogens and 4.2 ppm (-CH_2O-triphenylene) also integrating to 12 hydrogens with the remaining peaks appearing at 2.0 ppm, 1.75 ppm, 1.65 ppm and 1.55 ppm.

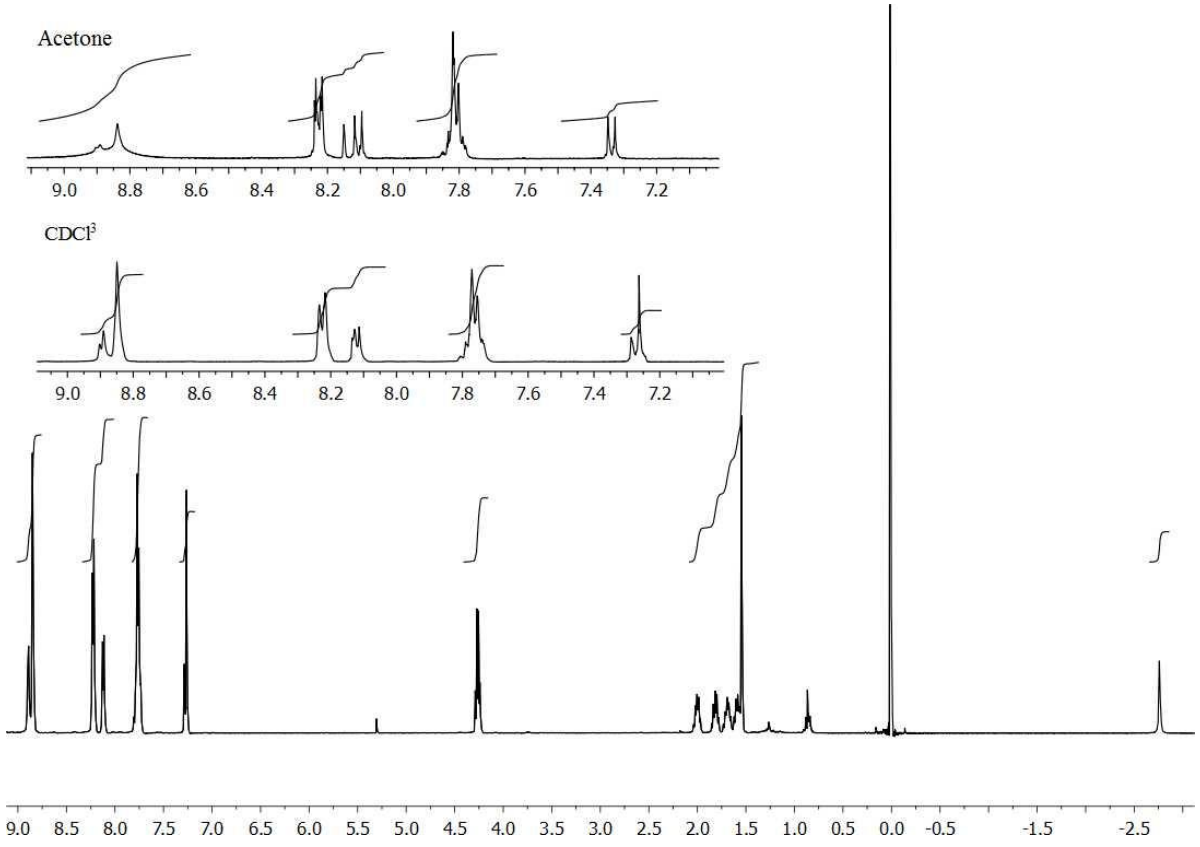

Figure 15. ^{1}H NMR spectra consistent with hexa(porphyrin)triphenylene **24**

We were unable to obtain a good MALDI-MS for compound **24**. Given the difficulties in obtaining MALDI-MS for the two model compounds, this was somewhat expected.

2.7. Increasing the number of chromophores

Following synthesis of the first generation compounds it was decided to extend the project by creating a multichromophore with twelve porphyrins around a central triphenylene core. The proposed synthesis for this was to attach a dimethoxyphenyl group to each of the 2,3,6,7,10,11-positions on the triphenylene core. We have performed a similar Suzuki reaction in the synthesis of triphenylenes so no real difficulties were expected, other than those associated with performing six sequential couplings on a triphenylene substrate. For this reaction we required use of triphenylene hexatriflate.[30]

2.7.1. Triflation of hexahydroxytriphenylene 3

As we have already produced the triphenylene core hexahydroxytriphenylene **3**, it was decided to convert this compound to its hexatriflate. This can be done easily using trifluoromethanesulphonic acid anhydride. Consequently, hexahydroxytriphenylene **3** was reacted with trifluoromethanesulphonic acid anhydride in a mixture of dry DCM and pyridine at -20 °C. After a work up, triphenylenehexatriflate **25** was produced as a cream powder (Scheme 25).[38]

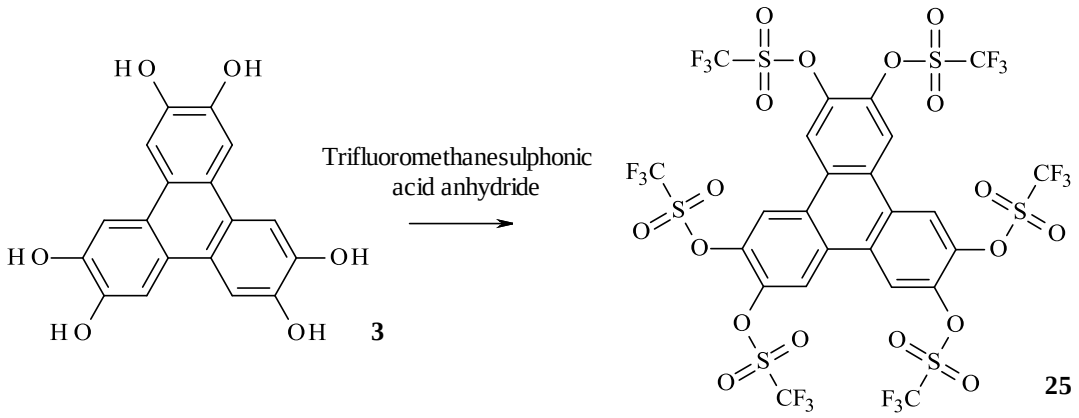

3 **25**

Scheme 25. Synthesis of triphenylenehexatriflate **25**

2.7.2. Synthesis of di(methoxy)benzeneboronic acid 26

Bromoveratrole is readily available so was selected for conversion to its corresponding boronic acid. The method used to produce this boronic acid is similar to that used earlier for the synthesis of the bis(hexyloxy)phenylboronic acid **13**. Bromoveratrole, in dry THF at -80°C, was lithiated with n-butyllithium to produce the intermediate. This was reacted with trimethylborate to form a boronic acid ester and hydrolysed with aqueous HCl to form di(methoxy)benzeneboronic acid **26** (Scheme 26).[30]

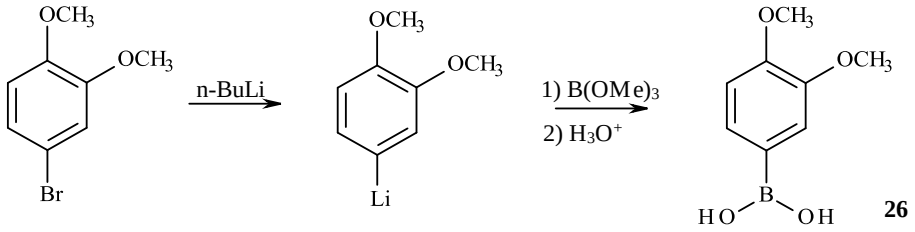

26

Scheme 26. Synthesis of di(methoxy)benzeneboronic acid **26**

2.7.3. Attempted synthesis of hexakis(dimethoxyphenyl)triphenylene 27

To make the hexakis(dimethoxyphenyl)triphenylene **27** we needed to react triphenylenehexatriflate **25** and di(methoxy)benzeneboronic acid **26**. The method chosen for this was adapted from a method by Flegeau and co-workers (Scheme 27),[38] where the boronic acid is reacted with the triflate in 1,4-dioxane. Therefore triphenylenehexatriflate **25** was reacted with boronic acid **26** in 1,4-dioxane employing $PdCl_2/PPh_3$ and K_3PO_4. However, after seven days TLC showed that there was essentially no reaction. Therefore it was decided to use a method from a different publication.[8] Suzuki-Miyaura cross coupling between triphenylenehexatriflate **25** and **26** was attempted in a refluxing mixed solvent system of toluene, ethanol and water (3:3:1) employing $PdCl_2$, PPh_3 and Na_2CO_3. After this time a TLC showed that a large number of products were present. Therefore we chose to investigate this reaction further.

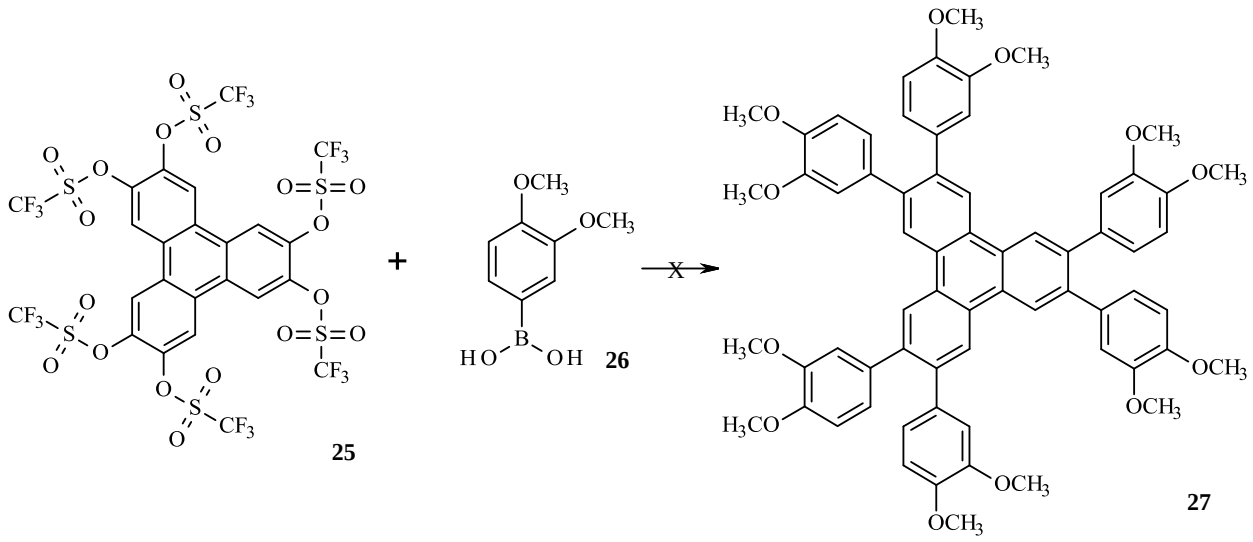

Scheme 27. Attempted synthesis of hexakis(dimethoxyphenyl)triphenylene **27**

2.7.4. Triflation of 2,3-bis(hydroxy)triphenylene 10

We chose to investigate what was happening within this reaction by performing the same reaction sequences on the model compound 2,3-dihydroxytriphenylene **10**. As 2,3-bis(hydroxy)triphenylene **10** only has two reaction sites instead of six, the number of side products is limited and therefore results should be much easier to interpret. Triphenylene-2,3-ditriflate **28** was prepared by the reaction of 2,3-dihydroxytriphenylene **10** with trifluoromethanesulphonic acid anhydride in the presence of pyridine in DCM (-20 °C). After work up the product, triphenylene-2,3-ditriflate **28** was isolated (Scheme 28).[8]

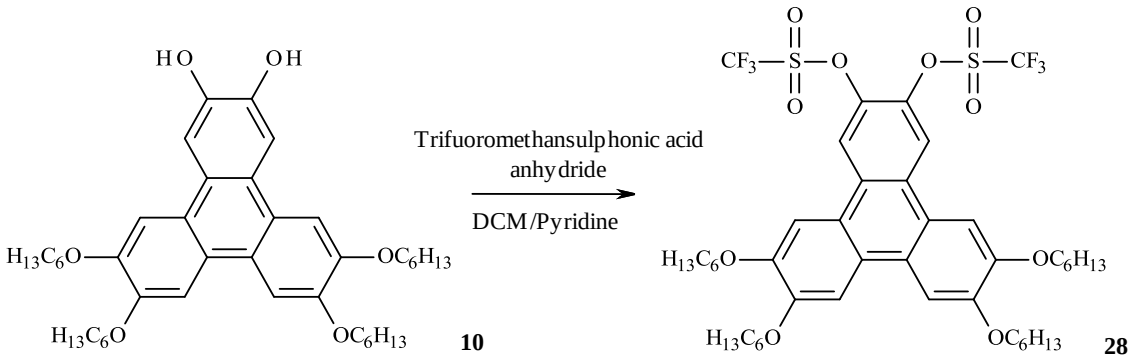

Scheme 28. Synthesis of triphenylene-2,3-ditriflate **28**

2.7.5. Attempted synthesis of 2,3-bis(3,4-dimethoxyphenyl)triphenylene 29.

The Synthesis of 2,3-bis(3,4-dimethoxyphenyl)triphenylene **29** was attempted by Suzuki reaction between triphenylene-2,3-ditriflate **28** and di(methoxy)benzeneboronic acid **26** in a mixed solvent system of refluxing toluene, ethanol and water (in a 3:3:1 ratio) employing $PdCl_2$, PPh_3 and Na_2CO_3 (Scheme 29).[8] After several days TLC showed one major product and this was isolated by column chromatography.

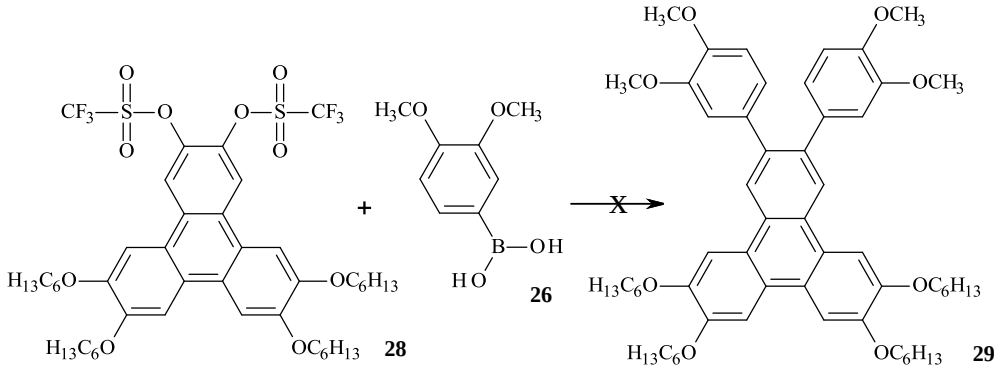

Scheme 29. Attempted synthesis of 2,3-bis(3,4-dimethoxyphenyl)triphenylene **29**

However it was discovered that the isolated compound was not the desired product **29** but rather (dimethoxyphenyl)triphenylene **30** (Figure 16).

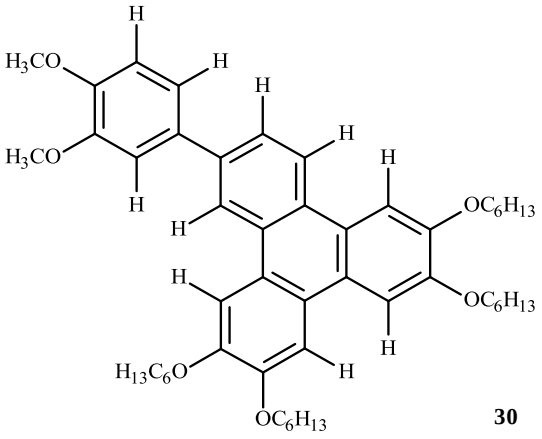

Figure 16. (Dimethoxyphenyl)triphenylene **30**

This is clearly shown in the ^{1}H NMR spectra (figure 17). The dimethoxyphenyl hydrogens are seen at ca. 7.4, 7.35 and 7.05 ppm, integrating to one hydrogen each. Five of the six remaining peaks integrate to one hydrogen each with the last peak integrating to two hydrogens. A characteristic signal for the methylene groups of the alkyl chains appear at 4. 5 ppm (-OCH_2-), 2.0 ppm, 1.6 ppm (masked my water), 1.4 ppm and 1.0 ppm. There are also signals for the two methoxy groups at ca. 4.0 ppm.

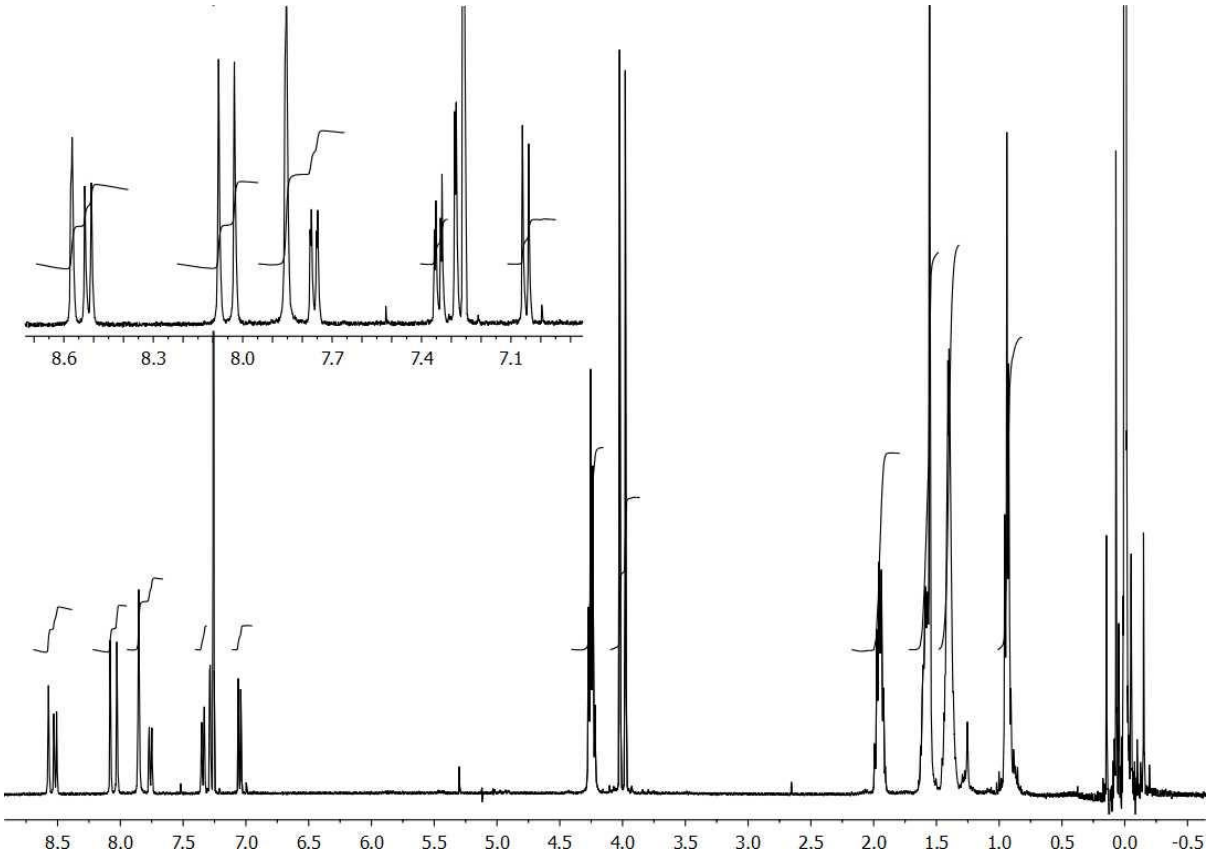

Figure 17. ^{1}H NMR spectra of (dimethoxyphenyl)triphenylene **30** in $CDCl_3$

The conclusion was reached that the 3,4-di(methoxy)benzeneboronic acid **26** reacts easily with one of the triflate groups on the triphenylene. However the second addition of **26** is very slow due to the lack of space around the triphenylene caused by the addition of the first dimethoxyphenyl fragment. As a result a second kinetically favoured reaction occurs preferentially. This is the reduction (protonolysis) of the triflate group (Scheme 30).

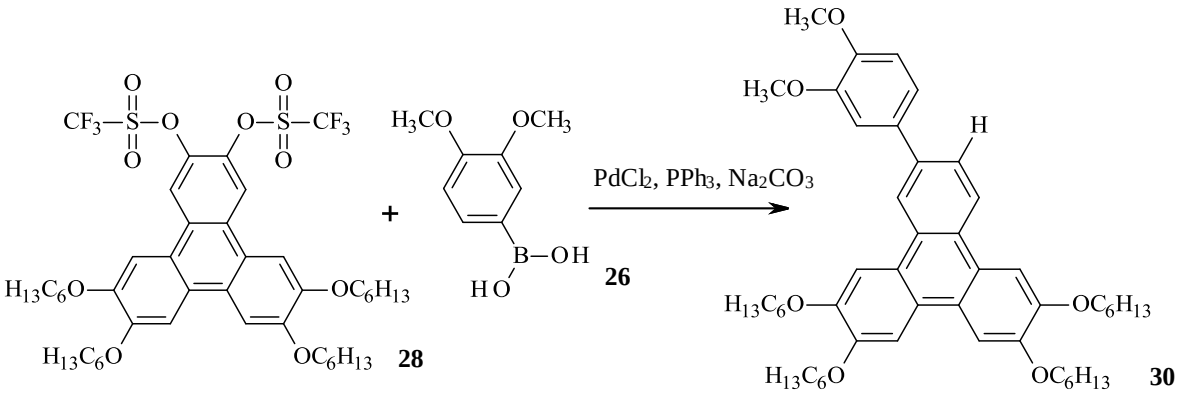

Scheme 30. Reaction between di(methoxy)benzeneboronic acid **26** and triphenylene-2,3-ditriflate **28**

This explains well the result from the attempted synthesis of hexakis(dimethoxyphenyl)triphenylene **27**. As there are six substitution points on triphenylenehexatriflate **25**, there are many more possible isomers that could be created when this is reacted with the di(methoxy)benzeneboronic acid **26**. These isomers along with a small amount of desired product explains the large number of products that produced a very complex TLC in the attempted synthesis of hexakis(dimethoxyphenyl)triphenylene **27** (figure 18). The reaction was not investigated further.

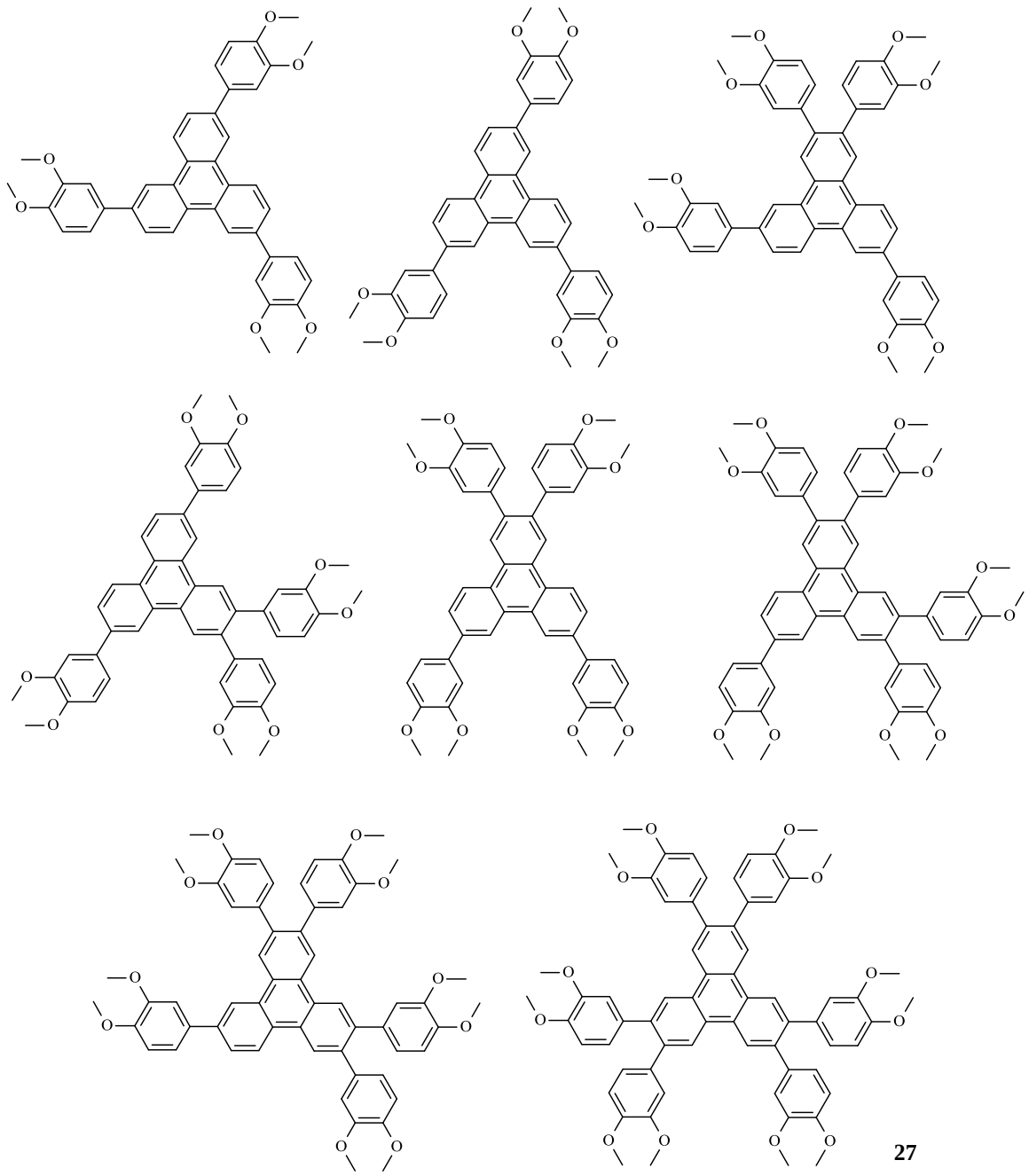

Figure 18. Isomers and products produced when triphenylenehexatriflate **25** and dimethoxyphenylboronic acid **26** are reacted

2.8. Metalation of the model compounds and the final multichromophore

2.8.1. Song method[39]

All of the multichromophore arrays synthesised had to be metalated with zinc. One method for this reaction was developed by Song *et al.*[39] Zinc-2,3-bis(porphyrin)triphenylene **5** was prepared by reaction of 2,3-bis(porphyrin)triphenylene **4** in DMF with an excess of zinc acetate at 80 °C. The reaction was monitored by UV-Vis spectroscopy (This is explained in further detail in section 2.8.3 below). After work up the product zinc-2,3-bis(porphyrin)triphenylene **5** was smoothly produced (Scheme 31).

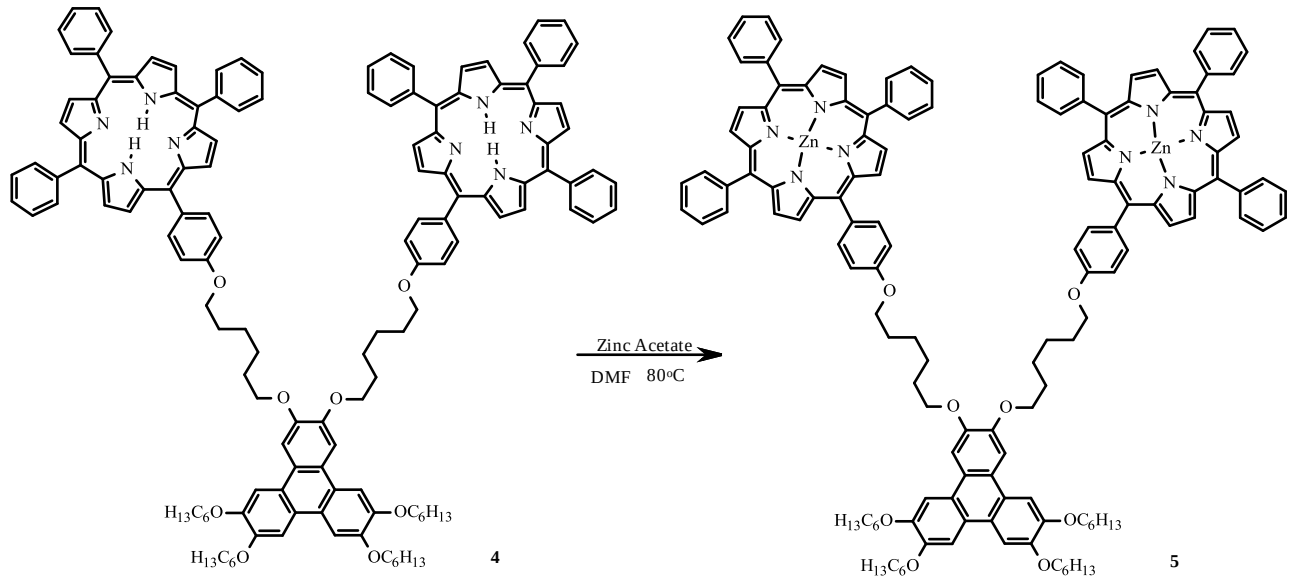

Scheme 31. Song method for the synthesis of zinc-2,3-bis(porphyrin)triphenylene **5**

The ^{1}H NMR spectrum clearly shows the completion of the metalation, as the distinctive signal for hydrogens in the centre of the porphyrins which was observed at ca. -2.7 ppm has now completely disappeared (figure 19). However the remaining signals are essentially the same as that observed for 2,3-bis(porphyrin)triphenylene **4**.

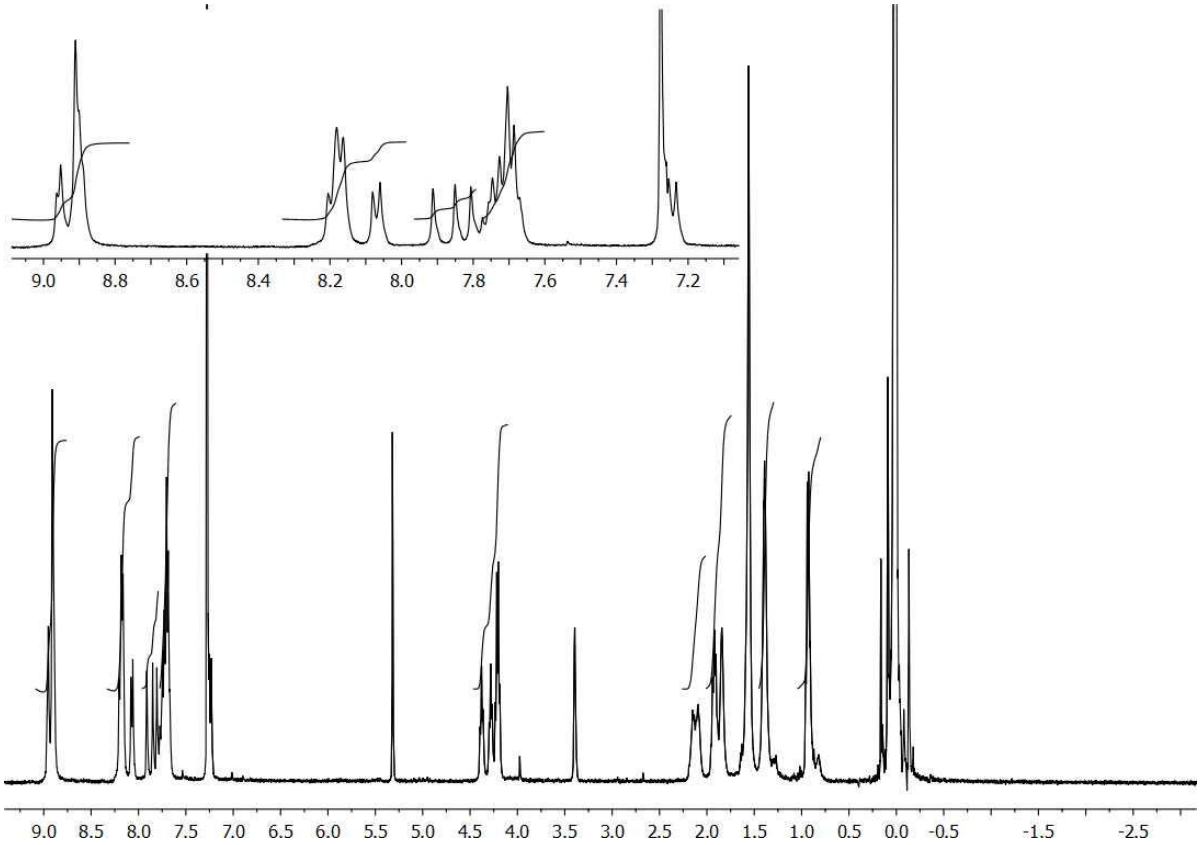

Figure 19. ^{1}H NMR spectra of zinc-2,3-bis(porphyrin)triphenylene **5**

The MALDI mass spectrum of **5** is shown in figure 20 and shows a peak at 2216 corresponding to the molecular ion. However, the spectrum also shows a peak at 2248 which corresponds to compound **5** with a single methanol molecule bound to one of the zinc metal centres. The peak at 2087 corresponds to the unmetalated compound 2,3-bis(porphyrin)triphenylene **4**. This compound was not visible in either the ^{1}H NMR spectrum or within the UV-Visible spectrum of compound **5** and therefore the amount present must be negligible. The MALDI-MS was difficult to obtain, and showed some clustering of peaks of low intensity around M^{+} and some higher intensity fragment ions.

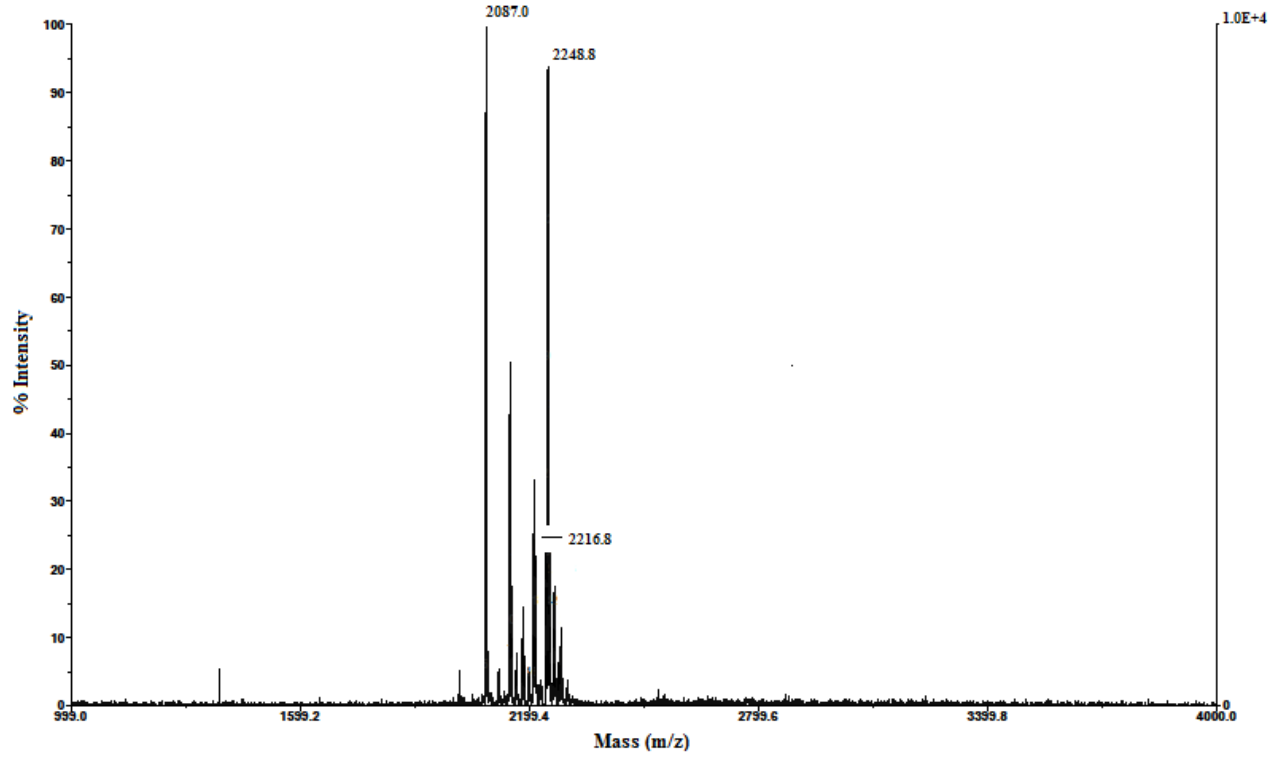

Figure 20. MALDI-MS spectra of zinc-2,3-bis(porphyrin)triphenylene **5**

2.8.2. Fukuzumi method

Although the previous reaction works well we found that it was very difficult to remove all of the DMF after the reaction was complete. Consequently it was decided to adapt a method developed by Fukuzumi *et al.*[40] The solvent was changed to DCM and the reaction performed at room temperature. This method worked very well and so was repeated for the second model compound 3,6-bis(porphyrin)triphenylene **23** and the final multichromophore hexa(porphyrin)triphenylene **24**. Both of these reactions produced the products zinc-3,6-bis(porphyrin)triphenylene **6** and (we presumed) zinc hexa(porphyrin)triphenylene **7** in good yields of 80 % and 63 % respectively (figure 21).

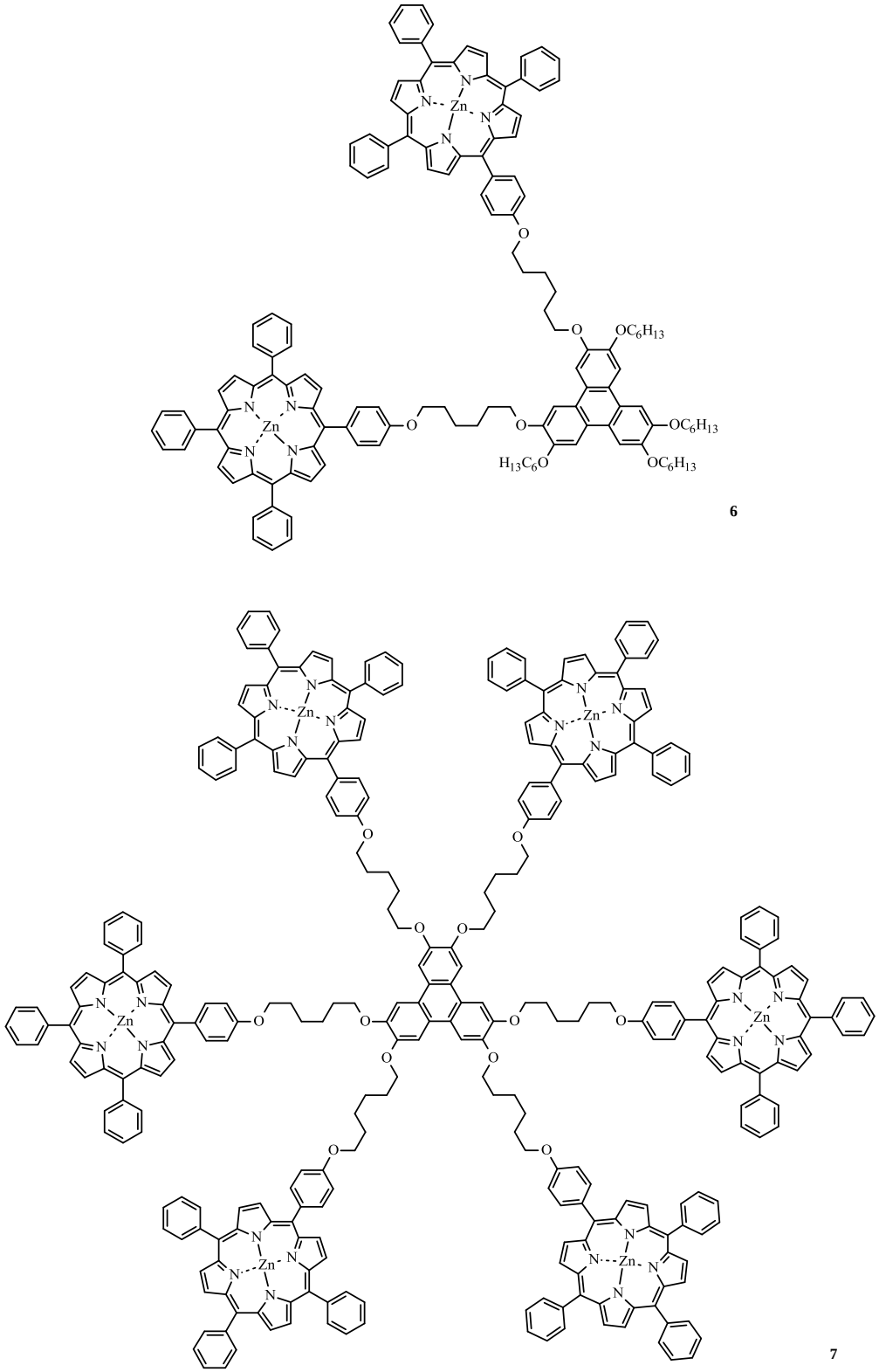

Figure 21. Zinc-3,6-bis(porphyrin)triphenylene **6** and zinc hexa(porphyrin)triphenylene **7**

The ^{1}H NMR spectra of both of these compounds reinforce what we have seen previously. Both molecules have comparable ^{1}H NMR spectra to that of the unmetalated compounds excepting the peak assigned to the signal for the hydrogens in the centre of the porphyrins (figure 22).

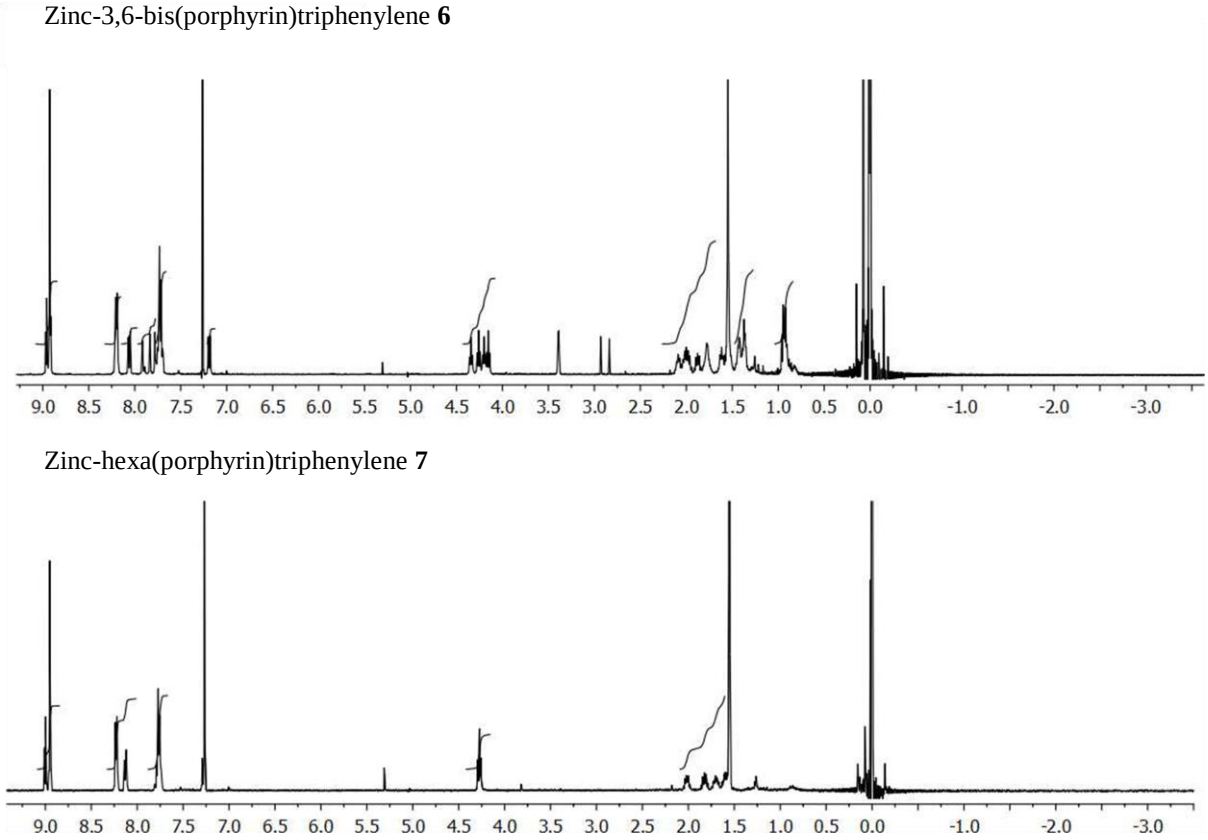

Figure 22. ^{1}H NMR spectra of zinc-3,6-bis(porphyrin)triphenylene **6** in $CDCl_3$ and the compound assumed to be zinc-hexa(porphyrin)triphenylene **7**

The MALDI mass spectrum of **6** is also shown in figure 23 and shows a peak at around 2216 corresponding to the molecular ion. However, the spectrum also shows a peak at 2248 which corresponds to compound **6** with a single methanol molecule bound to one of the zinc metal centres. The peak at 2086 corresponds to the unmetalated compound 2,3-bis(porphyrin)triphenylene **23**. This compound was not visible in either the ^{1}H NMR spectrum or within the UV-Visible spectrum of compound **6** and therefore the amount present must be negligible. Again, MALDI-MS was difficult to obtain, and showed some clustering of peaks of low intensity around M^{+} and some higher intensity fragment ions.

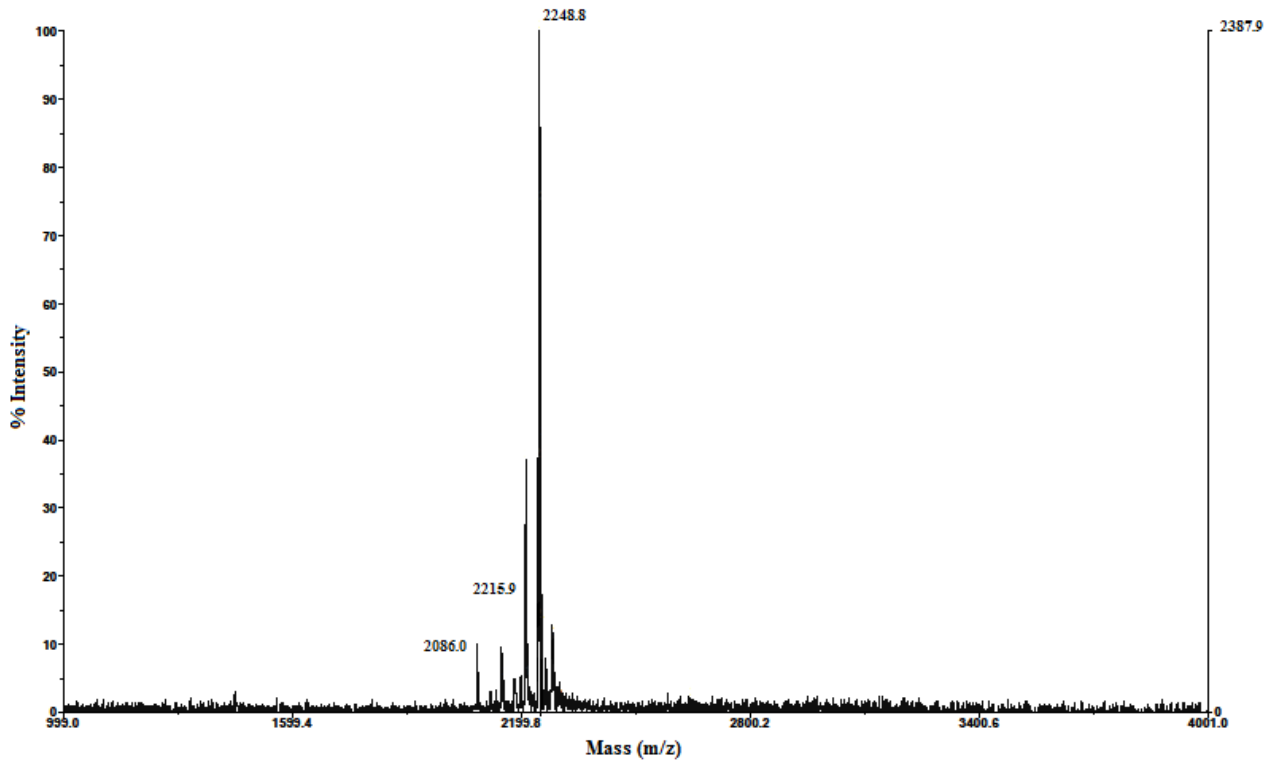

Figure 23. MALDI-MS of zinc-3,6-bis(porphyrin)triphenylene **6**

The MALDI mass spectrum of **7** shows a very small peak at 4981 corresponding to the molecular ion. However due to the difficulties in obtaining a MALDI-MS for the two model compounds, and for the unmetalated compound hexa(porphyrin)triphenylene **24** it could be foreseen that compound **7** may not give a strong molecular ion peak.

It was also decided to metalate bromoalkoxyporphyrin **22** and TPP with zinc using the same procedure so they could be used as model compounds as they best represent the individual porphyrin units within the multichromophore arrays (Figure 24). Zinc-TPP **31** will make a good reference point as the binding constants for zinc-TPP **31** are well documented.[41,42] Also zinc-bromoalkoxyporphyrin **32** is a good model for the arrays without the complication of having more than one chromophore present, and it was expected that this would make the analysis of the results of the final multichromophore much easier to interpret.

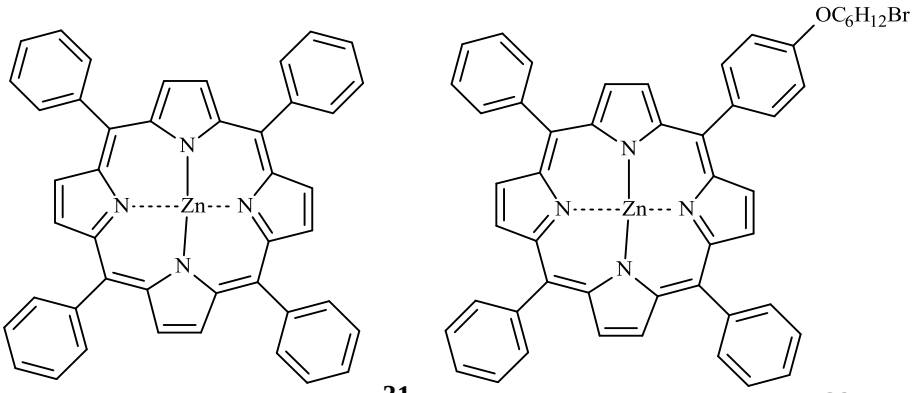

31 **32**

Figure 24. Zinc-TPP **31** and zinc-bromoalkoxyporphyrin **32**

2.8.3. Analysis of the metalation end point

The end point of the metalation can be monitored easily by UV-visible spectroscopy. This is because the metalation increases the symmetry of the porphyrin which in turn reduces the number of Q bands in UV-Vis spectrum from 4 to 2. This is demonstrated by the spectra of TPP and zinc-TPP **31** shown in figure 25.

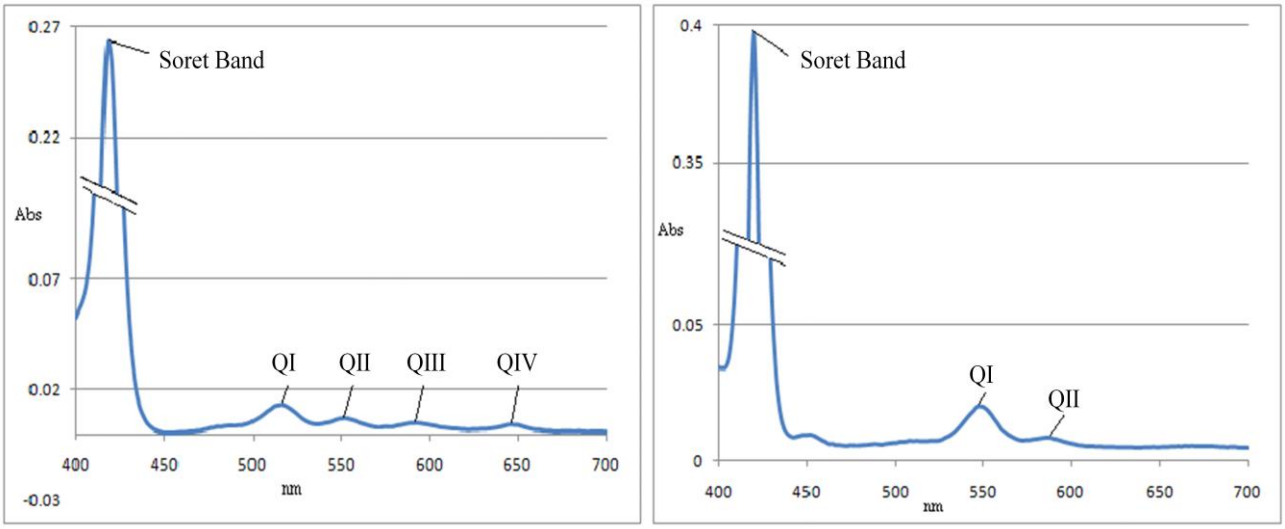

Figure 25. UV-Vis spectra of TPP and zinc-TPP **31**

2.9. UV-Vis analysis of binding

The main aim of this research was to produce a non-interacting multichromophore. To do this the porphyrins on the multichromophore arrays have been metalated with zinc and now ligands must be inserted between the metal centres to separate the porphyrins from each other. UV-Vis spectroscopy can be used to analyse the binding of ligands to the zinc metal centres within the porphyrin arrays. This can be done because the binding causes the Soret band and the two Q bands in the spectra to shift towards the red end of the spectrum.[41,43] This is demonstrated by the spectra in figure 26 of zinc-TPP **31** both bound and unbound to pyridine. The visible spectrum can also be used to calculate the binding constants of the ligands to the metal centres and this will be described later.

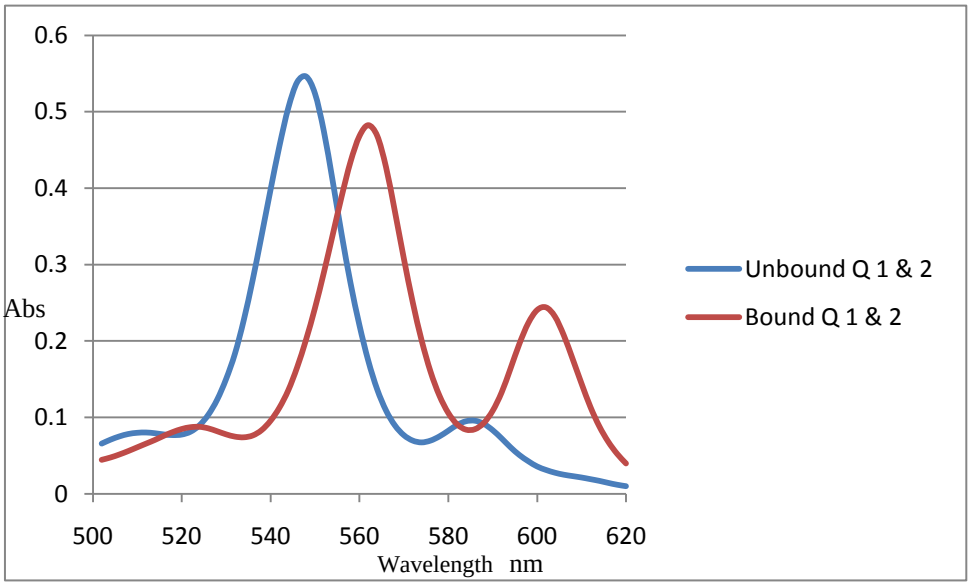

Figure 26. Spectra of zinc-TPP **31** both unbound and bound to pyridine

However we need to not only be able to tell if the ligands are bound but also if they are binding one ligand per chromophore or if each bidentate ligand is binding two of the chromophores within the same molecule. This can be done by comparing the binding constants calculated from the visible spectra. If the ligand is binding two adjacent chromophores from the same array in a cooperative fashion then it expected that the binding constant will increase dramatically. This is termed a cooperative effect of binding.[44] When one end of the bidentate ligand is bound to one of the chromophores in an array the other end should bind easily to another chromophore in the array due to its close proximity (high effective concentration). As the ligand is then bound at two points to the same molecule it

would be much harder to dissociate that if it were bound by just one. This causes the binding constant to be much higher. However we will not know if the binding constant is high unless we compare it to the binding constant of a ligand that has no cooperative effect *i.e.* monodentate. We can easily do this by calculating the binding constants of our metalated arrays to pyridine.

2.9.1. Calculation of binding constants

The method[41] we chose had been previously used by our lab.[45] A UV-Vis spectrum is taken with no ligand present then the concentration of ligand is gradually increased keeping the concentration of the chromophore array constant. A UV-Vis spectrum is then taken of the array completely bound. If only two species are present then when the spectra are overlaid an isosbestic point will be present (figure 27). The two species are the metalated porphyrin array and the metalated porphyrin array bound to a ligand.

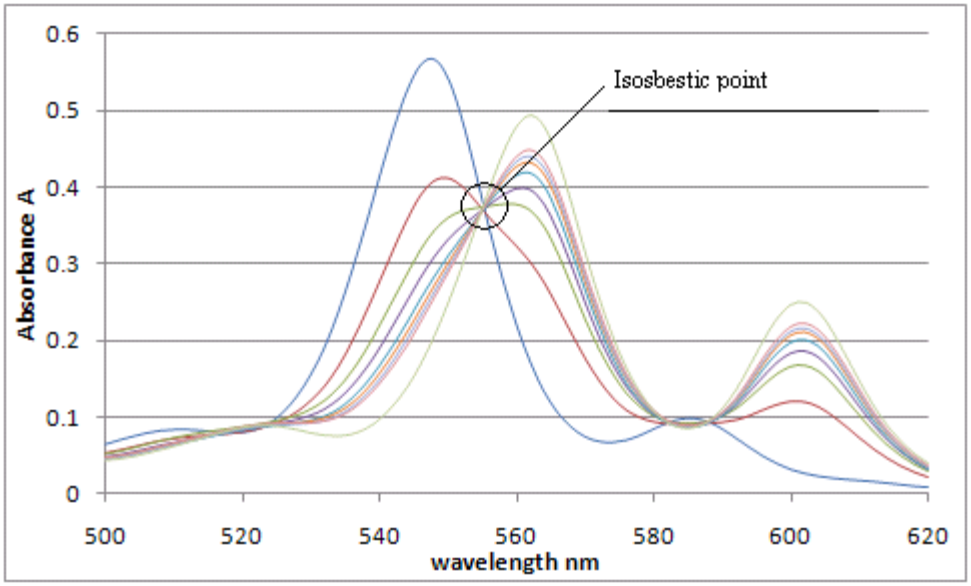

Figure 27. UV-Vis spectra demonstrating an isosbestic point

2.9.1.1. Scatchard plot

The information gained from these spectra is put in to a Scatchard Plot. A Scatchard plot is a plot created from the Scatchard equation.[46] $(A-A_0)/[Py]$ is plotted against $(A-A_0)$ producing a gradient of -k, where [Py] is the concentration of free ligand, A_0 is the absorbance of the porphyrin array without any binding ligand present at a specific wavelength, A is the absorbance of the porphyrin array with a certain concentration of binding ligand present at a specific wavelength and k is the binding constant. Both A and A_0 are obtained from the UV-Vis spectra and the concentration of ligand is known. Once each these points are plotted in the Scatchard plot, they should fall on a straight line. The gradient of this line is the binding constant of the ligand to the metal centre of the porphyrin array. An example of a Scatchard plot is shown in figure 28.

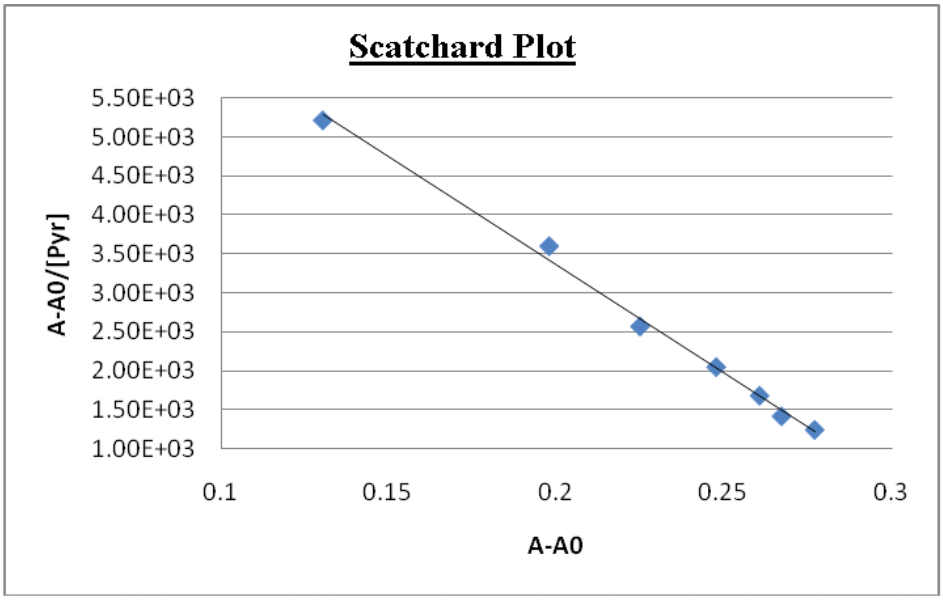

Figure 28. An example of a Scatchard plot

2.9.1.2. Binding of pyridine to zinc-TPP 31

Pyridine was chosen as the monodentate ligand because the binding constant of pyridine to a number of zinc porphyrins is well documented which allows us to confirm that our method is correct.[42,43] For the first experiment we decided to ligate zinc-TPP **31** with pyridine. [41-43] The binding constant in the literature for this experiment is relatively low (3.64 - 3.86)[41] meaning there is reasonably high concentration of ligand required before binding of the ligand to the zinc metal centre will begin. As the concentration of ligand is high in comparison to the

amount of ligand bound to the porphyrin, it was thought that this did not need to be taken away from the overall ligand concentration to gain the concentration of the free ligand. The concentration of the porphyrin compound must stay the same throughout the experiment even with the addition of the ligand. Therefore the same amount of a stock solution of porphyrin was to be used along with a varying amount of a stock ligand solution followed by sample being made up to the same volume i.e.

- Solution 1- 10 mL porphyrin stock sol + 2.5 mL ligand stock sol, made up to 25 mL in a volumetric flask.
- Solution 2- 10 mL porphyrin stock sol + 5 mL ligand stock sol, made up to 25 mL in a volumetric flask
- Solution 3- 10 mL porphyrin stock + 7.5 mL ligand stock sol, made up to 25 mL in a volumetric flask

This would only allow six samples to be analysed before the amount of porphyrin solution plus the amount of ligand solution equalled 25 mL. To increase the number of samples taken, after six samples the concentration of the ligand stock solution was doubled, table 1. The first UV-Vis spectrum taken was that of zinc-TPP **31** with no ligand present. However the porphyrin already appeared to be partially bound. This could be explained by a stabilisation molecule present in the dichloromethane (DCM) solvent. To fix this problem the solvent was changed to a higher spectroscopic grade DCM. The experiments were then continued and the results are presented in table 1.

Sample	Porphyrin Stock mL	Ligand Stock mL	Concentration of Ligand solution
1	10	2.5	3.7939×10^{-4} M
2	10	5	3.7939×10^{-4} M
3	10	7.5	3.7939×10^{-4} M
4	10	10	3.7939×10^{-4} M
5	10	12.5	3.7939×10^{-4} M
6	10	15	3.7939×10^{-4} M
7	10	8.75	7.5879×10^{-4} M
8	10	10	7.5879×10^{-4} M
9	10	11.25	7.5879×10^{-4} M
10	10	12.5	7.5879×10^{-4} M
11	10	13.75	7.5879×10^{-4} M
12	10	15	7.5879×10^{-4} M
13	10	8.75	1.5175×10^{-3} M
14	10	10	1.5175×10^{-3} M
15	10	11.25	1.5175×10^{-3} M
16	10	12.5	1.5175×10^{-3} M
17	10	13.75	1.5175×10^{-3} M
18	10	15	1.5175×10^{-3} M

Table 1. UV-Vis experiment of pyridine binding to zinc-TPP **31**

2.9.2. New method for the calculation of binding constants

After performing this binding experiment on Zinc-TPP **31** the results were not as expected and they were outside the values reported by Nappa and Valentine (3.64-3.86).[41] The conclusion was reached that the calculations performed on the spectra taken when the concentration of ligand is low were not accurate. This is because at these low concentrations the amount of bound ligand was in fact a large percentage of the overall concentration of ligand. Therefore the amount of bound ligand would need to be taken away from the amount of ligand added to calculate the concentration of free ligand in solution.[45] This can be done by looking at the equilibrium equation for the binding of pyridine to zinc-TPP **31**, represented as:

$$ZnTPP + Py \rightleftharpoons PyZnTpp \qquad \text{Equation 1.0}$$

Therefore the equilibrium binding constant k, can be represented by:

$$K = [PyZnTPP]/[ZnTPP][Py] \qquad \text{Equation 1.1}$$

The equilibrium constant may be extracted from the absorption data by solving the above equation for each spectrum. However the only known concentrations are the total amount of ZnTPP added $[ZnTPP]_0$ and the amount of ligand added $[Py]_0$. However the equilibrium values can be calculated as long as the absoptions of the bound and unbound porphyrin compound occur at different wavelengths (i.e. the first Q band) using the following equations.

$$A^{548} = A(PyZnTPP)^{548} + A(ZnTPP)^{548} \qquad \text{Equation 1.3}$$
$$A^{562} = A(PyZnTPP)^{562} + A(ZnTPP)^{562} \qquad \text{Equation 1.4}$$

The Beer-Lambert law states that

$$A = \varepsilon.c.\ l \qquad \text{Equation 1.5}$$

Where ε is the molar extinction coefficient of the compound at the stated wavelength, c is the concentration in $moldm^{-3}$ (M) and l is the path length in cm. Therefore the absorbencies in equations 1.3 and 1.4 can be substituted to form the equation below.

$$A^{548} = \varepsilon^{548}{}_{PyZnTPP}.\ l.[PyZnTPP] + \varepsilon^{548}{}_{ZnTPP}.l.[ZnTPP] \qquad \text{Equation 1.6}$$
$$A^{562} = \varepsilon^{562}{}_{PyZnTPP}.\ l.[PyZnTPP] + \varepsilon^{562}{}_{ZnTPP}.l.[ZnTPP] \qquad \text{Equation 1.7}$$

Obviously if there is no ligand present i.e. [Py] = 0 the there will be no bound porphyrin compound i.e. [PyZnTPP] = 0. Therefore values for $\varepsilon^{548}{}_{ZnTPP}$ (C_2) and $\varepsilon^{562}{}_{ZnTPP}$ (C_4) can be calculated. Also if excess ligand is added it can be assumed that there will be no unbound ligand remaining i.e. [ZnTPP] = 0 and that the concentration of the porphyrin complex doesn't change once the ligand is bound i.e. $[PyZnTPP] = [ZnTPP]_0$. Therefore values for $\varepsilon^{548}{}_{PyZnTPP}$ (C_1) and $\varepsilon^{562}{}_{PyZnTPP}$ (C_3) can also be calculated. [ZnTpp] can be eliminated to give the equation below.

$$[PyZnTPP] = ((C_2/C_4)*A^{548}-A^{562})/((C_2/C_4)*C_3-C_1) \quad \text{Equation 1.8}$$

Therefore the concentration of free pyridine in the Scatchard plot can be calculated by

$$[Py] = [Py]_0 - [PyZnTPP] \quad \text{Equation 1.9}$$

When this new correction factor was applied to the data already obtained the results appeared to be much closer to what we were expecting, the resulting binding constant of pyridine to zinc-TPP **31** was 3.87. Due to this the UV-Vis experiments were repeated for the next porphyrin compound. The binding constant of pyridine bound to zinc-bromoalkoxyporphyrin **32** calculated was 3.57. This is similar to that of pyridine bound to zinc-TPP **31**. As pyridine is monodentate this result is what is expected, for only one pyridine is bound to one metal centre as in the first experiment. However on closer inspection of the Scatchard plot, the results although roughly linear deviated from the line of best fit too much to be reliable (figure 29). This caused us to lose confidence in the chosen method and in the assumptions made and to seek out a new method.

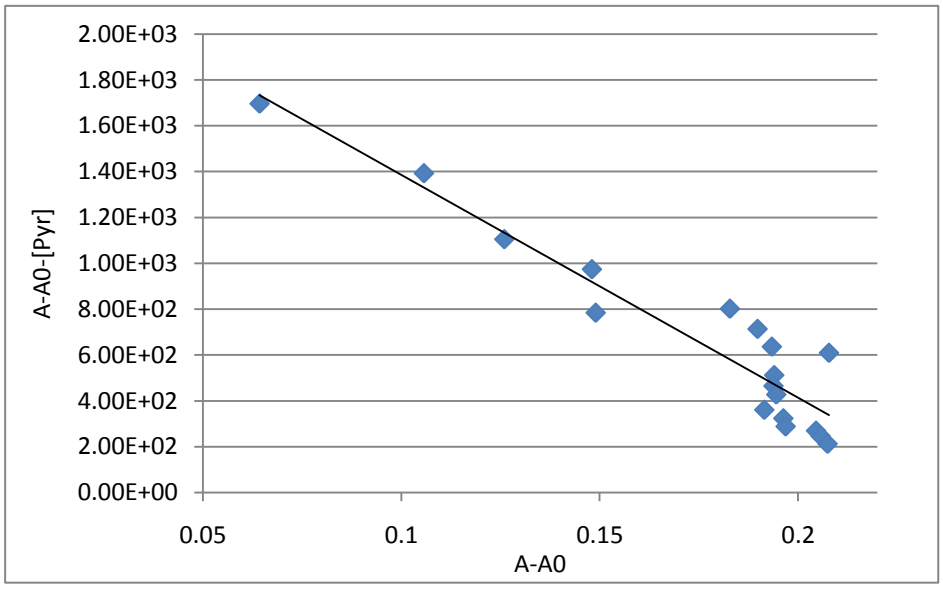

Figure 29. Scatchard plot of zinc-bromoalkoxyporphyrin **32** binding to pyridine

2.9.3. A new method for UV-Vis analysis of binding

Previous experiments have allowed us to find the optimal range of concentrations of ligand for binding studies. However we now needed to find a more accurate method to perform the UV-Vis experiments. One of the first issues to tackle was that for the current number of experiments per porphyrin compound, two solutions of stock porphyrin must be produced. For the stock porphyrin solution 0.005 g of product is dissolved in 100 mL of DCM (this gives an absorbance of the Q bands in the desired range of absorbance). Therefore the error in the weighing could produce two slightly different concentrations of solution. Although this difference is very small it is enough to affect the results of the experiment. To correct this we limited the experiments to the number we could obtain from one solution of stock porphyrin and concentrate the research on a smaller range of ligand concentrations. The same issue was identified with the ligand stock solution, so it was decided to use only one stock solution of the ligand also. However, previously, to gain a large range of ligand concentrations within the 25 mL volumetric flask, the concentration of the stock solution was doubled every few experiments (as seen in table 1), however there is not enough room in the 25 mL volumetric flask to allow for a large enough range in ligand concentrations. To solve this problem the concentration of the stock porphyrin was doubled and half the amount used i.e. 5 mL. This allowed much more free volume for the ligand solution but still preserved the same overall concentration of porphyrin. The new set of solution amounts are stated in table 2 below. It also became apparent that the porphyrin solution degrades over time (also affecting the intensity of the absorbance of the porphyrin), and to prevent this, the stock solution must be used immediately after dilution.

Sample	Porphyrin Stock mL	Ligand Stock mL
1	5	2
2	5	4
3	5	6
4	5	8
5	5	10
6	5	12
7	5	14
8	5	16

Concentration of the ligand solution = 0.000914 M

Concentration of the porphyrin Solution = 1.17E-04 M

Table 2. New experimental method for UV-Vis experiments

Once all of the UV-Vis experiments were repeated the accuracy of the results was much improved and the -log k for the zinc-TPP **31** binding with pyridine shown in the Scatchard plot shown in figure 30 was 3.82 and is within the region reported by Nappa and Valentine[41] i.e. 3.64-3.86.

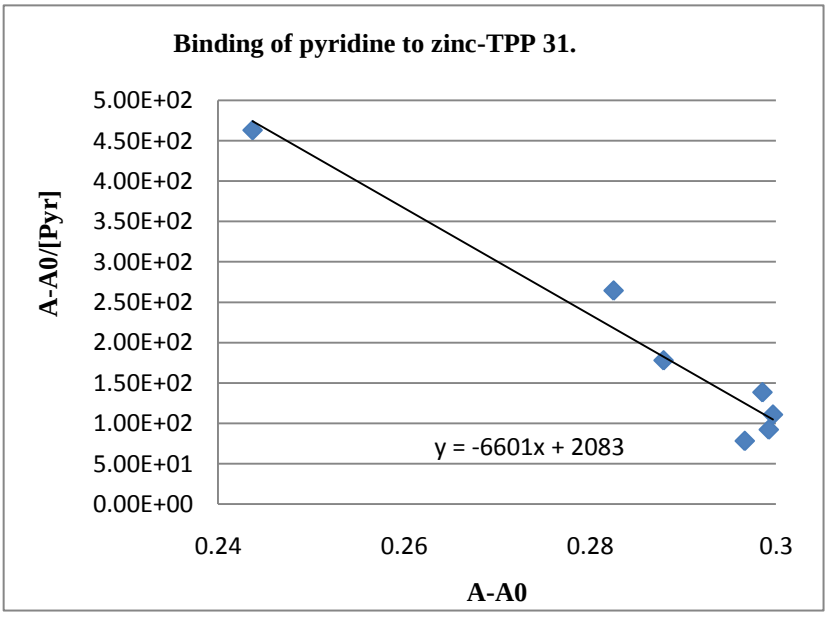

Figure 30. Scatchard plot of zinc-TPP **31** binding with pyridine in DCM

2.9.3.1. Binding of pyridine to zinc-bromoalkoxyporphyrin 32, zinc-2,3-bis(porphyrin)triphenylene 5 and zinc-3,6-bis(porphyrin)triphenylene 6

A similar result was also obtained for zinc-bromoalkoxyporphyrin **32**. The binding constant of pyridine to zinc-bromoalkoxyporphyrin **32** was calculated to be 3.82. This was obtained by calculating the –log of the gradient of the Scatchard plot shown in figure 31.

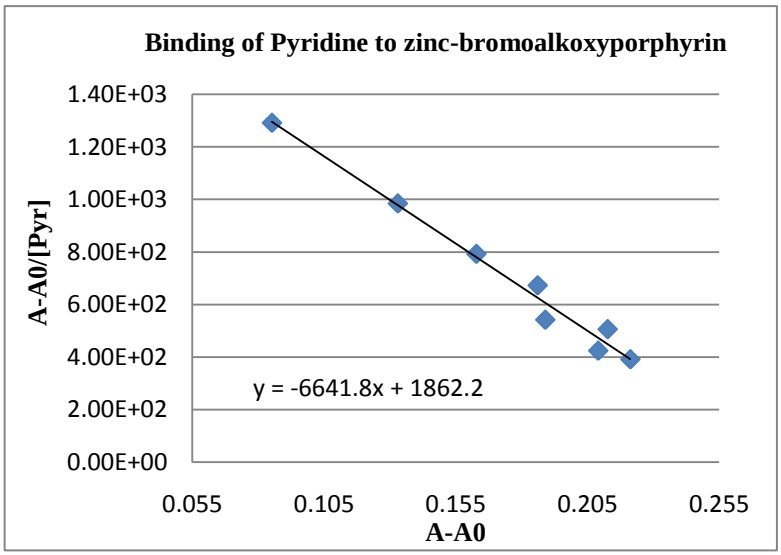

Figure 31. Scatchard plot of pyridine binding to zinc-bromoalkoxyporphyrin **32**

The experiment was then repeated using this method for the zinc-2,3-bis(porphyrin)triphenylene **5** and zinc-3,6-bis(porphyrin)triphenylene **6** (the plots for which are shown in figure 32).

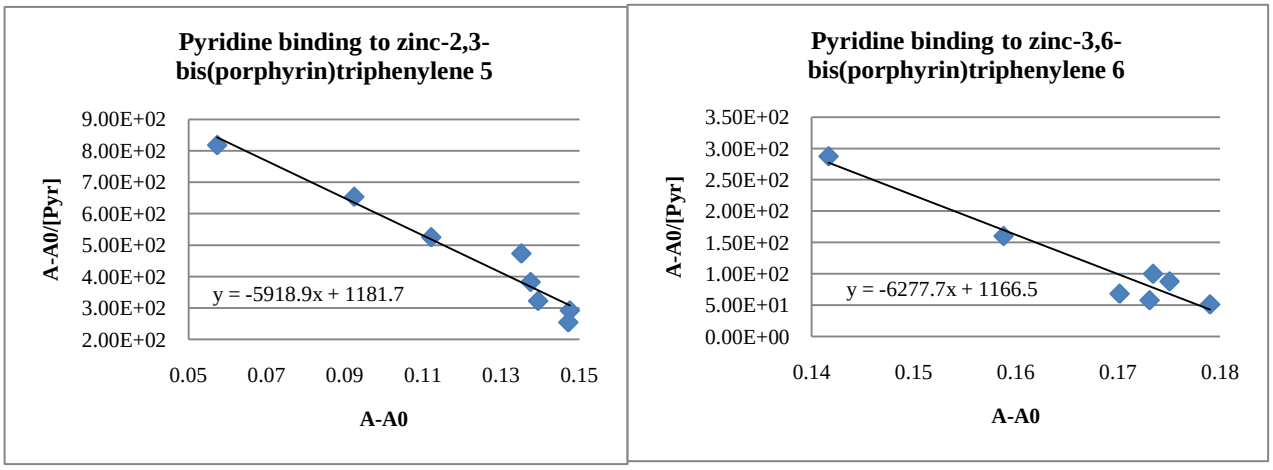

Figure 32. Scatchard plots of pyridine binding to zinc-2,3-bis(porphyrin)triphenylene **5** and to zinc-3,6-bis(porphyrin)triphenylene **6**

As expected, these experiments gave similar results compared to the binding constants for the two previous experiments. For example 3.77 for the binding of zinc-2,3-bis(porphyrin)triphenylene **5** to pyridine and 3.79 for the binding of zinc-3,6-bis(porphyrin)triphenylene **6** to pyridine**.** This is as expected due to pyridine being monodentate and so its binding is directly comparable to that of pyridine to Zinc-TPP **31.**

2.9.3.2. Binding of pyridine to zinc-hexa(porphyrin)triphenylene 7

The binding analysis of zinc-hexa(porphyrin)triphenylene **7** to pyridine was performed in the same manner as above. The Scatchard plot obtained is shown in figure 33 and the resulting binding constant was calculated to be 4.03. This is close to the value for binding of pyridine to zinc-TPP **31**.

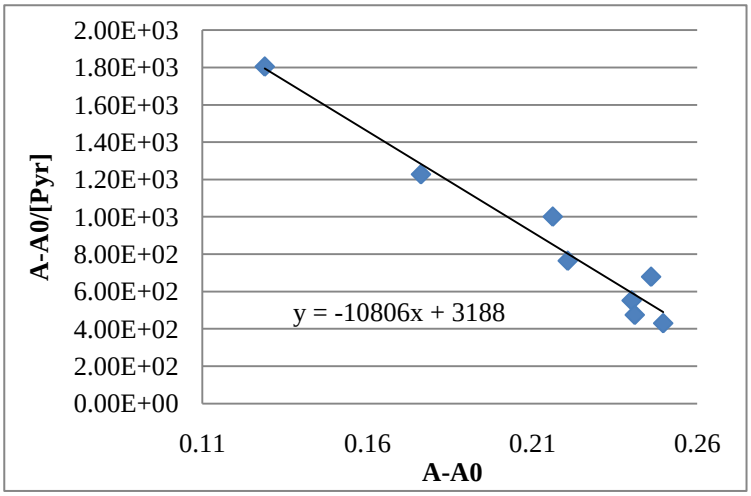

Figure 33. Scatchard plot of the binding of the molecule assumed to be zinc-hexa(porphyrin)triphenylene **7** to pyridine

2.9.3.3. Binding between our metalated arrays and 4,4-bipyridine

As mentioned earlier the aim of our work was to insert ligands between pairs of porphyrins around a triphenylene core. This should increase the binding constants of the ligand binding to the zinc metal centre significantly. The method of the experiment was kept the same and the ligand changed to 4,4-bipyridine. The experiment was carried out on zinc-TPP **31**, zinc-bromoalkoxyporphyrin **32**, the two model compounds zinc-2,3-bis(porphyrin)triphenylene **5**

and zinc-3,6-bis(porphyrin)triphenylene **6** plus the final multichromophore zinc hexa(porphyrin)triphenylene **7**.

2.9.3.4. Binding of zinc-TPP 31 and zinc-bromoalkoxyporphyrin 32 to 4,4-bipyridine

The experiment was performed on the mono porphyrin compounds zinc-TPP **31** and zinc-bromoalkoxyporphyrin **32** to determine the difference in binding constants between mono binding and cooperative bidentate binding ligands. The results for the zinc-TPP **31** and zinc bromoalkoxyporphyrin **32** where as expected in that they were similar to that gained from reaction between zinc-TPP **31** and pyridine. The binding constant of zinc-TPP **31** to 4,4-bipyridine was calculated to be 4.34 and the binding constant of zinc bromoalkoxyporphyrin **31** to the same ligand was 3.91 from the Scatchard plots shown in figure 34. This is a little higher than for those calculated for pyridine; however this is to be expected when binding a ligand with different electronic properties.

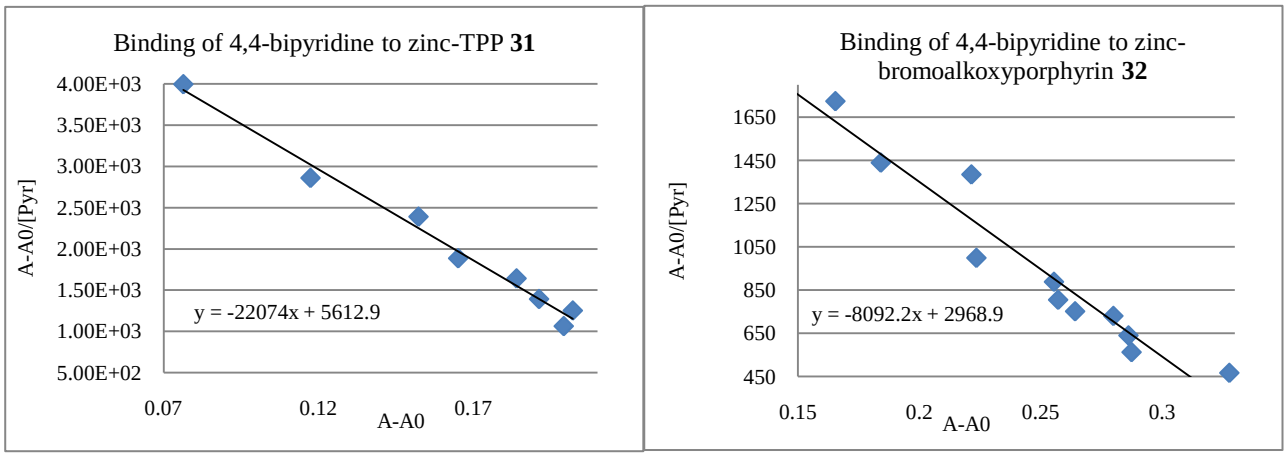

Figure 34. Scatchard plots of both zinc-TPP **31** and zinc bromoalkoxyporphyrin **32** to binding to 4,4-bipyridine

2.9.3.5. Binding of zinc-2,3-bis(porphyrin)triphenylene 5 and zinc-3,6-bis(porphyrin)triphenylene 6 to 4,4-bipyridine

The binding reactions between 4,4-bipyridine and both of the model compounds zinc-2,3-bis(porphyrin)triphenylene **5** and zinc-3,6-bis(porphyrin)triphenylene **6** were very different from the start. Using the same concentrations as used for the previous experiments was not an option as even the smallest amount of this concentration of ligand caused the porphyrin compounds to become fully bound. This could be seen by eye, but was also verified by UV-

Vis spectroscopy. This was our first indication that the binding was much stronger between the model compounds and the bidentate ligand than with the monodentate ligand. We had to dilute the concentration of the ligand by around thirty before the amount of binding to the porphyrin was within the measurable range. This is indicative of a high binding constant. The concentrations used for the experiments are listed in table 3.

Sample Number	Porphyrin sol mL	Ligand sol mL	Conc of ligand sol
A0	5	0	N/A
1	5	5	3.25×10^{-6}
2	5	10	3.25×10^{-6}
3	5	15	3.25×10^{-6}
4	5	4	1.63×10^{-5}
5	5	5	1.63×10^{-5}
6	5	6	1.63×10^{-5}
7	5	7	1.63×10^{-5}
A0B	5	20	3.25×10^{-5}

Conc of Porphyrin sol = 4.37×10^{-5}

Table 3. Concentrations and amounts used for the new experiments all made up in DCM

After performing the calculations, the binding constant (negative log of the gradient from the Scatchard plot) (figure 35) of the zinc-2,3-bis(porphyrin)triphenylene **5** binding with 4,4-bipyridine came to around 6.0. This is much higher than for the monodentate ligand binding constant which is around 3.77, and shows that the ligand is binding cooperatively i.e. the ligand inserts between the two porphyrin metal centres creating a sandwich complex.

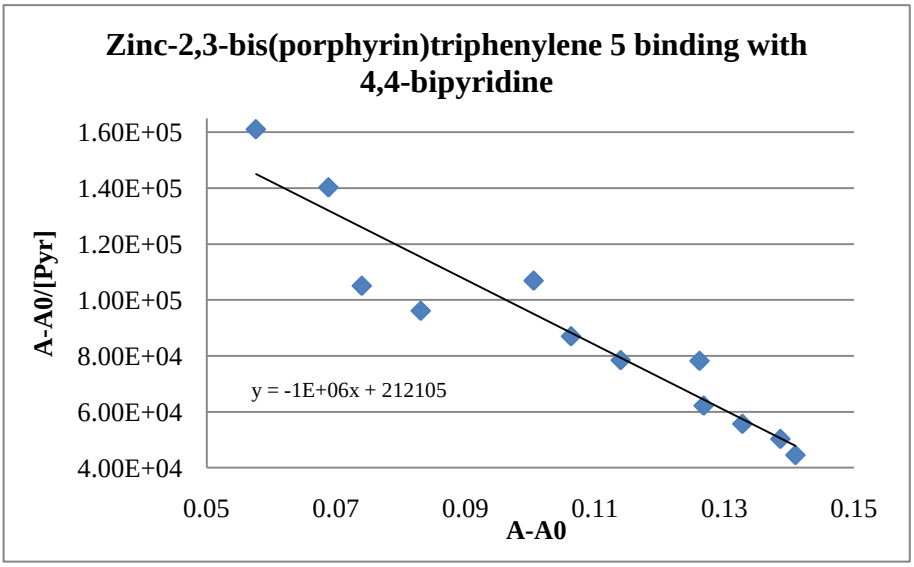

Figure 35. Scatchard plot of zinc-2,3-bis(porphyrin)triphenylene **5** binding with 4,4-bipyridine

The same UV-Vis experiments were performed for the binding of zinc-3,6-bis(porphyrin)triphenylene **6** to 4,4-bipyridine. The Scatchard plot (figure 36) shows the binding constant to be 6.30 which is much higher than that of the binding between compound **6** and the monodentate ligand, pyridine (3.79). Therefore this plot also shows that the ligand is binding cooperatively i.e. the ligand inserts between the two porphyrin metal centres creating a sandwich complex.

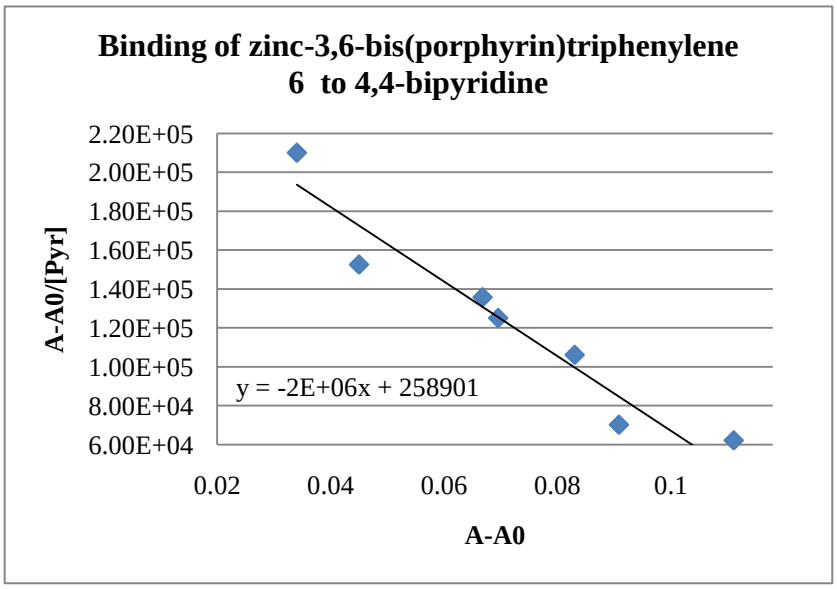

Figure 36. Scatchard plot of the binding of zinc-3,6-bis(porphyrin)triphenylene **6** to 4,4-bipyridine

2.9.3.6. Binding of zinc-hexa(porphyrin)triphenylene 7 with 4,4-bipyridine

The same UV-Vis experiments were then performed for the binding of zinc-hexa(porphyrin)triphenylene **7** with 4,4-bipyridine. However, when we repeated the experiment it was obvious from the beginning that the results would not be as we expected. We expected to use similar concentrations of porphyrin **7** to that used for the model compounds **5** and **6**. However, even the more concentrated solutions within this range showed no measurable binding of the ligand to the metal centres. We expected the binding constant to be similar to that of the model compounds as each of the bidentate ligands should bind two porphyrin metal centres within the multichromophore creating three pairs. However we found that the concentrations had to be similar to those used for the binding of **7** to pyridine. Once the experiments were completed and a Scatchard plot drawn (figure 37), the binding constant for the binding of 4,4-bipyridine to zinc-hexa(porphyrin)triphenylene **7** was calculated to be 4.10. This is very similar to that of the binding of **7** to the monodentate ligand pyridine (4.03). To confirm that this was a genuine result and not an error we repeated all of the binding experiments with a slightly larger bidentate ligand 1,2-bispyridylethane using the same conditions and similar concentrations throughout.

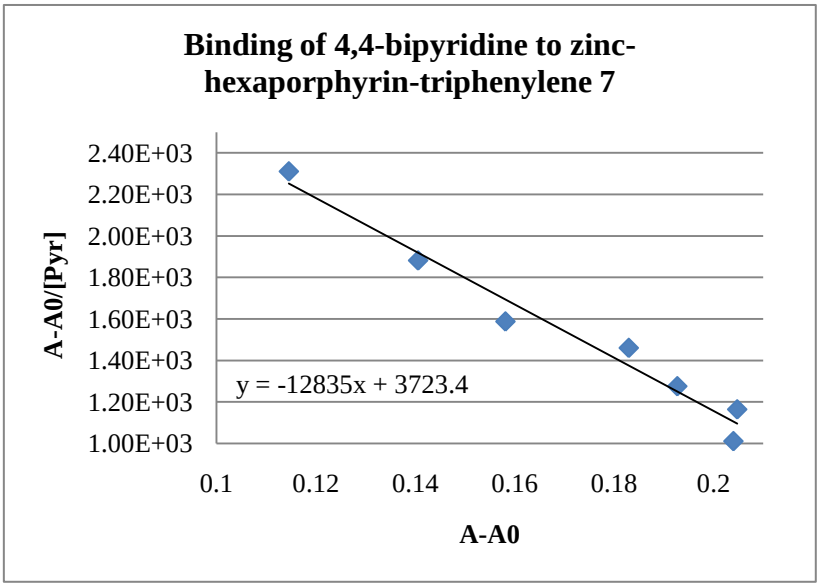

Figure 37. Scatchard plot of the binding of 4,4-bipyridine to zinc-hexa(porphyrin)triphenylene **7**

2.9.3.7. Binding of 1,2-bispyridylethane to zinc-TPP 31 and zinc-bromoalkoxyporphyrin 32

The binding of 1,2-bispyridylethane to zinc-TPP **31** and zinc-bromoalkoxyporphyrin **32** was as expected, in that they were similar to the results found from the binding of **31** and **32** to 4,4-bipyridine (4.34 and 3.91 respectively). This is shown in the Scatchard plots below (Figure 38). The binding constant of 1,2-bispyridylethane to zinc-TPP **31** was calculated to be 4.44 and to zinc-bromoalkoxyporphyrin **32** to be 4.05.

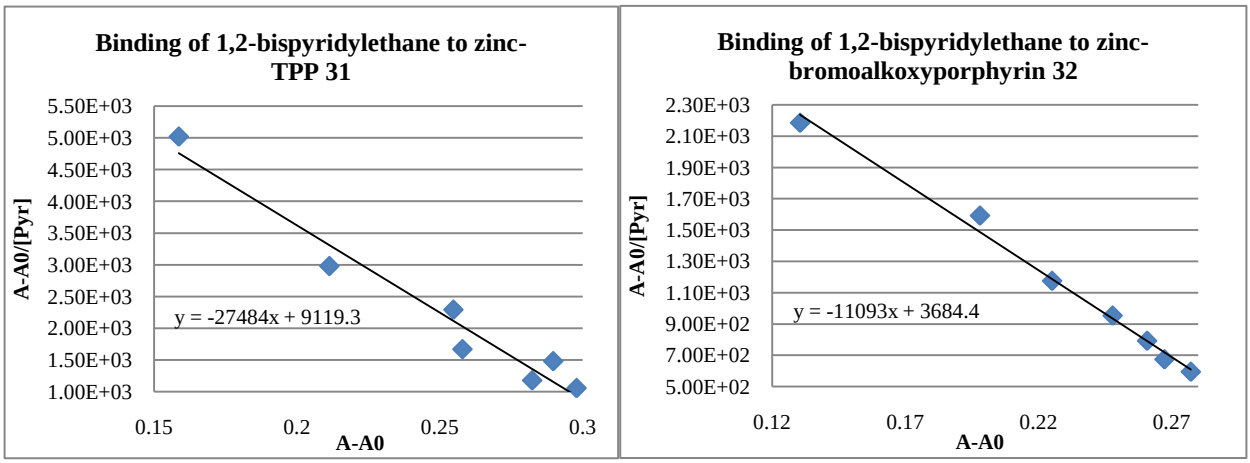

Figure 38. Scatchard plots of the binding of 1,2-bispyridylethane to both zinc-TPP **31** and to zinc-bromoalkoxyporphyrin **32**

2.9.3.8. Binding of zinc-2,3-bis(porphyrin)triphenylene 5 and zinc-3,6-bis(porphyrin)triphenylene 6 to 1,2-bispyridylethane

As with the binding of compounds **5** and **6** to the bidentate ligand 4,4-bipyridine, a much higher binding constant was apparent from the onset. Using the same concentrations as used for the previous experiments (binding of **5** and **6** to a monodentate ligand) was not an option, again even the smallest amount of this concentration of ligand caused the porphyrin compounds to become fully bound. This could be seen by eye, but was also verified by UV-Vis spectroscopy. Again we had to dilute the concentration of the ligand by around thirty before the amount of binding to the porphyrin was within the measurable range. The UV-Vis experiments were carried out in the same manner as above and the resulting Scatchard plots shown in figure 39. The binding constant of 1,2-bispyridylethane binding to zinc-2,3-

bis(porphyrin)triphenylene **5** was calculated to be 7.60 and to zinc-3,6-bis(porphyrin)triphenylene **6** calculated to be 7.0. These binding constants were as expected in that they are much higher than that of the binding constants of compounds **5** and **6** to pyridine (3.77 and 3.79 respectively) and are comparable to the binding constants of compounds **5** and **6** to 4,4-bipyridine (6.0 and 6.30 respectively). This shows cooperative binding between both of the model compound **5** and **6** and the bidentate ligand 1,2-dipyridylethane.

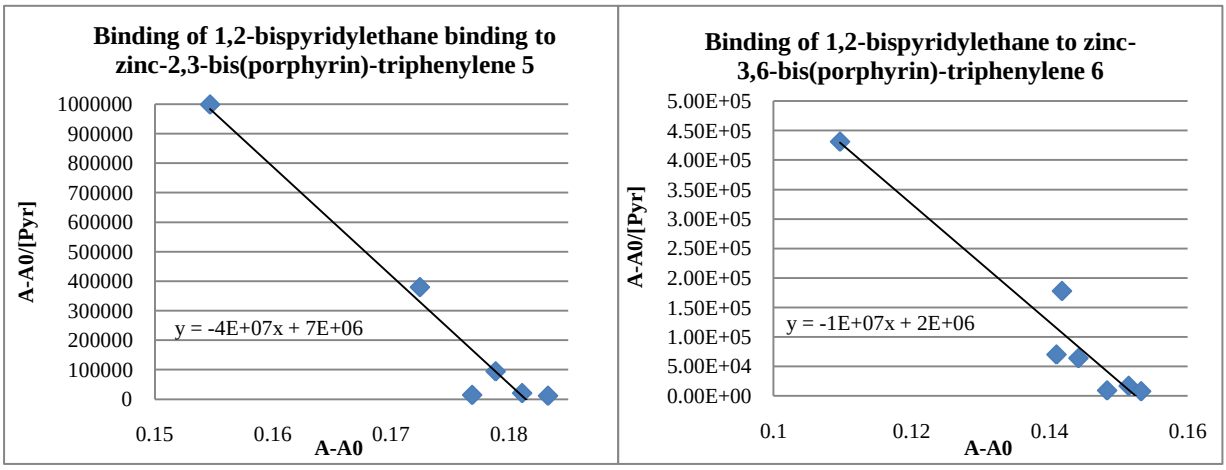

Figure 39. Scatchard plots of the binding of 1,2-bispyridylethane to both zinc-2,3-bis(porphyrin)triphenylene **5** and zinc-3,6-bis(porphyrin)triphenylene **6**

2.9.3.9. Binding of zinc-hexa(porphyrin)triphenylene 7 with 1,2-bispyridylethane

However, once again the binding constant between zinc-hexa(porphyrin)triphenylene **7** and the bidentate ligand 1,2-bispyridylethane was not as expected. Concentration ranges similar to those employed for the analysis of the monochromophore compounds had to be used before meaningful spectra were obtained. Once the experiments were conducted and the Scatchard plot drawn (figure 40) the binding constant was calculated to be 4.01 and is comparable to both the binding of **7** to pyridine (4.03) showing no cooperative binding. It is also similar in behaviour to the binding of zinc-bromoalkoxyporphyrin **32** to 1,2-bispyridylethane (4.04) also showing no cooperative binding. This would indicate that either there is a complicated binding system taking place making it impossible for the bidentate ligand to bind two metal centres, or that the zinc-hexa(porphyrin)triphenylene **7** is not as is appears in the characterisation performed so far.

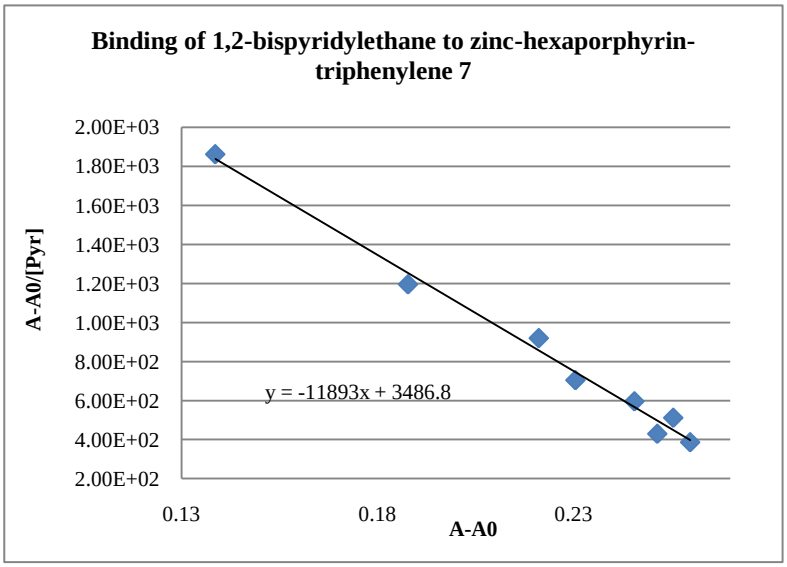

Figure 40. Scatchard plot of 1,2-bispyridylethane binding to zinc-hexa(porphyrin)triphenylene **7**

This caused us to investigate further and look back into the zinc-hexa(porphyrin)triphenylene **7** compound in more detail.

2.10. Investigation of zinc-hexa(porphyrin)triphenylene 7

We were fortunate enough at this point to have grown a crystal of what was thought to be the compound zinc-hexa(porphyrin)triphenylene **7**. X-ray crystal analysis was performed on these crystals and revealed a surprising result. We discovered that rather than zinc hexa(porphyrin)triphenylene **7** being present we found the crystal to be a formate ester, formate **33** (figure 41). We repeated this analysis on more crystals of what was thought to be compound **7**. We also repeated the ^{1}H NMR analysis on the crystals to confirm they are the same as was used for the UV-Vis experiments.

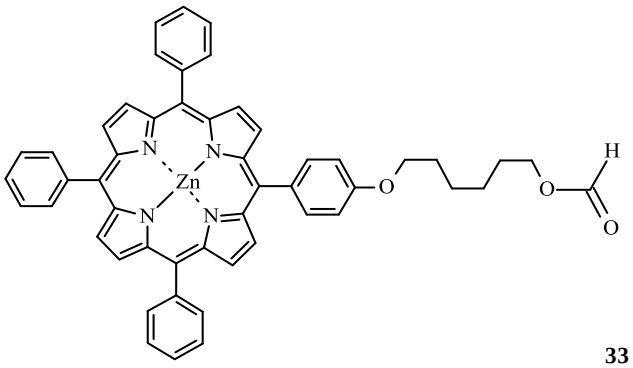

33

Figure 41. Formate **33**

When we went back to the ^{1}H NMR (figure 15) we discovered that the compound **33** would give peaks in the same areas as the zinc-hexa(porphyrin)triphenylene **7** with the same integration ratios. Most significantly, the singlet previously attributed to the triphenylene proton is clearly in fact from the formate ester. Also as the quaternary carbons did not show in the ^{13}C NMR the peaks for the zinc-hexa(porphyrin)triphenylene **7** would appear very similar to that of the formate ester **33**. We had also assumed that zinc-hexa(porphyrin)triphenylene **7** would be difficult to see in mass spectra as we expected the molecular ion peak to be very small (this was indicated by the MALDI-MS spectra of the two model compounds). However, on review, although there is a small peak of the correct mass, a large peak at 821 was also present which corresponds to the mass of the crystallised product **33** (figure 42).

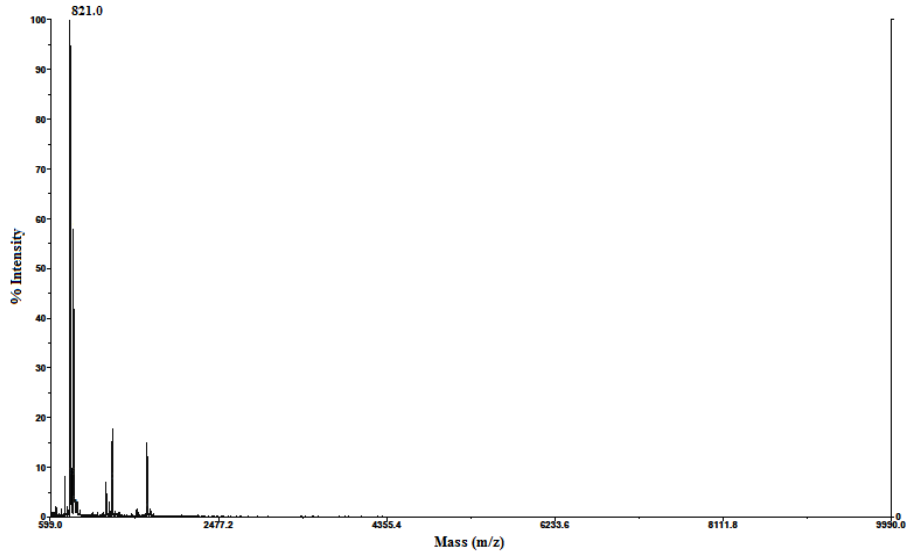

Figure 42. MALDI-MS of formate **33**

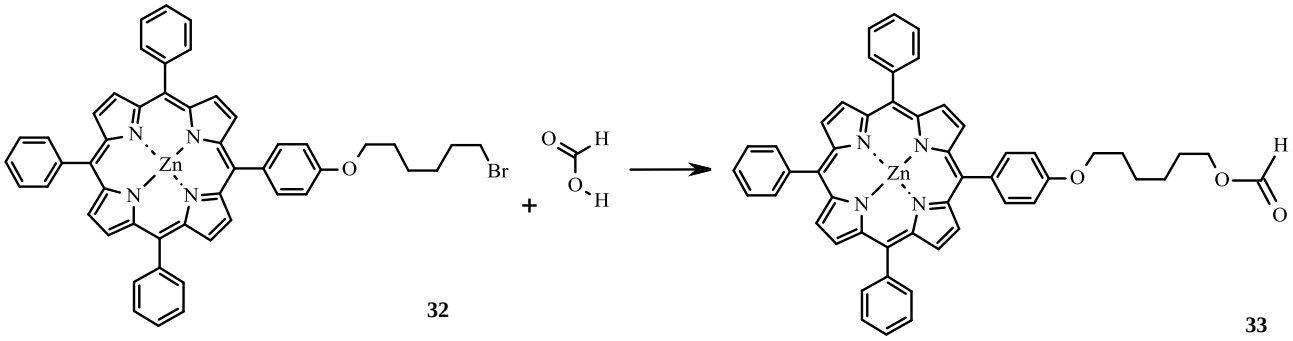

Scheme 32. Synthesis of formate **33**

After re-evaluating the experimental procedure to produce hexa(porphyrin)triphenylene **24**, the conclusion was reached that the bromoalkoxyporphyrin **22** could react with the degradation products from the DMF solvent rather than the hexa(hydroxy)triphenylene **3** (Scheme 32). As mentioned earlier under certain conditions DMF can break down to form dimethylamine and formic acid. Although the temperature was kept below 80°C the length of the reaction time could cause this breakdown to occur. Also as the hexa(hydroxy)triphenylene **3** is unstable it could be that this degrades quickly leaving the bromoalkoxyporphyrin **22** and the formic acid (a product of the degraded DMF) to react. There is also very little room around the triphenylene so the constraints might have been enough to prevent the reaction from occurring between the porphyrin and the triphenylene. This explains well the formation of formate **33** rather than the expected hexa(porphyrin)triphenylene **24** and why this was not picked up immediately.

2.11. Extended metalation of 2,3-bis(porphyrin)triphenylene 4

Due to these difficulties we chose to concentrate on our most interesting compound and expand our research into this molecule. The molecule chosen to expand on was the 2,3-bis(porphyrin)triphenylene **4**. As insertion of zinc into the porphyrin centre was achieved easily we chose to try inserting other metals and to briefly investigate the properties of these new compounds.

2.11.1. Metalation with copper

We chose to insert copper into 2,3-bis(porphyrin)triphenylene **4** as we expect similar binding properties of the resulting compound with pyridyl ligands. Copper is inserted easily into porphyrins using cooper acetate (Scheme 33).[47] Copper acetate in a minimum volume of methanol was reacted with 2,3-bis(porphyrin)triphenylene **4** in refluxing DCM. Purification by column chromatography gave the product, copper-2,3-bisporphyrintriphenylene **34**, in a high yields of 90%. This compound cannot undergo the same UV-Vis experiments as performed on the zinc compounds, as the Soret and Q bands in the UV-Vis spectra do not shift significantly upon ligation.

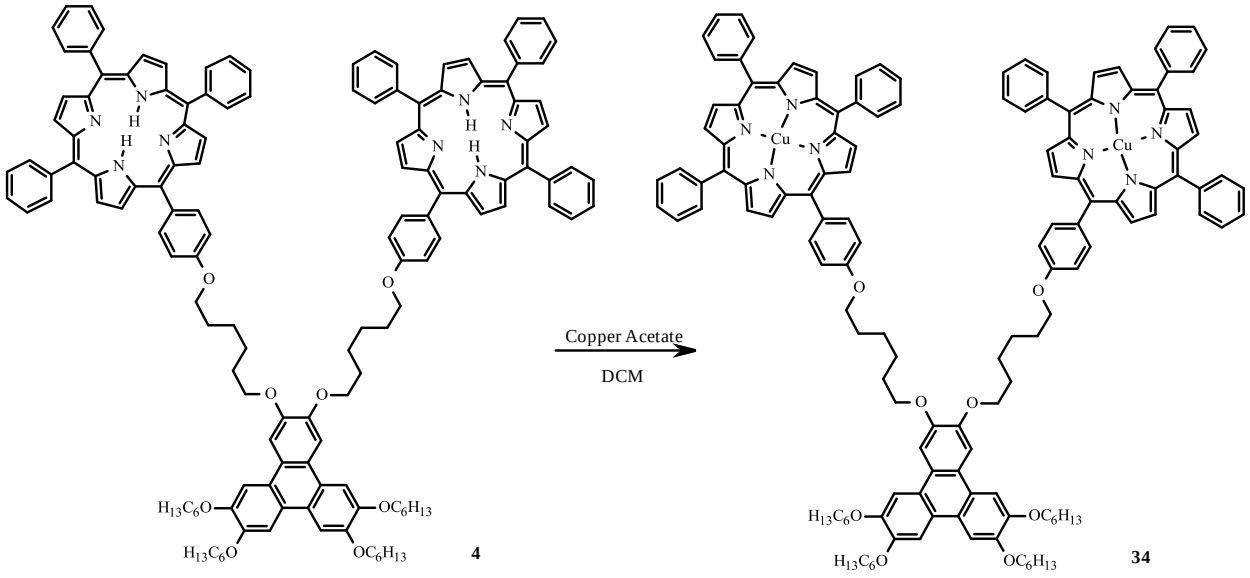

Scheme 33. Synthesis of copper-2,3-bisporphyrintriphenylene **34**

Also, ^{1}H NMR spectra of copper-2,3-bisporphyrintriphenylene **34** could not be obtained due to the copper derivatives being paramagnetic yielding very broad signals. The MALDI-MS however, shown in figure 43, shows a large peak around 2209. Samples in the presence of bispyridyl ligands were set aside to attempt to grow crystals for X-ray analysis.

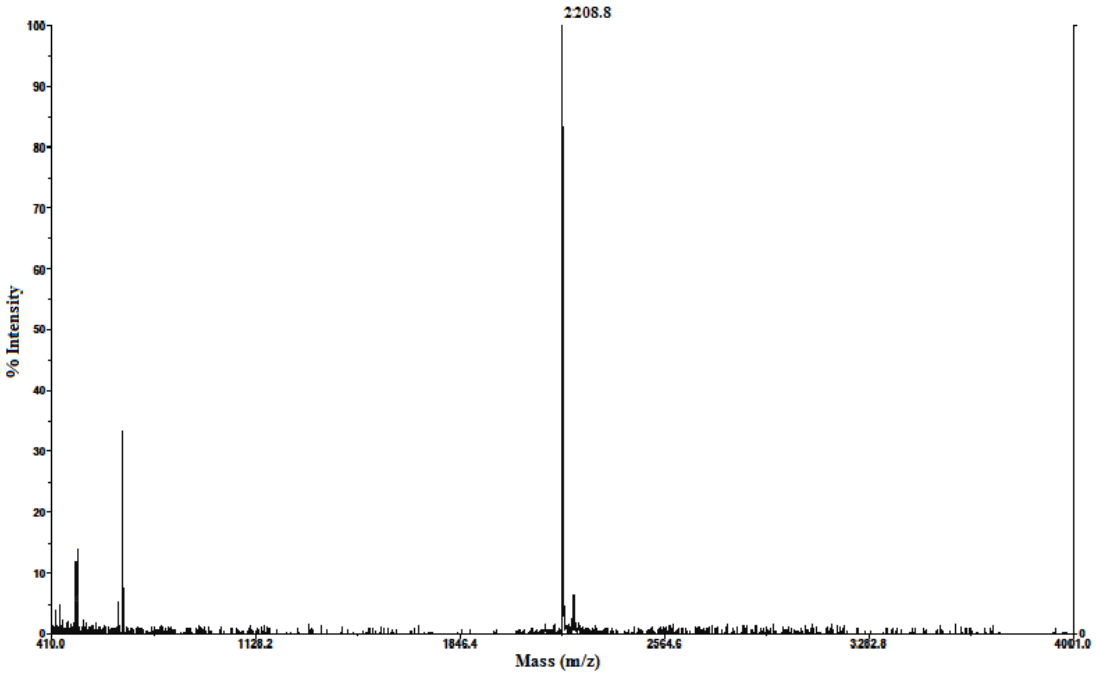

Figure 43. MALDI-MS of copper-2,3-bisporphyrintriphenylene **34**

2.12.2. Metalation with ruthenium

Next we chose to insert ruthenium into 2,3-bis(porphyrin)triphenylene **4**. Ruthenium was chosen because it has the ability to easily bind two ligands once bound to the porphyrin. This can be done easily by reaction of the porphyrin with triruthenium dodecacarbonyl (Scheme 34).[48] Ruthenium-2,3-bisporphyrintriphenylene **35** was achieved by metalation of 2,3-bis(porphyrin)triphenylene **4** with triruthenium dodecacarbonyl in refluxing benzene. Purification was achieved by column chromatography. Again this compound cannot undergo the same UV-Vis experiments as performed on the zinc compounds, as the Soret and Q bands in the UV-Vis spectra do not shift enough upon ligation to be able to perform the calculations. However, samples in the presence of bispyridyl ligands were set aside to attempt to grow crystals for X-ray analysis.

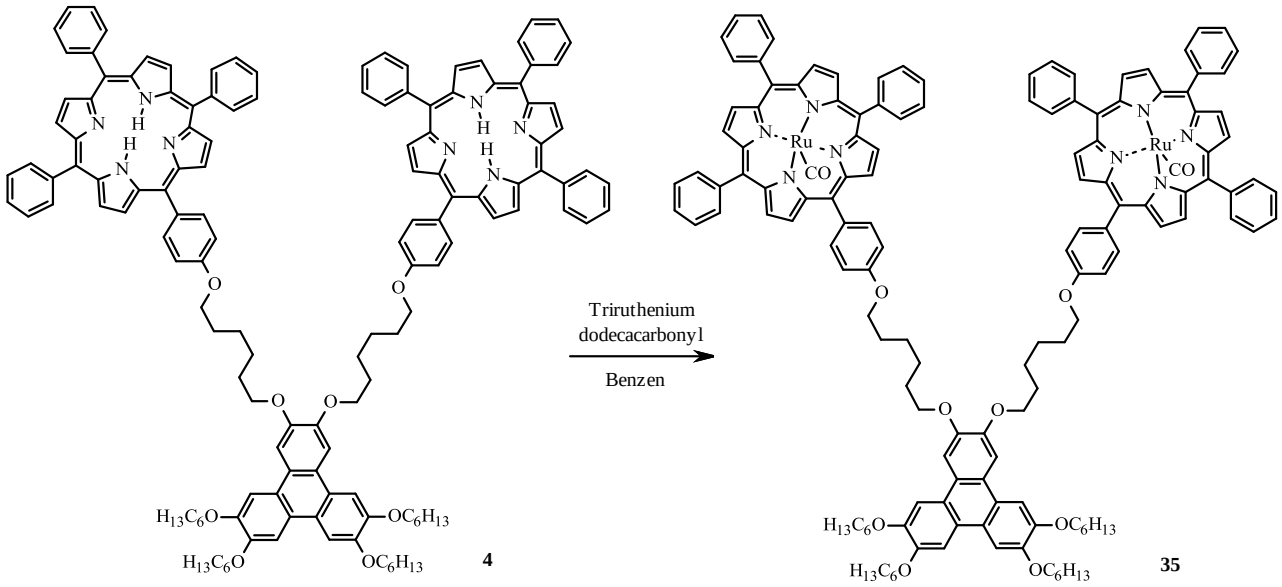

Scheme 34. Synthesis of ruthenium-2,3-bisporphyrintriphenylene **35**

The ^{1}H NMR spectra of the ruthenium-2,3-bisporphyrintriphenylene **35** has the same spectral pattern as for that of the unsymmetrical bromoalkoxyporphyrin **22**. The distinctive signal for hydrogens in the centre of the porphyrins is observed at ca. -2.7 ppm is no longer present (Figure 44).

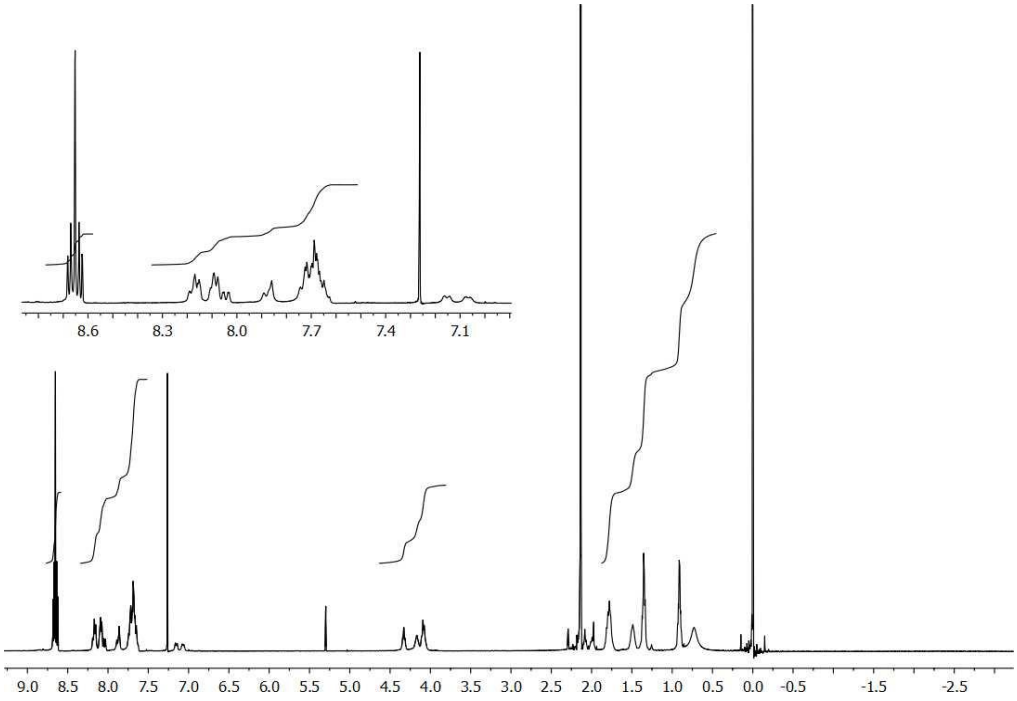

Figure 44. ^{1}H NMR spectra of ruthenium-2,3-bisporphyrintriphenylene **35** in $CDCl_3$

The MALDI-MS of ruthenium-2,3-bisporphyrintriphenylene **35** is shown in figure 45 and shows a small peak at 2086.1 corresponding to the molecular ion. The small size of this peak is no surprise as we have had difficulties in the past seeing molecular ions for similar compounds, therefore it could be foreseen that compound **35** may not give a strong peak peak.

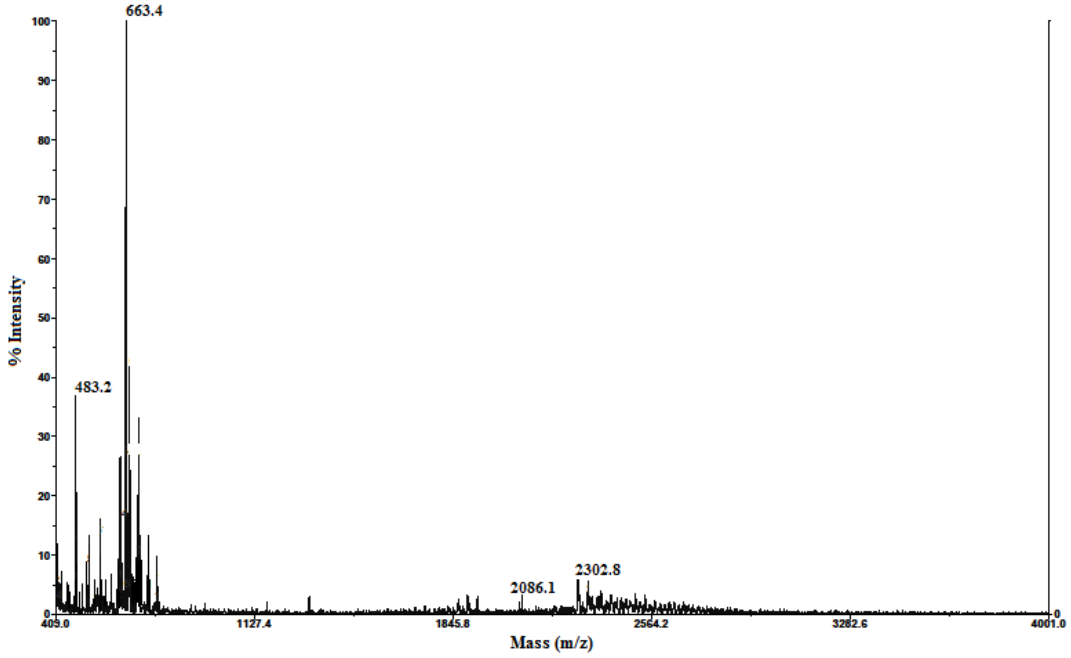

Figure 45. MALDI-MS of ruthenium-2,3-bis(porphyrin)triphenylene **35**

2.13. Conclusion

Triphenylene cores have been employed in the synthesis of model compounds for investigation of non-interacting multichromophore arrays. Two regioisomeric models were successfully synthesised in which the chromophore (a zinc porphyrin) was linked to the 2,3 or 3,6-positions of the triphenylene core via a flexible spacer. The binding was investigated quantitatively through UV-vis titrations and, as expected, the models showed strong, cooperative binding to matched bispyridyl ligands.

Synthesis of the related hexaporphyrin array initially appeared successful. However, analysis of binding gave unexpected results that matched binding to simple monomeric zinc porphyrins. These results led to further investigation and it was found that the synthesised compound was in fact the monomeric porphyrin substituted with a terminal formate ester. The origin of this compound is likely to stem from decomposition of the DMF reaction solvent.

Further metalation of the model diporphyrins was undertaken to give the copper and ruthenium analalogues. A very interesting expansion to this work could be to investigate the two model compounds **5** and **6** further as tweezer complexes.

2.12. References

(1) Karrasch, S. Bullough, P. A.; Ghosh, R. *EMBO J.* **1995**, *14*, 631-638.

(2) Cammidge, A. N.; Lifsey, K. M. *Tetrahedron Lett.* **2000**, *41*, 6655-6656.

(3) Cammidge, A. N.; Öztürk, O. *Tetrahedron Lett.* **2001**, *42*, 355-358.

(4) Cammidge, A. N.; Öztürk, O. *J. Org. Chem.* **2002**, *67*, 7457-7464.

(5) Gonsalves, R.; Pereia, M. M. *J. Heterocycl. Chem.* **1985**, *22*, 931-933.

(6) Lindsey, J. S. MacCrum, K. A. Tyhonas, J. S.; Chuang, Y. Y. *J. Org. Chem.* **1994**, *59*, 579-587.

(7) Prathapan, S. Johnson, T. E.; Lindsey, J. S. *J. Am. Chem. Soc.* **1993**, *115*, 7519–7520.

(8) Boden, N. Bushby, R. J. Lu, Z.; Headdock, G. *Tetrahedron Lett.* **2000**, *41*, 10117-10120.

(9) Boden, N. Rushby, R. J.; Cammidge, A. N. *J. Mater. Chem.* **1997**, *7*, 601-605.

(10) Boden, N. Bushby, R. J.; Cammidge, A. N. *Liq Cryst* **2006**, *33*, 1443-1448.

(11) Li, J. He, Z. Zhao, H. Gopee, H. Kong, X. Xu, M. An, X. Jing, X.; Cammidge, A. N. *Pure Appl Chem* **2010**, *82*, 1993-2003.

(12) Krebs, F. C. Schiodt, N. C. Batsberg, W.; Bechgaard, K. *Synthesis* **1997**, 1285-1290.

(13) Kadish, K. M. Smith, K. M.; Guilard, R. *The Porphyrin Handbook. Inorganic, Organometalic and Coordination Chemistry.* Academic Press, **2000**; Vol. 3, p96-112.

(14) Vogel, G. C.; Beckmann, B. A. *Inorg. Chem.* **1976**, *15*, 483-484.

(15) Becker, D. S.; Hayes, R. G. *Inorg. Chem.* **1983**, *22*, 3050–3053.

(16) Lindsey, J. S. Kadish, K. M. Smith, K. M.; Guilard, R. *The Porphyrin Handbook*; Achademic Press, **2000**; Vol. 1, p60-80.

(17) Little, R. G. Anton, J. G. Bullough, P. A.; Ibers, J. A. *J. Heterocycl. Chem.* **1975**, *12*, 343-349.

(18) Little, R. G. *J. Heterocycl. Chem.* **1981**, *18*, 129-133.

(19) Rao, P. Dhanalekshmi, S. Littler, B.; Lindsey, J. *J. Org. Chem.* **2000**, *65*, 7323-7344.

(20) Alder, A. D. Longo, F. R.; Shergalis, W. *J. Am. Chem. Soc.* **1964**, *86*, 3145–3149.

(21) Alder, A. D. Longo, F. R. Finarelli, J. D. Goldmacher, J. Assour, J.; Korsakoff, L. *J. Org. Chem.* **1967**, *32*, 476–476.

(22) Alder, A. D. Sklar, L. Longo, F. R. Finarelli, J. D.; Finarelli, M. G. *J. Heterocycl. Chem.* **1968**, *5*, 669-678.

(23) Longo, F. R. *J. Heterocycl. Chem.* **1969**, *6*, 972-931.

(24) Rao, P. Littler, B. Geier, G.; Lindsey, J. *J. Org. Chem.* **2000**, *65*, 1084-1092.

(25) Piattelli, M. Fattorusso, E. Nicolaus, R. A.; Magno, S. *Tetrahedron* **1965**, *21*, 3229–3236.

(26) Howard, M. Heirtzler, F.; Dias, S. *J. Org. Chem.* **2008**, *73*, 2548-2553.

(27) Haufe, G. Alvernhe, G. Laurent, A. Ernet, T. Goj, O. Kroger, S.; Sattler, A. *Org. Synth.* **2004**, *10*, 128-132.

(28) Meier, H.; Rose, B. *J. Prakt. Chem* **1998**, *340*, 536-543.

(29) Suzuki, A. Miyaura, N.; Yangi, T. *Synth. Commun.* **1981**, *11*, 513-519.

(30) Miyaura, N.; Suzuki, A. *Chem. Rev.* **1995**, *95*, 2457–2483.

(31) Anderson, N. G. Maddaford, S. P. A.; Keay, M. A. *J. Org. Chem.* **1996**, *61*, 9556-9559.

(32) Beattie, D. R. Hindmarsh, P. Goodby, J. W. Haslam, S. D.; Richardson, R. M. *J. Mater. Chem.* **1992**, *2*, 1261-1266.

(33) Fujimori, I. Mita, T. Maki, K. Shiro, M. Sato, A. Furusho, S. Kanai, M.; Shibasaki, M. *Tetrahedron* **2007**, *63*, 5820-5831.

(34) Li, J. He, Z. Gopee, H.; Cammidge, A. N. *Org. Lett.* **2010**, *12*, 472–475.

(35) Chen, W. Zhao, Q. Xu, M.; Lin, G. *Org. Lett.* **2010**, *12*, 1072-1075.

(36) Ogasawara, F. Kasai, H. Nagashima, Y. Yoshihiro, K. Kawagachi, T.; Yoshizama, A. *Ferroelectrics* **2008**, *365*, 48-57.

(37) International Programme On Chemical Safty *http://www.inchem.org/documents/ehc/ehc/ehc114.htm* **05/04/2011**.

(38) Ferrer Flegeau, E. Popkin, M.; Greaney, M. *Org. Lett.* **2006**, *8*, 2495-2498.

(39) Song, H. Taniguchi, M. Speckbacher, M. Yu, L. Bocian, D. Lindsey, J.; Holten, D. *J. Phys. Chem. B* **2009**, *113*, 8011-8019.

(40) El-Khouly, M. Ryu, J. Kay, K. Ito, O.; Fukuzumi, S. *J. Phys. Chem. C* **2009**, *113*, 15444-15453.

(41) Nappa, M.; Valentine, J. S. *J. Am. Chem. Soc.* **1978**, *100*, 5075–5080.

(42) Miller, J. R.; Dorough, G. D. *J. Am. Chem. Soc.* **1952**, *74*, 3977–3981.

(43) Kolling, O. W. *Inorg. Chem.* **1979**, *18*, 1175–1176.

(44) Monod, J. Wyman, J.; Changeux, J.-P. *J. Mol. Biol.* **1965**, *12*, 88-118.

(45) Hard, A. P. Sensing and Analysis with Raman Spectroscopy. Thesis, (PHD), University of East Anglia: UEA, **2002**, p84-87.

(46) Conner, K. A. *Binding Constants*; John Wiley and sons, New York,**1987**, p62-65.

(47) Beavington, R.; Burn, P. L. *J. Chem. Soc., Perkin Trans. 1* **1999**, *5*, 583-592.

(48) Gallo, E. Caselli, A. Ragaini, F. Fantauzzi, S. Masciocchi, N. Sironi, A.; Cenini, S. *Inorg. Chem.* **2005**, *44*, 2039-2049.

Chapter 3: Experimental

3.1. General Methods

3.1.1. Physical Measurements

^{1}H NMR spectra were recorded at either 300 MHz on a Varian Gemini-300 spectrometer or 400 MHz on a Varian Gemini-400 spectrometer in $CDCl_3$, unless otherwise stated. Signals are quoted in ppm as δ downfield from tetramethylsilane (δ 0.00) as internal standard, unless otherwise stated. ^{13}C NMR spectra were recorded at 75.4 MHz or 100.5 MHz on the Varian Gemini-300 spectrometer and the 400 MHz on a Varian Gemini-400 spectrometer respectively in $CDCl_3$, unless otherwise stated. The spectra were recorded at room temperature and the nucleus and operating frequency are indicated for each set of data. The coupling constants *J* are given in Hertz.

Infrared spectra were recorded on a Perkin-Elmer FT-IR system spectrum BX spectrometer. For solids a Pike MIRacle ATR attachment was used. UV-Vis spectra were taken on a Perkin-Elmer Lambda 3**5** UV/Vis spectrometer in dichloromethane.

Elemental analyses were performed by Stephen Boyer at the London Metropolitan University. Mass spectra produced were + ve MALDI using DCTB, Dithranol and anthracene matracies and nanospray on an orbitrap all *via* the EPSRC National Mass Spectroscopy Service Centre at the university of Wales, Swansea. Crystal structures where obtained by the EPSRC x-ray crystallography service.

TLC was carried out on a Merck aluminium backed silica gel 60 F_{254} coated plates, and the compounds were visualised by viewing under UV at 254 nm or 366 nm. Column chromatography was performed at ambient temperature using Davisil chromatographic silica media 40-63 micron at ambient pressure or occasionally at moderate pressure. Solvent ratios are given as v : v.

Melting points were recorded on an Olympus BH-2 microscope.

3.1.2. Reagents, Solvents and Reaction Conditions

Unless otherwise stated, all chemicals were obtained from commercial sources and were used without purification.

Nitrogen gas used was oxygen free. Petroleum ether is light petroleum (Bp 40-60 °C). If stated THF, DMF and pyridine were dried by stirring over molecular sieves. Other solvents were SLR-grade and used without drying, unless otherwise stated. Water refers to distilled water. Brine is a saturated aqueous solution of sodium chloride. Organic layers were dried over magnesium sulphate. Evaporation of solvent was carried out on a Büchi rotary evaporator at reduced pressure.

Temperatures quoted in the reaction conditions are the temperatures of the reaction mixtures and not the cooling or heating baths.

3.2. Synthesis of the Porphyrin Unit

3.2.1. Synthesis of hydroxyphenylporphyrin 1

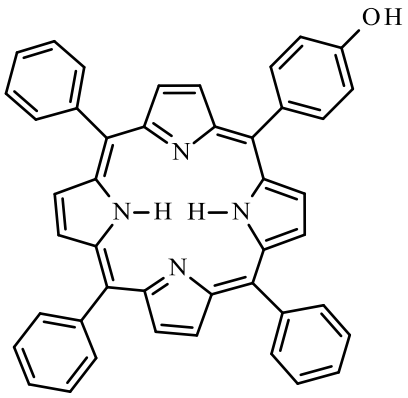

1

Following a modification to the procedure described by Alder,[1] 4-hydroxybenzaldehyde (3.05 g, 25.00 mmol) and benzaldehyde (7.64 mL 75.00 mmol) were dissolved in propionic acid (250 mL), to this was added pyrrole (6.94 mL, 0.10 mol). This was refluxed in the dark for 30 min then cooled to room temperature. To this ethanol (150 mL) was added and the mixture left to crystallise overnight. The crystals were filtered off and purified by column chromatography on silica eluting with dichloromethane petroleum ether (3:7) followed by

THF pet ether (1:1). The hydroxyphenylporphyrin **1** was gained as purple crystals. (0.69 g, 4 %).

Mp >290 °C decomposed, lit[2] mp >300 °C; δ_H ($CDCl_3$, TMS, 400 MHz) 8.92 (s, 2H), 7.79 (m, 9H), 8.87 (d, J = 2.7 Hz, 6H), 8.25 (dd, J = 5.7 Hz, J = 0.9 Hz, 6H), 8.10 (d, J = 6.3 Hz, 2H), 7.26 (d, J = 6.3 Hz, 2H), -2.73 (s, 1H).

3.3. Synthesis of the hexa(hydroxy)triphenylene core 3

3.3.1. Synthesis of hexa(methoxy)triphenylene 2

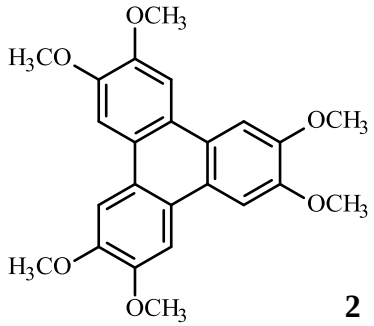

2

Following a modification to the procedure first described by Piattelli *et al*,[3] 1,2-dimethoxybenzene (15.00 g, 0.11 mol) was dissolved in DCM (500 mL), $FeCl_3$ (88.04 g, 0.54 mol) was added and stirred for 2 h. This was then poured onto cold methanol (1.5 L) and filtered to produce the hexa(methoxy)triphenylene **2** (10.64 g, 24 %).

Mp 296 °C, lit[3] mp 297-298 °C; δ_H ($CDCl_3$, TMS, 400 MHz) 7.81 (s, 6H) 4.13 (s, 18H).

3.3.2. Deprotection of hexa(methoxy)triphenylene 2

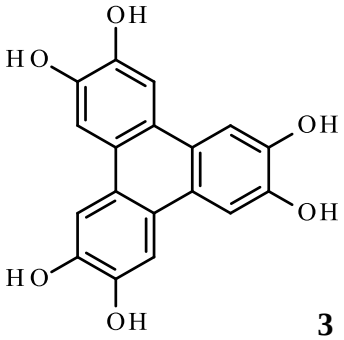

3

Following a modification to the procedure described by Piattelli,[3] hexa(methoxy)triphenylene **2** (10 g, 24.45 mmol) was added to a mixture of HBr (100 mL) and acetic acid (100 mL) and refluxed over night. Water (500 mL) was added and hexa(hydroxy)triphenylene **3** filtered off. (7.25 g, 86 %).

Mp >300 °C decomposed, lit[3] mp >310 °C; δ_H ($CDCl_3$, TMS, 400 MHz) 8.26 (s, 6H).

3.4. Synthesis of the 2,3-bis(hydroxy)triphenylene core 10

3.4.1. 1,2-Bis(hexyloxy)benzene 11

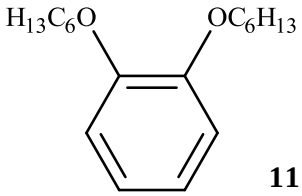

11

Following a modification to the procedure described by Howard *et al*,[4] Catechol (44.04 g 0.40 mol), 1-bromohexane (140.37 mL, 1.00 mol) and potassium carbonate (138.21 g, 1.00 mol) were suspended in ethanol (300 mL) and refluxed for 48 h. The mixture was then cooled to room temperature, filtered and the solvents removed in vacuo. The crude product was purified by distillation to give 1,2-bis(hexyloxy)benzene **11** as a pale brown oil. (106.33 g, 78 %).

δ_H ($CDCl_3$, TMS, 400 MHz) 6.90 (s, 4H), 4.00 (t, *J* = 5.1 Hz, 4H), 1.79-1.86 (m, 4H), 1.46-1.52 (m, 4H), 1.33-1.38 (m, 8H), 0.90-0.94 (m, 6H).

3.4.2. Bis(hexyloxy)phenylbromide 12

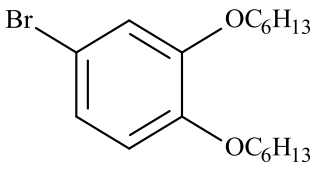

12

1,2-Bis(hexyloxy)benzene **11** (8.08 g, 29.00 mmol) was dissolved in DCM (125 mL) and cooled to -5 ˚C. To this was added a solution of bromine (6.64 g, 29.00 mmol) in DCM (5 mL) slowly. The solvents are then removed in vacuo and the bis(hexyloxy)phenylbromide **12** oil was used without further purification. (20.85 g, 97 %).

δ_H ($CDCl_3$, TMS, 400 MHz) 6.98 (d, *J* = 4.2 Hz, 1H), 6.88 (s, 1H), 6.72 (d, *J* = 4.2 Hz, 1H), 3.92-3.97 (m, 4H), 1.75-1.84 (m, 4H), 1.42-1.48 (m, 4H), 1.29-1.39 (m, 8H), 0.89-0.92 (m, 6H).

3.4.3. Bis(hexyloxy)phenylboronic acid 13

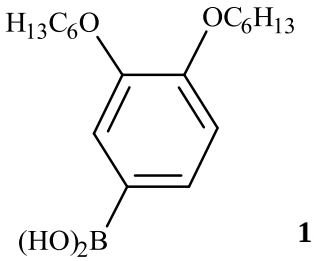

13

Following a modification to the procedure described by Meier,[5] bis(hexyloxy)phenylbromide **12** (20.85 g, 58.30 mmol) was dissolved in dry THF (250 mL) and the temperature reduced to -80˚C. To this BuLi (23.20 mL, 64.13 mmol) was added slowly over 1 h. $B(OMe)_3$ (13.24 mL, 0.1166 mol) was added slowly and the solution left to warm to room temperature over night. The solution was then stirred vigorously with HCl sol (200 mL, 1 M) and extracted with diethyl ether (3 x 50 mL). The combined organic extracts were then dried ($MgSO_4$) and

the solvent removed in vacuo. The resulting solid was washed with hexanes to leave the bis(hexyloxy)phenylboronic acid **13** as a white powder. (5.60 g, 30 %).

No Mp, degrades on heating, δ_H ($CDCl_3$, TMS, 400 MHz) 7.27 (d, J = 6.3 Hz, 1H), 6.90 (d, J = 6.3 Hz, 1H), 6.87 (s, 1H), 4.00-4.06 (m, 4H), 1.79-1.89 (m, 4H), 1.53-1.71 (m, 4H), 1.30-1.50 (m, 8H), 0.90 (t, J = 5.3 Hz, 6H).

3.4.4. Di(bromo)di(methoxy)benzene 14

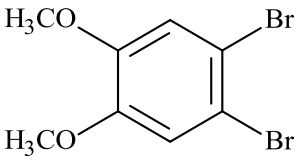

14

Following a modification to the procedure described by Fanta,[6] veratrole (9.26 mL, 72.37 mol) was added to DCM (150 mL) and cooled to 0 ˚C. To this bromine (8.20 mL, 0.16 mol) was added and the solution stirred for 2 h at 0 ˚C. This was then washed with 20 % sodium metabisulphite solution (3 x 50 mL) followed by water (3 x 50 mL), the washings were combined and extracted with DCM (3 x 50 mL). The organic extracts were combined, dried ($MgSO_4$) and the solvents removed in vacuo to produce the di(bromo)di(methoxy)benzene **14** as a white solid. (19.44 g, 91 %).

Mp 90 °C, lit[7] mp 90-92 °C; δ_H ($CDCl_3$, TMS, 400 MHz) 7.06 (s, 2H), 3.86 (s, 6H).

3.4.5. Synthesis of 2,3-bis(methoxy)triphenylene 9

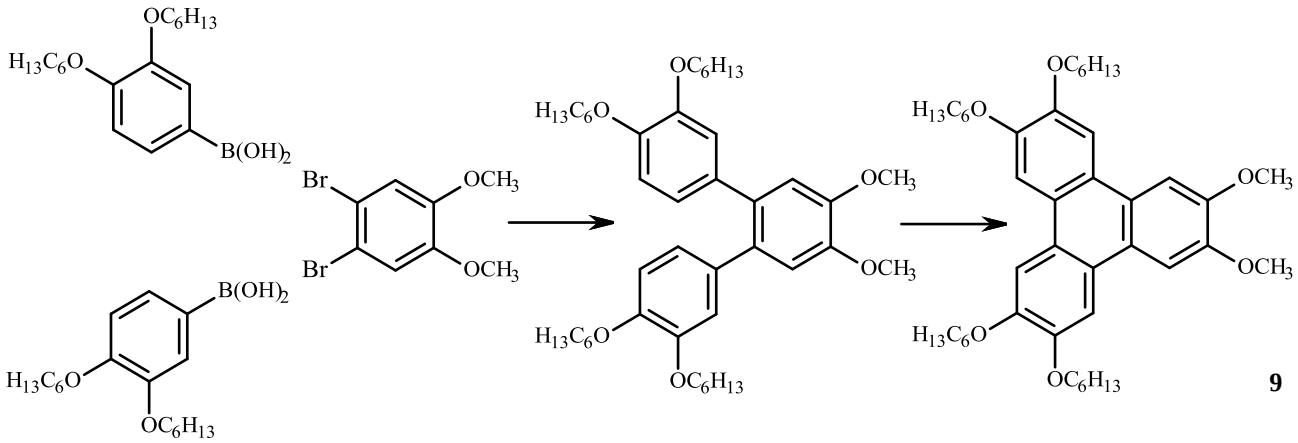

Bis(hexyloxy)phenylboronic acid **13** (14.52 g, 45.05 mmol), di(bromo)di(methoxy)benzene **14** (3.33 g, 11.26 mmol), CsF (6.84 g, 45.05 mmol), $PdCl_2$ (0.20 g, 1.126 mmol) and PPh_3 (1.48 g, 22.53 mmol) were refluxed in a mixture of toluene, ethanol and water (3:3:1, 200 ml) [8] for 4 days. The solvents were removed in vacuo and the residue redissolved in DCM (100 mL). The solution was then washed with water (2 x 100 mL) followed by brine (100 mL) and the washings extracted with DCM (2 x 100 mL). The extracts were then combined, dried ($MgSO_4$) and the solvents removed in vacuo. The crude *o*-terphenyl was purified by column chromatography eluting with DCM : petroleum ether (2:1) gradually increasing to 100 % DCM. The solvent was then evaporated in vacuo to a volume of 150 mL, $FeCl_3$ (3.00 g, 18.50 mmol) was added and the solution stirred for 3 h. The solution was poured onto methanol (300 mL) and cooled. The 2,3-bis(methoxy)triphenylene **9** was filtered off as a white powder. (5.99 g, 79 %).

Mp 82 °C, lit[9] mp 84 °C; δ_H ($CDCl_3$, TMS, 400 MHz) 7.85 (s, 4H), 7.81 (s, 2H), 4.24 (t, J = 4.9 Hz, 8H), 4.12 (s, 6H), 1.91-1.96 (m, 8H), 1.19-1.60 (m, 8H), 1.36-1.43 (m, 16H), 0.92-0.95 (m, 12H).

3.4.6. Tetra(hexyloxy)biphenyl 16

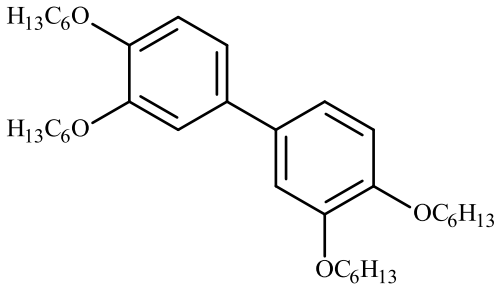

16

Following a modification to the procedure described by Boden *et al*,[10] bis(hexyloxy)phenylboronic acid **13** (10.00 g, 31.03 mmol), bis(hexyloxy)phenylbromide **12** (8.53 g, 23.87 mmol), $PdCl_2$ (0.17 g, 0.95 mmol), PPh_3 (1.30 g, 0.50 mmol) and Na_2CO_3 (9.87 g, 93.09 mmol) were refluxed in a mixture of toluene, ethanol and water (3:3:1, 250 mL) for 3 days. The mixture was filtered, the water was separated and the ethanol and toluene removed in vacuo. Ethanol (200 mL) was added to the remaining residue and heated to reflux. This was allowed to cool and the resulting tetrahexyloxybiphenyl **16** filtered off as a white crystalline solid. (25.57 g, 96 %).

Mp 66 °C, lit[11] mp 69-70 °C; δ_H ($CDCl_3$, TMS, 400 MHz) 7.04 (d, J = 6.3 Hz, 2H), 6.92 (d, J = 6.3 Hz, 1H), 4.01-4.07 (m, 8H), 1.79-1.87 (m, 8H), 1.47-1.52 (m, 8H), 1.30-1.40 (m, 16H), 0.86-0.93 (m, 12H).

3.4.7. Synthesis of 2,3-bis(methoxy)triphenylene 9 using biphenyl

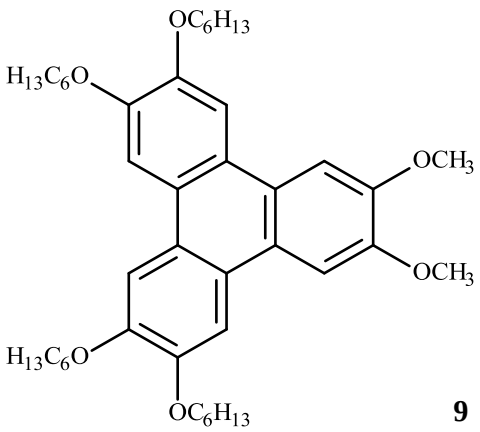

9

Tetra(hexyloxy)biphenyl **16** (8.00 g, 14.40 mmol), 1,2-dimethoxybenzene (22.80 g, 82.00 mmol) and $FeCl_3$[12] (45.00 g, 0.28 mol) were stirred in DCM (150 mL) for 1 h. This was then poured onto cold methanol (500 mL) and the resulting solid filtered. The solid was then redissolved in DCM (50 mL) and filtered again. The filtrate was then concentrated to a minimum and purified by column chromatography. The 2,3-bis(methoxy)triphenylene **9** was eluted with DCM and precipitated with cold methanol as a white solid. (7.14 g, 26 %).

Mp 82 °C, lit[9] mp 84 °C; δ_H ($CDCl_3$, TMS, 400 MHz) 7.85 (s, 4H), 7.81 (s, 2H), 4.24 (t, J = 4.9 Hz, 8H), 4.12 (s, 6H), 1.91-1.96 (m, 8H), 1.19-1.60 (m, 8H), 1.36-1.43 (m, 16H), 0.92-0.95 (m, 12H).

3.4.8. Deprotection of 2,3-bis(methoxy)triphenylene 9

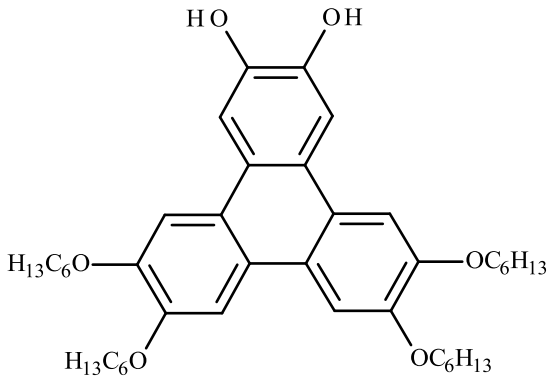

10

Following a modification to the procedure described by Cammidge *et al*,[13] 2,3-bis(methoxy)triphenylene **9** (1.000 g, 1.4997 mmol) and potassium carbonate (0.9328 g, 6.7488 mmol) were placed in an atmosphere of nitrogen. To this was added dry DMF (6 mL) and thiophenol (0.4958 g, 4.4992 mmol) then the mixture refluxed for 1.5 h. This was then poured onto concentrated HCl (10 mL) and ice (50 mL), filtered and the residue dissolved in a minimum of DCM. This was then purified using column chromatography and eluted with DCM : petroleum ether (2 : 1). The solvents were removed in vacuo and 2,3-bis(hydroxy)triphenylene **10** recrystalised from DCM and methanol as a white solid. (0.32 g, 33 %)

No mp, slow decomposition; δ_H ($CDCl_3$, TMS, 400 MHz) 7.86 (s, 2H), 7.70 (s, 2H), 7.76 (s, 2H), 6.11 (s, 2H), 4.15 – 4.26 (m, 4H), 3.95 – 4.08 (m, 4H), 1.72 – 1.81 (m, 4H), 1.58 – 1.69

(m, 4H), 1.39 – 1.45 (m, 4H), 1.21 – 1.34 (m, 12H), 1.10 – 1.19 (m, 8H), 0.77 – 0.83 (m, 12H).

3.5. Synthesis of 3,6-bis(hydroxy)triphenylene 18

3.5.1. 4-Bromo-2-methoxyhexyloxybenzene 19

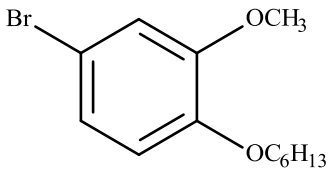

19

4-Bromo-2-methoxyphenol (5.00 g, 24.60 mmol), 1-bromohexane (40.00 g, 0.25 mol), potassium carbonate (10.00 g, 13.82 mol) and potassium iodide (16.60 mg, 0.10 mmol) were suspended in ethanol (200 mL) and refluxed for 2 days. This was then washed with water (3 x 50 mL) and the washings extracted with DCM (3 x 50 mL). The organic extracts were combined and dried using magnesium sulphate. The DCM was removed in vacuo and the remaining oil was distilled to gain 4-bromo-2-methoxyhexyloxybenzene **19** as a clear oil. (8.83 g, 83 %).

δ_H ($CDCl_3$, TMS, 400 MHz) 7.00 (d, *J* = 8.8 Hz, 1 H), 6.98 (d, *J* = 8.8 Hz, 1 H), 6.74 (d, *J* = 8.8 Hz, 1H), 3.97 (t, *J* = 6.8 Hz, 2H), 3.8**5** (s, 3H), 1.79 – 1.86 (m, 2H), 1.41 - 1.48 (m, 2H), 1.29 – 1.38 (m, 4H), 0.88 – 0.92 (m, 3H).

3.5.2. Di(hexyloxy)di(methoxy)biphenyl 20

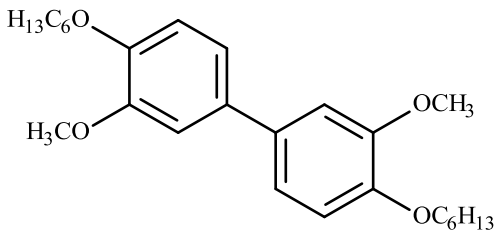

20

Following a modification to the procedure described by Lin *et al*,[14] 4-bromo-2-methoxyhexyloxybenzene **19** (9.00 g, 0.0313 mol), $NiCl_2$ (1.5668 mmol, 0.2030 mol), PPh_3

(2.47 g, 9.4011 mmol) and Zn powder (3.07 g, 0.0470 mol) were stirred in dry pyridine (22.5 mL) under nitrogen at reflux for 3 h. This was then left to cool overnight. DCM (50 mL) was added and the zinc powder filtered off. The solution was then washed with water (3 x 50 mL) and the aqueous washings extracted with DCM (3 x 50 mL). The extracts were combined and dried ($MgSO_4$). The solvent was reduced to a minimum in vacuo, cold methanol (50 mL) was then added and the product filtered off. This gives the di(hexyloxy)di(methoxy)biphenyl **20** as a white solid. (6.32 g, 49 %).

Mp 80 °C, lit[15] mp 82.5-83 °C; δ_H ($CDCl_3$, TMS, 400 MHz) 7.26 (s, 2H), 7.07 (d, J = 8.8 Hz, 2H), 6.93 (d, J = 8.8 Hz, 2H), 4.05 (t, J = 7.2 Hz, 4H), 3.93 (s, 6H), 1.89 – 1.82 (m, 4H), 1.49 - 1.44 (m, 4H), 1.37 – 1.34 (m, 8H), 0.89 - 0.93 (m, 6H).

3.5.3. Synthesis of 3,6-bis(methoxy)triphenylene 17

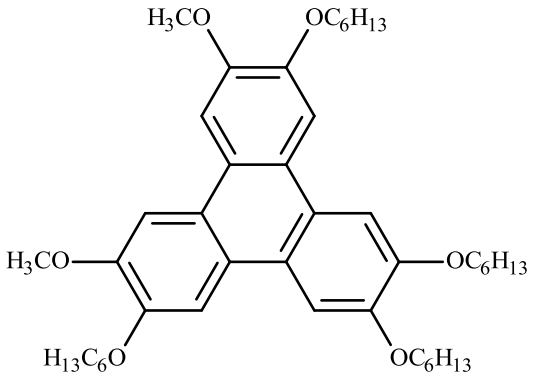

17

Following a modification to the procedure described by Cammidge et al,[15] di(hexyloxy)di(methoxy)biphenyl **20** (0.4480 g, 1.0806 mmol), 1,2-bis(hexyloxy)benzene **11** (0.6363 g, 2.1612 mmol) and $FeCl_3$ (1.0517 g, 6.4835 mmol) were dissolved in DCM (10 mL) and stirred for 3 h. This was poured onto cold methanol (50 mL) and the solid filtered off. The solid was then purified by column chromatography eluting with DCM : petroleum ether (1 : 1), the solvent was reduced to a minimum in vacuo and the product was then precipitated with cold methanol. This was filtered to give 3,6-bis(methoxy)triphenylene **17** as a white solid. (0.23 g, 48 %).

Mp 114 °C, lit[15] mp 116.5 °C; δ_H ($CDCl_3$, TMS, 400 MHz) 7.85 (s,2H), 7.84 (s,2H), 7.82 (s, 2H), 4.28 – 4.22 (m, 8H), 4.10 (s, 6H), 2.01 – 1.91 (m, 8H), 1.61 – 1.54 (m, 8H), 1.45 – 1.36 (m, 16H), 0.95 – 0.92 (m, 12H).

3.5.4. Deprotection of 3,6-bis(methoxy)triphenylene 17

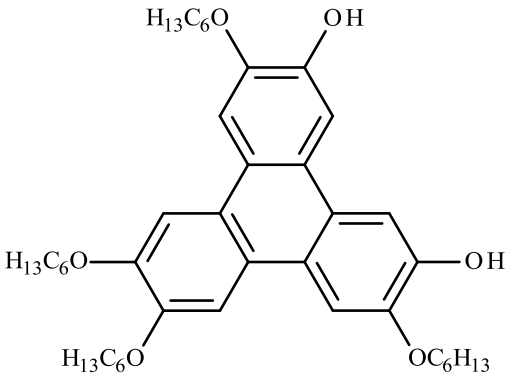

18

Following a modification to the procedure described by Cammidge *et al*,[13] 3,6-bis(methoxy)triphenylene **17** (0.39 g, 0.59 mmol) and K_2CO_3 (0.37 g, 2.66 mmol) were brought to reflux in dry DMF (4 mL). To this thiophenol (0.20 g, 1.77 mmol) was added slowly and the solution left to reflux for 1.5 h. DCM (50 mL), was added and the solution washed with water (3 x 50 mL), the aqueous washings were combined and extracted with DCM (3 x 50 mL). The extracts were then combined, dried with magnesium sulphate and the solvents removed in vacuo. The residue was purified by column chromatography eluting with DCM : Pet (1: 1) until the first spot was removed then the eluent was changed to DCM : pet ether : acetone (1 : 1 : 0.0001) to elute 3,6-bis(hydroxy)triphenylene **18** as a white solid. (0.33 g, 34 %).

Mp 101 °C, lit[15] mp 105 °C; δ_H ($CDCl_3$, TMS, 400 MHz) 7.94 (s, 2H), 7.81 (s, 2H), 7.76 (s, 2H), 4.29 (t, J = 6.4 Hz, 4H), 4.23 (t, J = 6.4 Hz, 4H), 1.98 – 1.90 (m, 8H), 1.62 – 1.53 (m, 8H), 1.42 – 1.36 (m, 16H), 0.96 – 0.89 (m, 12H)

3.6. Synthesis of 2,3-bis(porphyrin)triphenylene 4

3.6.1. Synthesis of 2,3-bis(bromohexyloxy)triphenylene 21

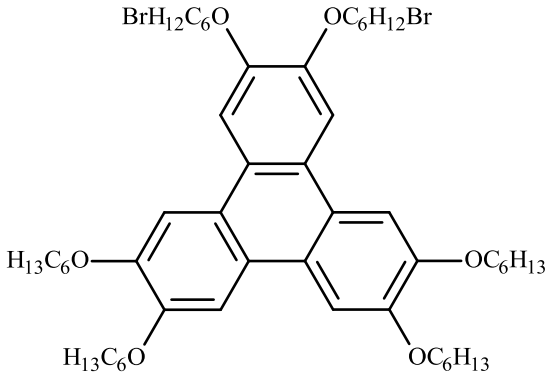

21

Following a modification to the procedure described by Ogasawara,[16] 2,3-bis(hydroxy)triphenylene **10** was then dissolved in MEK (10 mL), K_2CO_3 (0.31 g, 2.27 mmol) added and placed under nitrogen. This was followed by adding 1,6-dibromohexane (6.98 mL, 45.39 mmol) and the mixture refluxed overnight. The solution was filtered to remove the K_2CO_3. Cold methanol (100 mL) was added and the precipitate filtered and washed with cold methanol (50 mL) to produce the crude product as a white solid. This was then purified by column chromatography eluting with 2 % ethyl acetate in petroleum ether producing 2,3-bis(bromohexyloxy)triphenylene **21** as a white semi-solid. (0.61 g, 13 %).

δ_H ($CDCl_3$, TMS, 400 MHz) 7.83 (s, 6H), 4.21-4.24 (m, 12H), 3.46 (t, J = 5.1 Hz, 4H), 1.93 (t, J = 5.3 Hz, 12H), 1.90-1.99 (m, 16H), 1.54-1.61 (m, 16H), 1.33-1.45 (m, 16H), 0.91-0.95 (m, 12H).

3.6.2. Synthesis of 2,3-bis(porphyrin)triphenylene 4

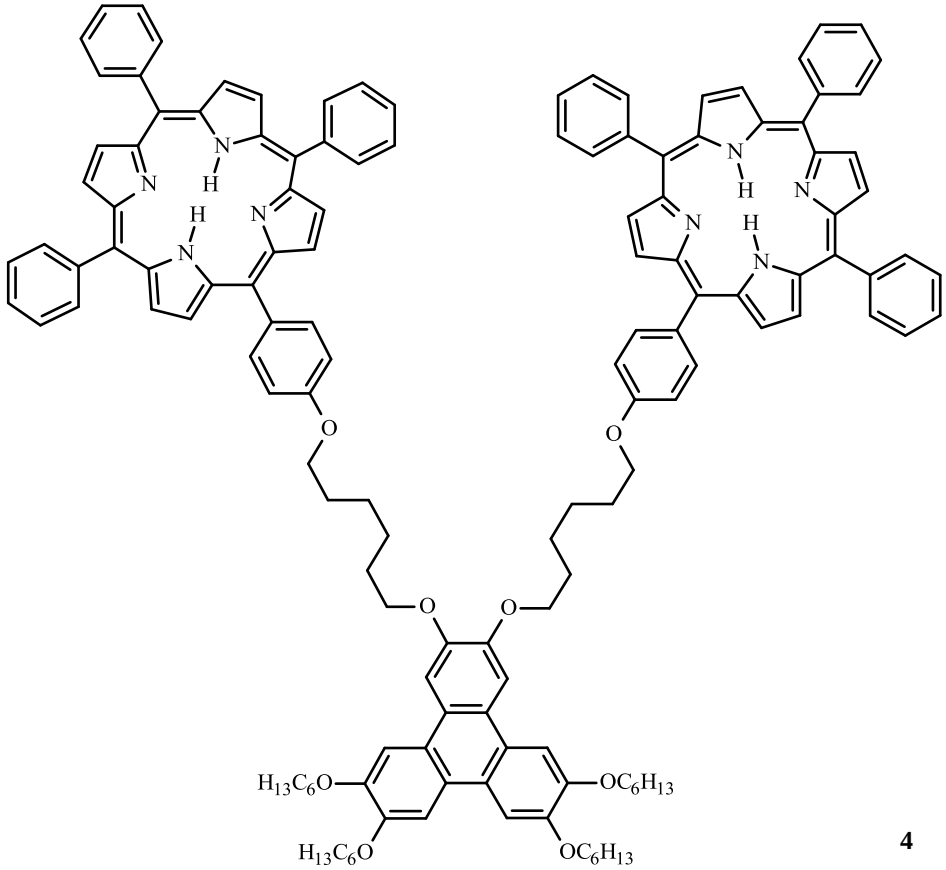

4

2,3-Bis(bromohexyloxy)triphenylene **21** (0.1 g, 0.10 mmol), hydroxyphenylporphyrin **1** (0.14 g, 0.22 mmol), K_2CO_3 (0.04 g, 0.25 mmol) and KI (0.02 g, 0.1 mmol) were suspended in MEK (5 mL) and refluxed for 7 days. This was then filtered and the solvent removed in vacuo. The residue was then purified by column chromatography (silica, PET:DCM, 50:50) to give 2,3-bis(porphyrin)triphenylene **4** as a purple solid (0.32 g, 30 %).

Mp 173 °C; Anal (Found; C 81.83, H 6.69, N 5.26, $C_{142}H_{140}N_8O_8$ Requires C 81.73; H 6.76; N 5.37 %); λ_{max} (DCM)/nm 418, ε=1.05x10^6; 516, ε=4.05x10^4; 552, ε=2.02x10^4; 590, ε=1.28x10^4; 646, ε=1.17x10^4; δ_H ($CDCl_3$, TMS, 400 MHz) 8.86 (s, 4H), 8.15 (s, 12H), 8.13-8.20 (m, 12H), 8.08 (d, *J* = 6.3 Hz, 4H), 7.93 (s, 2H), 7.90 (s, 2H), 7.86 (s, 2H), 7.62-7.77 (m, 18H), 7.75 (d, *J* = 6.3 Hz, 4H), 4.32-4.39 (m, 4H), 4.21-4.28 (m, 12H), 2.04-2.19 (m, 8H), 1.89-2.0 (m, 8H), 1.79-1.88 (m, 8H), 1.31-1.44 (m, 16 H), 1.50-1.62 (m, 8H), 0.90-0.94 (m, 12H), -2.79 (s, 4H). δ_C ($CDCl_3$, 75.45 MHz) 159.04, 149.08, 142.25, 135.67, 134.57, 134.43, 133.19, 130.56-132.10, 127.67, 126.66, 123.99, 123.77, 123.67, 120.17, 120.07, 112.73, 107.45, 69.77, 69.66, 68.09, 31.58, 29.47, 29.34, 26.09, 26.00, 25.75, 25.68, 22.53, 13.93

3.6.3. Synthesis of bromoalkoxyporphyrin 22

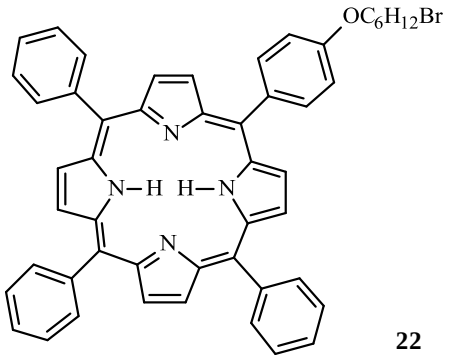

22

Following a modification to the procedure described by Ogasawara,[16] hydroxyphenylporphyrin **1** (0.20 g, 0.32 mmol), 1,6-dibromohexane (0.48 mL, 3.17 mmol) and potassium carbonate (0.44 g, 3.17 mmol) was added to dry DMF (40 mL) and the mixture stirred at room temp for 20 h. The solvent was removed and the residue redissolved in DCM (50 mL). This was washed with water (100 mL) and the washings extracted with DCM (3 x 50 mL). The combined organic extracts were dried ($MgSO_4$) and the solvent removed in vacuo. The product was purified by column chromatography (eluting with DCM : petroleum ether, 1:1). Recrystallisation from hexane gave bromoalkoxyporphyrin **22** as a purple solid. (0.12 g, 47 %).

Mp 173 °C; Anal (Found: C 75.55; H 5.32; N 6.96. $C_{50}H_{41}BrN_4O$ Requires C 75.65; H 5.21; N 7.06 %); λ_{max} (DCM/nm) 418, 5 $\varepsilon=4.88x10^5$; 516, $\varepsilon=2.04x10^4$; 522, $\varepsilon=9.87x10^3$; 590, $\varepsilon=6.05x10^3$; 646, $\varepsilon=5.10x10^3$; δ_H ($CDCl_3$, TMS, 300 MHz) 8.89 (s, 2H), 8.85 (s, 6H), 8.23 (d, *J* = 4.8 Hz, 6H), 8.13 (d, *J* = 5.4 Hz, 2H), 7.62-7.81 (m, 9H), 7.28 (d, *J* = 5.4 Hz, 2H), 4.27 (t, *J* = 4.1 Hz, 2H), 3.52 (t, *J* = 4.8 Hz, 2H), 1.95-2.09 (m, 4H), 1.60-1.78 (m, 4H), -2.77 (s, 2H). δ_c (75.45 MHz; $CDCl_3$) 159.02, 142.33, 135.71, 134.66, 134.49, 131.66-132.79, 127.78, 126.76, 120.15, 120.04, 112.74, 67.94, 33.80, 32.67, 29.19, 27.95, 25.38; *m/z* (MALDI) 794 (M^+, 100%).

3.6.4. **Synthesis of 2,3-bis(porphyrin)triphenylene 4**

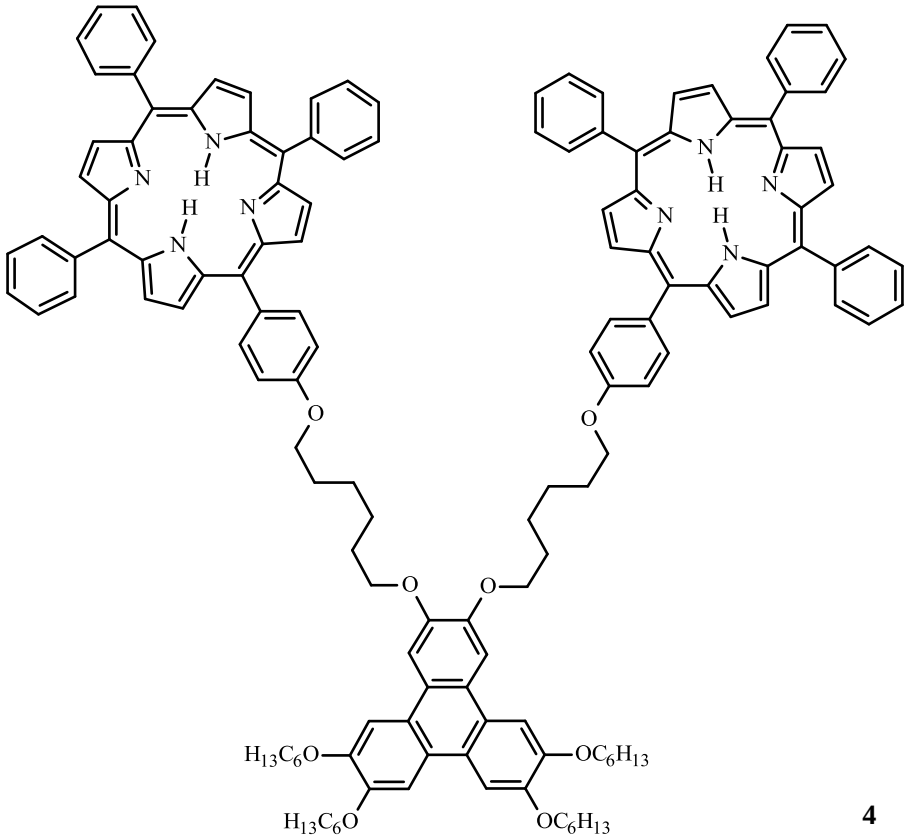

4

Bromoalkoxyporphyrin **22** (1.000 g, 1.2857 mmol), 2,3-bis(hydroxy)triphenylene **10**, potassium carbonate (0.2019 g, 1.4610 mmol) and potassium iodide (0.0166 g, 0.1000 mmol) were added to dry DMF (10 mL). This was placed under nitrogen and heated at 80°C for 5 days. The mixture was cooled to room temperature and DCM (50 mL) added, washed with water (3 x 50 mL) and the aqueous washings extracted with DCM (3 x 50 mL). The organic extracts were then combined and reduced to a minimum. Purification was achieved by column chromatography, eluting the product with DCM : petroleum ether 1 : 1 to produce 2,3-bis(porphyrin)triphenylene **4** as a purple solid. (0.59 g, 84 %).

Mp 173 °C; Anal (Found; C 81.83, H 6.69, N 5.26, $C_{142}H_{140}N_8O_8$ Requires C 81.73; H 6.76; N 5.37 %); λ_{max} (DCM)/nm 418, ε=1.05x10^6; 516, ε=4.05x10^4; 552, ε=2.02x10^4; 590, ε=1.28x10^4; 646, ε=1.17x10^4; δ_H ($CDCl_3$, TMS, 400 MHz) 8.86 (s, 4H), 8.15 (s, 12H), 8.13-8.20 (m, 12H), 8.08 (d, *J* = 6.3 Hz, 4H), 7.93 (s, 2H), 7.90 (s, 2H), 7.86 (s, 2H), 7.62-7.77 (m, 18H), 7.75 (d, *J* = 6.3 Hz, 4H), 4.32-4.39 (m, 4H), 4.21-4.28 (m, 12H), 2.04-2.19 (m, 8H), 1.89-2.0 (m, 8H), 1.79-1.88 (m, 8H), 1.50-1.62 (m, 8H), 1.31-1.44 (m, 16 H), 0.90-0.94 (m,

12H), -2.79 (s, 4H). δ_C ($CDCl_3$, 300 MHz) 142.4, 135.8, 134.8, 127.9, 126.8, 123.9, 120.2, 112.9, 69.9, 68.3, 31.8, 29.6, 29.5, 26.3, 25.9, 22.7, 14.1. *m/z* (MALDI) 2086 (M+, 30%).

3.7. Synthesis of 3,6-bis(porphyrin)triphenylene 23

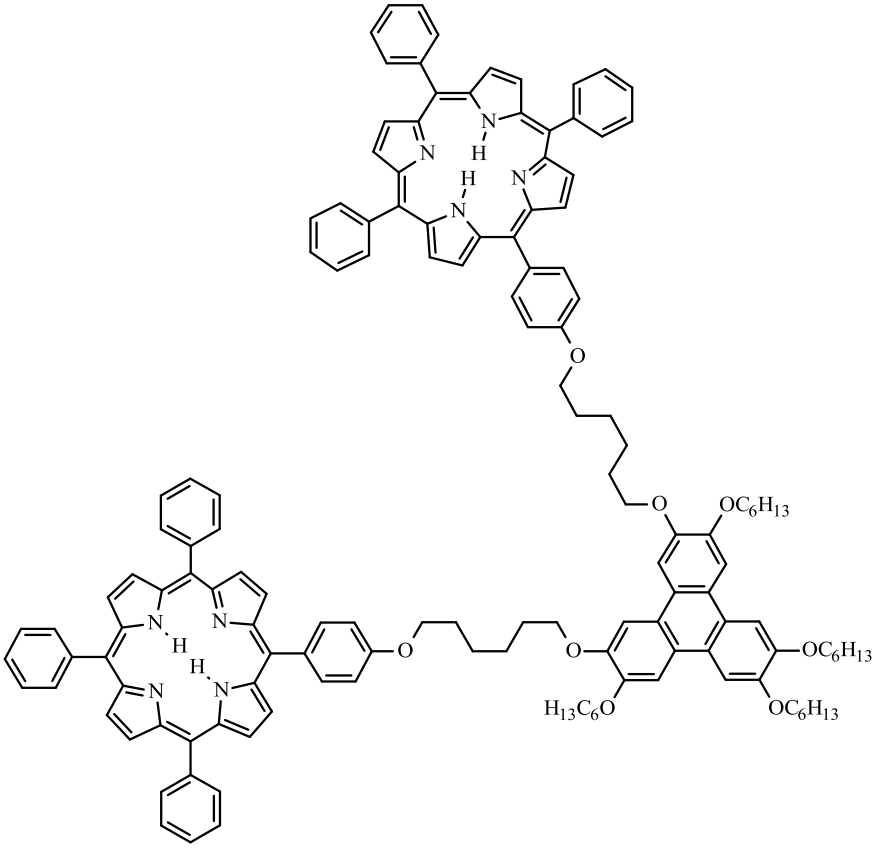

23

3,6-Bis(hydroxy)triphenylene **18** (0.10 g, 0.16 mmol), bromoalkoxyporphyrin **22** (0.27 g, 0.34 mmol), K_2CO_3 (0.05 g, 0.39 mmol) and KI (16.6 mg, 0.01 mmol) were all added to dry DMF (5 mL) and stirred at 80 °C in an atmosphere of nitrogen for 7 days. DCM (50 mL) was then added and the mixture washed with water (3 x 50 mL). The aqueous washings were extracted with DCM (3 x 50 mL) and the organic extracts combined, dried ($MgSO_4$) and the solvent removed in vacuo. The residue was then purified by column chromatography, the remaining starting material was eluted with DCM : Pet (1 : 1) and the product was eluted with DCM. 3,6-bis(porphyrin)triphenylene **23** precipitated out with addition of cold methanol as a purple solid. (0.10 g, 31 %).

Mp 187 °C; Anal (Found: C 78.63; H 6.37; N 4.90. $C_{142}H_{140}N_8O_8.CH_2Cl_2$ Requires C 79.09 H 6.59 N 5.16%); λ_{max} (DCM)/nm 418, ε=1.10x10^6; 516, ε=4.10x10^4; 552, 2.04x10^4; 590, 1.24x10^4; 646, 1.01x10^4; δ_H ($CDCl_3$, TMS, 400 MHz) 8.87 (s, 4H), 8.83 (s, 12H), 8.20 – 8.18 (m, 12H), 8.06 (d, *J* = 8 Hz, 4H), 7.95 (s, 2H), 7.88 (s, 2H), 7.87 (s, 2H), 7.68 – 7.75 (m, 18H), 7.19 (d, *J* = 8, 4H), 4.35 (t, *J* = 6.4 Hz, 4H), 4.28 (t, *J* = 6.4 Hz, 4H), 4.23 (t, *J* = 6 Hz, 4H), 4.17 (t, *J* = 6.4 Hz, 4H), 2.07 – 2.11 (m, 4H), 1.97 – 2.04 (m, 8H), 1.90 – 1.95 (m 4H), 1.74 – 1.79 (m, 8H), 1.54 – 1.64 (m, 8H), 1.37 – 1.46 (m, 16H), 0.85 – 0.97 (m, 12H), -2.79 (s, 4H). δ_C ($CDCl_3$, 300 MHz) 143.5, 139.6, 138.3, 126.5, 125.5, 124.3, 122.5, 112.4, 70.1, 68.2, 38.2, 29.7, 29.5, 26.3, 25.9, 22.7, 15.1. *m/z* (MALDI) 2086 (M^+, 100%).

3.8. Attempted synthesis of hexa(porphyrin)triphenylene 24

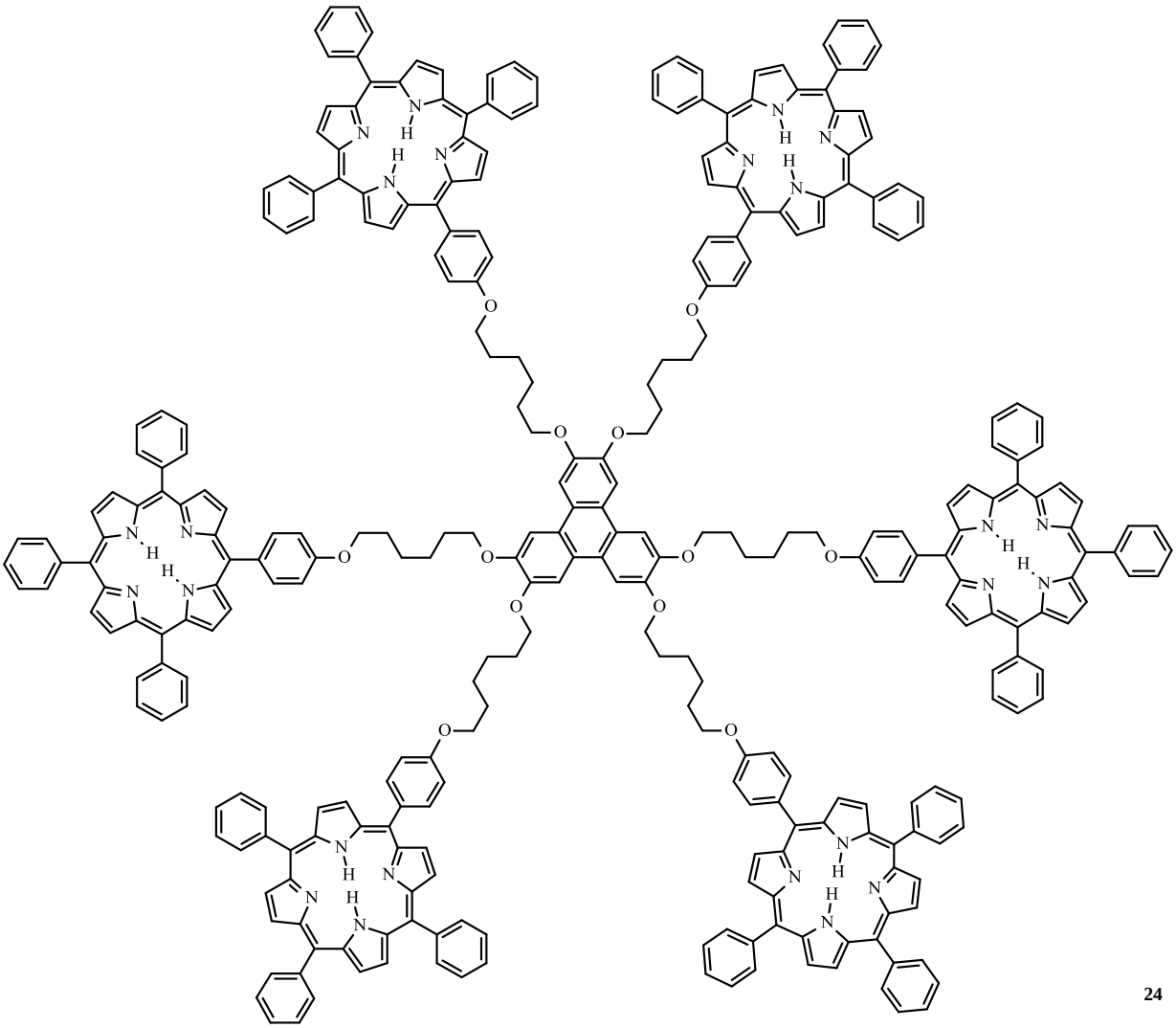

24

Hexa(hydroxy)triphenylene **3** (39.7 mg, 0.16 mmol), bromoalkoxyporphyrin **22** (1.00 g, 1.26 mmol), K_2CO_3 (0.20 g, 1.42 mmol) and KI (16.6 mg, 0.01 mmol) were all added to dry DMF

(15 mL) and stirred at 80 °C in an atmosphere of nitrogen for 7 days. DCM (50 mL) was then added and the solution washed with water (3 x 50 mL) and the aqueous washings extracted with DCM (3 x 50 mL), the organic extracts were combined, dried with magnesium sulphate and the solvent removed in vacuo. The residue was then purified by column chromatography. The remaining starting material was eluted with DCM : petroleum ether (1 : 1) and the product was eluted with DCM. A product was precipitated with cold methanol as a purple solid. (0.15 g, 22 %).

Mp 278 °C; Anal (Found: C 82.85; H 5.43; N 7.24. $C_{318}H_{252}N_{240}O_{12}$ Requires C 83.00; H 5.52; N 7.31%); Log ε λ_{max} (DCM) ; 419 (6.9979), 515 (5.0475), 551 (4.7344), 591 (4.5209), 647(4.4421). δ_H ($CDCl_3$, TMS, 400 MHz) -2.79 (s, 12H), 1.81 – 1.28 (m, 12H), 1.54 – 1.60 (m, 12H), 1.64 – 1.71 (m, 12H), 1.74 – 1.81 (m, 12H), 4.21 (t, *J* = 6.4 Hz, 12H), 4.29 (t, *J* = 6 Hz, 12H), 7.35 (d, *J* = 8.4 Hz, 12H), 7.78 – 7.86 (m, 54H), 8.12 (d, *J* = 8.4 Hz, 12H), 8.15 (s, 6H), 8.22 – 8.24 (m, 36H), 8.84 (s, 36H), 8.90 (s, 12H). δ_c ($CDCl_3$, TMS, 400 MHz) 161.34, 159.01, 142.30, 135.69, 134.63, 134.48, 130.58-132.25, 127.74, 126.73, 120.11, 119.99, 112.73, 67.97, 63.95, 29.25, 28.43, 25.78, 25.66.

3.9. Extension of project, increasing the number of chromophores

3.9.1. Synthesis of di(methoxy)benzeneboronic acid 26

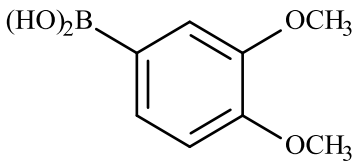

26

Following a modification to the procedure described by Suzuki *et al*,[17] bromoveratrole (13.81 mL, 0.12 mol) was dissolved in dry THF (200 mL) and cooled to -80 °C, to this n-BuLi (2.5 M in hexanes) (52.36 mL, 0.13 mol) was added drop wise. This was stirred at -80 °C for 1 h then left over night to warm to room temperature. To this was added 1 M HCl solution (250 mL) and stirred for 1.5 h. The solvents were removed in vacuo and the remaining residue dissolved in hot ethylacetate, to this was added hexanes and the mixture allowed to cool to

room temperature. The dimethoxybenzeneboronic acid crystallised out as a white solid. (1.3 g, 6 %).

Mp 234 °C, lit[18] mp 240 °C; δ_H ($CDCl_3$, TMS, 400 MHz) 7.88 (d, J = 8 Hz, 1H), 7.70 (s, 1H), 7.04 (d, J = 8 Hz, 1H), 4.03 (s, 3H), 3.99 (s, 3H).

3.9.2. Synthesis of triphenylenehexatriflate 25

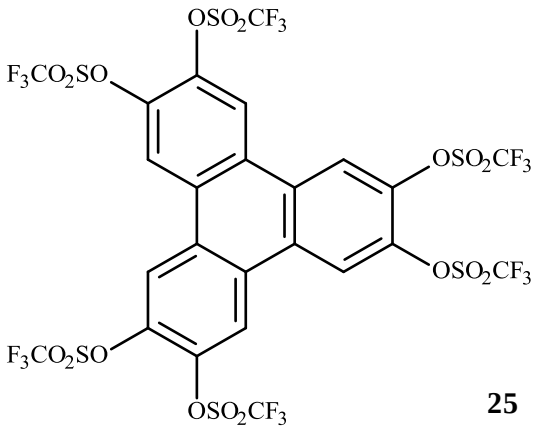

25

Following a modification to the procedure described by Bagui,[19] dry DCM (50 mL) and pyridine (13 mL, 0.15 mol) were cooled to -20 °C. Hexa(hydroxy)triphenylene **3** (2 g, 6.17 x 10^{-3} mol) was added and stirred for 10 min. Trifloromethanesulphonic anhydride (7.47 mL, 0.05 mol) was added drop wise and the reaction allowed to warm to room temperature and left to stir over night. This was then washed with water (3 x 50 mL), and the aqueous washings extracted with DCM (3 x 50 mL). The organic extracts were combined and dried ($MgSO_4$). The solvent was reduced to a minimum in vacuo and cold methanol added (50 mL). The resulting solid was filtered off to produce triphenylenehexatriflate **25** as a cream powder (0.80 g, 12 %).

Mp 166 °C, lit[20] mp 169 °C; δ_H ($CDCl_3$, TMS, 400 MHz) 8.58 (s, 6H).

3.9.3. Synthesis of triphenylene-2,3-ditriflate 28

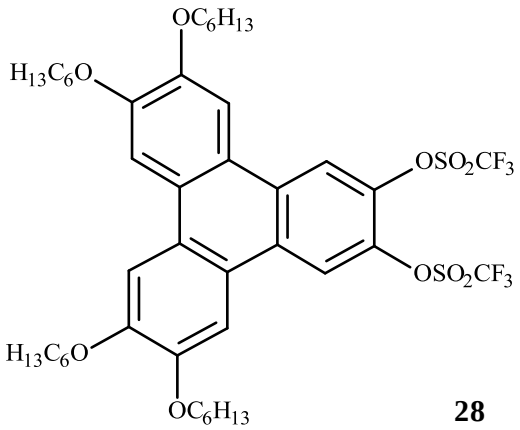

28

Following a modification to the synthesis used for **25**, 2,3-bis(hydroxy)triphenylene **10** (1.00 g, 1.51 mmol) and pyridine (6 mL) were added to dry DCM and cooled to -20 ºC. This was stirred for 10 minutes followed by the addition of triflouromethanesulphonic anhydride (1.28 g, 4.59 mmol) slowly, the solution was then left to warm to room temperature overnight. This was then washed with water (3 x 50 mL), and the aqueous washings extracted with DCM (3 x 50 mL). The organic extracted were combined, dried ($MgSO_4$) and the solvent reduced to a minimum in vacuo. Cold methanol was added (50 mL) and the precipitate filtered to produce triphenylene-2,3-ditriflate **28** as a cream semi-solid. (1.37 g, 97 %).

δ_H ($CDCl_3$, TMS, 400 MHz) 8.44 (s, 2H), 7.81 (s, 2H), 7.77 (s, 2H), 4.22 – 4.28 (m, 8H), 1.92 – 1.99 (m, 8H), 1.55 – 1.63 (m, 8H), 1.37-1.45 (m, 16H), 0.92 – 0.96 (m, 12H).

3.9.4. Attempted synthesis of 2,3-bis(methoxyphenyl)triphenylene 29

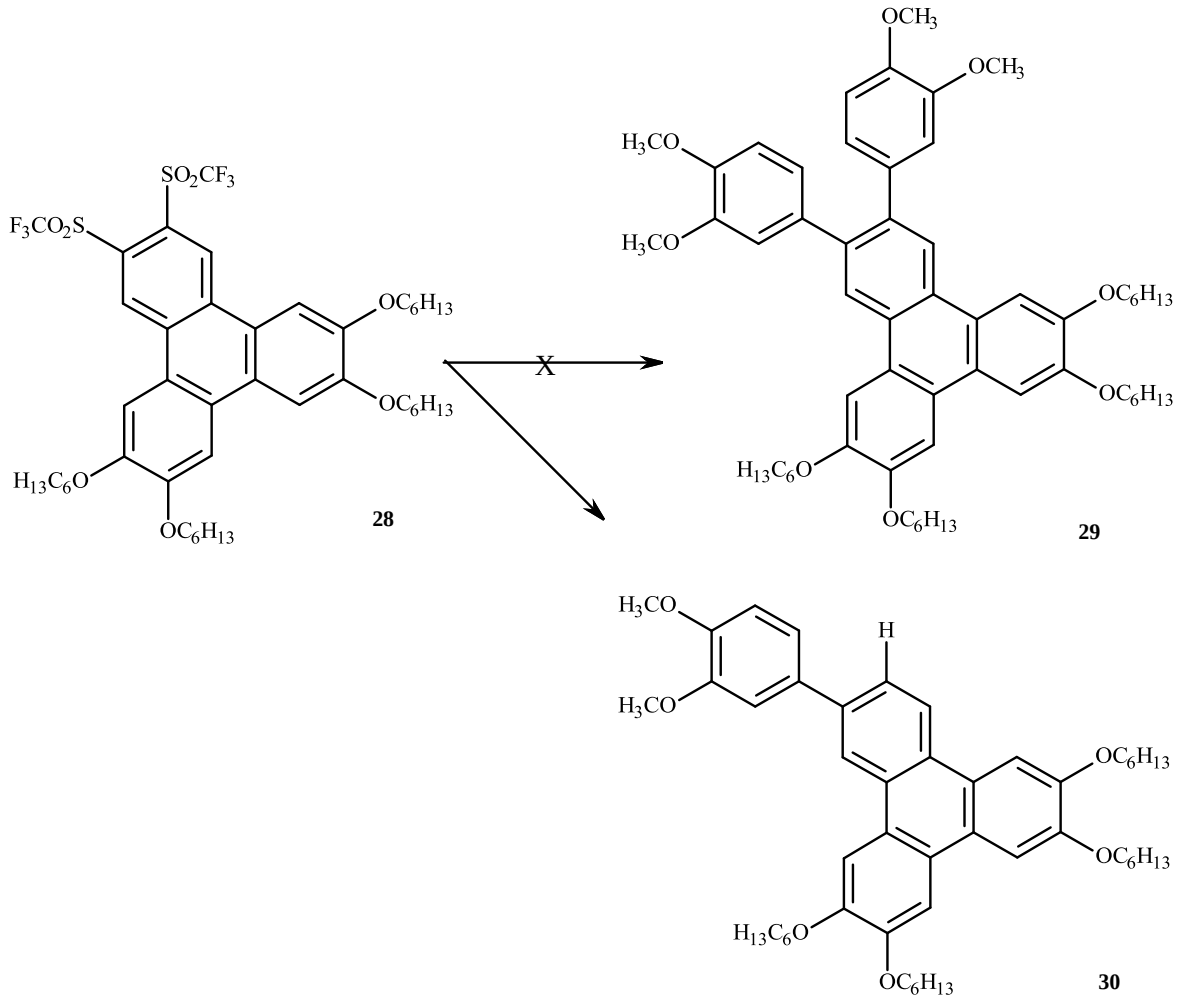

Following a modification to the procedure by Boden *et al*,[10] di(methoxy)benzeneboronic acid **26** (0.05 g, 0.29 mmol), triphenylene-2,3-ditriflate **28** (0.2 g, 0.22 mmol), $PdCl_2$ (1.57 mg, 0.0088 mmol), PPh_3 (9.13 mg, 0.03 mmol) and $NaCO_3$ (0.07 g, 0.67 mmol) were refluxed in a mixture of toluene, ethanol and water (3:3:1, 10 mL) for three nights. The water was separated and the ethanol and toluene removed in vacuo. The remaining residue was dissolved in DCM then washed with water (3 x 50 mL), and the aqueous washings extracted with DCM (3 x 50 mL). The organic extracted were combined, dried ($MgSO_4$) and the solvent reduced to a minimum in vacuo. The major product (dimethoxyphenyl)triphenylene **30** was then isolated by column chromatography eluting with DCM.

δ_H ($CDCl_3$, TMS, 400 MHz) 8.57 (s, 1H), 8.52 (d, J = 8.8Hz, 1H), 8.08 (s, 1H), 8.03 (s, 1H), 7.85 (s, 2H), 7.76 (d, J = 8.0Hz, 1H) 7.28 (s, 1H), 7.05 (d, J = 8.0Hz, 1H), 4.27-4.22 (m, 8H),

4.02 (s, 3H), 3.98 (s, 3H), 1.99-1.91 (m, 8H), 1.64-1.55 (m, 8H), 1.45-1.39 (m, 16H), 0.96-0.85 (m, 12H).

3.10. Metalation with zinc

3.10.1. Zinc-2,3-bis(porphyrin)triphenylene 5 - Song method[21]

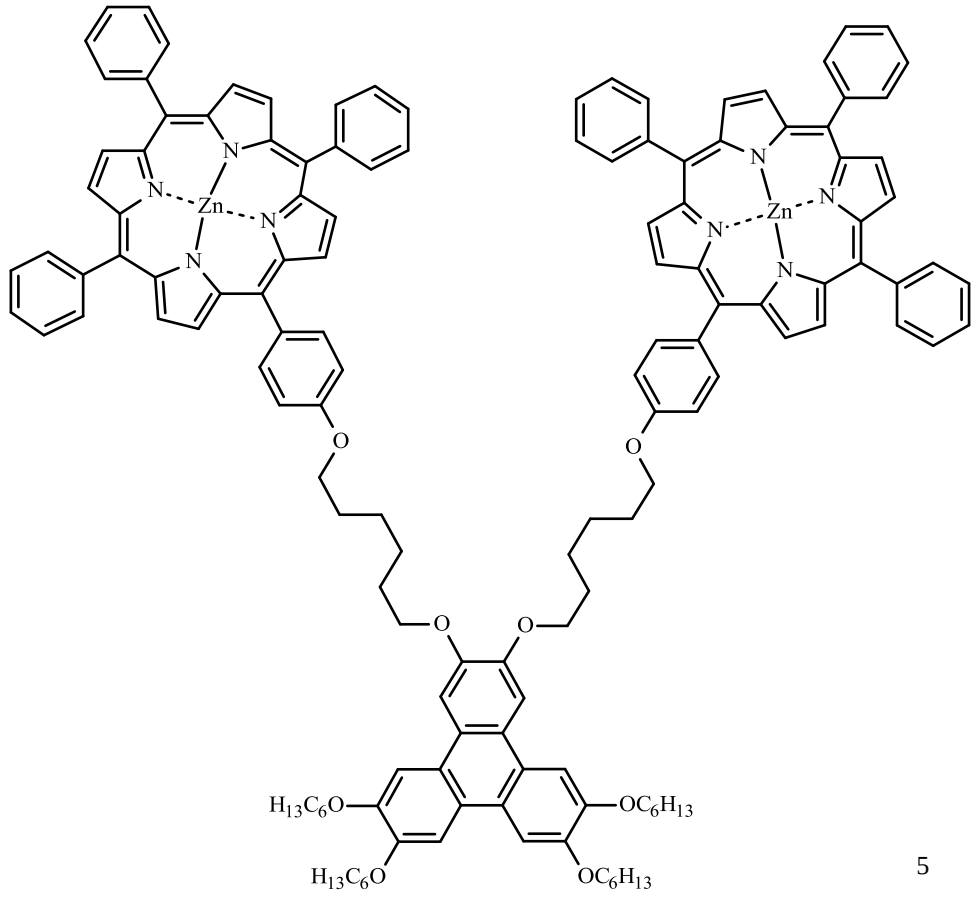

5

Hexa(porphyrin)triphenylene **24** (0.05 g, 0.01 mmol) was dissolved in DMF (5 mL) and to this zinc acetate (0.06 g, 0.33 mmol) was added and heated to 80°C for 12 h. The solution was then washed with water (3 x 50 mL), and the aqueous washings extracted with DCM (3 x 50 mL). The organic extracts were combined, dried ($MgSO_4$) and the solvent removed in vacuo. The product zinc-2,3-bis(porphyrin)triphenylene **5** was recrystallised from DCM : petroleum ether. (0.03 g, 63 %).

Mp 173 °C; Anal (Found C 76.96; H 6.28; N 4.88. $C_{142}H_{136}N_8O_8Zn_2$ Requires C 77.06; 6.19; N 5.06%); λ_{max} (DCM)/nm: 420, ε=9.24x10^5; 548, ε=3.86x10^4; 588, ε=9.67x10^3; δ_H ($CDCl_3$,

TMS, 400 MHz) 8.95 (s, 2H), 8.91 (s, 6H), 8.16 – 8.21 (m, 6H), 8.07 (d, *J* = 8.0Hz, 2H), 7.91 (s, 2H), 7.85 (s, 2H), 7.81 (s, 2H), 7.69 – 7.77 (m, 9H), 7.24 (d, *J* = 8.0Hz, 2H), 4.38 (t, *J* = 6.4 Hz), 4.28 (t, *J* = 6.4Hz, 4H), 4.19 – 4.23 (m, 8H), 2.10 – 2.15 (m, 12H), 1.84 – 1.94 (m, 16H), 1.38 – 1.40 (m, 20H), 0.91 – 0.96 (m, 12H). δ_c ($CDCl_3$, TMS, 300 MHz) 158.83, 150.62, 142.88, 135.49, 134.45, 131.88, 127.45, 126.52, 123.68, 121.04, 112.60, 109.89, 107.43, 69.71, 68.09, 31.56, 29.45, 29.27, 26.06, 25.71, 22.52, 13.91; *m/z* (MALDI) 2213 (M^+, 100%).

3.10.2. Zinc-2,3-bis(porphyrin)triphenylene 5 - Fukuzumi method[22]

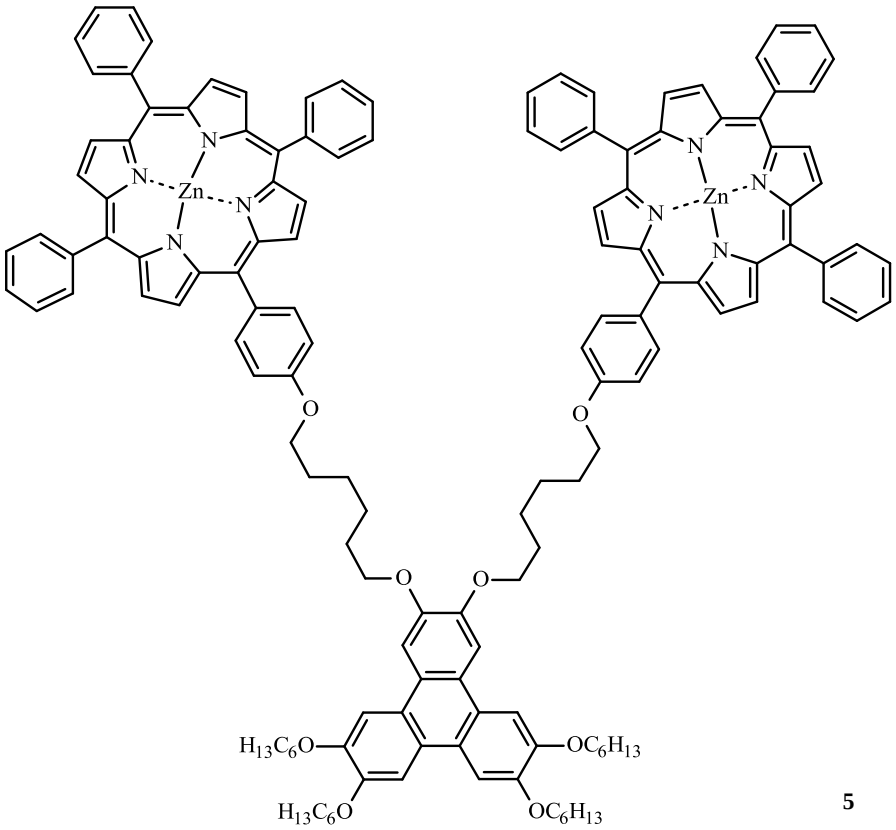

5

2,3-Bis(porphyrin)triphenylene **4** (0.10 g, 0.05 mmol) and zinc acetate (0.88 g, 0.48 mmol) were added to DCM (10 mL) and stirred at room temperature for 1 h. This was then washed with water (3 x 50 mL), and the aqueous washings extracted with DCM (3 x 50 mL). The organic extracts were combined, dried ($MgSO_4$) and the solvent removed in vacuo. The crude zinc-2,3-bis(porphyrin)triphenylene **5** was re-crystallised from DCM : petroleum ether. (0.0965 g, 76 %).

Mp 173 °C; Anal (Found C 76.96; H 6.28; N 4.88. $C_{142}H_{136}N_8O_8Zn_2$ Requires C 77.06; 6.19; N 5.06%); λ_{max} (DCM)/nm: 420, ε=9.24x10^5; 548, ε=3.86x10^4; 588, ε=9.67x10^3; δ_H ($CDCl_3$, TMS, 400 MHz) 8.95 (s, 2H), 8.91 (s, 6H), 8.16 – 8.21 (m, 6H), 8.07 (d, *J* = 8.0Hz, 2H), 7.91 (s, 2H), 7.85 (s, 2H), 7.81 (s, 2H), 7.69 – 7.77 (m, 9H), 7.24 (d, *J* = 8.0Hz, 2H), 4.38 (t, *J* = 6.4 Hz), 4.28 (t, *J* = 6.4Hz, 4H), 4.19 – 4.23 (m, 8H), 2.10 – 2.15 (m, 12H), 1.84 – 1.94 (m, 16H), 1.38 – 1.40 (m, 20H), 0.91 – 0.96 (m, 12H). δ_c ($CDCl_3$, TMS, 300 MHz) 158.83, 150.62, 142.88, 135.49, 134.45, 131.88, 127.45, 126.52, 123.68, 121.04, 112.60, 109.89, 107.43, 69.71, 68.09, 31.56, 29.45, 29.27, 26.06, 25.71, 22.52, 13.91; *m/z* (MALDI) 2213 (M^+, 100%).

3.10.3. Zinc-3,6-bis(porphyrin)triphenylene 6

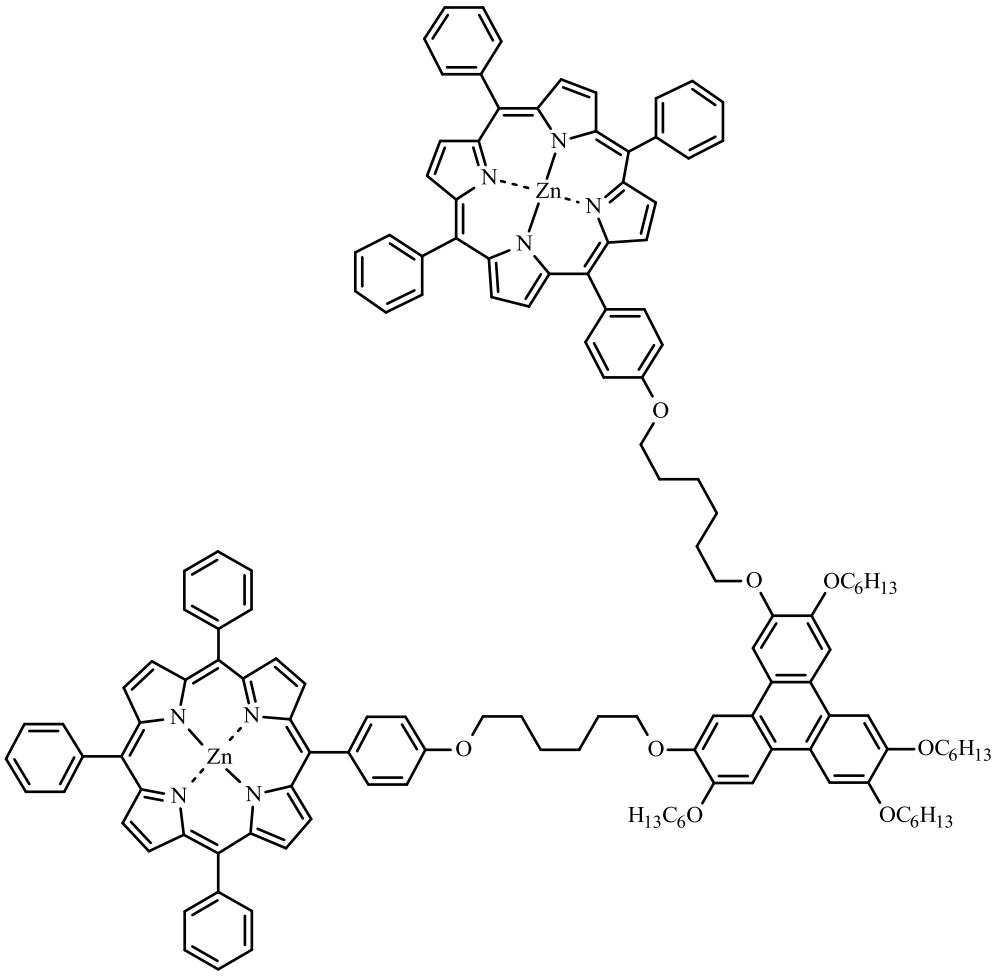

6

3,6-Bis(porphyrin)triphenylene **23** (0.03 mmol, 0.05 g) and zinc acetate (0.86 mmol, 0.16 g) were added to DCM (10 mL) and stirred at room temperature for 1 h. This was then washed

with water (3 x 50 mL), and the aqueous washings extracted with DCM (3 x 50 mL). The organic extracts were combined, dried ($MgSO_4$) and the solvent removed in vacuo. The zinc-3,6-bis(porphyrin)triphenylene **6** was re-crystallised from DCM : petroleum ether. (0.05 g, 80 %).

Mp 177 °C; Anal (Found C 74.83; H 6.36; N 4.66. $C_{142}H_{136}N_8O_8Zn_2.CH_2Cl_2$ Requires C 74.73; H 6.05; N 4.88%); λ_{max} (DCM)/nm: 420, $\varepsilon=4.67x10^5$; 548, $\varepsilon=3.27x10^4$; 588, $\varepsilon=8.06x10^3$; δ_H ($CDCl_3$, TMS, 400 MHz) 8.96 (s, 4H), 8.92 (s, 12H), 8.17 – 8.21 (m, 12H), 8.06 (d, *J* = 8.4 Hz, 4H), 7.92 (s, 2H), 7.84 (s, 2H), 7.78 (s, 2H), 7.64 – 7.79 (m, 18H), 7.19 (d, *J* = 8.4 Hz, 4H), 4.34 (t, *J* = 6.4 Hz, 4H), 4.26 (t, *J* = 6.4Hz, 4H), 4.20 (t, *J* = 6.4 Hz, 4H), 4.15 (t, *J* = 6.4 Hz, 4H), 2.09 – 2.05 (m, 4H), 1.94 – 2.04 (m, 8H), 1.89 – 1.81 (m, 4H), 1.72 – 1.83 (m, 8H), 1.58 – 1.68 (m, 8H), 1.48 – 1.57 (m, 16H), 0.86 – 0.99 (m, 12H). δ_c ($CDCl_3$, TMS, 300 MHz) 156.82, 150.29, 142.28, 135.63, 134.60, 134.47, 131.98-131.32, 127.69, 127.48, 126.55, 126.69, 123.16, 120.08, 112.58, 107.78, 69.64, 68.05, 31.58, 29.33, 25.77, 25.69, 22.51, 13.95 *m/z* (MALDI) 2213 (M+, 100%).

3.10.4. Attempted synthesis of zinc-hexa(porphyrin)triphenylene 7

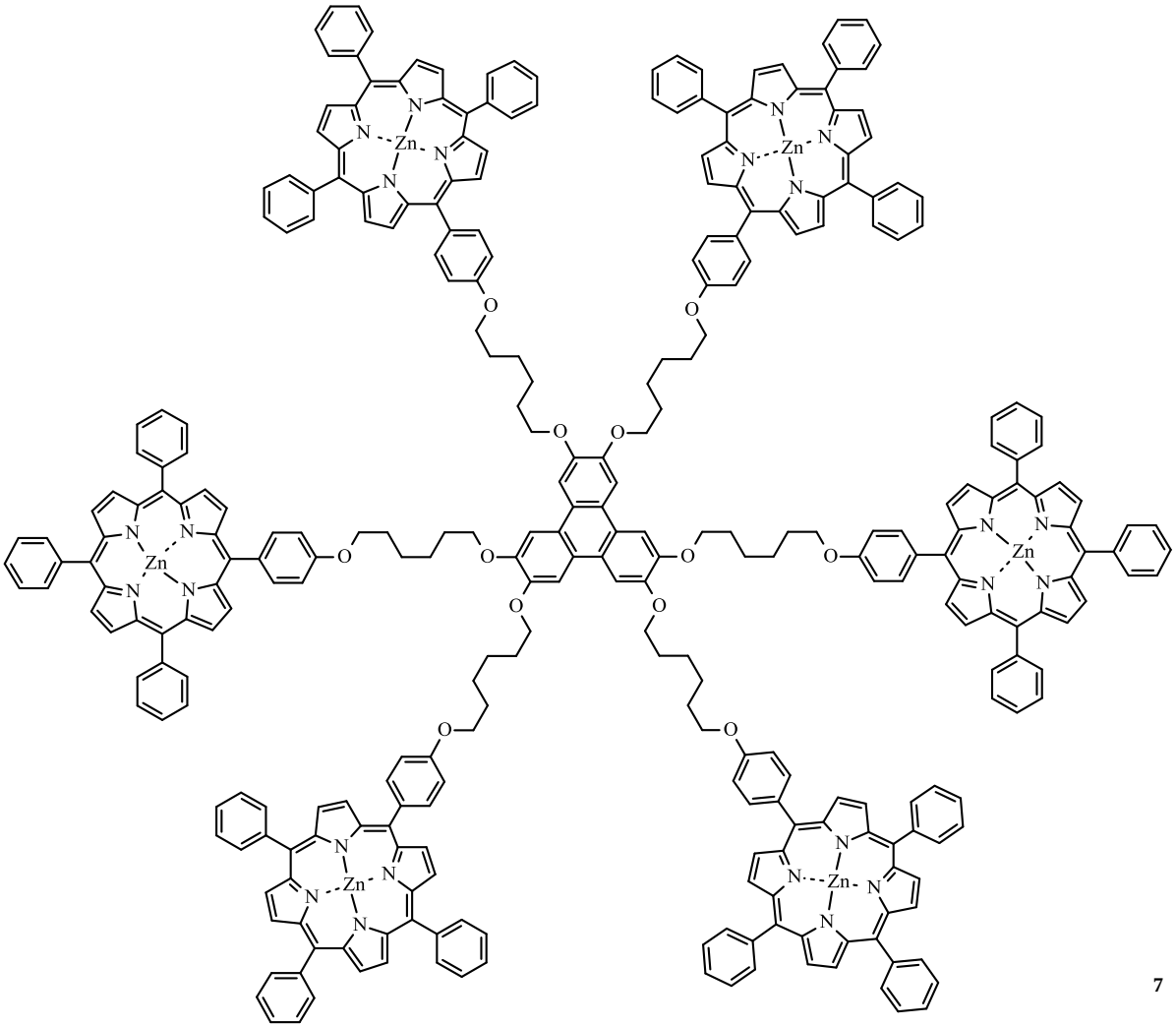

7

Hexa(porphyrin)triphenylene **24** (0.01 mmol, 0.05 g) and zinc acetate (0.33 mmol, 59.80 mg) were added to DCM (10 mL) and stirred at room temperature for 1 h. This was then washed with water (3 x 50 mL), and the aqueous washings extracted with DCM (3 x 50 mL). The organic extracts were combined, dried ($MgSO_4$) and the solvent removed in vacuo. A material was then re-crystallised from DCM : petroleum ether. (29.00 mg, 63 %).

Mp 197 °C; Anal (Found C 73.00; H 4.78; N 6.24. $C_{318}H_{240}N_{24}O_{12}Zn_6.2Cl_2CH_2$ Requires C 72.67; H 4.70; N 6.24%); λ_{max} (DCM)/nm: 420, ε=6.04x10^6; 548, ε=2.28x10^5; 587, ε=4.96x10^4; δ_H ($CDCl_3$, TMS, 400 MHz) 9.40 – 9.42 (m, 36H), 8.77 – 8.79 (m, 36H), 8.74 (s, 6H), 8.65 – 8.69 (m, 12H), 8.47 (s, 12H), 8.33 – 8.40 (m, 12H), 7.89 – 7.92 (m, 12H), 4.87 (t, *J* = 6.4 Hz, 12H), 4.79 (t, *J* = 6.8 Hz, 12H), 2.53 – 2.65 (m, 12H), 2.32 – 2.40 (m, 12H), 2.23 – 2.30 (m, 12H), 2.13 – 2.19 (m, 12H). δ_c ($CDCl_3$, TMS, 300 MHz) 158.84, 150.67, 150.31,

150.23, 142.92, 135.48, 134.48, 131.95-132.34, 127.53, 126.59, 121.11, 112.59, 63.94, 29.26, 28.41, 25.77, 25.65. *m/z* (MALDI) 2213 (M+, 100%).

3.10.5. Zinc-TPP 31

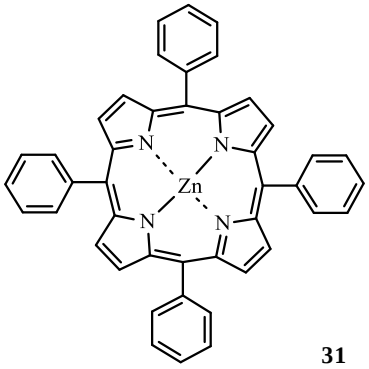

31

TPP (0.05 g, 8.1332×10^{-5} mol) and zinc acetate (0.1492 g, 8.1332×10^{-4} mol) were added to DCM (10 mL) and stirred at room temperature for 1 h. This was then washed with water (3 x 50 mL), and the aqueous washings extracted with DCM (3 x 50 mL). The organic extracts were combined, dried ($MgSO_4$) and the solvent removed in vacuo. The crude zinc-TPP **31** was then re-crystallised from DCM : methanol. (0.0424 g, 85 %).

Mp 445 °C; Anal (Found: C 77.82; H 4.09; C 8.19. $C_{44}H_{28}N_4Zn$ Requires C 77.94; H 4.16; N 8.26%); λ_{max} (DCM)/nm: 419, $\varepsilon=6.31 \times 10^5$; 547, $\varepsilon=1.89 \times 10^4$; 587, $\varepsilon=3.17 \times 10^3$; δ_H ($CDCl_3$, TMS, 400 MHz) 8.96 (s, 8H), 8.22 – 8.24 (m, 8H), 7.73 – 7.78 (m, 12H); δ_c ($CDCl_3$, TMS, 300 MHz). 150.22, 142.80, 134.44, 132.01, 127.52, 126.57, 121.15 m/z (MALDI) 678 (M^+, 100%).

3.10.6. Zinc-bromoalkoxyporphyrin 32

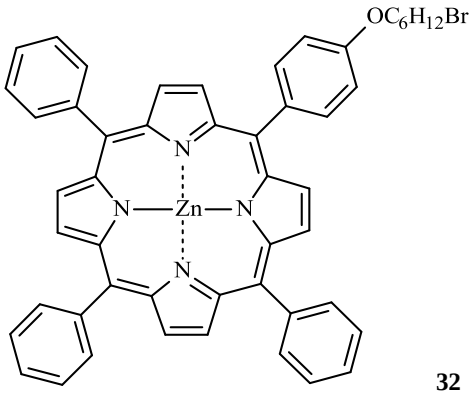

32

Bromoalkoxyporphyrin **22** (0.05 g, 0.06 mmol), zinc acetate (0.63 mmol, 0.12 g) were added to DCM (10 mL) and stirred at room temperature for 1 h. This was then washed with water (3 x 50 mL), and the aqueous washings extracted with DCM (3 x 50 mL). The organic extracts were combined, dried ($MgSO_4$) and the solvent removed in vacuo. The crude zinc-bromoalkoxyporphyrin **32** was then re-crystallised from DCM : petroleum ether. (46.70 mg, 87 %).

Mp 190 °C; Anal (Found: C;H;N. $C_{50}H_{39}BrN_4OZn$ Requires C;H;N%); λ_{max} (DCM)/nm: 420, ε=6.81x105; 548, ε=2.30x104; 586, ε=4.95x103; δ_H ($CDCl_3$, TMS, 400 MHz) 9.01 (d, *J* = 4.4 Hz, 2H), 8.97 (s, 6H), 8.24 (d, *J* = 6.8 Hz, 6H), 8.13 (d, *J* = 8 Hz, 2H), 7.75 – 7.81 (m, 9H), 7.29 (d, *J* = 8, 2H), 4.28 (t, *J* = 6.4 Hz, 2H), 3.53 (t, *J* = 6.8 Hz, 2H), 2.00 – 2.05 (m, 2H), 1.66 – 1.68 (m, 2H), 1.54 – 1.63 (m, 4H). δ_c ($CDCl_3$, TMS, 300 MHz) 158.82, 142.93, 135.49, 134.49, 132.12, 132.00, 131.94, 127.52, 126.59, 121.10, 112.60, 67.97, 33.78, 32.66, 29.21, 27.95, 25.38 m/z (MALDI) 856 (M^+, 100%).

3.11. Metalation with copper

3.11.1. Copper-2,3-Bisporphyrintriphenylene 34

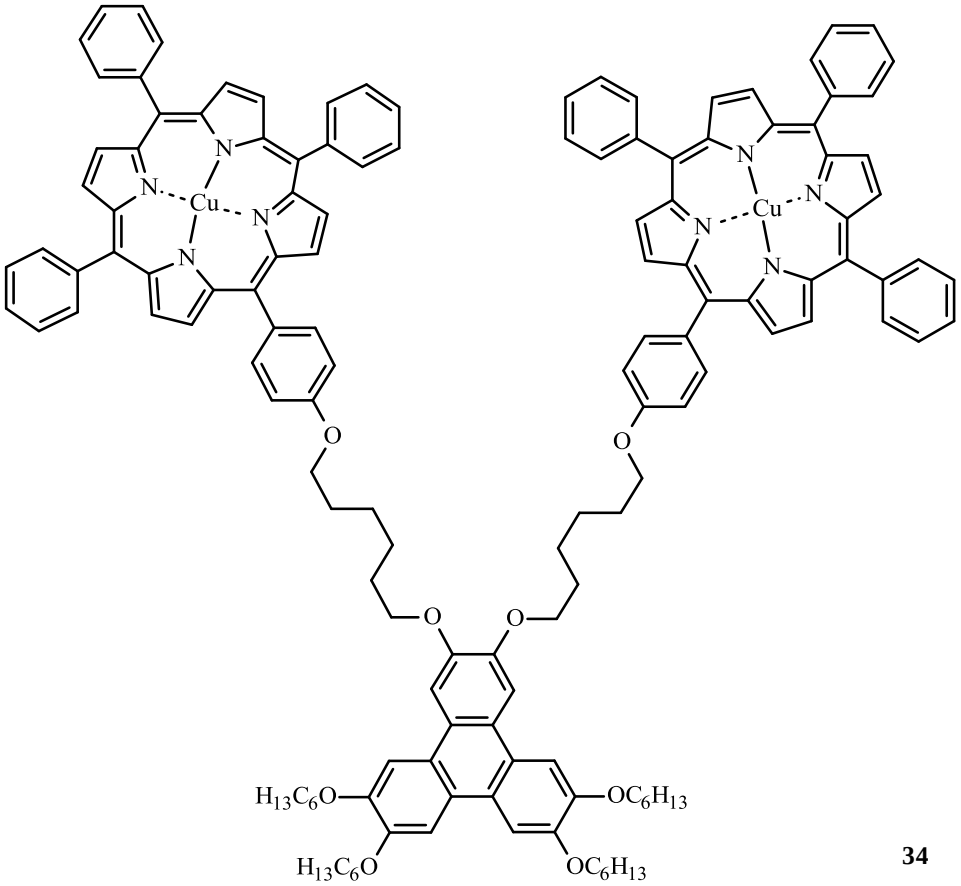

34

Copper acetate (0.0071 g, 0.13594 mmol) was dissolved in a minimum of methanol and added to 2,3-bisporphyrin-triphenylene **4** (0.025 g, 0.1198 mmol) in DCM (10 mL).[23] This was refluxed for 2 h, washed with water (3 x 50 ml) and the washings extracted with DCM. The organic extracts were combined, dried ($MgSO_4$) and the solvent removed in vacuo. The crude product underwent column chromatography (DCM : PET, 50:50) to produce copper-2,3-bisporphyrintriphenylene **36** as a red solid (0.0239 g, 90 %).

Mp 191 °C; λ_{max} (DCM)/nm: 539, ε=4.29x10^4; 574, ε=6.20x10^3; 416, ε=8.61x10^5; δ_H ($CDCl_3$, TMS, 400 MHz) very broad spectrum; δ_c ($CDCl_3$, TMS, 300 MHz) very broad spectrum. m/z (MALDI) 2208.8 (M^+, 100%).

3.12. Metalation with ruthenium

3.12.1. Ruthenium-2,3-bis(porphyrin)triphenylene 35

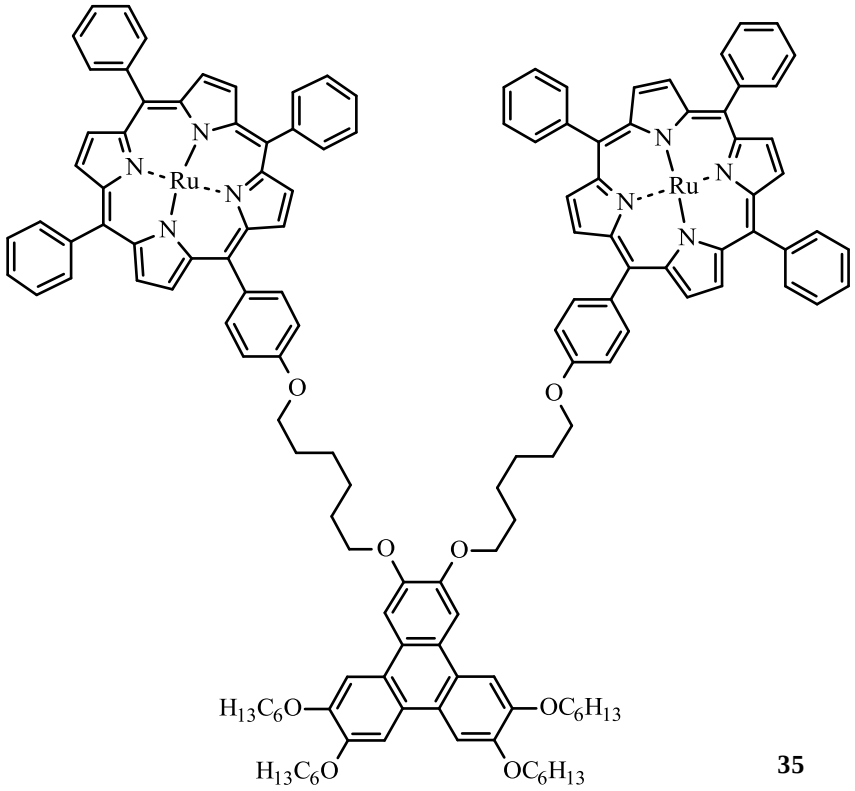

35

Following a modification to the procedure described by Gallo *et al*,[24] 2,3-bis(porphyrin)triphenylene **4** (0.1 g, 0.0479 mmol) and triruthenium dodecacarbonyl (0.0919 g, 0.1438 mmol) were dissolved in benzene (5 ml) and refluxed for 48 h. This was then washed (3 x 50 ml) with water and the washings extracted with DCM (3 x 50 ml). The organic extracts were combined, dried ($MgSO_4$) and the solvent removed in vacuo. The crude product was then column chromatography (DCM → DCM : Methanol 100:1). The ruthenium-2,3-bis(porphyrin)triphenylene **35** was isolated as a red solid (0.066 g, 60 %).

Mp >250 decomposed; (DCM)/nm: 416, ε=4.02x10^4; 567, ε=1.33x10^4; 412, ε=4.82x10^5; δ_H ($CDCl_3$, TMS, 400 MHz) 8.68-8.62 (m, 16H), 8.19-8.07 (m, 12H), 8.04 (d, J=8.4, 2H), 7.89 (s, 2H), 7.86 (s, 2H) 7.74-7.63 (m, 22), 7.15 (d, J=8.4, 2H), 7.07 (d, J=6.8), 4.33 (t, J=6, 4H), 4.17 (s, 4H), 4.09 (t, J=6, 8H), 2.01-1.97 (m, 8H), 1.81-1.79 (m, 16H), 1.49 (s, 8H), 1.39-1.35 (m, 16H), 0.91-0.89 (m, 12H) ; δ_c ($CDCl_3$, TMS, 300 MHz)155.36, 149.11, 142.52, 135.45, 134.52, 1131.88, 131.75, 127.37, 126.45, 126.63, 123.60, 121.76, 112.72, 109.06, 69.54, 68.08, 32.07, 31.51, 29.09, 28.81, 28.83, 25.60, 22.49, 13.89; m/z (MALDI) 2086.1 (M^+, 10%)

3.13. References

(1) Alder, A. D. Longo, F. R. Finarelli, J. D. Goldmacher, J. Assour, J.; Korsakoff, L. *J. Org. Chem.* **1967**, *32*, 476–476.

(2) Tome, J. P. C. Neves, M. G. Tome, A. C. Cavaleiro, J. A. S. Mendonca, A. F. Pegado, I. N. Duarte, R.; Valdeira, M. L. *Bioorg.Med.Chem.* **2005**, *13*, 3878–3888.

(3) Piattelli, M. Fattorusso, E. Nicolaus, R. A.; Magno, S. *Tetrahedron* **1965**, *21*, 3229–3236.

(4) Howard, M. Heirtzler, F.; Dias, S. *J. Org. Chem.* **2008**, *73*, 2548-2553.

(5) Meier, H.; Rose, B. *J. Prakt. Chem* **1998**, *340*, 536-543.

(6) Fanta, P. E. *Synthesis* **1974**, *9*, 9-21.

(7) Bannard, R. A. B.; Latremouille, G. *Can. J. Chem.* **1953**, *31*, 469–469.

(8) Anderson, N. G. Maddaford, S. P. A.; Keay, M. A. *J. Org. Chem.* **1996**, *61*, 9556-9559.

(9) Li, J. He, Z. Gopee, H.; Cammidge, A. N. *Org. Lett.* **2010**, *12*, 472–475.

(10) Boden, N. Bushby, R. J. Lu, Z.; Headdock, G. *Tetrahedron Lett.* **2000**, *41*, 10117-10120.

(11) Boden, N. Bushby, R. J. Cammidge, A. N.; Martin, P. S. *J. Mater. Chem.* **1995**, *5*, 1857.

(12) Boden, N. Bushby, R. J.; Cammidge, A. N. *J. Chem. Soc., Chem. Commun.* **1994**, 465.

(13) Li, J. He, Z. Gopee, H.; Cammidge, A. N. *Org. Lett.* **2010**, *12*, 472–475.

(14) Chen, W. Zhao, Q. Xu, M.; Lin, G. *Org. Lett.* **2010**, *12*, 1072-1075.

(15) Boden, N. Bushby, R. J.; Cammidge, A. N. *J. Am. Chem. Soc.* **1995**, *117*, 924–927.

(16) Ogasawara, F. Kasai, H. Nagashima, Y. Yoshihiro, K. Kawagachi, T.; Yoshizama, A. *Ferroelectrics* **2008**, *365*, 48-57.

(17) Miyaura, N.; Suzuki, A. *Chem. Rev.* **1995**, *95*, 2457–2483.

(18) Alfa http://www.alfa.com/en/GP100w.pgm?DSSTK=B24240. *http://www.alfa.com/en/GP100w.pgm?DSSTK=B24240* **21/07/2011**.

(19) Bagui, M. Melinger, J. Chakraborty, S. Keightley, J.; Peng, Z. *Tetrahedron* **2009**, *65*, 1247-1256.

(20) Cammidge, A. N.; Gopee, H. *Mol.Cryst.Liq.Cryst* **2003**, *397*, 117-128.

(21) Song, H. Taniguchi, M. Speckbacher, M. Yu, L. Bocian, D. Lindsey, J.; Holten, D. *J. Phys. Chem. B* **2009**, *113*, 8011-8019.

(22) El-Khouly, M. Ryu, J. Kay, K. Ito, O.; Fukuzumi, S. *J. Phys. Chem. C* **2009**, *113*, 15444-15453.

(23) Beavington, R.; Burn, P. L. *J. Chem. Soc., Perkin Trans. 1* **1999**, *5*, 583-592.

(24) Gallo, E. Caselli, A. Ragaini, F. Fantauzzi, S. Masciocchi, N. Sironi, A.; Cenini, S. *Inorg. Chem.* **2005**, *44*, 2039-2049.